CHARACTERISATION OF THE RUVB BRANCH MIGRATION MOTOR

BY

HELEN MARION GEORGE

Thesis submitted to the University of London, for the degree of Doctor of Philosophy

December 1999

ProQuest Number: U643994

All rights reserved

INFORMATION TO ALL USERS
The quality of this reproduction is dependent upon the quality of the copy submitted.

In the unlikely event that the author did not send a complete manuscript
and there are missing pages, these will be noted. Also, if material had to be removed,
a note will indicate the deletion.

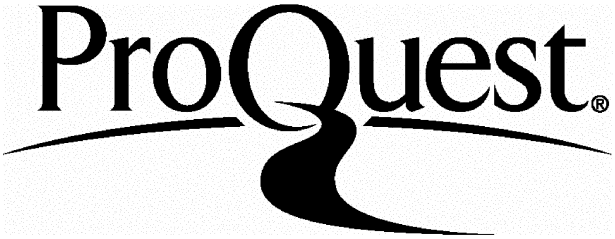

ProQuest U643994

Published by ProQuest LLC(2016). Copyright of the Dissertation is held by the Author.

All rights reserved.
This work is protected against unauthorized copying under Title 17, United States Code.
Microform Edition © ProQuest LLC.

ProQuest LLC
789 East Eisenhower Parkway
P.O. Box 1346
Ann Arbor, MI 48106-1346

ACKNOWLEDGEMENTS

I particularly wish to thank Steve West, my supervisor, for his guidance and enthusiasm throughout my PhD, and to the members of the West lab, both past and present, for being such good colleagues. They are Addie, Alain, Alison, Angie, Angelos, Anthony, Brenda N., Boris, Carol, Christine, Claire, Dave, Didier, Eric, Fiona, Jean-Yves (alias JYM!), Les, Madalena, Mike, Peter, Rajvee and Simon. Special thanks to Christine who took me under her wing when I first started and taught me the ropes in the lab and, in particular, in the cold room! Also, a huge thankyou to all those who proof-read my thesis, especially Steve, Simon and Carol who did overtime! On a less scientific note, I'd like to thank the West lab for being so sociable; for all the badminton and tennis matches, Friday night pub trips, Christmas bowling days and so it goes on. I couldn't have worked with a nicer crowd and I will miss them.

I would also like to say thanks to all the people in Clare Hall who have helped in my research either directly, by giving technical advice, or indirectly, by providing a happy and friendly atmosphere in which to work. In particular, I'd like to thank Brenda M., Frank and Sue, for the smooth day-to-day running of Clare Hall, Judy, for all her help with ordering papers, John, for his photography expertise, the security guards, for looking after me (!), and the canteen crowd, for keeping me well-fed!

On a more personal note, I'd like to thank Mum and Dad for the unconditional love and support they have given me over the years; also my brother Nick and his wife Janette for their love and encouragement. Finally, thanks to my friends, especially the eight who got married this year providing me with welcome weekend breaks from my PhD!

ABSTRACT

The *Escherichia coli* Ruv proteins process Holliday junction intermediates during the recombinational repair of DNA damage. RuvA and RuvB promote branch migration, a reaction responsible for the formation and extension of heteroduplex DNA, whilst RuvC mediates junction resolution to form recombinant products. A tripartite RuvAB-Holliday junction complex has been observed by electron microscopy. RuvA is bound to the crossover and is flanked by two RuvB hexameric rings threaded on opposite arms of the junction. The RuvB rings provide a novel dual motor for branch migration, using the energy from ATP hydrolysis to pump duplex DNA out through their central cavities.

RuvB belongs to a family of hexameric helicases and, in the presence of RuvA, exhibits a 5′ to 3′ DNA helicase activity *in vitro*. To investigate the role of DNA unwinding in branch migration, site-directed mutagenesis has been used to knock-out a residue in RuvB that is important for its helicase activity. The resultant protein, $RuvB^{D113E}$, has been purified and characterised *in vivo* and *in vitro*. Despite being severely compromised in its DNA helicase activity, $RuvB^{D113E}$ was able to hydrolyse ATP and promote branch migration in the presence of RuvA. The results indicate that extensive helicase activity is not required for RuvAB-mediated branch migration.

It is possible that transient opening of the duplex arms within the RuvB rings may occur which would provide a single strand for unidirectional translocation. However, introduction of an interstrand cross-link into a synthetic junction did not affect the efficiency of RuvAB-mediated branch migration. Based on the results of these studies, and on observations made with the other hexameric helicases, models for DNA translocation by RuvB are proposed.

CONTENTS

LIST OF FIGURES

CHAPTER ONE

CHAPTER TWO

CHAPTER THREE

CHAPTER FOUR

CHAPTER FIVE

ABBREVIATIONS

A_x	absorbance at wavelength of x nm (e.g. 650 nm)
Ac	acetate
ADP	adenosine 5'-diphosphate
ATP	adenosine 5'-triphosphate
ATPγS	adenosine 5′-O-(3-thiotriphosphate)
bp	base pair
Brij 58	polyoxyethylene 20 cetyl ether
BSA	bovine serum albumin
ddH_2O	double distilled water
DNA	deoxyribonucleic acid
dsDNA	double-stranded DNA
gDNA	gapped circular duplex DNA
ssDNA	single-stranded DNA
DSB	double-strand break
DSBR	double-strand break repair
DTT	dithiothreitol
EDTA	ethylenediaminetetraacetic acid
FPLC	fast protein liquid chromatography
HPLC	high pressure liquid chromatography
IPTG	isopropyl β-D-thiogalactopyranoside
kbp	kilobase pair
kDa	kilodalton
LB	Luria broth
nt	nucleotide
NTP	nucleoside 5′-triphosphate
oligo	oligonucleotide

ORF	open reading frame
PAGE	polyacrylamide gel electrophoresis
Polymin P	polyethylenimine
rpm	revolutions per minute
SDS	sodium dodecyl sulphate
SSB	single-stranded DNA binding protein
TEA	triethanolamine
TEMED	N,N,N′,N′-tetramethylethylenediamine
TLC	thin-layer chromatography
Tris	tris(hydroxymethyl)aminomethane
Tween 20	polyoxyethylenesorbitan monolaurate
U	unit
UV	ultraviolet
vol	volume

CHAPTER ONE : INTRODUCTION

I. ROLE OF THE HOLLIDAY JUNCTION IN HOMOLOGOUS RECOMBINATION AND REPAIR

Homologous genetic recombination is a universal biological process that involves the exchange of DNA sequences between two homologous chromosomes or DNA molecules. It functions to (i) generate genetic diversity through the random assortment of genes; (ii) maintain genomic integrity by repairing damaged DNA; and (iii) guide the proper segregation of chromosomes during meiosis (in higher organisms).

THE HOLLIDAY MODEL FOR HOMOLOGOUS RECOMBINATION

In the early 1960s, Robin Holliday proposed a model for homologous recombination to explain the aberrant segregations, or gene conversions, seen in fungal tetrads (Holliday, 1964). The model, shown in Figure 1.1, involves the alignment of homologous DNA molecules, followed by the reciprocal exchange of single DNA strands with like polarity. The exchange reaction results in strands from each parental molecule becoming base paired with the other partner to form a four-way heteroduplex joint. This crossover was later referred to as a Holliday junction. Subsequent movement of the junction occurs by a process known as branch migration, which acts to extend the region of heteroduplex DNA. Finally, the Holliday junction is resolved by endonucleolytic cleavage. Resolution occurs in one of two possible orientations to generate 'patch' recombinant products, in which flanking markers retain their parental configurations, or 'splice' products, in which there is exchange of the markers (Figure 1.1 (iv) and (v), respectively).

Over the years, a number of new models have been proposed for homologous recombination. However, the idea originally proposed by Holliday that recombining DNA molecules might become linked by a heteroduplex joint

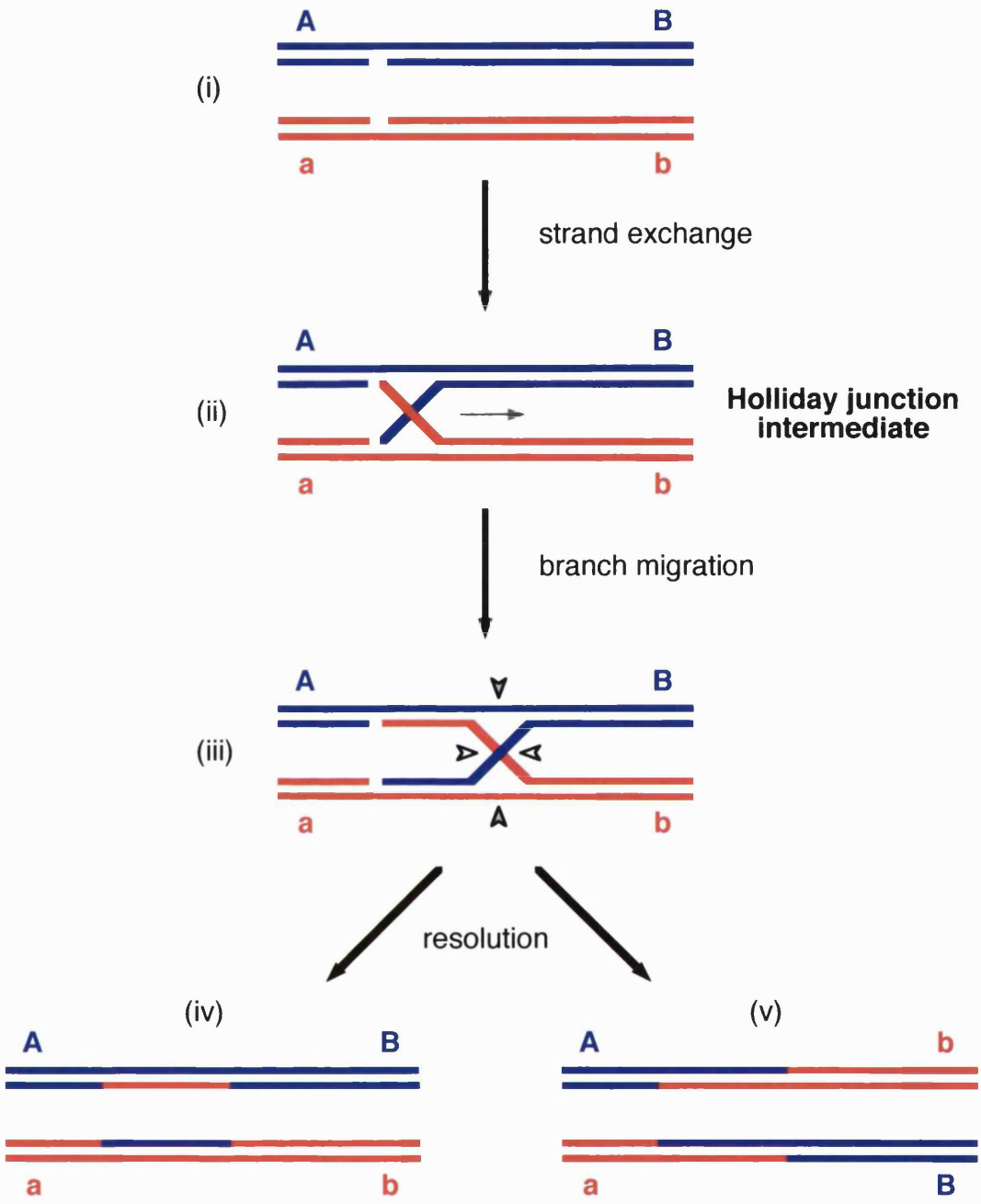

FIGURE 1.1. THE HOLLIDAY MODEL FOR HOMOLOGOUS RECOMBINATION

Identical strands in two aligned homologous duplexes are nicked (i), allowing the reciprocal exchange of DNA strands and resulting in the formation of a Holliday junction (ii). Branch migration of the crossover point produces a region of hybrid DNA (iii). The Holliday junction is then resolved by cleavage either east-west or north-south to generate 'patch' (iv) or 'splice' (v) products, respectively, and the nicks are repaired by DNA ligase. In this figure, the two DNA molecules are oriented such that strands of the same polarity are next to each other. 'A' and 'B' represent two genetic markers in the DNA molecules (with 'a' and 'b' denoting different alleles of these markers).

has withstood the test of time. In addition to being a key intermediate in homologous recombination, the Holliday junction also plays an important role in the other major class of genetic recombination, site-specific recombination. However, this section will focus on the Holliday junction as an intermediate in homologous recombination and, in particular, on its role in the repair of damaged DNA.

DOUBLE-STRAND BREAK REPAIR BY HOMOLOGOUS RECOMBINATION

Double-strand breaks (DSBs) in DNA are caused by environmental agents (e.g. X-rays and other ionising radiation), by mechanical stress during chromosome segregation and, in particular, by the collapse of replication forks (Kuzminov, 1995). In addition, DSBs in cells are voluntarily induced by enzymatic cleavage during processes such as meiotic recombination (Keeney *et al.*, 1997). It was suggested that recombination events could be initiated from DSBs, leading to the repair of DNA (Orr-Weaver *et al.*, 1981; Resnick, 1976). This led to the proposal of the DSB-repair (DSBR) model for recombination (Szostak *et al.*, 1983; Figure 1.2A). Following the formation of DSBs, the DNA ends are resected by a 5′-3′ exonuclease activity and the resulting 3′ ssDNA tails invade the homologous duplex DNA to displace a loop (D-loop). The ends act as primers for the initiation of DNA synthesis, allowing genetic information to be copied from the intact homologous duplex. The D-loop is enlarged by repair synthesis leading to the formation of two Holliday junctions, which are subsequently processed by branch migration and resolution reactions. Cleavage of the junctions in the same orientation leads to the generation of patch products whereas cleavage in opposite orientations leads to the exchange of flanking markers and the formation of splice products (Figure 1.2A (vi) and (vii), respectively). In support of the DSBR model, double Holliday junction

FIGURE 1.2. THE REPAIR OF DOUBLE-STRAND BREAKS BY HOMOLOGOUS RECOMBINATION

A. The DSBR model. DSB formation (i) is followed by 5' to 3' resection of the ends (ii). The 3' ssDNA tails invade a homologous duplex, forming a D-loop (iii), and initiate repair DNA synthesis (iv). The D-loop is extended by DNA synthesis to create two Holliday junctions (v) which are resolved in the same or opposite orientation to generate patch (vi) or splice (vii) recombinant products, respectively.

B. A version of the synthesis-dependent strand-annealing model. DSBs (i) are processed as described above (ii) and one ssDNA tail invades the homologous duplex (iii). The resulting D-loop is pushed along by DNA replication (iv). The 3' tail at the other end of the DSB can then anneal with the newly-synthesised strand (v), or with the D-loop to form a pair of Holliday junctions (vi) that can be resolved as in A. Figure adapted from Haber (1999).

In the figures, the two DNA molecules are oriented such that strands of like polarity are closest together. In both models, the intact homologous duplex acts as a template for retrieving lost genetic information at the DSB. Repair DNA synthesis is indicated by the green dashed line.

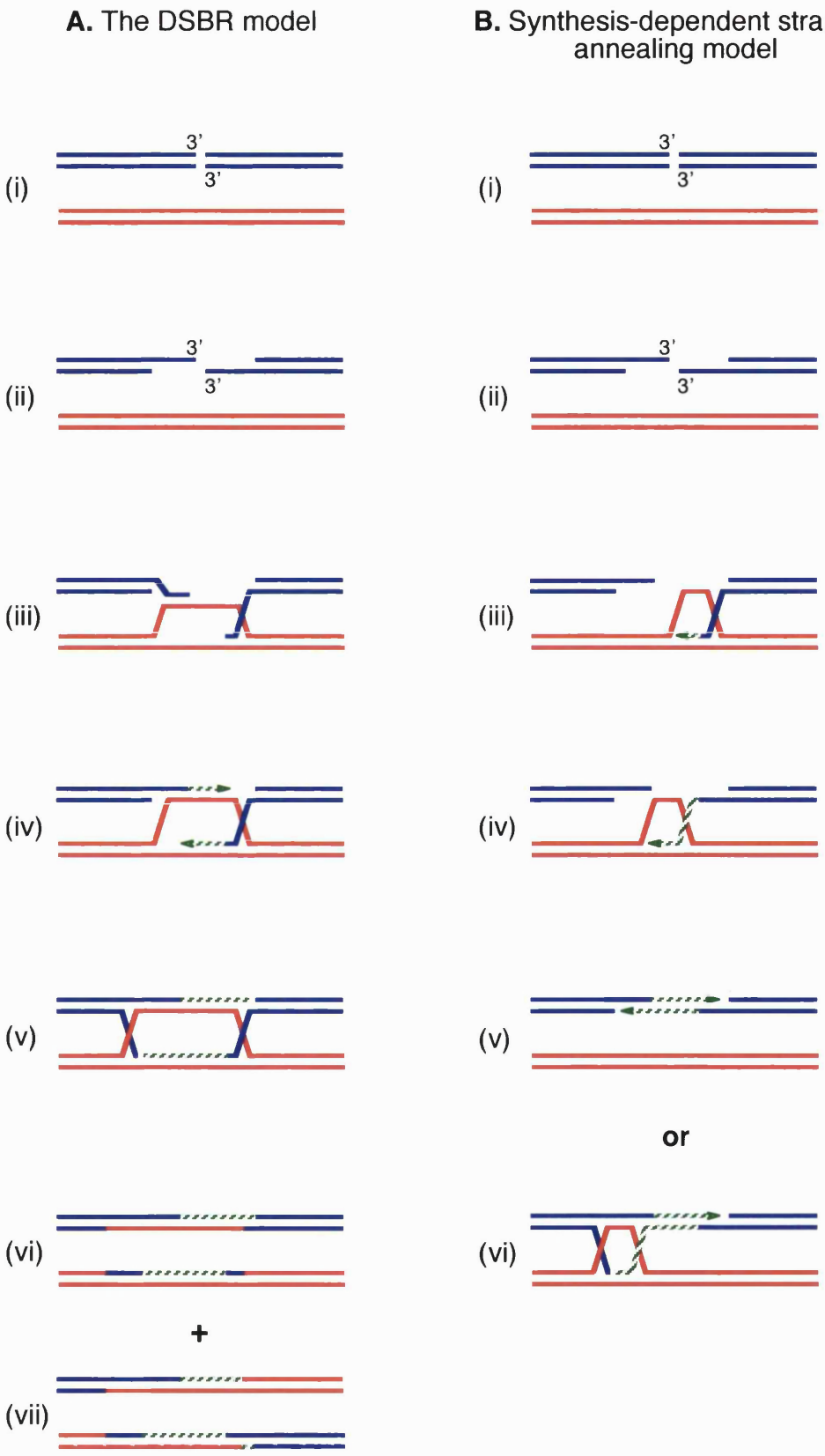
A. The DSBR model
B. Synthesis-dependent strand-annealing model
(i)
3'
3'
(ii)
3'
3'
(iii)
(iv)
(v)
(vi)
+
(vii)
or

FIGURE 1.2

intermediates have been identified in meiotic cells (Byers and Hollingsworth, 1994; Schwacha and Kleckner, 1995).

A variation of the DSBR model, called the synthesis-dependent strand-annealing model (Figure 1.2B), has been proposed by a number of groups (Ferguson and Holloman, 1996; Nassif *et al.*, 1994; Paques *et al.*, 1998). In this model, strand invasion and DNA synthesis are initiated from one 3′ ssDNA end of the processed DSB. In this case, the D-loop is not extended but instead pushed along the DNA as repair synthesis occurs from the 3′ invading end. At this stage, strand annealing may occur between the newly-synthesised strand and the other 3′ end at the DSB (Figure 1.2B (v)). Alternatively, the second end may anneal to the D-loop to produce a pair of Holliday junctions (vi), that are subsequently resolved. It should be noted that in this and the DSBR model, the positions of the two Holliday junctions, and thus the nature of the recombinant products, can be altered by tandem branch migration (Fu *et al.*, 1994; Schwacha and Kleckner, 1995).

DAUGHTER-STRAND GAP REPAIR BY HOMOLOGOUS RECOMBINATION

UV-induced DNA lesions, such as pyrimidine dimers, are usually removed by a repair process called nucleotide excision repair (deLaat *et al.*, 1999; Jaspers and Hoeijmakers, 1995). In the 1960s, Howard-Flanders and colleagues examined the replicated DNA from excision-defective bacterial cells following UV treatment, and observed single-strand gaps in the nascent daughter strands (Howard-Flanders *et al.*, 1968; Rupp and Howard-Flanders, 1968). The postreplication gaps were thought to result from the DNA replication machinery stalling at each unexcised photoproduct in the template strand and then reinitiating downstream of the blocking lesion. As the UV-irradiated cells were incubated for increasing lengths of time, the daughter-strand gaps were

found to disappear. Furthermore, the cells exhibited an increased recombination frequency, suggesting a role for homologous recombination in the repair of these gaps (Howard-Flanders *et al.*, 1968; Rupp *et al.*, 1971). These studies led to the proposal of the so-called postreplicational repair model (described below). It should be noted that this pathway does not repair the primary DNA lesions themselves, but rather permits the cell to tolerate these lesions by repairing the gaps resulting from replication of the damaged templates. To make this distinction, the mechanism is more often termed 'daughter-strand gap repair' (Hanawalt *et al.*, 1979).

The model, shown in Figure 1.3, involves invasion of the daughter-strand gap with the undamaged sister strand of the homologous duplex molecule. This exchange is likely to require nicking of the transferred strand by an endonuclease (West *et al.*, 1981b; West *et al.*, 1982). Further strand exchange into the duplex region results in reciprocal exchange and the formation of a Holliday junction. This allows the daughter-strand gap to be filled by repair synthesis, using the intact homologue as a template. Finally, the Holliday intermediate is processed by branch migration and resolution into mature recombinant products. Following gap repair, the UV-induced lesion may be removed by an excision repair system (deLaat *et al.*, 1999; Jaspers and Hoeijmakers, 1995).

In some cases, a polymerase may be unable to reinitiate downstream of a lesion. A model for how DNA synthesis could continue past the lesion, in a continuous manner, has been proposed that involves the formation and branch migration of a Holliday junction intermediate. This is discussed in more detail in the next section (pp. 47).

FIGURE 1.3. MODEL FOR DAUGHTER-STRAND GAP REPAIR

Replication of UV-damaged DNA (i) results in a daughter-strand gap opposite the DNA lesion (pyrimidine dimer) (ii). A nick is introduced into the complementary strand of the intact sister duplex allowing strand transfer at the site of the gap (iii). Reciprocal strand exchange generates a Holliday junction (iv) and provides an intact template strand for repair of the daughter-strand gap by DNA synthesis (indicated by green dashed line) (v). Finally, branch migration and resolution of the junction results in mature products (vi). The initial parental strands are represented by blue solid lines and their daughter strands by blue dashed lines. Figure adapted from Friedberg *et al* (1995).

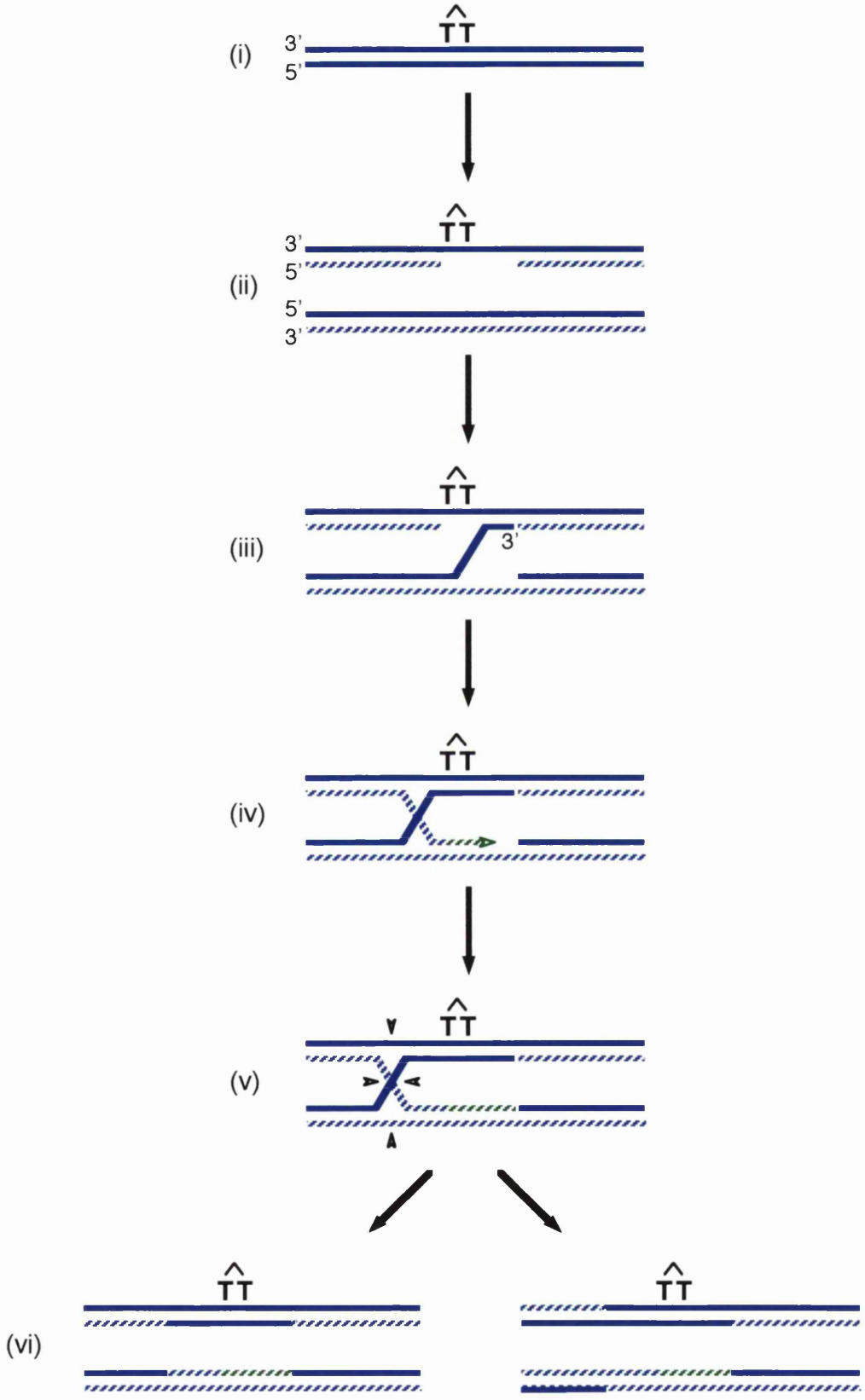

FIGURE 1.3

FORMATION OF HOLLIDAY JUNCTION INTERMEDIATES

E. coli RecA Protein

In *Escherichia coli*, efficient recombination requires the products of at least 15 genes, in addition to enzymes involved in general DNA metabolism such as DNA ligase (reviewed in Camerini-Otero and Hsieh, 1995; Clark and Sandler, 1994; Kowalczykowski *et al.*, 1994; Lloyd and Low, 1996). The most extensively characterised of these is the product of the *recA* gene. This gene was discovered in 1965, following the isolation of *E. coli* mutants that were defective in conjugational recombination and sensitive to UV-irradiation (Clark and Margulies, 1965). Furthermore, *recA*$^-$ mutants are sensitive to X-rays (Howard-Flanders and Theriot, 1966), and are unable to promote postreplicational repair thus accounting for the UV-sensitive phenotype (Clark and Margulies, 1965; Smith and Meun, 1970). This early genetic data thus indicated that the *recA* gene product is essential for genetic recombination and related DNA repair processes. This was later confirmed by extensive biochemical analysis of the RecA protein (38 kDa) showing that the protein promotes homologous pairing and strand exchange reactions between two DNA molecules, central processes in homologous recombination that generate the Holliday junction intermediate.

In order to assemble on duplex DNA, RecA requires a region of single-stranded DNA. The main pathway for DNA end-processing is mediated by the RecBCD complex, which catalyses the formation of 3′ single-stranded tails via its combined helicase and nuclease activities (reviewed in Eggleston and West, 1997). With the assistance of a number of accessory factors (e.g. SSB) (Cox *et al.*, 1983; Kowalczykowski and Krupp, 1987; Muniyappa *et al.*, 1984; Umezu *et al.*, 1993; Umezu and Kolodner, 1994), RecA cooperatively binds to the ssDNA to form a continuous filament that extends into the duplex region in a 5′ to 3′ direction (Cassuto and Howard-Flanders, 1986; Chiu *et al.*, 1990; Shaner and

Radding, 1987; West *et al.*, 1980). In an active nucleoprotein filament, which will only assemble in the presence of ATP, the DNA is underwound and stretched by a factor of approximately 1.5 compared to normal B-form DNA (DiCapua *et al.*, 1990; Egelman and Stasiak, 1986; Heuser and Griffith, 1989; Howard-Flanders *et al.*, 1984; Stasiak and DiCapua, 1982; Stasiak *et al.*, 1981; Yu and Egelman, 1992).

Once formed, the RecA-DNA filament conducts a rapid and efficient search for homologous DNA duplex sequences. Upon finding a match, homologous contacts are thought to be established between the duplex molecules (Cassuto *et al.*, 1982; Chiu *et al.*, 1990; Conley and West, 1989; Conley and West, 1990; West and Howard-Flanders, 1984). Strand exchange is then initiated at the ssDNA region by 3′ terminal end invasion to form a stable joint molecule (West *et al.*, 1981a; West *et al.*, 1982). The 3′ end is more invasive than the 5′ end because RecA polymerises along ssDNA with a 5′ to 3′ polarity; thus, since initial binding is random, the 3′ end is more likely to be coated with protein (Konforti and Davis, 1992; Register and Griffith, 1985). Further strand exchange into the duplex region results in pairing of the complementary strand of the invading molecule with the displaced strand of the homologous duplex. This exchange is reciprocal and gives rise to a Holliday junction intermediate (DasGupta *et al.*, 1981; Müller *et al.*, 1992; West *et al.*, 1983).

RecA protein is a DNA-dependent ATPase (Ogawa *et al.*, 1979; Roberts *et al.*, 1979). However, experiments conducted in the presence of ATPγS or ADP.AlF_4^-, which mimics the transition state in ATP hydrolysis, have shown that RecA-mediated strand exchange occurs in the absence of ATP hydrolysis (Kowalczykowski and Krupp, 1995; Menetski *et al.*, 1990; Rosselli and Stasiak, 1990). Furthermore, a mutant RecA protein ($RecA^{K72R}$) that binds but does not hydrolyse ATP is able to form joint molecules (Rehrauer and Kowalczykowski,

1993). These exchange reactions, however, were conducted between ssDNA and duplex DNA (3-strand reaction). In contrast, ATP hydrolysis is essential for the reciprocal exchange between two duplexes (4-strand reaction) described in the previous paragraph (Kim *et al.*, 1992b; Shan *et al.*, 1996). In addition, it is absolutely required for the bypass of short heterologous insertions or other structural barriers in both the 3-strand and 4-strand reactions (Kim *et al.*, 1992a; Rosselli and Stasiak, 1991; Shan *et al.*, 1996). So what is the role of ATP hydrolysis in these exchange reactions?

A number of groups have proposed a facilitated DNA rotation model in which RecA acts as an ATP-driven motor, using the energy from ATP hydrolysis to rotate the DNA substrates about each other within the nucleoprotein filament (Bedale and Cox, 1996; Cox, 1994; MacFarland *et al.*, 1997; Shan and Cox, 1997; Shan *et al.*, 1996). In the 4-strand reaction, DNA rotation within the filament would generate torsional stress in the 'incoming' homologous duplexes and may result in their transient unwinding, thereby allowing reciprocal strand exchange to occur (MacFarland *et al.*, 1997). This ATP-coupled mechanism would be consistent with the observation that the bypass of heterology involves the unwinding of heterologous inserts in the duplex DNA through torsional stress (Jwang and Radding, 1992), and would also explain the requirement for ATP hydrolysis in these reactions (Kim *et al.*, 1992a; Rosselli and Stasiak, 1991). In a recent study, a mutant RecA protein ($RecA^{S69G}$) was described that hydrolysed various nucleotide cofactors at different rates (Nayak and Bryant, 1999). Significantly, the rate of strand exchange was found to be directly proportional to the rate of hydrolysis, thereby supporting a mechanism, such as the facilitated rotation model, in which strand exchange is coupled to ATP hydrolysis. A model for RecA-mediated strand exchange is shown in Figure 1.4.

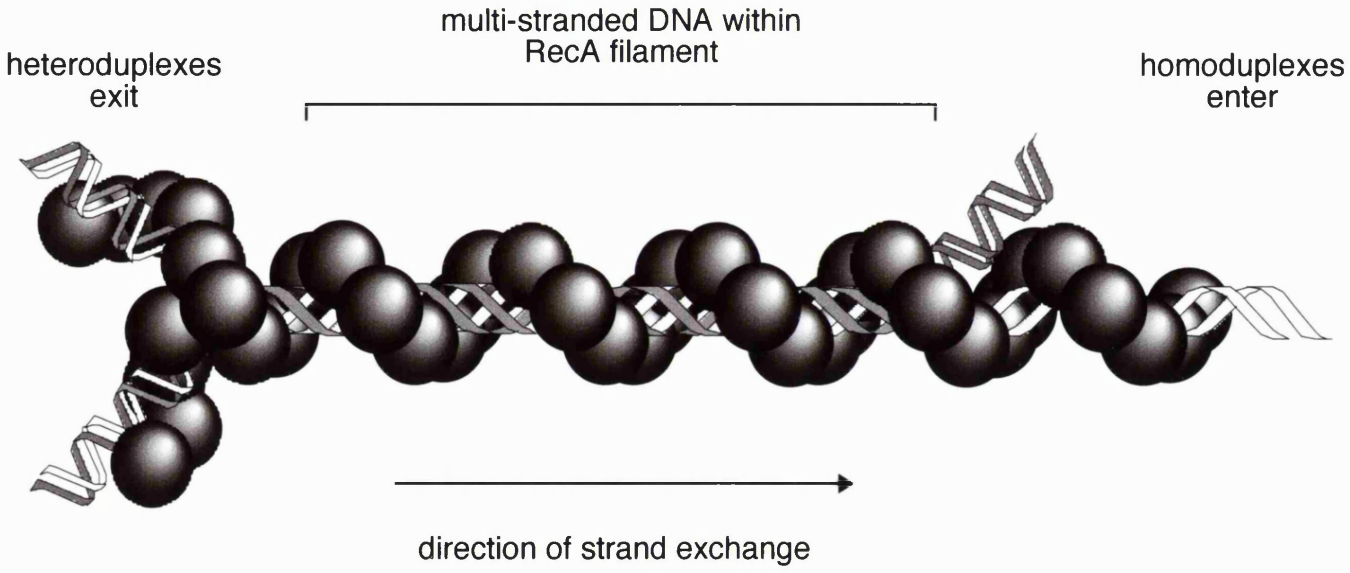

FIGURE 1.4. RECA-MEDIATED STRAND EXCHANGE

RecA promotes strand exchange between two homologous duplexes, which are proposed to become interwound within the RecA nucleoprotein filament. Rotation of the DNA in the filament is thought to unwind the incoming homoduplexes allowing strand exchange to occur. The heteroduplexes formed are then spooled out further along the filament. Deproteinisation of the intermediate would produce a classical Holliday junction. Figure adapted from Adams and West (1995a) and Müller *et al* (1992).

In addition to its crucial role in homologous recombination, RecA also plays a central role in the induction of the SOS response to DNA damage by catalysing the autodigestion of the LexA repressor protein (Little, 1984; Little *et al.*, 1980). LexA cleavage results in the transcriptional derepression of approximately 20 genes, most of which are involved in DNA repair (Little and Mount, 1982).

Eukaryotic Homologues of RecA

In recent years, a number of homologues of the *E. coli* RecA protein have been identified in eukaryotes as well as in bacteriophage (Yonesaki and Minagawa, 1985; Yu and Egelman, 1993), Archaea (Sandler *et al.*, 1996; Seitz *et al.*, 1998), and other eubacteria (Karlin and Brocchieri, 1996; Karlin *et al.*, 1995), indicating that at least some of the fundamental steps of homologous recombination and recombinational repair may have been conserved throughout evolution. In the yeast *Saccharomyces cerevisiae*, four proteins with sequence homology to RecA have been identified: Rad51, Rad55, Rad57 and Dmc1 (Aboussekhra *et al.*, 1992; Basile *et al.*, 1992; Bishop *et al.*, 1992; Kans and Mortimer, 1991; Lovett, 1994; Shinohara *et al.*, 1992). Yeast *rad51*, *rad55* and *rad57* mutants display pleiotropic phenotypes, including defects in DSB repair and meiotic recombination (Game, 1993; Petes *et al.*, 1991; Shinohara *et al.*, 1992). In addition, mutations in *RAD51* give rise to defects in mitotic recombination (Petes *et al.*, 1991). In contrast, *ScDmc1* mutants are defective in exclusively meiotic functions (Bishop *et al.*, 1992; Rockmill *et al.*, 1995).

*Sc*Rad51 shows the most striking homology with RecA, sharing a 33% sequence identity over a 207-amino acid core domain. Furthermore, functional similarities have been observed between the two proteins (reviewed in Bianco *et al.*, 1998). *Sc*Rad51 forms nucleoprotein filaments similar to those of RecA

(Ogawa *et al.*, 1993), and catalyses homologous pairing and strand exchange (Sung, 1994; Sung and Robberson, 1995). Homologues of Rad51 have been identified in a wide range of higher eukaryotes, including lily (Terasawa *et al.*, 1995), *Xenopus laevis* (Maeshima *et al.*, 1995) and humans (Shinohara *et al.*, 1993; Yoshimura *et al.*, 1993). Biochemical analysis has shown that both *X*Rad51 and *h*Rad51 promote strand exchange reactions (Baumann *et al.*, 1996; Maeshima *et al.*, 1996). In addition, eukaryotic homologues of *Sc*Dmc1 have been identified in humans (Habu *et al.*, 1996; Li *et al.*, 1997; Masson *et al.*, 1999; Passy *et al.*, 1999), mouse (Habu *et al.*, 1996; Yoshida *et al.*, 1998) and *Arabidopsis thaliana* (Doutriaux *et al.*, 1998).

In the past few years, a further five human *RAD51*-like genes have been identified (reviewed in Thacker, 1999): *RAD51B* (also known as *RAD51L1/hREC2/R51H2*), *RAD51C* (*RAD51L2*), *RAD51D* (*RAD51L3/R51H3*), *XRCC2* and *XRCC3* (Albala *et al.*, 1997; Cartwright *et al.*, 1998a; Cartwright *et al.*, 1998b; Dosanjh *et al.*, 1998; Liu *et al.*, 1998; Pittman *et al.*, 1998; Rice *et al.*, 1997; Tambini *et al.*, 1997). The role of the products of these genes is not clear at present, although it has been suggested that they may be functional homologues of the yeast Rad55 and Rad57 proteins (Dosanjh *et al.*, 1998; Jeanmougin *et al.*, 1998; Liu *et al.*, 1998).

II. STRUCTURE AND MANIPULATION OF THE HOLLIDAY JUNCTION

As highlighted in the last section, the Holliday junction is the central intermediate in homologous recombination and in a number of recombinational repair pathways, and arises from the reciprocal exchange of single strands between two homologous DNA duplexes. In this section, I will describe the

structure of the Holliday junction and the proteins that recognise and process this intermediate during the late stages of recombination in *E. coli*.

VISUALISATION AND STRUCTURE OF THE HOLLIDAY JUNCTION

Direct evidence for the existence of the Holliday junction has been obtained by electron microscopy. Potter and Dressler (1976) isolated DNA of the ColE1 plasmid from *E. coli* and observed dimer-sized 'figure-8' molecules. Although such structures could theoretically arise from the mere interlocking of two monomeric circles, digestion of the figure-8 species with a unique-site restriction enzyme generated 4-armed 'chi' (χ) structures, indicating that the pairs of plasmids were covalently-linked. Since figure-8 and chi structures were not obtained from *recA*$^-$ strains, they most likely represent Holliday junction intermediates of recombination (Potter and Dressler, 1976). Figure-8 structures were also observed in yeast (Bell and Byers, 1979) and in viral DNA isolated from *E. coli*, including ΦX174 and λ DNA (Benbow *et al.*, 1975; Doniger *et al.*, 1973; Thompson *et al.*, 1975; Valenzuela and Inman, 1975). More recently, recombination intermediates generated *in vitro* using purified RecA protein have been visualised by electron microscopy (DasGupta *et al.*, 1981; Müller *et al.*, 1992; West *et al.*, 1983).

Initial efforts to deduce the structure of the Holliday junction employed a range of techniques, including gel electrophoresis (Cooper and Hagerman, 1987; Duckett *et al.*, 1988), chemical probing (Churchill *et al.*, 1988) and fluorescence resonance energy transfer (Murchie *et al.*, 1989). Naturally-occurring recombination intermediates are inherently unstable due to internal sequence symmetry that allows them, under certain *in vitro* conditions, to undergo spontaneous branch migration (see next section). Therefore, these studies made use of small synthetic Holliday junctions produced by annealing

four oligonucleotides. Synthetic junctions can be designed that lack homology (i.e. such that any movement of the crossover point would result in mismatched bases); these junctions are immobile and therefore stable (Kallenbach *et al.*, 1983).

Ten years ago, Lilley and coworkers proposed the 'stacked X-structure' for the Holliday junction (Duckett *et al.*, 1988; Murchie *et al.*, 1989). The structure is two-fold symmetric with the four helical arms of the junction stacked in pairs, as depicted in Figure 1.5A (Churchill *et al.*, 1988; Duckett *et al.*, 1988; Murchie *et al.*, 1989). The junction consists of two 'continuous strands' that are anti-parallel and cross at the junction point (subtending an angle of ~60°), and two 'exchanging strands' that pass between the stacked helical pairs at the point of strand exchange. It should be noted that in models for recombination pathways, such as those shown in Figures 1.1-1.3, the Holliday junction intermediate is usually drawn with the continuous (non-exchanging) strands in a parallel orientation for simplicity.

Confirmation of the stacked X-structure awaited a crystal structure of the Holliday junction which was finally obtained this year (Ortiz-Lombardia *et al.*, 1999). The structure closely corresponds to that proposed by Lilley and his group, the main difference being that the acute angle between the helical axes is 40° as opposed to 60°. The crystal structure is shown in Figure 1.5B in side view, i.e. looking directly into the major groove side of the stacked X-structure depicted in Figure 1.5A. The junction contained two pairs of G-A mismatches flanking the crossover point and, as a result, minor distortion of the DNA helices can be observed at these positions.

The structure of the Holliday junction, described above, is in the presence of divalent cations. In the absence of cations, the Holliday junction unfolds into an open four-fold symmetric structure in which the helical arms

FIGURE 1.5. RIBBON DIAGRAMS TO SHOW THE PROPOSED AND ACTUAL STRUCTURE OF THE HOLLIDAY JUNCTION

A. The 'stacked X-structure' originally proposed, based on electrophoretic studies. The junction is shown in face view. The 'continuous strands' (indicated by yellow asterisks) are anti-parallel and cross over each other at the junction point, whilst the 'exchanging strands' pass from one stacked helical pair to the other without crossing. Clegg *et al* (1994).

B. Crystal structure of a synthetic Holliday junction as observed from the major groove side, i.e. from the left side of the junction in A (in the plane of the paper). The DNA is distorted as a result of two pairs of G-A mismatches, at the positions indicated by arrows. Reproduced from Ortiz-Lombardía *et al* (1999).

C. Effect of divalent cations on the structure of the Holliday junction. The structures shown in A and B are in the presence of divalent cations (e.g. Mg^{2+}). In their absence, the junction adopts an 'open square' conformation with four-fold symmetry. Adapted from Clegg *et al* (1994).

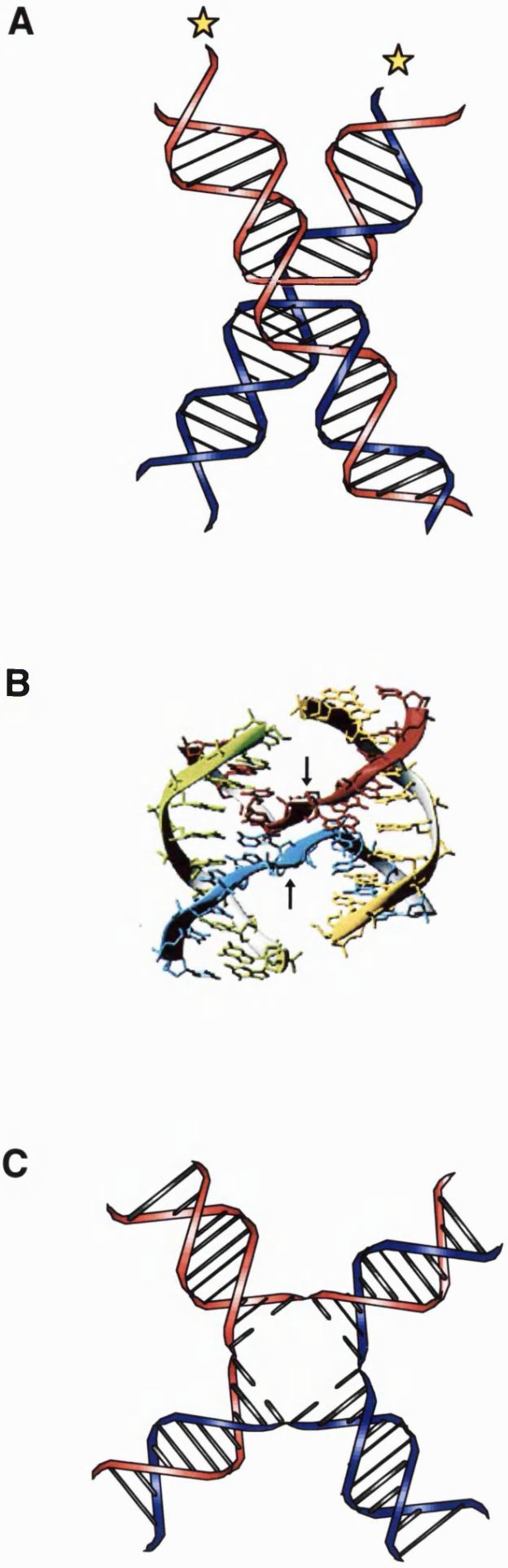

FIGURE 1.5

are unstacked and extended towards the four corners of a square (Figure 1.5C) (Duckett *et al.*, 1988; Duckett *et al.*, 1990). However, it was shown that folding occurs at Mg^{2+} concentrations of ≥ 100 μM, indicating that Holliday junctions most likely exist in the stacked X form under physiological conditions (Duckett *et al.*, 1990). The Mg^{2+} ions are thought to stabilise the folded structure by binding close to the crossover point and shielding the negatively charged phosphate groups that are in close proximity to each other (Duckett *et al.*, 1990; Møllegaard *et al.*, 1994).

SPONTANEOUS BRANCH MIGRATION OF THE HOLLIDAY JUNCTION

Movement of the Holliday junction, by the process of branch migration, is an important step in homologous recombination and results in the exchange of DNA strands between the recombining molecules. Where recombination occurs between two similar but not identical duplexes, this process results in the formation and extension of heteroduplex DNA. Theoretically, branch migration between homologous sequences is an isoenergetic process in which the breakage of hydrogen bonds is balanced by their reformation. Thus branch migration was initially believed to occur spontaneously, by a random walk process (Thompson *et al.*, 1976). However, more recently, spontaneous branch migration in the presence of Mg^{2+} was found to be too slow to account for genetic recombination where strand exchange occurs over long regions (Panyutin and Hsieh, 1994). Furthermore, branch migration in Mg^{2+} is blocked by a single base mismatch (Panyutin and Hsieh, 1993).

In the absence of Mg^{2+}, the rate of spontaneous branch migration is approximately 1000-fold faster than in the presence of divalent cations (Panyutin and Hsieh, 1994). This difference in rate is thought to relate to changes in the conformation of the Holliday junction that are known to occur

under different ionic conditions (described in the previous section). Indeed when branch migration assays were conducted in the presence of decreasing Mg^{2+} concentrations, a dramatic increase in the rate of spontaneous branch migration was observed at ~100 μM Mg^{2+} which coincided with the loss of base stacking across the four-way junction (Panyutin *et al.*, 1995).

Collectively, these studies indicate that both DNA mismatches and base stacking at the crossover present kinetic barriers to spontaneous branch migration (Panyutin *et al.*, 1995; Panyutin and Hsieh, 1993; Panyutin and Hsieh, 1994). Therefore, since Holliday junctions adopt a stacked X-structure at physiological concentrations of Mg^{2+} and are likely to encounter mismatches, insertions and deletions *in vivo*, proteins must be recruited in the cell to promote the process of branch migration.

RecA-Mediated Branch Migration

Following joint molecule formation by RecA-mediated strand exchange, the reaction may proceed into a kinetically-distinct branch migration phase (Cox and Lehman, 1981b). Branch migration catalysed by RecA protein is unidirectional, proceeding with 5′ to 3′ polarity relative to the single strand on which filament formation was initiated, and requires ATP hydrolysis (Cox and Lehman, 1981a; Cox and Lehman, 1981b; Kahn *et al.*, 1981; Schutte and Cox, 1987; West *et al.*, 1981a; West *et al.*, 1982). In four-strand reactions, movement of the Holliday junction is slow, occurring at a rate of ~3 bp/sec (West, 1992). Furthermore, RecA-mediated branch migration is blocked by insertions and deletions of ≥120 bp (Hahn *et al.*, 1988). This sluggish rate and poor heterology bypass indicate that RecA is not the major protein responsible for branch migration *in vivo*. Indeed, other proteins in *E. coli* that promote this reaction

more efficiently have now been identified; these are the RuvAB and RecG proteins.

RUVAB-MEDIATED BRANCH MIGRATION

Among the proteins known to act in the late stages of genetic recombination are those encoded by the *ruv* locus, i.e. products of the *ruvA*, *ruvB* and *ruvC* genes (Benson *et al.*, 1991; reviewed in West, 1997). Cells carrying *ruv* mutations are sensitive to UV light, ionising radiation and mitomycin C, and form long non-septate filaments after treatment with these DNA-damaging agents (Lloyd *et al.*, 1984; Otsuji *et al.*, 1974; Sharples *et al.*, 1990). Surprisingly, mutations in *ruv* only result in a mild defect in conjugational recombination (<2.5-fold) (Lloyd and Buckman, 1991). In combination with *recG* mutations, however, *ruv* mutants become severely defective (>100-fold), indicating an overlap in the function of these gene products (see pp. 50).

The *ruv* locus, which maps at minute 41 on the *E. coli* chromosome, consists of two operons: *orf26-ruvC* and *ruvA-ruvB* (Sharples *et al.*, 1990; Sharples and Lloyd, 1991; Shinagawa *et al.*, 1988; Takahagi *et al.*, 1991). The latter operon is regulated by the LexA repressor protein and the gene products, RuvA and RuvB, are induced as part of the SOS response to DNA damage (Benson *et al.*, 1988; Shinagawa *et al.*, 1988; Shurvinton and Lloyd, 1982). The RuvA and RuvB proteins have been shown to act together *in vitro* to promote the branch migration of Holliday junctions (Iwasaki *et al.*, 1992; Mitchell and West, 1996; Müller *et al.*, 1993a; Parsons *et al.*, 1992; Parsons and West, 1993; Tsaneva *et al.*, 1992b). In contrast to the RecA-mediated reaction, branch migration catalysed by RuvAB is bidirectional and rapid (Iwasaki *et al.*, 1992; Tsaneva *et al.*, 1992b), and is able to bypass heterologous inserts of >1 kbp, in 3-strand reactions, or up to 300 bp, in 4-strand reactions (Adams and West, 1996;

Iype *et al.*, 1994). Moreover, using χ-shaped plasmid molecules, RuvAB have been shown to drive branch migration through 1800 bp of heterology in a reaction facilitated by the presence of single-stranded binding protein (SSB) (Parsons *et al.*, 1995b).

Properties of RuvA

RuvA is a 22 kDa DNA binding protein that exhibits a high affinity for Holliday junctions (Iwasaki *et al.*, 1992; Parsons *et al.*, 1992; Shiba *et al.*, 1991). RuvA interacts with RuvB and is thought to act as a specificity factor for targeting RuvB to the junction (Hiom and West, 1995b; Iwasaki *et al.*, 1992; Parsons *et al.*, 1992; Parsons and West, 1993; Shiba *et al.*, 1993). Gel filtration studies have shown that RuvA forms stable tetramers in solution (Shiba *et al.*, 1993; Tsaneva *et al.*, 1992a) and this has been confirmed more recently by X-ray crystallography (Hargreaves *et al.*, 1998; Rafferty *et al.*, 1996).

The structure of RuvA was first solved in the absence of DNA, at a resolution of 1.9 Å, and consists of four RuvA subunits that are related by four-fold symmetry (Rafferty *et al.*, 1996). The two faces of the tetramer exhibit different properties; one is convex and predominantly negatively charged, whilst the other is concave, more highly conserved and largely positively charged. By modelling a Holliday junction onto the RuvA tetramer, it was proposed that the four DNA duplex arms lie in positively charged grooves on the concave surface of the protein (Rafferty *et al.*, 1996). Using band-shift assays (Parsons *et al.*, 1995a), it was proposed that RuvA unfolds and traps the junction in an open-square planar configuration that is more energetically favourable for branch migration (Panyutin *et al.*, 1995; Figure 1.6). Furthermore, four 'acidic pins' were identified on the concave face, each composed of the conserved Glu55 and Asp56 residues. These pins are located in the grooves near the centre

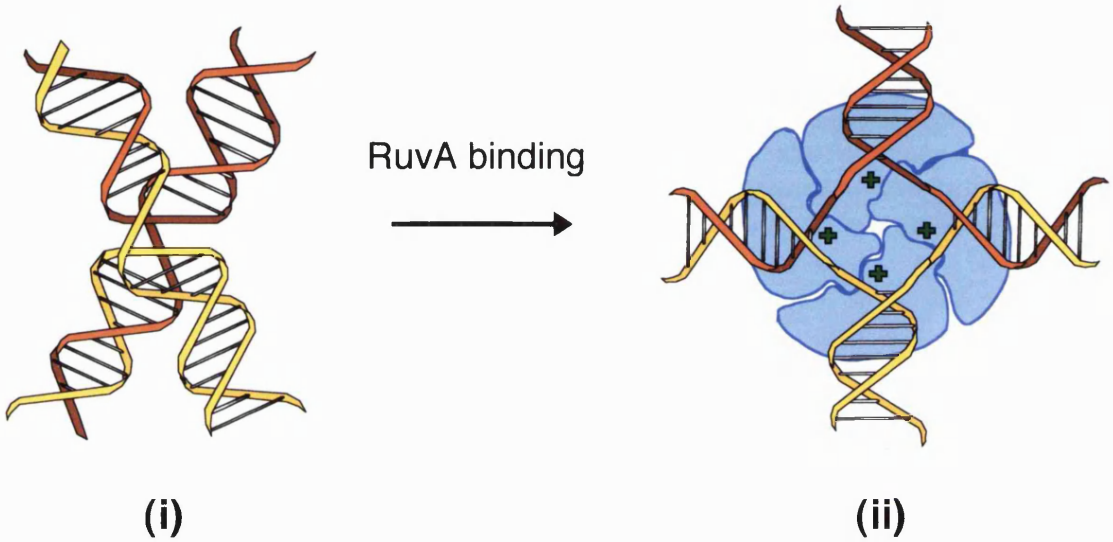

FIGURE 1.6. STRUCTURAL CHANGES TO THE HOLLIDAY JUNCTION UPON FORMATION OF A RUVA-JUNCTION COMPLEX

In the presence of physiological concentrations of metal ions, the junction adopts a stacked X-structure (i). The coaxial stacking interactions in this structure present a kinetic barrier for branch migration. Upon binding of a RuvA tetramer, however, the junction is unfolded into a four-fold symmetric open-square structure (ii) similar to the unfolded protein-free junction observed in the absence of cations (Figure 1.5C). The four acidic pins in the RuvA tetramer (indicated by green crosses) facilitate DNA strand separation at the crossover. Figure adapted from West (1997).

of the RuvA tetramer (Figure 1.6), and are thought to facilitate separation of the DNA duplexes during branch migration (Rafferty *et al.*, 1996).

The structure of a RuvA-junction complex was recently solved at 6 Å resolution (Hargreaves *et al.*, 1998). As predicted by the modelling studies (Rafferty *et al.*, 1996) and band-shift assays (Parsons *et al.*, 1995a), the junction arms lie in the positively charged grooves on the concave face of the RuvA tetramer and adopt an open-square conformation. The junction was not strictly planar, however, but depressed slightly towards the centre of the RuvA tetramer resulting in a shallow pyramidal arrangement (Hargreaves *et al.*, 1998). The RuvA-junction structure further revealed that RuvA interacts with the side of the junction containing its major groove at the crossover point.

Although the crystal structure of the *E. coli* RuvA-junction complex contains only one RuvA tetramer, band-shift assays have indicated that a Holliday junction may be bound by one or two tetramers of RuvA, depending on the protein concentration (Parsons *et al.*, 1992). Moreover, analysis of *Mycobacterium leprae* RuvA, using X-ray crystallography and neutron scattering techniques, have shown that the junction is sandwiched between two RuvA tetramers that bind to opposite faces of the DNA (Chamberlain *et al.*, 1998; Roe *et al.*, 1998). It has been suggested that both the tetrameric and octameric forms have biological relevance (West, 1998). Binding of a single RuvA tetramer to one face of a Holliday junction would leave the other face accessible for interaction with RuvC (Whitby *et al.*, 1996), resulting in a RuvABC complex that is capable of both branch migration and resolution (see pp. 54). In contrast, a RuvAB complex containing two tetramers of RuvA would be specifically active in branch migration.

Properties of RuvB

The RuvB protein (37 kDa) is a DNA-dependent ATPase whose activity is stimulated by RuvA (Iwasaki *et al.*, 1989a; Shiba *et al.*, 1991; Shinagawa *et al.*, 1991). RuvB is thought to be the motor for driving branch migration, a notion supported by the observation that saturating amounts of RuvB can catalyse the reaction in the absence of RuvA (Mitchell and West, 1996; Müller *et al.*, 1993a; Tsaneva *et al.*, 1992b). The RuvB-mediated reaction also requires high levels of Mg^{2+} to overcome the low binding affinity that RuvB shows for DNA (Müller *et al.*, 1993b).

Gel filtration studies indicate that the quaternary state of RuvB in solution varies greatly depending on the protein concentration and buffer conditions. In the absence of metal ions, RuvB forms dimers or tetramers in a concentration-dependent manner (Mitchell and West, 1994; Shiba *et al.*, 1993; Tsaneva *et al.*, 1992a). In the presence of Mg^{2+} and ATP or ATPγS, however, hexamers or a mixture of hexamers and dodecamers were detected, respectively (Mitchell and West, 1994). RuvB-dsDNA complexes, formed in the presence of Mg^{2+} and ATPγS, were visualised by electron microscopy and found to consist of double hexameric rings that encircle the duplex DNA (Stasiak *et al.*, 1994). Image reconstruction of the RuvB dodecamer indicated that each hexamer was composed of a large and small tier and possessed a central hollow through which the DNA passed. The hexamer, which may be composed of a trimer of dimers, is thought to be the functionally active form of the protein (Mitchell and West, 1994; Parsons *et al.*, 1995a).

Sequence comparisons indicate that DNA and RNA helicases contain seven conserved motifs (Gorbalenya and Koonin, 1993; Gorbalenya *et al.*, 1989), motifs I and II of which correspond to the NTP binding Walker A and B boxes (Walker *et al.*, 1982). Six of the seven helicase motifs have been identified in

FIGURE 1.7. ALIGNMENT OF THE *E. COLI* RUVB SEQUENCE WITH TWELVE BACTERIAL HOMOLOGUES, SHOWING THE CONSERVED HELICASE MOTIFS

RuvB homologues from *Mycobacterium leprae* (Smith *et al.*, 1997), *Mycobacterium tuberculosis* (Cole *et al.*, 1998), *Haemophilus influenzae* (Fleischmann *et al.*, 1995), *Pseudomonas aeruginosa* (Hishida *et al.*, 1996), *Thermus thermophilus* (Tong and Wetmur, 1996), *Thermotoga maritima* (Tong and Wetmur, 1996), *Synechocystis sp* (Kaneko *et al.*, 1995), *Mycoplasma genitalium* (Fraser *et al.*, 1995), *Mycoplasma pneumoniae* (Himmelreich *et al.*, 1996), *Bacillus subtilis* (Swiss-Prot database accession number O32055), *Helicobacter pylori* (Tomb *et al.*, 1997) and *Borrelia burgdorferi* (accession number P70828) were aligned with the *E. coli* sequence using PileUp (Wisconsin Package Version 10.0, Genetics Computer Group, Madison, Wisc.). Identical and similar amino acids are boxed in black and grey, respectively. Helicase motifs I - VI are indicated above the alignment by a solid or dashed red line, representing highly and poorly conserved motifs, respectively.

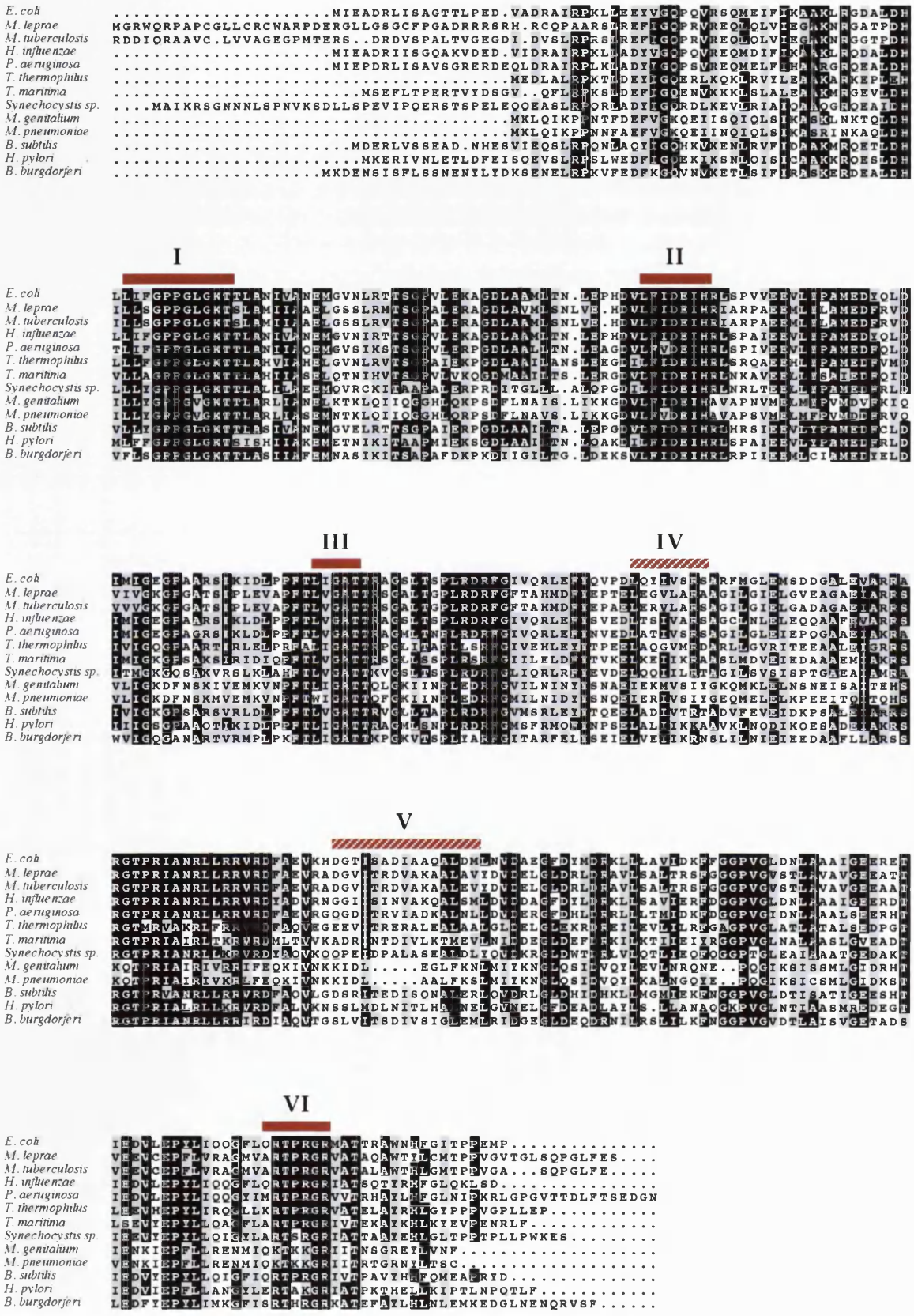
E. coli
M. leprae
M. tuberculosis
H. influenzae
P. aeruginosa
T. thermophilus
T. maritima
Synechocystis sp.
M. genitalium
M. pneumoniae
B. subtilis
H. pylori
B. burgdorferi
I
II
III
IV
V
VI

FIGURE 1.7

RuvB (Figure 1.7); motifs I, II, III and VI are well conserved between *E. coli* RuvB and other bacterial homologues, whilst motifs IV and V are poorly conserved in RuvB and correlate weakly with the original motifs defined by Gorbalenya *et al.* (1989, 1993). Using standard DNA helicase substrates (i.e. a single-stranded DNA circle carrying a short annealed fragment), RuvB together with RuvA was shown to possess a 5′ to 3′ DNA helicase activity that is capable of unwinding up to 558 bp in length (Tsaneva *et al.*, 1993). The helicase activity, which is ATP-dependent, has an absolute requirement for RuvA and can be specifically targeted to Holliday junctions (Tsaneva *et al.*, 1993; Tsaneva and West, 1994). In addition, RuvAB can transiently unwind covalently closed circular duplex DNA, although this reaction also occurs to a limited extent in the presence of RuvB alone (Adams and West, 1995b).

In recent years, a number of other helicases that form hexameric rings have been identified, including the replicative DNA helicases *E. coli* DnaB (Bujalowski *et al.*, 1994; Reha-Kranz and Hurwitz, 1978; Yu *et al.*, 1996c) and bacteriophage T7 gene 4 protein (Egelman *et al.*, 1995; Patel and Hingorani, 1993). The structural similarities between RuvB and the other hexameric ring proteins, and its mechanistic implications are discussed in section III (pp. 61).

Formation of a RuvAB-Holliday Junction Complex

RuvAB-Holliday junction complexes, formed in the presence of Mg^{2+} and ATPγS, have been studied by band-shift assays (Parsons and West, 1993) and, more recently, by glycerol gradient centrifugation, DNase I footprinting (Hiom and West, 1995b) and electron microscopy (Parsons *et al.*, 1995a). In the latter case, a tripartite complex was observed in which RuvA binds the crossover and is flanked on either side by a RuvB hexameric ring (Figure 1.8A). The two RuvB rings are 'threaded' on opposite arms of the junction and are oriented in a

FIGURE 1.8. FORMATION OF A RUVAB-HOLLIDAY JUNCTION COMPLEX

A. Visualisation of a tripartite RuvAB-Holliday junction complex by electron microscopy. Image taken from Parsons *et al* (1995a).

B. Model for the RuvAB-Holliday junction complex. The RuvA tetramer binds the crossover with the junction arms in an open square configuration and directs the assembly of two RuvB hexamers to opposite arms of the junction. The RuvB rings are oppositely oriented. Branch migration occurs as the DNA is pumped out through the central cavities of the RuvB rings in the directions indicated. The branch migration complex may contain two RuvA tetramers, one bound to each face of the junction, but only one tetramer is shown in this figure. The RuvB structure shown is hypothetical. This image was provided courtesy of P. Artymiuk (University of Sheffield).

A

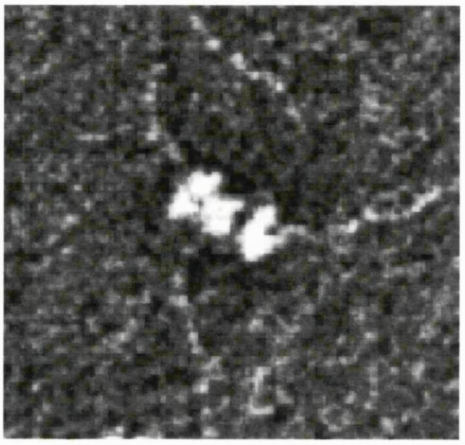

B

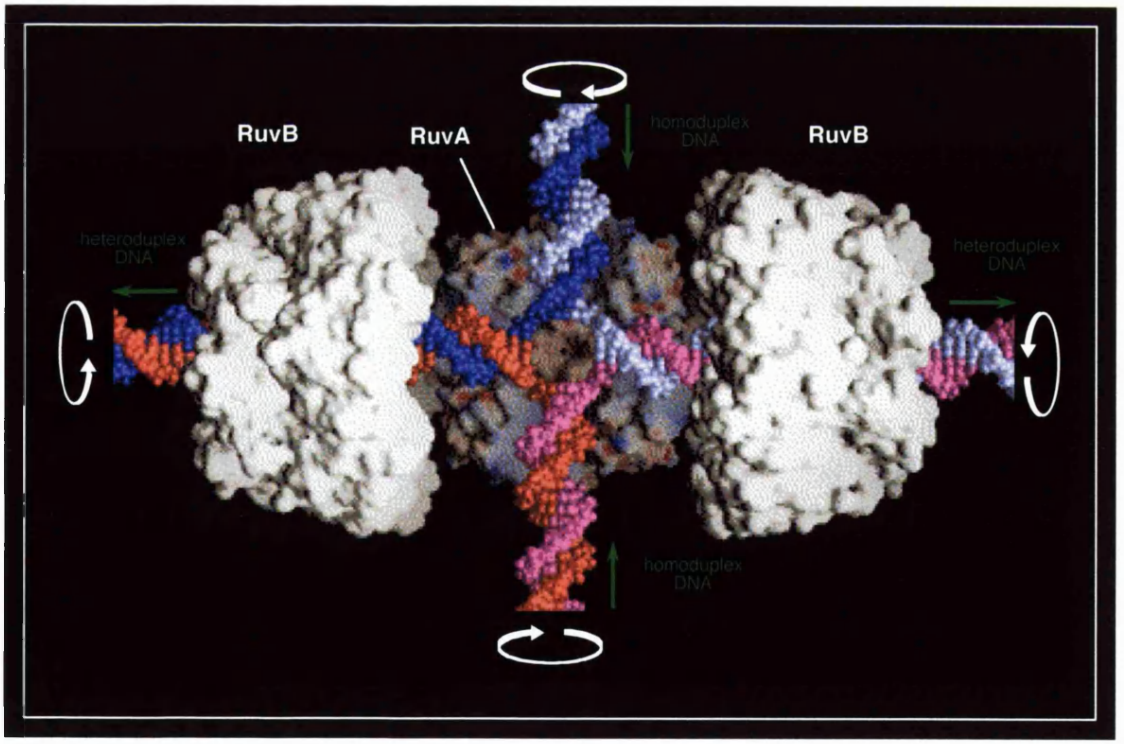
RuvB
RuvA
homoduplex DNA
RuvB
heteroduplex DNA
heteroduplex DNA
homoduplex DNA

FIGURE 1.8

bipolar manner, with their smaller, more convex, surfaces pointing outwards (Parsons *et al.*, 1995a; Yu *et al.*, 1997).

Mechanism of RuvAB-Mediated Branch Migration

Based on the tripartite RuvAB-junction complex observed by electron microscopy (Parsons *et al.*, 1995a), and on the crystallographic structure of RuvA (Hargreaves *et al.*, 1998; Rafferty *et al.*, 1996), a model for the structure of the RuvAB-junction complex has been proposed (Figure 1.8B). Catalysis of branch migration by RuvAB requires ATP hydrolysis, which is provided by the RuvB ATPase activity. The two opposing RuvB rings are thought to exert equal and opposite forces on the DNA (Parsons *et al.*, 1995a). However, because the rings are tethered by RuvA, simple translocation along the DNA is restricted. Consequently the DNA is drawn into the RuvAB complex and pumped out through the centre of each hexameric ring, as shown in Figure 1.8B. The net motion of DNA through the RuvAB complex, driven by the twin RuvB 'molecular pump', results in branch migration.

At present, the precise mechanism of RuvAB-mediated branch migration is poorly understood. Because RuvB possesses conserved helicase motifs and exhibits *in vitro* DNA helicase activity in the presence of RuvA, it has been suggested that ATP-dependent DNA unwinding by RuvB is an essential step in the mechanism of branch migration (Adams and West, 1995b; Tsaneva *et al.*, 1993). However, the RuvB hexamers sit on the 'outgoing' arms of the junction (Hiom *et al.*, 1996; Hiom and West, 1995a). Therefore, strand separation and exchange have already occurred before the DNA enters the RuvB rings, thereby questioning the need for DNA unwinding by RuvB.

RuvA plays an important role in branch migration, both by directing RuvB to the Holliday junction (Parsons and West, 1993), and during catalysis,

by holding the junction in an unfolded configuration that facilitates its movement (Parsons *et al.*, 1995a). Furthermore, as DNA passes into the RuvAB complex, the four acidic pins located near the centre of the RuvA tetramer are thought to facilitate separation of the DNA strands as they pass from one helical axis to the other (Hargreaves *et al.*, 1998; Rafferty *et al.*, 1996).

RuvB-Mediated Branch Migration

Previous studies with recombination intermediates made by RecA have shown that RuvB can promote branch migration in the absence of RuvA (Müller *et al.*, 1993a; Tsaneva *et al.*, 1992b). Unlike RuvAB-mediated branch migration, reactions catalysed by RuvB alone require saturating amounts of protein and elevated (≥15 mM) Mg^{2+} concentrations, and are highly sensitive to inhibition by NaCl, ADP and ATPγS (Mitchell and West, 1996). RuvB-mediated branch migration is likely to result from non-specific binding and translocation of the hexameric rings along DNA, and is unlikely to be relevant *in vivo*. Indeed, *ruvA* mutants exhibit a similar repair-defective phenotype to *ruvB* mutants (Lloyd *et al.*, 1984; Mandal *et al.*, 1993; Sharples *et al.*, 1990). Furthermore, *in vitro* studies have shown that both RuvA and RuvB are required to drive branch migration through heterology (Adams and West, 1996).

Dissociation of RecA by RuvAB

RecA filaments are stable and have been shown to remain associated with the Holliday junction following strand exchange *in vitro* (Pugh and Cox, 1987a; Pugh and Cox, 1987b; Shan and Cox, 1996). A number of studies suggest that, *in vivo*, RuvAB may dissociate RecA filaments from duplex DNA, thereby recycling RecA for subsequent strand exchange reactions (Adams *et al.*, 1994; Eggleston *et al.*, 1997). Certainly the addition of RuvAB to an ongoing RecA-

mediated strand exchange reaction results in rapid branch migration, suggesting that the specialised branch migration 'machinery' takes over from RecA (Eggleston *et al.*, 1997; Tsaneva *et al.*, 1992b). Similar reactions have been conducted in the presence of ATPγS at concentrations that stabilise the RecA-DNA filament and block strand exchange. Addition of RuvAB, which is less sensitive to ATPγS, resulted in branch migration through regions initially bound by RecA. This result strongly supports the active displacement of the RecA filament by RuvAB.

The Action of RuvAB at Stalled Replication Forks

Upon encountering a blocking lesion, such as a pyrimidine dimer, a DNA polymerase may pause and reinitiate downstream, giving rise to a daughter-strand gap that is repaired by homologous recombination (pp. 19). However, in some cases, the polymerase may stall at the lesion. A model for the rescue of arrested replication forks was originally proposed to account for replication repair in mammalian cells (Higgins *et al.*, 1976), and was later adapted by Echols and Goodman (1991). In the model, shown in Figure 1.9, leading strand synthesis is blocked by the lesion whilst lagging strand synthesis can progress further. It is proposed that the two newly synthesised strands anneal to form a Holliday junction that may be moved further away from the block by branch migration. Following repair synthesis, using the lagging strand as a template, a reverse branch migration reaction would resolve the junction, without the need for endonucleolytic cleavage, and provide a site for replication restart.

Recent work conducted by Michel and colleagues suggests that blocked replication forks in *E. coli* are processed by certain recombination proteins, including RuvAB which are thought to promote branch migration (Seigneur *et al.*, 1998). In contrast with daughter-strand gap repair, however, this pathway is

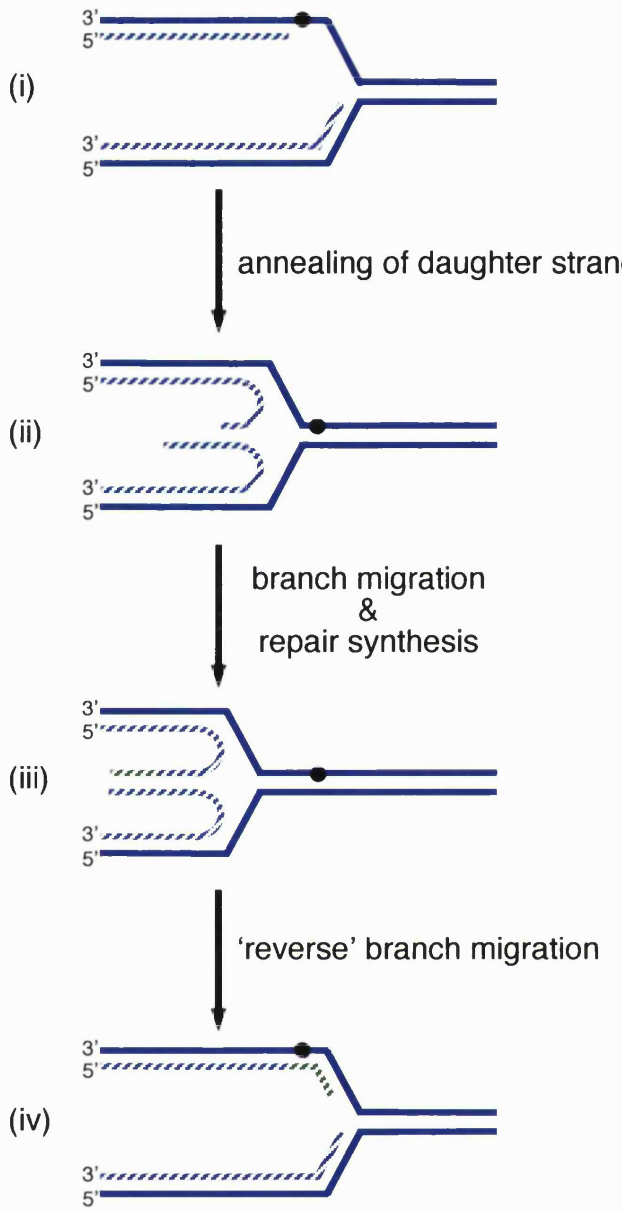

FIGURE 1.9. MODEL FOR THE RESCUE OF STALLED REPLICATION FORKS

Upon encountering a blocking lesion (●), leading strand synthesis is arrested whilst lagging strand synthesis progresses further (i). Annealing of the two daughter strands results in the formation of a Holliday junction (ii), which may be moved away from the lesion by branch migration (iii). The lagging strand provides a template for DNA synthesis from the 3′ end of the leading strand (indicated by a green dashed line) (iii). Finally, the junction is 'resolved' by branch migration in the reverse direction, allowing replication to resume beyond the lesion. Repair of the blocking lesion, by an excision repair pathway, can occur during step (iii) or (iv). The parental strands are represented by blue solid lines and their daughter strands by blue dashed lines. Figure adapted from Friedberg *et al* (1995)

not thought to involve the action of the RuvC resolvase (Seigneur *et al.*, 1998). Furthermore it does not involve the formation of postreplicational gaps; instead it allows DNA synthesis to occur past the lesion in a continuous manner (Friedberg *et al.*, 1995). Similar strand switching models have been proposed to account for error-prone translesion synthesis in *E. coli* (Koffel-Schwartz *et al.*, 1996), yeast (Torres-Ramos *et al.*, 1997) and mammalian cells (Cordeiro-Stone *et al.*, 1997).

Prokaryotic and Eukaryotic Homologues of RuvB

Homologues of *E. coli* RuvB have been identified in a wide range of other eubacteria, including both Gram-positive and Gram-negative species (see Figure 1.7). These bacterial homologues are highly conserved, particularly in the regions corresponding to the conserved helicase motifs. *Thermus thermophilus* RuvB, which is 56% identical and 88% similar to its *E. coli* counterpart, has been recently purified and was shown to promote ATP-dependent branch migration of Holliday junctions (Yamada *et al.*, 1999). Furthermore, the ATPase and branch migration activities of the protein were enhanced by *E. coli* RuvA, suggesting that the interaction between RuvA and RuvB is structurally and functionally conserved between these two bacterial species.

To date, no RuvB homologues have been identified in Archaea (Bult *et al.*, 1996). A putative rat RuvB homologue, TIP49a, has been reported (Kanemaki *et al.*, 1997), and homologues and related proteins have since been identified in a range of eukaryotes (Bauer *et al.*, 1998; Holzmann *et al.*, 1998; Kanemaki *et al.*, 1999; Kikuchi *et al.*, 1999; Qiu *et al.*, 1998). TIP49a (Kanemaki *et al.*, 1997), or p50 as it is also called (Kikuchi *et al.*, 1999), shares ~21% sequence identity with *Thermus thermophilus* RuvB and contains the Walker A and B

motifs (Walker *et al.*, 1982). However, at present there is no genetic or biochemical evidence to suggest that the TIP49a family of proteins are functional homologues of *E. coli* RuvB.

RecG-Mediated Branch Migration

The observation that mutations in *ruv* have only mild effects on conjugational recombination was initially surprising considering the key roles of the Ruv proteins in the processing of recombination intermediates. However, in combination with *recG* mutations, *ruv* mutants are severely defective in conjugational recombination (Lloyd and Buckman, 1991). Based on this genetic evidence, it was argued that the *ruv* and *recG* gene products provide alternative recombination pathways in wild-type cells. Indeed, biochemical studies have shown that the 76 kDa RecG protein binds specifically to Holliday junctions and promotes ATP-dependent branch migration (Lloyd and Sharples, 1993a; Lloyd and Sharples, 1993b; Sharples *et al.*, 1994b; Whitby *et al.*, 1993). Furthermore, RecG contains conserved helicase motifs and possesses DNA helicase activity, although with opposite polarity (3′ to 5′) to RuvAB (Lloyd and Sharples, 1993b; Whitby *et al.*, 1994)

However, despite the ability of both RuvAB and RecG to promote branch migration, there is growing evidence that the proteins have quite distinct cellular roles. For example, RecG is unable to complement the UV-sensitive phenotype of *ruv* mutants, indicating that the functional overlap between the RuvAB and RecG systems does not extend to recombinational repair (Lloyd, 1991). Furthermore, mutations in *recG*, but not those in *ruvA* or *ruvB*, affect constitutive stable DNA replication (cSDR) (Hong *et al.*, 1995). cSDR is a form of chromosomal replication that is primed by RNA-DNA hybrids, called R-loops, at non-*oriC* initiation sites (Asai and Kogoma, 1994). RecG has been shown to

dissociate R-loops *in vitro* (Fukuoh *et al.*, 1997; Vincent *et al.*, 1996) and over-expression of RecG in *E. coli* results in a severe reduction in the copy number of pUC plasmids (Fukuoh *et al.*, 1997). These plasmids require R-loop formation for the initiation of replication from their ColE1 site.

In addition to R-loops, D-loops can prime cSDR (Asai and Kogoma, 1994). These are formed during recombination by RecA-mediated strand exchange between a ssDNA end and a duplex molecule (see pp. 18). The initiation of cSDR from R- and D-loops requires the assembly of a specialised replication complex, or primosome, by the helicase PriA (Masai *et al.*, 1994). Interestingly, mutations in *priA* suppress the repair and recombination defects in *recG* mutants, suggesting that RecG is functionally linked in some aspect with the replication protein (Al-Deib *et al.*, 1996). The precise roles of these two helicases in replication and recombination at D-loops are not known at present, but it is interesting to note that PriA is also a key component in replication restart, for example following the rescue of stalled replication forks.

RESOLUTION OF THE HOLLIDAY JUNCTION

RuvC-Mediated Resolution

Following branch migration, Holliday junctions are processed into mature recombinant products by RuvC. The *ruvC* gene is located upstream of *ruvA* and *ruvB*, in a separate operon with *orf26* (Sharples and Lloyd, 1991; Takahagi *et al.*, 1991). Whilst mutations in *ruvC* produce the same phenotype as *ruvA* and *ruvB* mutants (Sharples *et al.*, 1990), *orf26* mutants do not exhibit a *ruv* phenotype and the function of the gene product (Orf26) is unknown (Sharples and Lloyd, 1991; Takahagi *et al.*, 1991). The *orf26-ruvC* operon is not SOS inducible, and the product of the *ruvC* gene is produced at low levels.

The 19 kDa RuvC protein is an endonuclease that resolves Holliday junctions *in vitro* to form recombinant duplex products (Connolly *et al.*, 1991; Dunderdale *et al.*, 1991; Iwasaki *et al.*, 1991). RuvC resolvase activity was initially detected in fractionated *E. coli* cell extracts (Connolly *et al.*, 1991; Connolly and West, 1990) and was subsequently over-expressed and purified (Dunderdale *et al.*, 1991; Dunderdale *et al.*, 1994; Iwasaki *et al.*, 1991). The RuvC-mediated resolution reaction was found to involve three distinct steps, illustrated in Figure 1.10. These are: (i) structure-specific junction binding (Bennett *et al.*, 1993; Benson and West, 1994; Takahagi *et al.*, 1994); (ii) structural modification of the junction (Ariyoshi *et al.*, 1994b; Bennett and West, 1995); and (iii) sequence-specific cleavage (Shah *et al.*, 1994b; Shah *et al.*, 1997; Shida *et al.*, 1996).

The RuvC protein binds to Holliday junctions as a dimer, as suggested by gel filtration (Iwasaki *et al.*, 1991), SDS-PAGE (Dunderdale *et al.*, 1994), X-ray crystallography (Ariyoshi *et al.*, 1994a; Ariyoshi *et al.*, 1994b) and by the symmetrical incision of two strands of like polarity during resolution, as shown in Figure 1.10 (Bennett *et al.*, 1993). Analysis of the RuvC-junction complex by band-shift assays has shown that the junction is unfolded by RuvC (Bennett and West, 1995). The arms of the junction are unstacked and, in contrast to a RuvA-bound junction, are oriented in a two-fold symmetric configuration. Upon RuvC binding, the DNA strands near the crossover became hypersensitive to permanganate ions, indicating that base-pairing is disrupted at the junction point.

Resolution of the Holliday junction involves the introduction of symmetrically related nicks in the pair of strands that constitute the wide angles in the RuvC-bound junction (Bennett *et al.*, 1993; Figure 1.10). These strands correspond to the continuous strands in the stacked X-structure. As originally

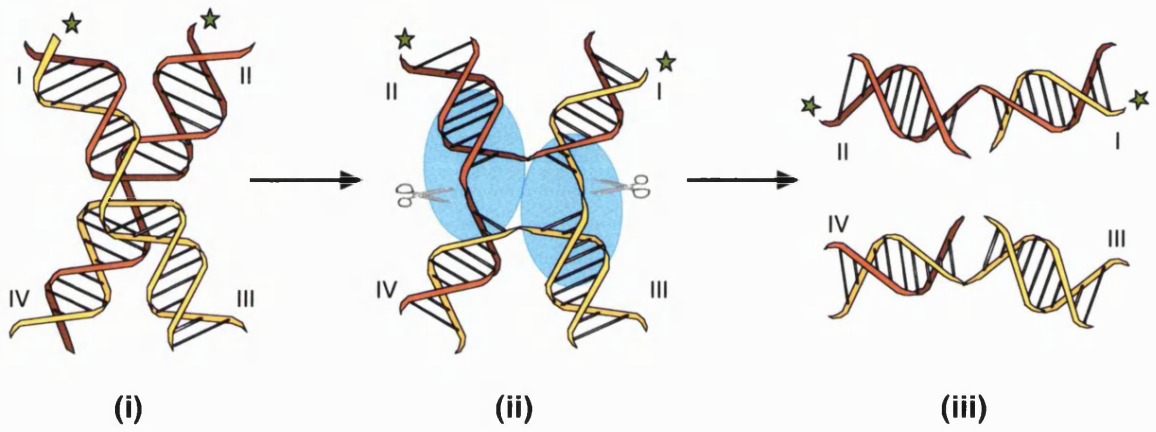

FIGURE 1.10. HOLLIDAY JUNCTION BINDING AND RESOLUTION BY RUVC

Dimeric RuvC binds to the Holliday junction (i) and orients the arms in a two-fold symmetric unfolded configuration (ii). Resolution occurs by the introduction of nicks in the pair of strands that form the wide angles (indicated by green asterisks); these correspond to the continuous strands in the stacked X-structure (i). The sites of incision are indicated by scissors. Cleavage results in nicked duplex products (iii) that can be repaired by ligation. Figure adapted from Bennett and West (1995).

predicted by the Holliday model (Holliday, 1964), either pair of strands may be nicked, depending on which pair form the large angle. Cleavage occurs preferentially at the 3′ side of the thymidine residues in the consensus sequence 5′-(A/T)TT↓(G/C)-3′ (Shah *et al.*, 1994b), and occurs most efficiently when the consensus site is located at or near the site of the crossover (Bennett and West, 1996; Shida *et al.*, 1996). The nicked duplexes generated by RuvC-mediated resolution are subsequently repaired by *E. coli* DNA ligase.

The crystal structure of RuvC has been solved and indicates that the two subunits, related by dyad symmetry, face in opposite directions (Ariyoshi *et al.*, 1994a; Ariyoshi *et al.*, 1994b). The catalytic centre of RuvC is located at the bottom of the putative DNA binding cleft and is composed of four acidic amino acids. These residues are thought to coordinate a divalent cation which is known to be required for junction cleavage (Bennett *et al.*, 1993; Saito *et al.*, 1995; Takahagi *et al.*, 1994). The crystal structure of RuvC resembles that of *E. coli* RNaseH1, despite there being poor sequence similarity between the two proteins (Ariyoshi *et al.*, 1994b). Furthermore, the structures of the catalytic domains of RuvC and RNaseH1 are strikingly similar to that of human immunodeficiency virus type-1 (HIV-1) integrase (Dyda *et al.*, 1994) and Mu transposase (Rice and Mizuuchi, 1995).

Formation of a RuvABC-Holliday Junction Complex

A number of genetic observations indicate that the processes of RuvAB-mediated branch migration and RuvC-mediated resolution are linked. Firstly, mutations in *ruvA*, *ruvB* or *ruvC* confer similar phenotypes, i.e. UV sensitivity and a modest defect in recombination (Lloyd *et al.*, 1984; Lloyd and Buckman, 1991; Sharples *et al.*, 1990). Secondly, defects in all three *ruv* mutants can be corrected by the over-expression of RusA, a 14 kDa cryptic Holliday junction

resolvase in *E. coli* (Mahdi *et al.*, 1996; Mandal *et al.*, 1993; Sharples *et al.*, 1994a). Taken together, the data suggest that all three Ruv proteins are required for junction resolution *in vivo*.

The genetic observations have been supported by recent biochemical data. The late stages of homologous recombination have been reconstituted *in vitro* using purified RuvA, RuvB and RuvC proteins (Eggleston *et al.*, 1997). The addition of monoclonal antibodies directed against any one of the proteins was found to inhibit RuvC-mediated junction resolution. Furthermore, RuvB and RuvC have been shown to interact in solution (Eggleston *et al.*, 1997), and RuvA-RuvC-junction complexes have been detected by band-shift assays (Whitby *et al.*, 1996). More recently, a RuvABC-junction complex has been detected *in vitro* by immunoprecipitation and, in addition, functional interactions have been demonstrated between the Ruv proteins (Davies and West, 1998; van Gool *et al.*, 1998; Zerbib *et al.*, 1998). Using synthetic junctions, RuvB was shown to stabilise RuvC-junction binding and stimulate its resolvase activity (van Gool *et al.*, 1998). Conversely, RuvC appeared to target RuvB to the junction leading to limited branch migration in the absence of RuvA. Zerbib *et al.* (1998) conducted experiments using plasmid-sized junctions called χ-structures, generated by the cleavage of figure-8 molecules, and found that Holliday junction resolution by RuvC was stimulated by RuvAB-mediated branch migration.

Taken together, the genetic and biochemical data strongly indicate that branch migration and resolution are tightly coordinated *in vivo* via the formation of a RuvABC-Holliday junction complex. The detailed structure of the complex remains to be elucidated but it is thought to contain a tetramer of RuvA and a dimer of RuvC, bound to opposite faces of the junction, with RuvB rings binding to the two arms (van Gool *et al.*, 1998; West, 1998; Whitby *et al.*,

1996). Since Holliday junction resolution by RuvC is sequence-specific (Bennett and West, 1996; Shah *et al.*, 1994b; Shah *et al.*, 1997; Shida *et al.*, 1996), a RuvAB-facilitated scanning mechanism has been proposed for the RuvABC, or resolvasome, complex (van Gool *et al.*, 1998; Zerbib *et al.*, 1998). In this model, shown in Figure 1.11, the RuvAB proteins drive branch migration of the junction whilst RuvC 'scans' the DNA for preferred cleavage sites as it passes through the RuvABC complex. Such a mechanism would account for the stimulation of RuvC-mediated resolution observed *in vitro* upon addition of RuvAB (van Gool *et al.*, 1998; Zerbib *et al.*, 1998). The model is also supported by the recent observation that, in the presence of RuvAB, RuvC is able to cleave a synthetic junction at preferred sites located away from the initial junction point (van Gool *et al.*, 1999).

Prokaryotic and Eukaryotic Holliday Junction Resolvases

Homologues of RuvC have been found in a range of eubacteria although, as yet, a homologue has not been identified in *M. genitalium* despite the fact that the whole genome has been sequenced (Fraser *et al.*, 1995). RuvC appears to be less conserved in bacteria than RuvB. For example, in *Pseudomonas aeruginosa*, the RuvC protein is ~55% identical to its *E. coli* counterpart compared to the ~72% identity calculated for RuvB (Hishida *et al.*, 1996). A second resolvase, RusA, has been identified in *E. coli* which, like RuvC, cleaves Holliday junctions by the introduction of symmetrical nicks into strands of like polarity (Mahdi *et al.*, 1996; Sharples *et al.*, 1994a). RusA was originally thought to be a cellular enzyme. However, the *rusA* gene was later found to be 95% identical to a gene in lambdoid bacteriophage 82 and it is thought to form part of a defective lambdoid prophage DLP12 in the *E. coli* genome (Mahdi *et al.*, 1996). This

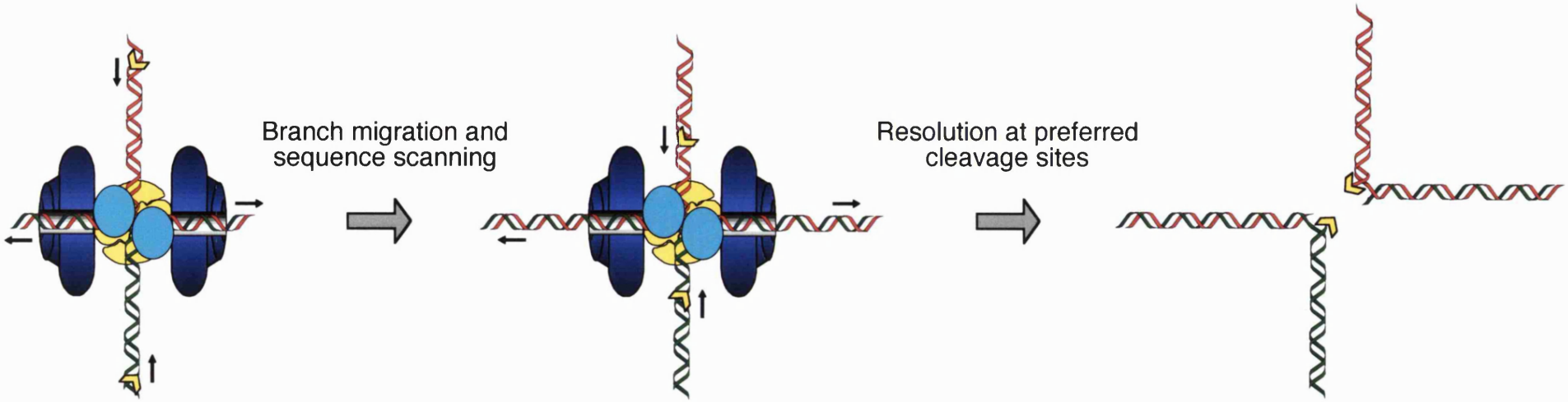

FIGURE 1.11. MODEL FOR THE ACTIVATION OF RUVC RESOLVASE BY A RUVAB-FACILITATED SCANNING MECHANISM

The Holliday junction is sandwiched between a RuvA tetramer (yellow) and a RuvC dimer (light blue), and is held in an unfolded square planar configuration. The RuvA-RuvC-junction complex is flanked by two hexameric RuvB rings (dark blue) that encircle the heteroduplex arms of the junction. The RuvB rings, which are oppositely oriented, pump the duplex DNA out through their central channels thereby driving the process of branch migration. The arrows indicate the direction of movement of the DNA. As the DNA is drawn into and through the RuvABC complex, it is 'scanned' by RuvC for preferred cleavage sites (indicated by yellow chevrons). Upon encountering a site, the RuvC dimer resolves the junction and the protein complex dissociates, leaving nicked duplex DNA which can be subsequently repaired by DNA ligase. Figure adapted from van Gool *et al* (1998) and Zerbib *et al* (1998).

cryptic resolvase is poorly expressed in *E. coli* and mutations in the encoding gene do not appear to affect recombination or repair.

Other junction resolving enzymes, that do not have sequence similarity to RuvC, have been identified in both bacteriophage and yeast. The most extensively studied of these is phage T4 endonuclease VII which binds and cleaves a variety of branched structures, including four-way junctions (Jensch and Kemper, 1986; Kemper and Garabett, 1981; Mizuuchi *et al.*, 1982; Mueller *et al.*, 1990; Nishimoto *et al.*, 1979; Parsons *et al.*, 1990). Mutations in the gene encoding T4 endonuclease VII can be complemented by bacteriophage T7 endonuclease I (de Massy *et al.*, 1984). T7 endonuclease I has been shown to resolve both three-way (Y) and four-way (X) junctions (de Massy *et al.*, 1987; Duckett *et al.*, 1995; Lu *et al.*, 1991b), as well as recombination intermediates made by RecA (Müller *et al.*, 1990). T4 endonuclease VII and T7 endonuclease I show much wider substrate and sequence specificity than *E. coli* RuvC (Bertrand-Burggraf *et al.*, 1994; Dickie *et al.*, 1987; Duckett *et al.*, 1988; Kemper *et al.*, 1984; Kleff and Kemper, 1988; Murchie and Lilley, 1993; Picksley *et al.*, 1990).

A junction-specific resolvase, CCE1 (or endo X2; Symington and Kolodner, 1985), has been identified in the yeast *S. cerevisiae* (Evans and Kolodner, 1987; Kleff *et al.*, 1992; Parsons *et al.*, 1989; Parsons and West, 1988), and an equivalent protein has been found in *Schizosaccharomyces pombe* (Oram *et al.*, 1998; Whitby and Dixon, 1997; White and Lilley, 1997). *S. cerevisiae* CCE1 behaves in a similar manner to RuvC and shows sequence-specificity, tending to cleave 3′ of a CT dinucleotide (White and Lilley, 1996). Using synthetic junctions, a resolvase activity has also been detected in a number of mammalian tissues, including calf thymus (Elborough and West, 1990; Hyde *et al.*, 1994), chinese hamster ovary (CHO) cells (Hyde *et al.*, 1994), and fractionated calf testes extracts (B. Kysela, A. A. Davies and S. C. West, unpublished data).

Unfortunately, attempts to isolate these activities have so far failed. A Holliday junction resolvase with functional similarity to RuvC has recently been identified in an archaeal strain, however, suggesting that the mechanism of junction resolution is conserved in eubacteria, Archaea and Eukarya (Komori *et al.*, 1999).

III. HELICASES: STRUCTURE AND MECHANISMS

Helicases are a diverse class of enzymes that utilise the energy from NTP hydrolysis to unwind duplex nucleic acids (DNA, RNA or RNA-DNA hybrids) (reviewed in Lohman and Bjornson, 1996; Matson *et al.*, 1994). They function in many key biological processes, including DNA replication, repair, recombination and transcription, as well as in RNA processing. Helicases were first discovered over 20 years ago (Abdel-Monem *et al.*, 1976; Scott *et al.*, 1977). Since then, at least 12 different helicases have been identified in *E. coli*, as many as 50 are thought to be present in yeast, and even more are predicted to exist in humans (Egelman, 1998). Genetic defects in helicases have been linked to a number of cancer-prone human disorders, including Xeroderma pigmentosum, Cockayne's syndrome, Bloom's syndrome and Werner's syndrome, highlighting the importance of these enzymes *in vivo* (Ellis *et al.*, 1995; Johnson and Squires, 1992; Yu *et al.*, 1996a). In addition to unwinding duplex DNA, helicases use the energy from NTP hydrolysis to fuel their translocation along the DNA, in some cases at rates of 500-1000 bp/s (Roman and Kowalczykowski, 1989; Taylor and Smith, 1980).

CONSERVED HELICASE MOTIFS AND THEIR CATALYTIC ROLES

Sequence comparisons indicate that many DNA and RNA helicases contain seven conserved motifs, denoted I, Ia and II-VI (Gorbalenya and Koonin, 1993;

Gorbalenya *et al.*, 1989). Motifs I and II are well conserved in all helicases, including RuvB, and correspond to the NTP binding Walker A and B boxes (Walker *et al.*, 1982). X-ray crystallographic studies of NTP-binding proteins have indicated that the Walker A motif forms a phosphate binding loop (P-loop) that interacts directly with the bound nucleotide, and that residues in the Walker B motif are involved in Mg^{2+}-coordinated ATP hydrolysis (Fry *et al.*, 1986; Milburn *et al.*, 1990; Pai *et al.*, 1990; Saraste *et al.*, 1990; Story and Steitz, 1992). Mutagenesis studies have indicated equivalent roles for these residues in helicases, with motifs I and II shown to be required for NTP binding and NTP hydrolysis, respectively (Pause and Sonenberg, 1992; Soultanas *et al.*, 1999).

The other helicase motifs are not so well defined, although the recent emergence of crystal structures of helicases has shed light on possible catalytic roles for these motifs (Korolev *et al.*, 1997; Subramanya *et al.*, 1996; Velankar *et al.*, 1999; Yao *et al.*, 1997). The first DNA helicase to be observed at atomic resolution was *Bacillus stearothermophilus* PcrA protein (Subramanya *et al.*, 1996). Significantly, the helicase motifs in the PcrA crystal structure were found to be clustered around the nucleotide binding site. More recently, the structure of PcrA complexed with a single strand tailed duplex has been solved and revealed the specific role of some of the amino acids in these motifs (Velankar *et al.*, 1999). A conserved residue in helicase motif III (Q254) was shown to interact with the bound nucleotide whilst two other residues in the motif (W259 and R260) form part of the ssDNA binding site of PcrA. The equivalent residues in *E. coli* Rep protein, another DNA helicase, are also thought to interact with ssDNA (Korolev *et al.*, 1997). Based on the crystallographic data, it was proposed that motif III of PcrA acts as a 'switch', coupling ATP hydrolysis to the helicase activity of the protein via changes in its ssDNA binding potential (Dillingham *et al.*, 1999). Such a model was tested and confirmed by site-

directed mutagenesis (Dillingham *et al.*, 1999; Velankar *et al.*, 1999). Furthermore, mutational analysis of motif III in mammalian translation initiation factor eIF-4A, an RNA helicase, also indicates a crucial role for this motif in coupling ATP hydrolysis with helicase activity (Pause and Sonenberg, 1992).

Motif Ia of PcrA is thought to form part of a putative DNA binding groove (Subramanya *et al.*, 1996). More recently, it was suggested that the conserved phenylalanine residue (F64) in this motif modulates the binding of ssDNA in the motif III 'binding pocket' in response to changes in the state of the bound nucleotide (Velankar *et al.*, 1999). Mutational analyses of PcrA indicate that conserved residues in motifs IV and VI make direct contacts with the terminal phosphate group of the bound nucleotide and thus also play central roles in catalysis (Soultanas *et al.*, 1999). In *E. coli* Rep, motifs Ia, III and V are thought to contribute to the DNA binding site, whilst motif IV is thought to be involved in nucleotide binding (Korolev *et al.*, 1997). However, in the hepatitis C virus (HCV) NS3 protein, an RNA helicase, motif IV is proposed to function in nucleic acid binding (Korolev *et al.*, 1998; Yao *et al.*, 1997). Thus the roles of the motifs may vary between different helicase families.

THE HEXAMERIC HELICASE FAMILY

RuvB belongs to an emerging family of helicases that possess a common hexameric ring structure. Other members of this family identified to date are: *E. coli* DnaB (Bujalowski *et al.*, 1994; Reha-Kranz and Hurwitz, 1978; Yu *et al.*, 1996c) and Rho (Finger and Richardson, 1982; Geiselmann *et al.*, 1992a; Gogol *et al.*, 1991), bacteriophage T7 gp4 (Egelman *et al.*, 1995; Patel and Hingorani, 1993) and T4 gp41 (Dong *et al.*, 1995), the simian virus 40 (SV40) large T antigen (Dean *et al.*, 1992; Mastrangelo *et al.*, 1989; San Martin *et al.*, 1997; Wessel *et al.*, 1992b),

plasmid-encoded RepA (Scherzinger *et al.*, 1997), and bovine papilloma virus type 1 (BPV-1) E1 protein (Fouts *et al.*, 1999). The general properties and low-resolution structures of these proteins are shown in Table 1.1 and Figure 1.12, respectively.

TABLE 1.1. GENERAL PROPERTIES OF THE HEXAMERIC HELICASES

Protein	Subunit Mass	Helicase Polarity	Function
E. coli RuvB	37 kDa	5′ to 3′	Branch migration
E. coli Rho	46 kDa	5′ to 3′	Transcription termination
Simian virus 40 T antigen	92 kDa	3′ to 5′	Replication initiation
Bovine papilloma virus type 1 E1 protein	68 kDa	Not known	Replication initiation
E. coli DnaB	52 kDa	5′ to 3′	Replication fork unwinding
Phage T7 gene 4 protein	63, 56 kDa*	5′ to 3′	Replication fork unwinding
Phage T4 gene 41 protein	53 kDa	5′ to 3′	Replication fork unwinding
Plasmid RSF1010 RepA	30 kDa	5′ to 3′	Replication fork unwinding

* T7 gp4 protein exists in two forms: gp4A, which possesses both primase and helicase activity, and gp4B, which is translated from an internal initiation site in the same gene and possesses only helicase activity (Bernstein and Richardson, 1988a; Bernstein and Richardson, 1988b; Bernstein and Richardson, 1989; Dunn and Studier, 1983).

As shown in Figure 1.12, the hexameric helicases form very similar toroidal structures with hollow central channels (20-40 Å in diameter). Biochemical and structural studies have suggested that, with the exception of Rho, the DNA passes through the centre of the hexameric rings (Bujalowski and Jezewska, 1995; Dean *et al.*, 1992; Dong *et al.*, 1995; Egelman *et al.*, 1995; Fouts *et al.*, 1999; Jezewska *et al.*, 1998a; Stasiak *et al.*, 1994). In contrast with the other members of the family, *E. coli* Rho is a DNA-RNA helicase and is thought to

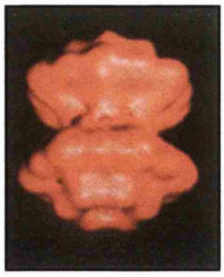

E. coli RuvB
(Stasiak *et al.*, 1994)

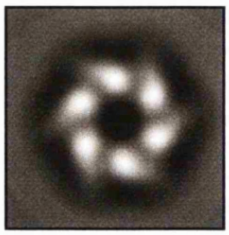

E. coli DnaB
(Yu *et al.*, 1996c)

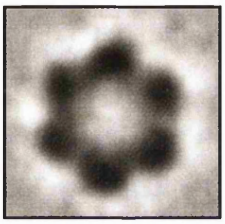

E. coli Rho
(Gogol *et al.*, 1991)

Phage T7
Gene 4 protein (gp4)
(Egelman *et al.*, 1995)

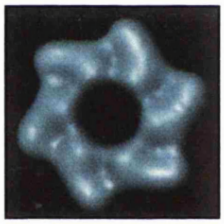

Simian virus 40 (SV40)
Large T antigen
(San Martin *et al.*, 1997)

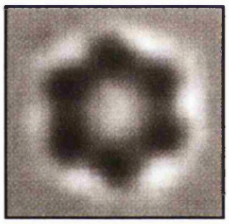

Phage T4
Gene 41 protein (gp41)
(Dong *et al.*, 1995)

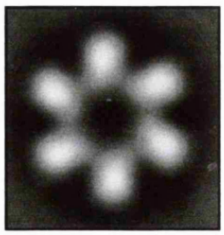

Bovine papilloma virus (BPV)
E1 protein
(Fouts *et al.*, 1999)

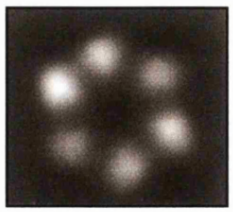

Plasmid RepA protein
(Scherzinger *et al.*, 1997)

FIGURE 1.12. THE HEXAMERIC RING HELICASES

The images shown were either obtained directly by electron microscopy, or from subsequent three-dimensional image reconstruction. With the exception of RuvB and T7 gp4, the ring proteins are shown as top views, allowing the central cavity through which DNA passes to be clearly seen. The images were reproduced from the indicated sources.

wrap the RNA around the outside of the hexamer (Geiselmann *et al.*, 1993; McSwiggen *et al.*, 1988).

Studies suggest that the replicative helicases T7 gp4 (Egelman *et al.*, 1995; Hacker and Johnson, 1997; Yong and Romano, 1996), T4 gp41 (Raney *et al.*, 1996) and DnaB (Jezewska *et al.*, 1998a; Jezewska *et al.*, 1997) encircle one DNA strand of the replication fork and exclude the other from the centre of the ring. In the case of RuvB and SV40 large T antigen, however, dsDNA is proposed to pass through the central cavity of the hexameric rings (Mastrangelo *et al.*, 1994; Mastrangelo *et al.*, 1989; Stasiak *et al.*, 1994; Wessel *et al.*, 1992a). Large T antigen forms a double hexameric ring structure at the core replication origin of SV40 (Dean *et al.*, 1992; Mastrangelo *et al.*, 1989). The palindromic nature of the origin suggests that the two rings lie in opposite orientations (Wessel *et al.*, 1992b), and it is possible that a dual pump action occurs similar to that described for RuvB (Parsons *et al.*, 1995a; West, 1996). In this case, the duplex DNA is drawn into the complex where it is unwound to form single-stranded loops, allowing the initiation of replication.

RuvB (Stasiak *et al.*, 1994), DnaB (San Martin *et al.*, 1995) and T7 gp4 (Egelman *et al.*, 1995) have all been shown to possess bilobed subunits, resulting in hexameric rings with a large and small tier. Interestingly, the T7 gp4 helicase translocates along ssDNA in a 5′ to 3′ direction such that the DNA passes out through the small end of the hexameric ring (Egelman *et al.*, 1995; Yu *et al.*, 1996b), the same structural polarity as that displayed by RuvB during branch migration (Parsons *et al.*, 1995a; Yu *et al.*, 1997).

The RuvB and T7 gp4 hexamers have both been shown to exhibit C6 symmetry (i.e. the subunits are related by a central six-fold axis). Furthermore, recent evidence suggests that Rho also possesses six-fold symmetry (Horiguchi *et al.*, 1997; Miwa *et al.*, 1995; Egelman, personal communication), as opposed to

the D3 symmetry originally proposed in which two trimers are stacked upon each other (Geiselmann *et al.*, 1992a; Geiselmann *et al.*, 1993; Geiselmann *et al.*, 1992b). Both DnaB and BPV-1 E1 protein, however, have been shown to exist in two quaternary states, one with C6 symmetry and the other with C3 symmetry (Fouts *et al.*, 1999; San Martin *et al.*, 1995; Yu *et al.*, 1996c). The latter form is thought to arise from the dimerisation of the six subunits into a trimer of dimers. These observations are particularly interesting in light of biochemical data indicating that DnaB (Bujalowski and Klonowska, 1993), Rho (Geiselmann and von Hippel, 1992; Stitt, 1988) and T7 gp4 (Hingorani and Patel, 1996; Hingorani *et al.*, 1997) contain three high-affinity and three low-affinity ATP binding sites. In addition, RuvB (Tsaneva *et al.*, 1992a), Rho (Geiselmann *et al.*, 1992a) and T4 gp41 (Dong *et al.*, 1995) have been shown to form dimers in solution.

At present, the precise molecular mechanisms of the hexameric helicases are poorly understood. Given the structural similarities between these proteins, especially considering their limited sequence homology (restricted to within the conserved helicase motifs), it is possible that the members of this family act by a similar helicase mechanism.

CRYSTAL STRUCTURES OF HELICASES AND EVIDENCE FOR A COMMON NUCLEOTIDE BINDING CORE

The crystal structure of *B. stearothermophilus* PcrA, a monomeric DNA helicase, has been solved in the presence and absence of ADP (Subramanya *et al.*, 1996). As shown in Figure 1.13, the protein is composed of two domains (1 and 2), each consisting of two subdomains (A and B). The bound ADP is located in a deep cleft between the two domains and is surrounded by the conserved helicase motifs. Interestingly, subdomains 1A and 2A of PcrA resemble the ATP

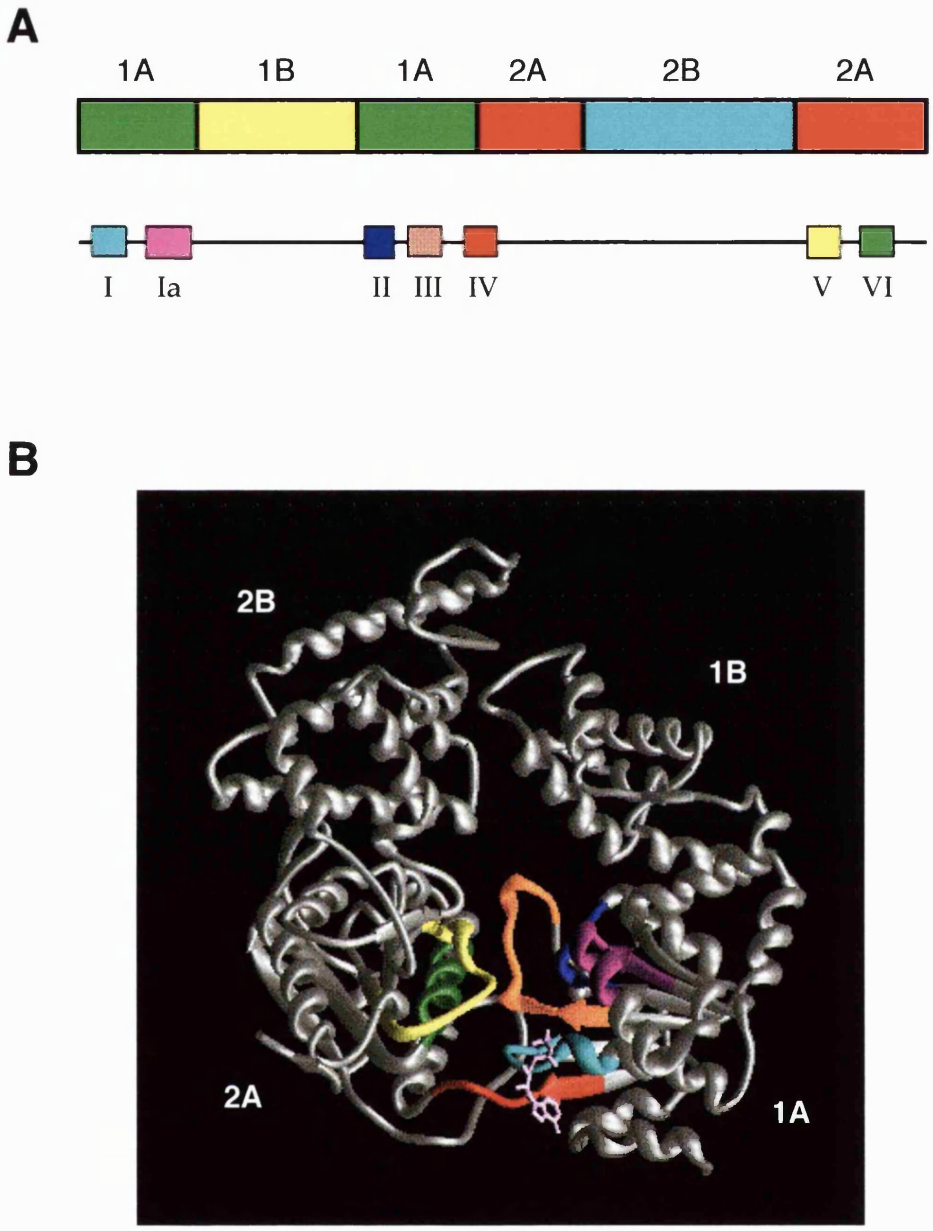

FIGURE 1.13. STRUCTURE OF *B. STEAROTHERMOPHILUS* PCRA

A. The conserved helicase motifs of PcrA and their positions in the four subdomains of the protein (1A, 1B, 2A and 2B).

B. Ribbon representation of the PcrA protein showing the locations of the different conserved motifs (indicated in the same colours as shown in A) and the position of the bound ADP (shown in lilac).

Figure reproduced from Subramanya *et al* (1996).

binding domain of *E. coli* RecA protein and all the key residues in the active sites of the two ADP-bound proteins were found to be spatially conserved (Story and Steitz, 1992; Story *et al.*, 1992). More recently, the structure of *E. coli* DNA helicase Rep, complexed with ssDNA and ADP, has been reported (Korolev *et al.*, 1997). The enzyme is also composed of four subdomains and these are arranged to give a similar crab claw-like appearance to PcrA (with one large and one small pincer). The nucleotide binding site is located in a cleft running between two subdomains that are nearly superimposable on the corresponding subdomains of PcrA.

The crystal structure of the RNA helicase domain of HCV NS3 protein has been determined, both alone and complexed with a single-stranded oligonucleotide (Kim *et al.*, 1998; Yao *et al.*, 1997). The RNA helicase was shown to consist of three domains, two of which contain all of the conserved helicase motifs and are structurally homologous to the 1A and 2A subdomains of PcrA and Rep. Furthermore, the nucleotide binding fold of another RNA helicase, the mammalian translation initiation factor eIF-4A, is reported to be nearly identical to that of HCV NS3 and PcrA (Benz *et al.*, 1999). The crystallographic data suggest that PcrA and Rep (DNA helicases) and NS3 and eIF-4A (RNA helicases) all share a common structural core that resembles the nucleotide binding fold of RecA.

At present, a complete high-resolution structure has not been obtained for any hexameric helicase. Recently, however, the crystal structure of the C-terminal helicase domain of T7 gp4 was reported. The structure of the nucleotide binding domain of this protein was found to closely resemble that of RecA (Sawaya *et al.*, 1999). Furthermore, the helicase domain crystallised as a helical filament reminiscent of that observed in the crystal structure of RecA (Story *et al.*, 1992). The SV40 large T antigen is proposed to be similar to RecA,

based on sequence homology and antibody cross-reactivity (Seif, 1982). The nucleotide binding core of RecA also resembles that of F_1-ATPase, an enzyme that converts ADP into ATP during oxidative phosphorylation (Abrahams *et al.*, 1994). Although F_1-ATPase is not a helicase, the α- and β-subunits of this protein form a ring-shaped heterohexamer that resembles the toroidal structure of the hexameric helicases. The *E. coli* Rho protein shares considerable sequence homology with F_1-ATPase and its structure has been modelled on the heterohexameric protein (Miwa *et al.*, 1995; Opperman and Richardson, 1994). Interestingly, using electron microscopy the *T. aquaticus* RecA protein has been shown to form stable hexameric rings in addition to the nucleoprotein filaments previously reported for *E. coli* RecA (Egelman and Stasiak, 1986; Yu and Egelman, 1997). The function of these RecA rings is, however, unknown at present.

Taken together, the structural and sequence data obtained to date suggest that all helicases, including the hexameric ring helicases, have a common 'RecA-like' nucleotide binding core.

MECHANISM OF ACTION OF HELICASES

Despite their importance and ubiquity, the precise molecular mechanisms of most DNA helicases are, at present, poorly understood. Helicases need to harness the energy released from NTP hydrolysis for duplex unwinding and, in some cases, for processive translocation along the DNA. This is thought to be achieved by conformational changes in the protein, caused by the binding and hydrolysis of ATP, that modulate its DNA binding properties (Velankar *et al.*, 1999; Wong and Lohman, 1992). Since helicases appear to share a common nucleotide binding core, it is possible that they utilise similar mechanisms for coupling ATP hydrolysis to helicase action.

Two popular models that have been proposed for the mechanism of helicase-catalysed unwinding are the 'active rolling' and 'inchworm' models (reviewed by Lohman and Bjornson, 1996; Bird et al., 1998; Figure 1.14). In the active rolling model, detailed in Figure 1.14A, the helicase possesses at least two subunits that alternately bind ssDNA and dsDNA in response to ATP binding and hydrolysis. This model has been proposed for *E. coli* Rep, which has been shown to form dimers on DNA by chemical cross-linking (Wong and Lohman, 1992).

In contrast to the active rolling model, which requires that the helicase is oligomeric, the inchworm model (Figure 1.14B) is equally applicable to a monomeric protein. The helicase must, however, possess two non-identical binding sites: a leading site, which binds duplex and ssDNA, and a tail site, which binds only ssDNA (Lohman, 1993; Yarranton and Gefter, 1979). Successive rounds of ATP binding and hydrolysis are thought to mediate conformational changes that allow the helicase to track along the DNA, separating the strands as it goes. Wigley and colleagues have proposed an inchworm mechanism for the action of the monomeric helicase PcrA (Velankar *et al.*, 1999). The leading site (in domain 2A) and tail site (in domain 1A) of PcrA are located either side of the cleft containing the nucleotide binding pocket (Subramanya *et al.*, 1996; Velankar *et al.*, 1999). The binding and hydrolysis of ATP at this site is thought to cause conformational changes in the two domains, thereby powering movement of the protein along the DNA in an 'inchworm' fashion. The leading site reaches forward to the forked region, where it binds and unwinds the duplex DNA. The tail site tracks along behind the leading site, gripping the single strand as it is formed (Velankar *et al.*, 1999).

A different model has been proposed for the hexameric helicase T7 gp4 in which the ssDNA is rotated between three catalytic subunits in the hexamer,

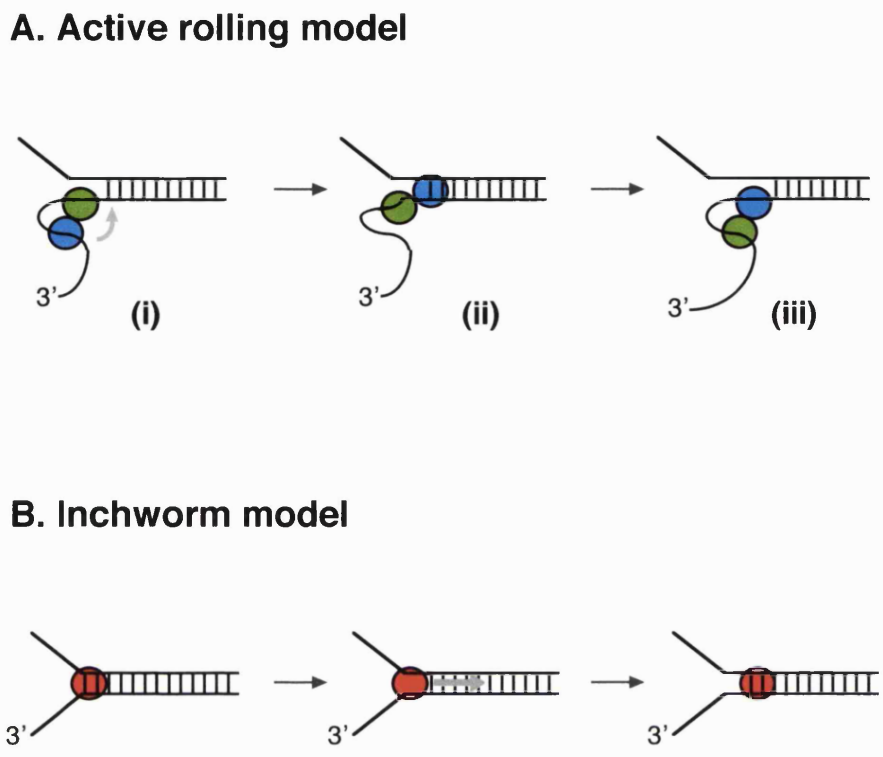

FIGURE 1.14. TWO POPULAR MODELS PROPOSED FOR HELICASE ACTION

A. The 'active rolling' model. In this model, the dimeric helicase (indicated by a blue and green circle) 'rolls' along the DNA as a result of an alternation in the affinity of the two subunits for ssDNA and dsDNA. Initially, both subunits are bound to the 3' ssDNA tail (i). Upon ATP binding, however, the affinity of the blue subunit for ssDNA decreases whilst its affinity for dsDNA increases. As a result, the dimer 'flips over' allowing the subunit to bind the duplex region ahead of the fork (ii). Finally, ATP hydrolysis is thought to induce protein conformational changes, resulting in unwinding of the duplex and release of the 5' strand ready for another cycle.

B. The 'inchworm' model. In this model, the monomeric helicase (indicated by a red circle) moves along the DNA in an 'inchworm' fashion, melting the duplex as it goes. The helicase possesses two DNA binding sites: the leading site, that binds ssDNA and dsDNA, and a tail site, that binds just ssDNA. As with the active rolling model, helicase action is coupled to successive rounds of ATP binding and hydrolysis.

Figure adapted from Bird *et al* (1998).

each at different stages of catalysis depending on the state of the bound nucleotide (Hingorani *et al.*, 1997). This model shows remarkable similarity to the cyclical binding change mechanism of F_1-ATPase (Abrahams *et al.*, 1994; Boyer, 1993).

The aim of my research was to investigate the mechanism by which the *E. coli* RuvB motor protein drives branch migration during homologous recombination and, in particular, to ascertain the role that DNA helicase activity plays in this process. The current model for the RuvAB-Holliday junction complex suggests that the two RuvB hexameric rings, which are assembled on the heteroduplex arms, may behave like a dual pump. The aim of this work is to understand the mechanics of this DNA pumping action and, in doing so, gain insight into the mechanisms of other hexameric DNA helicases.

CHAPTER TWO : MATERIALS AND METHODS

I. ENZYMES AND REAGENTS

2.1 ENZYMES

RecA and RuvB proteins were purified as described in sections 2.12 and 2.13. RuvA protein (Tsaneva *et al.*, 1992a) and wheat germ DNA topoisomerase I (Dynan *et al.*, 1981) were generously provided by Dr D. E. Adams and were purified as described. RuvC protein was a gift from Dr R. Shah, purified according to published protocols (Dunderdale *et al.*, 1991; Dunderdale *et al.*, 1994). *E. coli* DNA topoisomerase I was kindly provided by Dr I. R. Tsaneva and was purified as described (Lynn and Wang, 1989). Where necessary, proteins were diluted in enzyme dilution buffer before use. Other enzymes were purchased from the following companies:

Amersham Pharmacia Biotech: terminal deoxynucleotidyl transferase (3′ end-labelling kit), T4 polynucleotide kinase.

New England Biolabs Inc. (NEB): restriction enzymes and NEBuffers.

Sigma Chemical Co: lysozyme, proteinase K, creatine phosphokinase.

2.2 REAGENTS

Chemical reagents were obtained from Sigma, BDH (Merck) or Fisons unless indicated otherwise. Other materials were purchased from the following companies:

Aldrich: thymine.

Amersham Pharmacia Biotech: radiolabelled reagents, 5x cacodylate buffer (3′ end-labelling kit), One-Phor-All buffer.

Anachem: polyacrylamide solutions.

Bio-Rad: ammonium persulphate, BioGel A-0.5m, bromophenol blue, Coomassie brilliant blue R-250, protein (low molecular weight) standards,

DEAE Bio-Gel, hydroxyapatite Bio-Gel, protein assay dye reagent concentrate, xylene cyanol.

Boehringer Mannheim: DNA size marker (molecular weight marker III).

DAKO A/S Denmark: horseradish peroxidase-conjugated anti-rabbit antibodies.

Difco: bacto-tryptone, bacto-yeast extract, bacto-agar.

Duchefa: carbenicillin.

Gibco BRL: agarose, formamide, sucrose (UltraPure).

International Biotechnologies Inc: ethidium bromide.

ICN Biomedicals Inc: ammonium sulphate, urea, casein hydrochloride

Kodak: TEMED.

Medicell International Ltd: dialysis tubing (diameter 6.3 mm and 14.3 mm).

Melford Laboratories Ltd: DTT.

National Diagnostics Inc: EcoScintA scintillation fluid.

New England Biolabs Inc: ϕX174 virion ssDNA and form I (supercoiled) dsDNA.

Promega: bovine serum albumin (BSA), isopropyl β-D-thiogalactopyranoside (IPTG).

Whatman: phosphocellulose.

2.3 BUFFERS AND SOLUTIONS

Agarose gel loading buffer (10x): 50 mM Tris-HCl (pH 8.0), 50% (v/v) glycerol, 0.2% (w/v) bromophenol blue.

Annealing buffer (10x): 100 mM Tris-HCl (pH 7.5), 100 mM $MgCl_2$, 500 mM NaCl.

ATPase buffer: 20 mM Tris-HCl (pH 7.5), 15 mM $MgCl_2$ (RuvB reactions) or 10 mM $MgCl_2$ (RuvAB reactions), 1 mM ATP, 2 mM DTT, 100 μg/ml BSA.

BioGel column buffer: 10 mM Tris-HCl (pH 8.0), 1 mM EDTA, 100 mM NaCl.

Branch migration buffer A: 50 mM Tris-Ac (pH 7.5), 15 mM $Mg(OAc)_2$ (for RuvB reactions) or 10 mM $Mg(OAc)_2$ (for RuvAB reactions), 20 mM K(OAc), 2 mM ATP, 1 mM DTT, 100 μg/ml BSA.

Branch migration buffer B: 50 mM Tris-Ac (pH 8.0), 15 mM $Mg(OAc)_2$, 2 mM ATP, 1 mM DTT, 50 μg/ml BSA.

Branch migration buffer C: 20 mM Tris-HCl (pH 7.5), 10 mM $MgCl_2$, 10 mM NaCl, 2 mM ATP, 2 mM DTT, 100 μg/ml BSA.

Branch migration stop buffer A (5x): 4 mg/ml proteinase K, 4% (w/v) SDS.

Branch migration stop buffer B (10x): 10 mg/ml proteinase K, 2.5% (w/v) SDS.

Branch migration stop buffer C (10x): 250 mM EDTA, 5% (w/v) SDS.

Brij solution: 1% (w/v) Brij 58, 50 mM Tris-HCl (pH 7.5), 2 mM DTT.

Coomassie blue stain solution: 10% (v/v) glacial acetic acid, 10% (v/v) propan-2-ol, 0.1% (w/v) Coomassie brilliant blue R-250.

Destain solution: 10% (v/v) glacial acetic acid, 10% (v/v) propan-2-ol.

DNA binding buffer A: 20 mM triethanolamine-HCl (pH 7.5), 15 mM $Mg(OAc)_2$ (RuvB reactions) or 5 mM $Mg(OAc)_2$ (RuvAB reactions), 1 mM ATPγS, 1 mM DTT, 100 μg/ml BSA.

DNA binding buffer B: 20 mM triethanolamine-Ac (pH 7.5), 15 mM $Mg(OAc)_2$, 1 mM ATPγS.

Enzyme dilution buffer: 50 mM Tris-HCl (pH 8.0), 1 mM EDTA, 150 mM NaCl, 50% (v/v) glycerol, 1 mM DTT, 100 μg/ml BSA.

Fermenter medium: 32 g/l bacto-tryptone, 20 g/l bacto-yeast extract, 5 g/l NaCl, 10 g/l K_2HPO_4, 1.85 g/l KH_2PO_4, 10 mg/l thiamine, 10 mg/l biotin, 50 mg/l thymine.

Formamide loading buffer: 80% (v/v) deionised formamide, 89 mM Tris base, 89 mM boric acid, 2 mM EDTA, 0.2% (w/v) bromophenol blue, 0.2% (w/v) xylene cyanol.

Gel crush buffer: 1 mM EDTA, 0.5 M Na(OAc), 10 mM $Mg(OAc)_2$.

Helicase buffer: 50 mM Tris-HCl (pH 8.0), 15 mM $MgCl_2$, 10 mM NaCl, 2 mM ATP, 2 mM DTT, 100 μg/ml BSA.

Helicase stop buffer (5x): 100 mM Tris-HCl (pH 7.5), 200 mM EDTA, 5 mg/ml proteinase K, 2.5% (w/v) SDS.

High destaining solution: 40% (v/v) methanol, 10% (v/v) glacial acetic acid.

Junction binding buffer: 50 mM Tris-HCl (pH 8.0), 5 mM EDTA, 1 mM DTT, 100 μg/ml BSA.

Low ionic strength (LI) buffer: 6.7 mM Tris-HCl (pH 8.1), 2 mM EDTA, 3.3 mM Na(OAc).

LI gel loading buffer (5x): 40 mM Tris-HCl (pH 7.5), 4 mM EDTA, 25% (v/v) glycerol, 400 μg/ml BSA, 0.2% (w/v) bromophenol blue, 0.2% (w/v) xylene cyanol.

Luria broth (LB): 10 g/l bacto-tryptone, 5 g/l bacto-yeast extract, 5 g/l NaCl.

LB agar: Luria broth (as above), 1.5% (w/v) agar.

Lysis buffer A: 250 mM Tris-HCl (pH 7.5), 25% (w/v) sucrose.

Lysis buffer B: 40 mM Tris-HCl (pH 8.0), 1 mM EDTA, 10 mM $MgCl_2$, 2 mM $CaCl_2$, 100 mM NaCl, 1 mM DTT.

Lysis buffer C: 100 mM Tris-HCl (pH 8.0), 2 mM EDTA, 5% (v/v) glycerol, 0.5 mM DTT.

M9 minimal medium A: 6 g/l Na_2HPO_4, 3 g/l KH_2PO_4, 1 g/l NH_4Cl, 0.5 g/l NaCl.

M9 minimal medium B: M9 minimal medium A supplemented with 10 mM $MgSO_4$, 1 mM $CaCl_2$, 1 mg/l thiamine, 0.4% (w/v) glucose.

M9 agar: M9 minimal medium B (as above), 1.5% (w/v) agar.

NEBuffer 3 (NEB): 50 mM Tris-HCl (pH 7.9), 10 mM $MgCl_2$, 100 mM NaCl, 1 mM DTT.

NEBuffer 4 (NEB): 20 mM Tris-Ac (pH 7.9), 10 mM $Mg(OAc)_2$, 50 mM K(OAc), 1 mM DTT.

Neutral gel loading buffer: 50% (v/v) glycerol, 0.2% (w/v) bromophenol blue, 0.2% (w/v) xylene cyanol.

Neutral sucrose solution: 10 mM Tris-HCl (pH 7.5), 10 mM EDTA, 1 M NaCl, 5% or 20% (w/v) ultrapure sucrose.

One-Phor-All buffer (Amersham Pharmacia): 10 mM Tris-Ac (pH 7.5), 10 mM $Mg(OAc)_2$, 50 mM K(OAc).

P_1-buffer: 20 mM potassium phosphate (pH 6.5), 0.1 mM EDTA, 10% (v/v) glycerol, 0.1 mM DTT.

P_2-buffer: 10 mM potassium phosphate (pH 6.8), 10% (v/v) glycerol, 0.5 mM DTT.

Protein cross-linking buffer: 20 mM triethanolamine-HCl (pH 8.2), 10 mM $MgCl_2$, 50 mM NaCl, 1 mM ATP, 0.25 mM ATPγS.

Protein storage buffer A: 20 mM Tris-HCl (pH 7.5), 1 mM EDTA, 150 mM NaCl, 50% (v/v) glycerol, 1 mM DTT.

Protein storage buffer B: 50 mM Tris-HCl (pH 7.5), 1 mM EDTA, 100 mM KCl, 40% (v/v) glycerol, 0.5 mM DTT.

R-buffer: 20 mM Tris-HCl (pH 7.5), 0.1 mM EDTA, 10% (v/v) glycerol, 0.5 mM DTT.

SDS gel buffer A: 375 mM Tris-HCl (pH 8.8), 0.1% (w/v) SDS.

SDS gel buffer B: 125 mM Tris-HCl (pH 6.8), 0.1% (w/v) SDS.

SDS gel reservoir buffer: 25 mM Tris base, 190 mM glycine, 0.1% (w/v) SDS.

SDS gel storage buffer: 50 mM EDTA, 5% (v/v) glycerol.

SDS sample buffer A (4x): 125 mM Tris-HCl (pH 6.8), 10% (v/v) glycerol, 2% (w/v) SDS, 100 mM DTT, 0.02% (w/v) bromophenol blue.

SDS sample buffer B (4x): 200 mM Tris-HCl (pH 6.8), 40% (v/v) glycerol, 8% SDS, 40 mM DTT, 0.4% (w/v) bromophenol blue.

Sepharose column buffer: 50 mM Tris-Ac (pH 7.5), 5 mM $Mg(OAc)_2$, 20 mM K(OAc), 1 mM DTT, 100 μg/ml BSA.

Spermidine buffer: 20 mM Tris-Ac (pH 7.5), 7 mM spermidine-KOH (pH 7.5), 0.1 mM DTT.

Strand exchange buffer: 50 mM Tris-Ac (pH 7.5), 15 mM $Mg(OAc)_2$, 20 mM K(OAc), 2 mM ATP, 2 mM DTT, 100 μg/ml BSA.

TAE buffer: 40 mM Tris base, 1.1% (v/v) glacial acetic acid, 1 mM EDTA.

TBE buffer: 89 mM Tris base, 89 mM boric acid, 2 mM EDTA.

TBS-Tween: 20 mM Tris base, 137 mM NaCl, 15 mM HCl, 0.05% (v/v) Tween-20.

TE buffer: 10 mM Tris-HCl (pH 8.0), 1 mM EDTA.

TEGD buffer: 20 mM Tris-HCl (pH 7.5), 1 mM EDTA, 10% (v/v) glycerol, 0.5 mM DTT.

TESS buffer: 80 mM Tris-Ac (pH 7.5), 1 mM EDTA, 5 mM Na(OAc), 0.03% (w/v) SDS.

TNE buffer: 10 mM Tris-HCl (pH 8.0), 1 mM EDTA, 50 mM NaCl.

Topo I buffer (*E. coli*): 50 mM Tris-HCl (pH 7.5), 0.1 mM EDTA, 10 mM $MgCl_2$, 50 mM KCl, 0.5 mM DTT, 30 μg/ml BSA.

TPA medium: 9 g/l casein hydrochloride, 0.8 g/l Na pyruvate, 1.1 g/l NH_4Cl, 22.7 mg/l Na_2SO_4, 0.01 mg/l $FeCl_3$, 2 mg/l thymine, 100 mM Tris-HCl (pH 7.5), 8.5 mM NaCl, 108 mM KCl, 1 mM $MgCl_2$, 1 mM $CaCl_2$, 0.05 mM KH_2PO_4, 0.4% (w/v) glucose.

Unwinding buffer: 25 mM Tris-HCl (pH 7.5), 0.5 mM EDTA, 30 mM $MgCl_2$ (for RuvB reactions) or 15 mM $MgCl_2$ (for RuvAB reactions), 0.5 mM ATP, ATPγS (as stated), 2 mM DTT, 100 μg/ml BSA.

Unwinding stop buffer (5x): 200 mM EDTA, 0.1 mg/ml proteinase K, 2% (w/v) SDS.

Western blot transfer buffer: 25 mM Tris base, 190 mM glycine, 20% (v/v) methanol.

2.4 BACTERIAL STRAINS

JC12772 is *E. coli* strain AB1157 (Bachmann, 1972) containing plasmid pBEU14 (Uhlin and Clark, 1981; section 2.5). HRS1004 is a derivative of AB1157 containing a deletion of the *ruvAB* operon (Iwasaki *et al.*, 1989b), and was kindly provided by Prof H. Shinagawa (Osaka University). FB820, a gift from Dr F. E. Benson, is a Δ*ruvAB* derivative of JM101 (Yanisch-Perron *et al.*, 1985) generated by P1 transduction from HRS1004. HI24 is derived from AB1157 and contains a *ruvB4* mutation (Otsuji *et al.*, 1974; Sharples *et al.*, 1990) (provided by Prof R. G. Lloyd, Nottingham University). Other strains used were DH5α (Grant *et al.*, 1990) and JM109 (Yanisch-Perron *et al.*, 1985).

E. coli cells were grown in Luria broth (LB) or on LB agar plates, unless stated otherwise. Cells were stored at –20°C and –70°C in 30% (v/v) glycerol.

2.5 PLASMIDS

pBEU14 is a *recA*$^+$ derivative of the runaway-mutant plasmid pBEU1 and can be amplified, to increase the *recA* gene dosage, by shifting the growth temperature of the host cells (Uhlin and Clark, 1981). pGTI19 is a *ruvB*$^+$ derivative of pUC19 (Yanisch-Perron *et al.*, 1985) in which the *ruvB* gene is under control of the vector *lac* promoter (Sharples *et al.*, 1990). pME3 and pME4 are derivatives of

pGTI19 carrying the mutant $ruvB^{D113E}$ and $ruvB^{K68N}$ genes, respectively. The mutations were introduced into the *ruvB* gene of pGTI19, using the Transformer site-directed mutagenesis kit (Clontech), by Dr C. Mezard (George *et al.*, 1999). pDEA-7Z f(+) was constructed by Dr D. E. Adams by replacing the *Sca*I-*Bsa*I fragment of pGEM-7Z f(+) (Promega) with the *Sca*I-*Bsa*I fragment of pBR322 (Promega) (Shah *et al.*, 1994a). pAKE-7Z was made by Dr A. K. Eggleston by inserting the 1668 bp *Asp*700-*Hinc*II fragment of pACYC184 (Promega) into pDEA-7Z at the *Sca*I site (Eggleston *et al.*, 1997). Form I Bluescript KS plasmid DNA was purchased from Stratagene. pFB585, a 7667 bp derivative of pAcSG2, was provided by Dr F. E. Benson (Van Dyck *et al.*, 1998). pREP4 (Qiagen) is a low copy number plasmid, derived from pACYC, that contains the *lacI* gene (Farabaugh, 1978).

Plasmids were maintained in *E. coli* by adding the following antibiotics to the growth medium: 100 μg/ml (unless stated otherwise) carbenicillin (pBEU14, pGTI19, pME3, pME4, pDEA-7Z, pBluescript, pFB585), 35 μg/ml chloramphenicol (pAKE-7Z) or 25 μg/ml kanamycin (pREP4).

II. GEL ELECTROPHORESIS AND ANALYSIS

2.6 SDS-PAGE

SDS-PAGE allows proteins to be separated according to their molecular weight (Laemmli, 1970) and was conducted using Bio-Rad Mini-PROTEAN II or 20 x 13 cm Cambridge Biosciences gel apparatus. Running gels contained 10 or 12% (w/v) polyacrylamide, supplied as a 30% stock (37.5:1 ratio of acrylamide/bisacrylamide), in SDS gel buffer A. Stacking gels contained 6% (w/v) polyacrylamide in SDS gel buffer B. The acrylamide was polymerised by the addition of 0.08% (w/v) ammonium persulphate and 0.08% (v/v) TEMED. Protein samples were prepared by the addition of 1/3 vol SDS sample buffer A

(4x) (unless stated otherwise) and were boiled for 3 min prior to loading. Gel electrophoresis was performed in SDS gel reservoir buffer at 150 V for 70 min (Mini-PROTEAN II) or at 180 V for 100 min (Cambridge gel), unless stated otherwise.

Proteins were visualised by Western blotting (section 2.16) or by Coomassie blue staining. In the latter case, gels were soaked in Coomassie blue stain solution for ~30 min, and then soaked in several changes of destain solution until all background staining was removed. Gels were kept in SDS gel storage buffer for photography and subsequently dried between two sheets of cellophane.

2.7 AGAROSE GEL ELECTROPHORESIS

Gels containing 0.7-1.2% (w/v) agarose in TAE buffer were prepared using the Bio-Rad Wide Mini-Sub cell system, except where stated otherwise. 1/9 vol agarose gel loading buffer (10x) was added to DNA samples and gels were run in TAE buffer at 4.6 V/cm for 2-3.5 hrs, unless stated otherwise. Ethidium bromide (0.5 μg/ml) was included in the gel and electrophoresis buffer where indicated.

Following electrophoresis, DNA was stained with 1 μg/ml ethidium bromide (in ddH_2O) for 30-45 min and visualised under short-wave UV light (Sharp *et al.*, 1973). Images of stained gels were obtained using a digital camera with a Bio-Rad Gel Doc 1000 set up running Molecular Analyst software. ^{32}P-labelled DNA was detected by autoradiography (section 2.10) and quantified by PhosphorImager analysis (section 2.11).

2.8 NEUTRAL PAGE

Gels were prepared in Bio-Rad PROTEAN II apparatus and contained 6-10% (w/v) polyacrylamide, supplied as a 30% stock (37.5:1 ratio of acrylamide/bisacrylamide), in TBE buffer. The acrylamide was polymerised by the addition of 0.07% (w/v) ammonium persulphate and 0.15% (v/v) TEMED. DNA samples were prepared by the addition of 1/2 to 1/9 vol neutral gel loading buffer. Electrophoresis was conducted in TBE buffer at 150 V for 1-2 hrs, unless stated otherwise. Low ionic strength PAGE was conducted as described (section 2.36). ^{32}P-labelled DNA was detected by autoradiography (section 2.10) and quantified by PhosphorImager analysis (section 2.11).

2.9 DENATURING PAGE

Denaturing PAGE was conducted in Bio-Rad Sequi-Gen nucleic acid sequencing apparatus (small: 21x50 cm; large: 38x50 cm), except when gel purifying oligos for which the Bio-Rad PROTEAN II apparatus was used (section 2.28). Gels contained 7 M urea and 8-12% (w/v) polyacrylamide, supplied as a 40% stock (19:1 ratio of acrylamide/bisacrylamide), in TBE buffer. The acrylamide was polymerised by the addition of 0.03% (w/v) ammonium persulphate and 0.13% (v/v) TEMED (except for the plug where 0.13% and 0.5% were added, respectively). Gels were pre-run at 65 W (small gels) or 100 W (large gels) until preheated to 50°C (~2 hrs). DNA samples were then heated to 95°C for 3 min in formamide loading buffer, cooled on ice and loaded immediately. Electrophoresis was conducted in TBE buffer at 65 W/100 W for variable times according to the size of the DNA fragments analysed. ^{32}P-labelled DNA was detected by autoradiography (section 2.10) and quantified by PhosphorImager analysis (section 2.11).

2.10 AUTORADIOGRAPHY

Following electrophoresis, agarose and polyacrylamide gels were dried onto 3MM filter paper (BDH) or DE81 anion exchanger paper (Whatman) before being exposed to Kodak X-Omat or BioMax film. Intensifying screens were used at –80°C where necessary. Exposed film was developed using a Fuji RG II X-ray film processor.

2.11 PHOSPHORIMAGER ANALYSIS

Dried gels and thin-layer chromatography (TLC) plates were exposed to Molecular Dynamics storage phosphor screens for up to 24 hr. Screens were subsequently analysed using a Molecular Dynamics model 425E PhosphorImager running ImageQuant software.

III. PROTEIN PURIFICATION AND TECHNIQUES

2.12 EXPRESSION AND PURIFICATION OF RECA

A 1 litre culture of JC12772 was grown up overnight with aeration at 37°C in LB supplemented with carbenicillin (50 μg/ml). The starter culture was transferred into a 12-litre fermenter (Biolafitte) containing 8 litres of fermenter medium supplemented with 50 μg/ml carbenicillin and ~5 ml antifoam A (Sigma). The fermenter culture was grown at 30°C with aeration (2.5 l/min) and stirring (250 rpm). At an absorbance (A_{600}) of 3.5 (~3 hr growth), the fermenter was steam-blasted to rapidly shift the temperature to 42°C in order to induce the over-expression of RecA protein, and incubation was continued at 42°C for 4 hr (Figure 2.1A). Cells were chilled on ice and harvested by centrifugation at 4,000 rpm for 25 min at 4°C (Beckman J-6B centrifuge). The pellets were washed with ice-cold lysis buffer A and centrifuged at 8,000 rpm for 10 min at 4°C (Sorvall

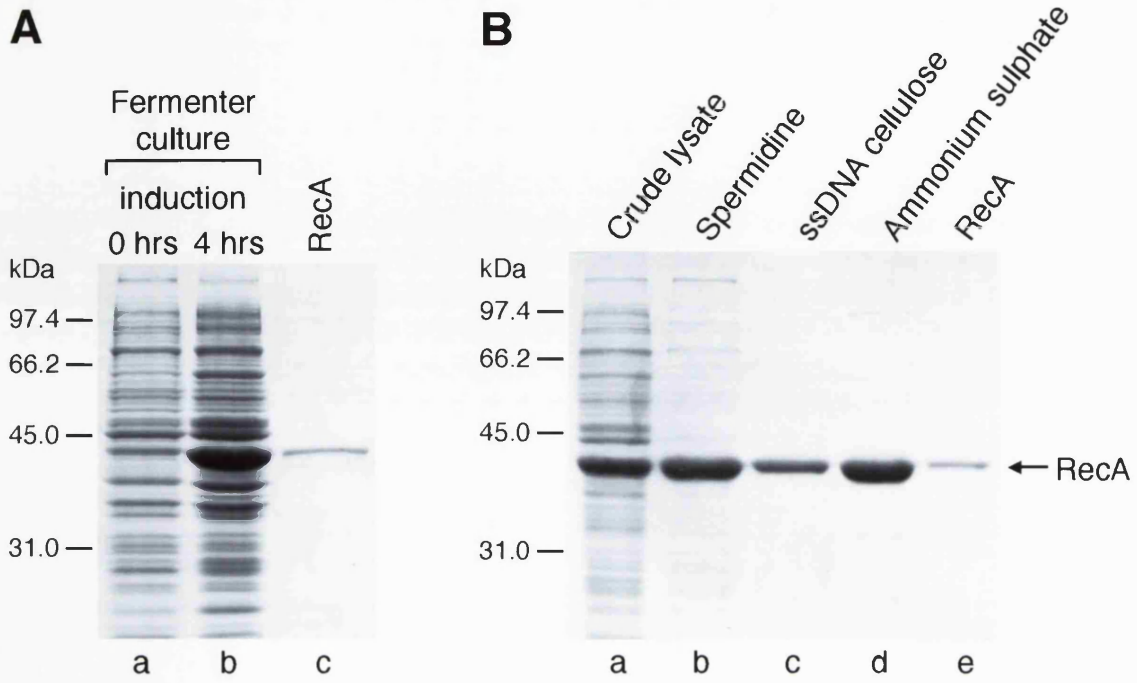

FIGURE 2.1. EXPRESSION AND PURIFICATION OF RECA

A. A 1 litre starter culture of JC12772 was grown up overnight at 37°C, in Luria broth supplemented with 50 μg/ml carbenicillin. Fermenter medium (8 litres) was inoculated with the starter culture and the cells were grown under fermenter conditions, at 30°C, as described in the text. At an OD_{600} of 3.5, the cells were induced by shifting the temperature to 42°C. Samples were taken 0 and 4 hrs after induction and analysed by 12% SDS-PAGE along with a RecA marker (lane c). Proteins were visualised by Coomassie blue staining. The positions of the molecular weight markers are indicated.

B. Purification of RecA. Samples at each stage in the purification scheme were analysed by 12% SDS-PAGE. Lane a, crude cell lysate; lane b, sample following spermidine precipitation; lane c, fraction eluted from ssDNA cellulose column; lane d, final purified RecA following ammonium sulphate precipitation; lane e, purified RecA marker (1 μg).

centrifuge, GSA rotor). Cell pellets were fast-frozen in dry ice/ethanol and stored at -80°C until required. Approximately 15 g wet cells were obtained per litre of culture.

RecA protein was purified by a modification of published procedures (Cox *et al.*, 1981; Griffith and Shores, 1985). 70 g frozen cells were thawed, resuspended in 70 ml lysis buffer A and lysed by the addition of 42 ml 5 mg/ml lysozyme solution (in 250 mM Tris-HCl, pH 7.5). After 10 min on ice, 175 ml Brij solution was added followed by a further 10 min incubation. Dimethyl sulfoxide (DMSO) was added to a final concentration of 0.75% (v/v) and 50 mM phenylmethylsulfonyl fluoride (PMSF) solution (in isopropanol) was added dropwise to 290 μM. The lysate was then incubated on ice for 20 min, after which DNase I (5 mg/ml solution in lysis buffer B containing 570 μM PMSF) was added to a final concentration of 20 μg/ml. Following 1 hr incubation at room temperature, the lysate was centrifuged at 13,000 rpm for 90 min at 4°C (Sorvall centrifuge, GSA rotor). All subsequent steps were performed at 4°C.

After centrifugation, the volume of the clear supernatant was measured and 0.3 g/ml ammonium sulphate was added slowly. After stirring for 1 hr, the suspension was centrifuged at 13,000 rpm for 1 hr (Sorvall centrifuge, GSA rotor). The protein pellet was carefully resuspended in 70 ml spermidine buffer and dialysed against 5 x 2 litres of spermidine buffer for a total of ~40 hr, with the occasional mixing of the dialysis bags. After dialysis, the white precipitate was recovered by centrifugation at 13,000 rpm for 30 min and gently resuspended in 150 ml P_1-buffer containing 200 mM NaCl and 25 mM EDTA. The sample was dialysed against 2 x 4 litres of P_1-buffer for 2 x 2 hr (with 25 mM EDTA included in the first dialysis buffer), centrifuged at 13,000 rpm for 30 min and then loaded onto a ssDNA cellulose column (100 ml) equilibrated with

P_1-buffer. After washing the column with P_1-buffer containing 50 mM NaCl, RecA protein was eluted with one column volume of the same buffer supplemented with 1 mM ATP. The column was then washed further with P_1-buffer containing 50 mM NaCl. Fractions containing RecA were pooled and diluted with 1/10 vol 1 M Tris-HCl (pH 8.0). Ammonium sulphate precipitation was carried out as described above and the suspension was centrifuged at 15,000 rpm for 1 hr (Sorvall centrifuge, SS-34 rotor). The protein pellet was resuspended in R-buffer containing 0.3 g/ml ammonium sulphate (using an equivalent volume to the pooled RecA fractions), stirred for 1 hr and then centrifuged as above. Finally, the pellet was resuspended in 12 ml R-buffer containing 1 mM DTT, and dialysed against the same buffer. After centrifuging at 10,000 rpm for 30 min, 50 μl aliquots of the protein were fast-frozen in dry ice/ethanol and stored at -80°C. Working stocks were stored at -20°C. The purification procedure yielded ~140 mg RecA protein from 70 g frozen cells. A sample at each step in the purification scheme was analysed by SDS-PAGE (Figure 2.1B).

2.13 EXPRESSION AND PURIFICATION OF RUVB

E. coli strain FB820 was streaked out onto M9 agar plates, to select for the F' plasmid which carries the *lacI*^{q} gene, and transformed with pGTI19 as described in section 2.26. Single colonies of freshly-transformed FB820 (pGTI19) were used to inoculate 2 x 1 litre of LB supplemented with carbenicillin and 0.2% (w/v) glucose. Cells were grown overnight at 37°C with rapid shaking and then transferred to fermenter medium. The fermenter culture (11 litres) was incubated at 37°C with aeration and stirring as described in 2.12. At an A_{650} of 3.0 (~4 hr growth), over-expression of RuvB protein was induced by the addition of IPTG to 1 mM. After a further 8 hr growth at 37°C, the cells were

chilled on ice and harvested by centrifugation at 4,000 rpm for 15 min at 4°C (Beckman J-6B centrifuge). Pellets were washed with lysis buffer C, centrifuged again, and resuspended in lysis buffer C (3 ml/g wet cells). The cell paste was fast-frozen in dry ice/ethanol and stored at -80°C until required. Approximately 10 g wet cells were obtained per litre of culture.

RuvB protein was purified according to a published procedure (Tsaneva *et al.*, 1992a). 50 ml of cell suspension (corresponding to ~13 g wet cells) were thawed and DTT was added to 1 mM, followed by lysozyme (10 mg/ml solution in 250 mM Tris-HCl, pH 8.0) to 1 mg/ml. After 30 min incubation on ice, Triton X-100 was added to 0.1% (v/v) and incubation was continued for 10 min. Finally, sodium deoxycholate was added to 0.4% (w/v) and insoluble material was removed by centrifugation at 42,000 rpm for 1 hr at 4°C (Beckman ultracentrifuge, Ti60 rotor). All subsequent steps were performed at 4°C.

After centrifugation, the crude lysate was filtered (using a Nalgene 0.45 μm disposable filter unit) and immediately loaded onto a phosphocellulose column (50 ml) equilibrated with TEGD buffer. The flow-through was passed directly onto a DEAE Bio-Gel column (50 ml), also equilibrated with TEGD buffer, and RuvB was eluted with a 500 ml 0 – 300 mM KCl linear gradient (in TEGD). Peak fractions containing RuvB, which eluted between 185 – 215 mM KCl, were pooled, dialysed against P_2-buffer containing 200 mM KCl and loaded onto a hydroxyapatite column (22 ml) equilibrated in the same buffer. Approximately 50% of the RuvB protein eluted from the column as a sharp peak by washing with one column volume of P_2-buffer without KCl (Fraction A). The column was then developed with a 220 ml linear gradient of 10 – 80 mM potassium phosphate (10% (v/v) glycerol, 0.5 mM DTT) and the remaining RuvB eluted between 25 – 45 mM potassium phosphate (Fraction B). Fractions A and B were dialysed against TEGD buffer containing 50 mM NaCl and

applied, in two separate batches, to a 1 ml pre-packed Mono Q FPLC column (Amersham Pharmacia) equilibrated in the same buffer. RuvB was eluted with a 30 ml 50 – 600 mM NaCl linear gradient. Peak fractions containing RuvB (300 – 370 mM NaCl) were pooled and dialysed against protein storage buffer A. 100 μl aliquots of the protein were fast-frozen in dry ice/ethanol and stored at -80°C. Working stocks were stored at -20°C. The purification procedure yielded ~70 mg RuvB protein from 13 g wet cells. A sample at each step in the purification scheme was analysed by SDS-PAGE (Figure 2.2).

2.14 PROTEIN CONCENTRATION DETERMINATION

Approximate protein concentrations were determined using the Bradford assay (Bradford, 1976). The protein solution of interest was diluted to a volume of 800 μl in ddH_2O and mixed with 200 μl of protein assay dye reagent concentrate (Bio-Rad). The colour was allowed to develop for 10 min at 20°C. The absorbance at 595 nm was then measured, using a Pharmacia Ultrospec 2000 spectrophotometer, and compared against a standard curve obtained in parallel with known concentrations of BSA.

The concentrations of purified RecA, RuvB and $RuvB^{D113E}$ were determined directly by spectrophotometry. The absorbance of an aqueous protein solution at 280 nm relates to the protein concentration according to the following equation:

$A_{280} = \varepsilon cd$ where A_{280} = absorbance at 280 nm

ε = extinction coefficient ($M^{-1}cm^{-1}$)

c = protein concentration (M)

d = pathlength, i.e. width of quartz cuvette (cm)

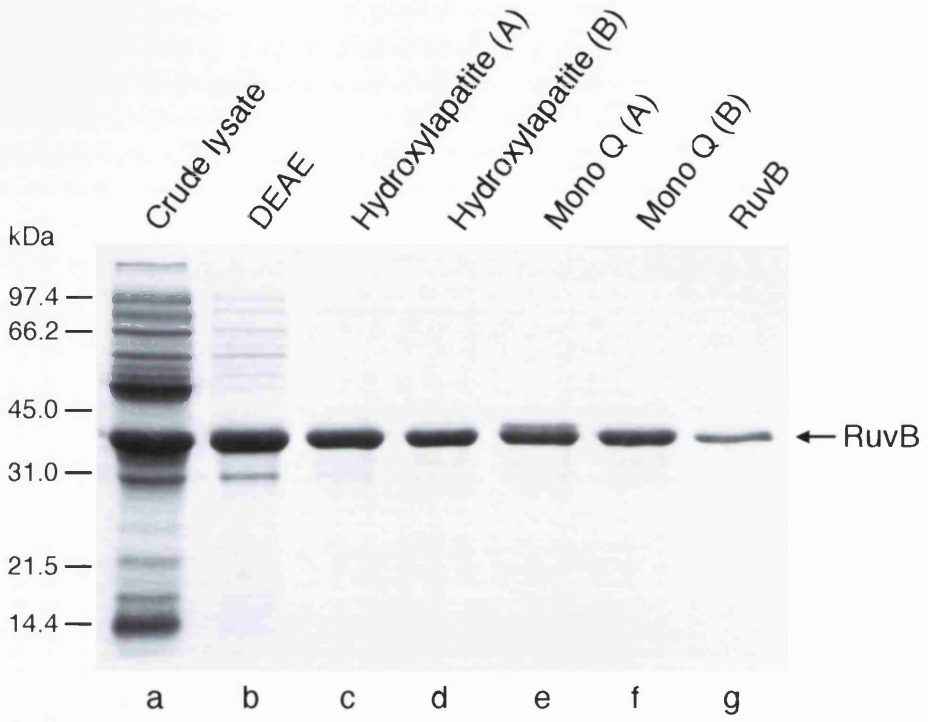

FIGURE 2.2. PURIFICATION OF RUVB

Samples at each stage in the purification scheme were analysed by 10% SDS-PAGE. Lane a, crude cell lysate; lanes b-f, fractions eluted from DEAE-Biogel, hydroxylapatite (A and B) and Mono Q (A and B); lane g, purified RuvB marker (2 μg). Proteins were visualised by Coomassie blue staining. The positions of the molecular weight markers are indicated.

Extinction coefficients of 27,000 $M^{-1}cm^{-1}$, for RecA, and 16,400 $M^{-1}cm^{-1}$, for RuvB (Marrione and Cox, 1995), have been determined based on their tryptophan and tyrosine residue content (Edelhoch, 1967). All protein concentrations are expressed in moles of monomer.

2.15 MOLECULAR WEIGHT STANDARDS

Protein standards (Bio-Rad low molecular weight standards) used for SDS-PAGE, except when preceding Western blotting, were: phosphorylase b (97.4 kDa), bovine serum albumin (66.2 kDa), ovalbumin (45 kDa), carbonic anhydrase (31 kDa), trypsin inhibitor (21.5 kDa) and lysozyme (14.4 kDa). SeeBlue pre-stained standards (Novex) used for Western blotting (section 2.16) were: myosin (250 kDa), bovine serum albumin (98 kDa), glutamic dehydrogenase (64 kDa), alcohol dehydrogenase (50 kDa), carbonic anhydrase (36 kDa), myoglobin (30 kDa), lysozyme (16 kDa), aprotinin (6 kDa) and insulin B chain (4 kDa).

2.16 WESTERN BLOTTING

Protein samples were subjected to SDS-PAGE as described in section 2.6. Gels were soaked in Western blot transfer buffer for 20 min before blotting onto Immobilon-P membrane (Millipore). Prior to use, the membrane was prepared by immersing for 2-3 min in methanol and rinsing in ddH_20 and transfer buffer. Western blotting was conducted, using a Hoefer Transphor electrophoresis blotting unit (TE22 model), in transfer buffer at 30 V/40 mA overnight (at 4°C). Following transfer, membranes were blocked with 5% (w/v) dried milk (Marvel) in TBS-Tween for 1 hr at room temperature, on a rocker. Primary polyclonal antibodies against RuvB (1/10,000) or RuvC (1/4,000) were added directly to the blocking solution and incubation was continued for 2 hrs. The

blots were rinsed with TBS-Tween briefly and then washed for 4 x 15 min in the same buffer. Horseradish peroxidase-conjugated anti-rabbit secondary antibodies (1/4,000 dilution) were applied to the membranes in a solution of 5% (w/v) dried milk/TBS-Tween. After 1 hr incubation, the membranes were washed in TBS-Tween, as described above, and then subjected to enhanced chemiluminescence (ECL) detection. After treatment with ECL reagents (Amersham Pharmacia) for 1 min, membranes were exposed to X-Omat film for different lengths of time, ranging from 5 sec to 5 min.

2.17 Electron Microscopy

For analysis by electron microscopy, RuvB or RuvB^{D113E} (4 μM) were incubated with *Pst*I-linearised duplex pAKE-7Z DNA (32 μM) in DNA binding buffer B. After 5 min incubation at 37°C, protein-DNA complexes were fixed by the addition of 1/10 vol 2.5% (v/v) glutaraldehyde (freshly diluted, from a 25% stock, in 50 mM triethanolamine-acetate, pH 7.5), followed by incubation for 15 min at 37°C. Samples were stained with 2% (w/v) uranyl acetate (Spiess *et al.*, 1987) and visualised at a magnification of 70,000x, using a Phillips CM10 electron microscope. All microscopy work was conducted by Dr A. Stasiak (University of Lausanne).

2.18 Covalent Cross-linking of Proteins

Reactions (20 μl) contained 1 μg RuvB or RuvB^{D113E} and 0.5 μg RuvC in protein cross-linking buffer, and were incubated for 10 min at 30°C. 1/18 vol 0.25% (v/v) glutaraldehyde (freshly diluted, from a 25% stock, in 50 mM triethanolamine-HCl, pH 8.2) was added and the reactions were incubated for 30 min at 30°C. The cross-linking was quenched by the addition of ethanolamine-HCl (pH 8.0) to a final concentration of 215 mM, followed by

incubation for 10 min at 30°C. Samples were diluted with 1/3 vol SDS sample buffer B (4x), boiled for 3 min and subjected to 10% SDS-PAGE (section 2.6). Proteins were visualised by Western blotting using rabbit polyclonal antibodies raised against either RuvB or RuvC (section 2.16).

IV. GENERAL METHODS OF DNA MANIPULATION

2.19 DNA CONCENTRATION DETERMINATION

DNA concentrations were determined by measuring the absorbance (A) at 260 nm, using a quartz cuvette and a Pharmacia Ultrospec 2000 spectrophotometer. Calculations were based on the assumption that the A_{260}= 1 (measured in a cuvette with a 1 cm pathlength) for a solution of 50 μg/ml dsDNA, 40 μg/ml ssDNA or 33 μg/ml oligonucleotide. Concentrations of ^{32}P-labelled oligonucleotides (section 2.25) and branch migration substrates (sections 2.31-2.33) were determined by calculating the specific activity using Whatman DE81 filters (Sambrook *et al.*, 1989). DNA concentrations are expressed in moles of nucleotides except where stated otherwise.

2.20 SOLVENT EXTRACTION

Solvents used were phenol/chloroform/iso-amyl alcohol (25:24:1), chloroform/iso-amyl alcohol (24:1), butan-2-ol and diethyl ether. Samples were mixed thoroughly with an equal volume of the relevant solvent and the two phases (organic and aqueous) separated by low speed centrifugation. In each case the aqueous phase was retained for further processing. To maximise recovery, solvent extraction was often followed by a back-extraction. In these cases, ddH_2O was mixed with the organic phase, centrifuged as above and the aqueous phases combined.

2.21 ETHANOL PRECIPITATION

DNA samples were mixed with 1/10 vol 3 M sodium acetate (pH 5.2) followed by 2.5 vol ethanol (ice-cold). After at least 15 min at -80°C, or 2 hr at -20°C, precipitated DNA was pelleted by centrifugation (14,000 rpm, 15-30 min, 4°C in an Eppendorf Model 5415 C benchtop centrifuge). DNA pellets were washed with 70% (v/v) ethanol (ice-cold), dried using a Savant speed vac concentrator (model SC110) and resuspended in TE buffer.

To analyse gel-purified oligonucleotides (section 2.28) by denaturing PAGE, ^{32}P-labelled DNA samples were precipitated by the addition of 20 μg carrier tRNA, 1/2 vol 7.5 M ammonium acetate (pH 5.2) and 3 vol ethanol (ice-cold). After 15 min at -80°C, precipitated DNA was collected, washed and air-dried as described above. Pellets were resuspended in formamide loading buffer.

2.22 SUCROSE DENSITY GRADIENT CENTRIFUGATION

5-20% (w/v) sucrose gradients were prepared in 40 ml polyallomer ultracentrifuge tubes (Beckman), using neutral sucrose solutions (section 2.3) and a gradient maker. DNA samples were applied in TE buffer (200 μl). Gradients were spun at 26,000 rpm for 18-20 hr (at 4°C) in a Beckman ultracentrifuge (SW28 rotor). 1 ml fractions were collected from the bottom of the gradient and 10 μl aliquots were analysed by 0.8% agarose gel electrophoresis (section 2.7).

2.23 ELECTROELUTION OF DNA

For electroelution of gDNA (section 2.31.1), each agarose gel slice was placed into one or two lengths of dialysis tubing each containing ~8 ml TAE buffer,

being careful to avoid trapping any air inside the tubing. DNA was recovered from the gel slices by electroelution at 50 V overnight (at 4°C) in BRL Horizon 20.25 gel tanks containing TAE buffer. The polarity of the current was then reversed for 2 min and the gDNA (in TAE) was collected for subsequent processing.

DNA was electroeluted from neutral and polyacrylamide gel slices using a Biotrap BT1000 chamber (Schleicher & Schuell). The gel slice was placed in the compartment between the two semi-permeable BT2 filters containing 0.5 ml TBE buffer (a non-permeable BT1 filter was placed at each end of the chamber and 0.5 ml/13 ml TBE buffer were added to the small and large BT1-BT2 compartments, respectively). The chamber was placed in a shallow layer of TBE buffer, in a BRL Horizon 20.25 gel tank, and the DNA was recovered by electroelution at 100 V for 1 hr (at 4°C). The polarity of the current was reversed for 30 sec before collecting the DNA from the small BT1-BT2 compartment.

2.24 Recovery of Gel-Purified Oligonucleotides

Oligonucleotides purified by denaturing PAGE were eluted in gel crush buffer (section 2.28) and recovered using Sep-Pak (C18) cartridges (Waters). After pre-treatment with 10 ml methanol followed by 10 ml ddH_2O, the DNA/gel sample was passed through the cartridge via a 0.2 μm Acrodisc filter (Gelman Sciences). The cartridge was washed with 5 ml ddH_2O and the DNA was eluted with 2 x 1 ml 60% (v/v) methanol.

2.25 ^{32}P-End-Labelling of DNA

Oligonucleotides were 5′ ^{32}P-end-labelled using T4 polynucleotide kinase and [γ-^{32}P]ATP. Typical labelling reactions (20 μl) contained 40 pmol oligonucleotide (in terms of molecules), 20-50 μCi [γ-^{32}P]ATP and 20 U T4 polynucleotide kinase

in One-Phor-All buffer. After incubation for 45 min at 37°C, reactions were diluted to 60 μl with ddH_20 and stopped by the addition of SDS and EDTA to 0.8% (w/v) and 25 mM, respectively. The DNA was extracted with phenol/chloroform/iso-amyl alcohol as described (section 2.20) and then back-extracted with 30 μl ddH_2O. Unincorporated label and residual organic solvent were removed on a G-25 MicroSpin column (Amersham Pharmacia). The column was prepared by centrifugation for 1 min at 3,000 rpm, in an Eppendorf Model 5415 C benchtop centrifuge. The combined aqueous phase from the extractions (~93 μl) was applied to the column and centrifugation was continued for a further 2 min. The eluate from the second spin (i.e. ^{32}P-labelled oligonucleotide DNA) was mixed with 1/2 vol ethanol, to help minimise radiolysis damage to the DNA, and stored at 4°C until required.

DNA was 3′ ^{32}P-end-labelled using the Amersham Pharmacia 3′ end-labelling kit and [α-^{32}P]ddATP. Reactions (50 μl) contained 8 μg *Pst*I-linearised pAKE-7Z DNA, 30 μCi [α-^{32}P]ddATP and 10 U terminal deoxynucleotidyl transferase in cacodylate buffer. After 90 min incubation at 37°C, labelling reactions were stopped by the addition of SDS and EDTA to 0.8% (w/v) and 25 mM, respectively. The DNA was extracted with phenol/chloroform/iso-amyl alcohol (section 2.20) and back-extracted with 50 μl ddH_2O. Unincorporated label was removed using a S-400 MicroSpin column (Amersham Pharmacia), as described above for a G-25 column. 1/2 vol ethanol was added to the eluate and the labelled DNA was stored at 4°C until required.

2.26 TRANSFORMATION OF DNA INTO BACTERIAL STRAINS

5 ml LB was inoculated with a single colony of the bacterial strain to be transformed and cells were grown up overnight at 37°C with aeration. 50 ml LB were inoculated with 0.5 ml of the starter culture and incubated at 37°C with

rapid shaking. At an A_{650} of 0.3-0.5 (~2.5 hrs growth), the culture was divided into 10 ml portions and chilled on ice for 10 min. Cells were pelleted by centrifugation at 5,000 rpm for 5 min (Sorvall centrifuge, SS-34 rotor) and washed twice with 5 ml ice-cold $CaCl_2$ solution (100 mM). Cells were resuspended in 0.6 ml 100 mM $CaCl_2$ and kept on ice for at least 30 min before being used in transformations.

To introduce plasmid DNA into competent cells, 50 ng DNA (in 5 μl TE) were mixed with 0.2 ml of the cell suspension. After 30 min incubation on ice, cells were heat-shocked for 2 min at 42°C and immediately transferred back onto ice. After 2 min, 0.8 ml LB was added and samples were incubated for 45 min at 37°C. Serial dilutions of the cell suspensions were made and 0.1 ml aliquots spread on LB agar plates containing the appropriate antibiotic (section 2.5). Plates were incubated at 37°C overnight, or until colonies were observed. Single colonies were streaked onto fresh selective LB agar plates.

V. PREPARATION OF DNA SUBSTRATES

2.27 PREPARATION OF PLASMID DNA

A 400 ml culture of DH5α (pBluescript), DH5α (pAKE-7Z) or JM109 (pDEA-7Z) was grown up overnight with aeration in a 37°C shaking incubator. Cells were harvested by centrifugation for 15 min at 6,000 rpm (Sorvall centrifuge, GSA rotor). Form I (native) plasmid DNA was isolated using the Qiagen plasmid purification kit (Maxi kit), according to the manufacturer's protocol. The DNA pellets obtained were air-dried, resuspended in 0.5 ml TE buffer and stored at -20°C. The procedure typically yielded 0.5 - 1 mg plasmid DNA.

2.28 OLIGONUCLEOTIDES

Ref.	Size (nt)	Sequence (5′ to 3′)	Use
SW141	20	CCCACAAAGTCCAGCGTACC	Helicase substrate
SW356	66	AGTGTTAACTTCTGCGTCATGGAAGCGATA AAACTCTGCAGGTTGGATACGCCAATCATT TTTATC	Helicase substrate
SW17	50	CGCTGCCGAATTCTACCAGTGCCATTGCTT TGCCCACCTGCAGGTTCACC	X-junction
SW36	50	GGTGAACCTGCAGGTGGGCAAAGCAATGG CAATCGTCAAGCTTTATGCCG	X-junction
SW37	50	CGGCATAAAGCTTGACGATTGCCATTGCTT TTCTAGAGGATCCGACTATC	X-junction
SW38	50	GATAGTCGGATCCTCTAGAAAAGCAATGG CACTGGTAGAATTCGGCAGCG	X-junction
SW275* (oligo 1)	26	GGTCTTCTTCTAGGCCTTCTTCTTCT	Y-junction
SW276 (oligo 2)	56	GATCTGTCGTGGCCTAGAAGAAGACCGGT ACGCTGGACTTTGTGGGATACCCTCGC	Y-junction
SW277 (oligo 3)	30	GCGAGGGTATCCCACAAAGTCCAGCGTAC C	Y-junction/ helicase substrate
SW278 (oligo 4)	24	AGAAGAAGAAGGCCACGACAGATC	Y-junction

*An additional oligonucleotide (oligo 1^{ps}) with the same sequence as SW275 but containing a *cis*-syn 2-carbomethoxypsoralen furan-side thymidine monoadduct (Kobertz and Essigmann, 1996) at the position of nt 11 was kindly provided by Dr J. M. Essigmann (MIT). The monoadduct was synthesised by Dr W. R. Kobertz and incorporated into the 26 nt oligonucleotide by Dr D. A. Nauman.

All oligonucleotides presented in the table above were prepared on PE Biosystems DNA synthesisers (models 394 and 3948) in the Oligonucleotide Synthesis Laboratory (Imperial Cancer Research Fund, Clare Hall) using PE

Biosystem reagents and protocols. Following synthesis, oligonucleotides SW276 and SW356 were purified by reverse-phase HPLC.

To remove nested fragments generated in the synthesis process, all oligonucleotides were gel-purified. 100-150 μg oligonucleotide DNA were ethanol precipitated by the addition of 1/9 vol 3M sodium acetate (pH 5.2), 1/99 vol 1M $MgCl_2$ and 3 vol ethanol (ice-cold) essentially as described in section 2.21. DNA pellets were resuspended in formamide loading buffer (without xylene cyanol) and subjected to 8 or 10% denaturing PAGE for 2.5 - 4 hr at 300 V (section 2.9). The gel was placed onto a TLC aluminium silica gel 60 plate (Merck) and the DNA was visualised (as dark blue bands) under short-wave UV light. The full-length oligonucleotide bands were excised, and the gel slices crushed and soaked overnight at 4°C in gel crush buffer (3 ml), with constant mixing. The eluted DNA was recovered using Sep-Pak (C18) cartridges (section 2.24), dried using a Savant speed vac concentrator and resuspended in TE buffer. To confirm the purity of the oligonucleotides, ~100-200 ng DNA were 5′ ^{32}P-end-labelled (section 2.25), ethanol precipitated (section 2.21) and analysed by 8% denaturing PAGE followed by autoradiography (sections 2.9 and 2.10).

2.29 PREPARATION OF HELICASE SUBSTRATES

Helicase substrates were prepared by annealing 20, 30 or 66 nt oligonucleotides (section 2.28) to ϕX174 virion DNA. The 20-mer (SW141) was complementary to ϕX174 DNA at nt 570-589, the 30-mer (SW277) was complementary to nt 570-599, and the 66-mer (SW356) to nt 5357-36. 5′ ^{32}P-end-labelled oligonucleotide DNA (section 2.25) was mixed with 8.5 μg ϕX174 virion DNA in a 4:1 (molecule per molecule) ratio in 100 μl annealing buffer, heated for 3 min at 95°C, incubated for 30 min at 68°C, and slowly cooled to room temperature.

Annealed substrates were purified by gel filtration through a 3 ml BioGel A-0.5m column equilibrated in BioGel column buffer. Two-drop fractions were collected from the column and two peaks of radioactivity were detected, corresponding to annealed substrate and free ^{32}P-labelled oligonucleotide. Fractions in the first peak were pooled and stored at -20°C. Helicase substrate concentrations were determined by the absorbance at 260 nm (section 2.19) and are expressed in moles of nucleotides.

2.30 PREPARATION OF ^{32}P-LABELLED PLASMID DNA

Uniformly ^{32}P-labelled pFB585 DNA was prepared by growth in *E. coli* JM109 cells in the presence of [^{32}P]orthophosphate. A 50 ml culture of JM109 (pFB585) was grown overnight with aeration at 37°C in LB supplemented with 50 μg/ml carbenicillin. The next day, 4 x 6.25 ml of the starter culture were used to inoculate four flasks each containing 250 ml TPA medium (+50 μg/ml carbenicillin), and cells were grown at 37°C with rapid shaking. After 2 hrs, chloramphenicol was added to a final concentration of 100 μg/ml and incubation was continued. 30 min later, 100 μCi [^{32}P]orthophosphate was added to each flask and the cultures were grown with aeration for a further 5.5 hrs at 37°C. The cells were then harvested by centrifugation at 4°C for 15 min at 6,000 rpm (Sorvall centrifuge, GS-3 rotor) and the ^{32}P-labelled form I plasmid DNA purified using the Qiagen plasmid purification kit (Mega kit). The DNA pellet obtained was resuspended in 2 ml TE and dialysed against 2 litres of TE/10% (v/v) ethanol overnight at 4°C. (The ethanol was essential to minimise radiolysis damage to the DNA). The procedure typically yielded 1 mg ^{32}P-labelled plasmid DNA.

Relaxed ^{32}P-labelled pFB585 DNA was prepared by treating form I (supercoiled) DNA with *E. coli* topoisomerase I. The amount of enzyme

required for complete relaxation was pre-determined by conducting titration experiments. *E. coli* topoisomerase I was then incubated with 60 μg ^{32}P-labelled form I DNA, in the presence of Topo I buffer, for 1 hr at 37°C. The reaction (3 ml) was stopped by the addition of 1/4 vol unwinding stop buffer (5x), followed by incubation for 15 min at 37°C. The DNA was extracted with phenol/chloroform/iso-amyl alcohol as described (section 2.20) and back-extracted with 2 ml TE. The combined aqueous phase was then extracted with chloroform/iso-amyl alcohol, to remove any remaining phenol. The ^{32}P-labelled relaxed pFB585 DNA was ethanol precipitated (section 2.21) and the pellet resuspended in 100-150 μl TE. In some cases, it was necessary to desalt the DNA solution by repeated dilution and re-concentration on a Microcon-30 microconcentrator (Amicon). Ethanol was added to 10% (v/v) to the final DNA sample and storage was at 4°C. DNA concentrations were determined by the absorbance at 260 nm (section 2.19) and are expressed in moles of nucleotides.

2.31 PREPARATION OF RECOMBINATION INTERMEDIATES (α-STRUCTURES)

2.31.1 Preparation of Gapped DNA

pDEA-7Z circular ssDNA was a gift from Dr C. Mézard, and was generated using the helper phage M13K07 as specified by the supplier (Promega). To prepare 2826 bp *Bsa*I-*Pst*I linear duplex DNA, a 4 ml reaction containing 250 μg form I (supercoiled) pDEA-7Z and 500 U *Bsa*I in NEBuffer 4 was incubated for 2 hr at 55°C. After checking a sample for complete digestion on a 0.8% agarose gel (section 2.7), the mixture was incubated for 90 min at 37°C with 200 U of *Pst*I. The digestion reaction was stopped by the addition of EDTA to 10 mM and the DNA was extracted with phenol/chloroform/iso-amyl alcohol and chloroform/iso-amyl alcohol (section 2.20), ethanol precipitated (section 2.21) and resuspended in 200 μl TE buffer. The 2826 bp and 174 bp linear duplex

products were separated by sucrose gradient centrifugation (section 2.22). Fractions containing the 2826 bp fragment were pooled and ethanol precipitated as before.

Trial annealing reactions were conducted between the 2826 bp linear duplex fragment (1 μg) and pDEA-7Z circular ssDNA (1, 1.4 or 2 μg) to determine the optimum ratio for generating gapped DNA (gDNA). Reactions, containing 1/10 vol annealing buffer (10x), were covered with mineral oil, heated in a water bath to 95°C for 6 min and slowly cooled to room temperature. Samples were analysed on a 0.8% agarose gel. Based on these results, 140 μg of the linear fragment were mixed with 280 μg circular ssDNA (total volume: 1.5 ml) and dialysed at 4°C for 2 hr against 2 litres of TE. The DNA mixture was divided into 4 x 375 μl aliquots, 50 μl annealing buffer (10x) and 75 μl ddH_2O were added, and annealing was conducted as described above.

The annealed DNA samples were diluted with 1/9 vol agarose gel loading buffer containing 0.2% (w/v) xylene cyanol and loaded onto 2 x 300 ml 1% agarose gels, prepared using BRL Horizon 20.25 gel apparatus. Gapped circular duplex DNA (gDNA) was separated from other DNA forms by electrophoresis at 200 V for 3 hr at 4°C (in this case, the gDNA migrates just below the xylene cyanol dye). A 2 cm slice was removed from each side of the gels and stained in a concentrated solution of ethidium bromide (2 μg/ml) for 10-15 min. The position of the gDNA was identified using an UV transilluminator and was used as a reference to excise the complete band in the absence of UV. DNA was electroeluted from the gel slices in TAE buffer, as described in section 2.23, and concentrated by extracting twice with butan-2-ol (section 2.20). The gDNA was then extracted once with diethyl ether, ethanol

precipitated (section 2.21), resuspended in 300 μl TE and dialysed overnight at 4°C against 2 x 2 litres of TE.

2.31.2 Preparation of ^{32}P-Labelled Linear Duplex DNA

30 μg form I (supercoiled) pAKE-7Z DNA was incubated for 90 min at 37°C with 100 U *Pst*I in NEBuffer 3. After checking a sample for complete digestion on a 0.8% agarose gel, the linearised DNA was extracted with phenol/chloroform/iso-amyl alcohol and chloroform/iso-amyl alcohol (section 2.20), ethanol precipitated (section 2.21) and resuspended in 35 μl TE buffer. The linear duplex DNA was 3′ ^{32}P-end-labelled as described in section 2.25.

2.31.3 Preparation of α-Structures

Optimum strand exchange conditions were established for each new preparation of gDNA and ^{32}P-labelled linear duplex DNA by conducting small-scale reactions in which the linear duplex and RecA protein concentrations were varied. Samples were run on a 1.2% agarose gel containing ethidium bromide (section 2.7) for 3.5 hr at 65V (with buffer recirculation), and ^{32}P-labelled DNA was visualised by autoradiography (section 2.10). Large-scale preparations (200 μl) typically contained 10 μM gDNA and 6 μM RecA protein in strand exchange buffer, supplemented with 20 mM phosphocreatine and 5 U/ml creatine phosphokinase (to provide an ATP regenerating system). After 5 min preincubation at 37°C, the reaction was initiated by the addition of 3-5 μM 3′ ^{32}P-labelled linear duplex DNA. Following incubation for 1 hr at 37°C, the strand exchange reaction was stopped and the α-structures deproteinised by the addition of 1/4 vol branch migration stop buffer A (5x) followed by incubation for a further 10 min at 37°C. Protein and unwanted chemicals were removed by gel filtration through a 3.5 ml Sepharose CL-2B column

equilibrated in Sepharose column buffer. Two-drop fractions were collected and the peak 6-8 fractions, as detected using a Geiger counter, were pooled. The recombination intermediates (α-structures) were stored in the column buffer at -20°C. DNA concentrations were determined by calculating the specific activity (section 2.19) and are expressed in moles of nucleotides.

2.32 PREPARATION OF SYNTHETIC X-JUNCTION SUBSTRATE

The synthetic Holliday junction X12 (van Gool *et al.*, 1998) was prepared by annealing four 50 nt oligonucleotides (section 2.28). SW17 (200 ng) was 5′ ^{32}P-end-labelled essentially as described in section 2.25. The reaction was stopped by the addition of EDTA to 45 mM, and an excess of oligonucleotides SW36-38 (1 μg of each) was added. Annealing was carried out by heating for 3 min at 90°C and then incubating for 10 min at 65°C, 10 min at 37°C and 10 min at room temperature. The sample was diluted with 1/3 vol neutral gel loading buffer followed by 1/10 vol 10% (w/v) SDS, and subjected to 10% neutral PAGE at 250 V for 100 min (section 2.8).

Annealed products were detected by exposing the wet gel to Kodak X-Omat film for 40 sec (section 2.10). The autoradiograph was used as a reference to excise the band containing X-junction DNA, using a phosphorescent tape, TrackerTape (Amersham Pharmacia), to allow the autoradiograph to be aligned over the gel exactly. Junction DNA was electroeluted from the gel slice in a Biotrap chamber, as described in section 2.23 and dialysed against 2 litres of TNE buffer for 90 min. DNA concentrations were determined by calculation of specific activity using the DE81 filter-binding method (section 2.19), and are expressed in moles of junction. Purified X12 was stored, in TNE, at 4°C.

2.33 PREPARATION OF SYNTHETIC Y-JUNCTION SUBSTRATES

2.33.1 Preparation of Junction Y-2

The cross-linked 3-armed junction Y-2 (Chapter 6, Figure 6.1) was prepared using oligo 1^{ps} (SW275 containing the psoralen monoadduct), oligo 2 (SW276), oligo 3 (SW277) and oligo 4 (SW278) (section 2.28). Oligo 1^{ps} (30 pmol, in terms of molecules) was 5′ ^{32}P-end-labelled as described in section 2.25. After 45 min incubation at 37°C, the labelling reaction was stopped by heat inactivation of the T4 polynucleotide kinase (3 min at 95°C). A 4-fold molar excess of oligo 2 (120 pmol) was added and DNA annealing was promoted as described for the preparation of synthetic X-junctions in section 2.32. Site-specific interstrand cross-links between oligo 1^{ps} and oligo 2 were induced by long-wave UV-irradiation (at 365 nm) using a BLAK-RAY model XX-15 UV lamp (UVP, California). A total dose of 33 kJ/m^2 was given over a 10 min period, as determined using a BLAK-RAY model J221 UV intensity meter. During irradiation, the sample was kept on ice and was covered with a plastic petri dish to eliminate 254 nm UV light which reverses psoralen photoadducts (Kanne *et al.*, 1982; Shim and Kim, 1983; Yeung *et al.*, 1988).

The sample was diluted in an equal volume of 'dye-free' formamide loading buffer (i.e. without both xylene cyanol and bromophenol blue), heated for 3 min at 90°C and immediately subjected to 12% denaturing PAGE at 65 W for 45 min (section 2.9). The cross-linked DNA (oligo 1^{ps} + oligo 2) was identified by autoradiography of the wet gel and recovered by band excision followed by electroelution, as described for the preparation of synthetic X-junctions in section 2.32. The eluted DNA was dialysed against 2 litres of TNE buffer for 1 hr at 4°C, and concentrated using a Microcon-10 microconcentrator (Amicon).

The cross-linked product (~3 pmol, in terms of molecules) was annealed to oligos 3 and 4 (added in 10-fold molar excess), in One-Phor-All buffer, as described (section 2.32). The sample was diluted with 1/2 vol neutral gel loading buffer (without xylene cyanol) and subjected to 10% neutral PAGE at 150 V for 8.5 hr at 4°C (section 2.8). Y-junction DNA was detected by autoradiography of the wet gel, and recovered by band excision followed by electroelution as described (section 2.32). Finally, the cross-linked substrate (Y-2) was dialysed against TNE buffer and concentrated as described above. The final yield of Y-2 obtained from this procedure was 1 pmol.

2.33.2 Preparation of Junctions Y and Y-1

The control junctions Y and Y-1 were prepared by annealing 10 pmol of 5′ ^{32}P-end-labelled oligo 1 or oligo 1^{ps}, respectively, to oligos 2-4 (added in 4-fold molar excess), as described in section 2.33.1. Instead of irradiating with UV light, annealed products were diluted with 1/2 vol neutral gel loading buffer (without xylene cyanol) and subjected to 10% neutral PAGE at 150 V for 8.5 hr at 4°C (section 2.8).

Y-junction DNA was detected by autoradiography, recovered by band excision followed by electroelution, dialysed against TNE buffer and concentrated as described for Y-2 (section 2.33.1). The concentrations of all three Y-junction substrates were determined by calculation of specific activity using the DE81 filter-binding method (section 2.19), and are expressed in moles of junction. The Y-junctions were stored in 5 μl aliquots at -20°C.

VI. *IN VIVO* AND BIOCHEMICAL ASSAYS

2.34 CELL SURVIVAL CURVES (UV SENSITIVITY)

E. coli strains AB1157 and HI24 were freshly transformed with pUC19, pGTI19, pME3 or pME4 as described in section 2.26. 5 ml cultures (LB + carbenicillin) of each strain/plasmid combination were incubated overnight at 37°C with rapid shaking. The next day, 200 μl of each starter culture was used to inoculate 20 ml LB, supplemented with carbenicillin, and cells were grown with aeration at 37°C. At an A_{600} of 0.4, a 100 μl sample of each culture was chilled on ice and diluted 10^1-, 10^2-, 10^3-, 10^4- and 10^5-fold with M9 minimal medium A. For each strain/plasmid combination, 10 μl aliquots of each dilution were spotted onto seven LB agar plates supplemented with carbenicillin. After allowing the plates to dry, cells were UV-irradiated with a total dose of 0, 5, 10, 20, 30, 45 or 60 J/m^2. The plates were incubated in the dark for ~16 hr, after which colonies of survivors were scored and expressed as a percentage of the total number of colonies observed on the non-irradiated control plate.

In some UV sensitivity studies, AB1157 and HI24 were initially transformed with pREP4 followed by selection on LB plates supplemented with kanamycin. Cells harbouring pREP4 were then co-transformed with pUC19, pGTI19, pME3 or pME4. To ensure complete repression of the vector *lac* promoter, cells were plated on LB agar containing 2% (w/v) glucose in addition to kanamycin and carbenicillin. 5 ml starter cultures were also supplemented with 2% glucose. Cell survival experiments were conducted as described above, except the 20 ml cultures and LB agar plates contained both carbenicillin and kanamycin (no glucose).

2.35 DNA BINDING ASSAY

Unless otherwise stated, binding reactions (20 μl) contained 60 μM form I DNA (either ϕX174 or pDEA-7Z) in DNA binding buffer A. Following preincubation for 5 min at 37°C, reactions were initiated by the addition of RuvB or $RuvB^{D113E}$ alone or premixed with 4 μM RuvA, as indicated. Reactions were incubated for 25 min at 37°C. Protein-DNA complexes were fixed by addition of 1/10 vol 2.5% (v/v) glutaraldehyde (freshly diluted, from a 25% stock, in 100 mM triethanolamine-HCl, pH 7.5), followed by incubation for a further 30 min at 37°C. Samples were diluted with 1/9 vol agarose gel loading buffer (10x) and analysed by electrophoresis through 0.8% agarose gels run at 4.6 V/cm for 2-3 hr (section 2.7). DNA was visualised by staining with ethidium bromide. In some band-shift assays, reactions contained 0.5 mM ATP and variable concentrations of ATPγS, as indicated.

2.36 JUNCTION BINDING ASSAY

Reactions (5 μl) contained 4 nM ^{32}P-labelled Y-junction DNA (in terms of junctions; section 2.33) and 200 or 800 nM RuvA, in junction binding buffer. After incubation for 5 min at 37°C, or 5 min on ice (in the case of the protein-free control reactions), 1/4 vol LI gel loading buffer was added to the reactions. Samples were immediately subjected to low ionic strength PAGE at 150 V for 2 hr at 4°C, with buffer recirculation. Gels were prepared as described for neutral polyacrylamide gels (section 2.8), except they contained 4% (w/v) polyacrylamide in low ionic strength (LI) buffer. Electrophoresis was conducted in the same LI buffer. ^{32}P-labelled DNA was detected by autoradiography (section 2.10).

2.37 ATPase Assay

Unless stated otherwise, reactions (60 μl) contained 150 μM form I pBluescript DNA in ATPase buffer supplemented with 10 μCi/ml [α-^{32}P]ATP. After preincubation for 5 min at 37°C, reactions were initiated by the addition of RuvB (5 μM) or RuvB^{D113E} (5 μM). In RuvAB reactions, RuvA (1 μM) was premixed with RuvB (4 μM) or RuvB^{D113E} (4 μM). Reactions were incubated at 37°C. At various times, samples (10 μl) were taken and ATP hydrolysis stopped by the addition of EDTA to 45 mM. Aliquots (1 μl) were spotted onto CEL 300 PEI/UV_{254} thin-layer chromatography plates (Polygram), which were subsequently developed in 1 M formic acid/500 mM LiCl for ~100 min. Plates were air-dried and the percentage of [α-^{32}P]ATP hydrolysed to [α-^{32}P]ADP was determined by PhosphorImager analysis (section 2.11). Background levels of hydrolysis observed in the absence of RuvB/RuvB^{D113E} were subtracted.

2.38 Helicase Assay

Helicase reactions (20 μl) containing 1 μM ^{32}P-labelled helicase substrate (section 2.29) and 30 nM RuvA, in helicase buffer, were preincubated for 5 min at 37°C. Reactions were initiated by the addition of appropriate amounts of RuvB or RuvB^{D113E}. After 25 min incubation at 37°C, reactions were stopped and the DNA deproteinised by the addition of 1/4 vol helicase stop buffer (5x). Samples were diluted with 1/5 vol neutral gel loading buffer, loaded directly onto neutral polyacrylamide gels and analysed by electrophoresis at 150 V (section 2.8). 66 nt displacement reactions were analysed by 6% neutral PAGE for 2 hr, whereas for 20 and 30 nt displacement assays, samples were subjected to 8% PAGE for 1 hr. ^{32}P-labelled DNA was detected by autoradiography (section 2.10) and quantified by PhosphorImager analysis (section 2.11).

2.39 TOPOLOGICAL ASSAY FOR DNA UNWINDING

Reactions (20 μl) containing 15 μM relaxed ^{32}P-labelled pFB585 DNA (section 2.30) in unwinding buffer, supplemented with varying concentrations of ATPγS, were preincubated for 5 min at 37°C. Reactions were initiated by the addition of RuvB or RuvB^{D113E} alone or premixed with 4 μM RuvA. After 15 min incubation at 37°C, ~5 U of wheat germ topoisomerase I was added and incubation was continued for a further 2 min. The reactions were then stopped and the DNA deproteinised by treatment with 1/4 vol unwinding stop buffer (5x) followed by incubation for 15 min at 37°C. DNA products were purified by extraction with phenol/chloroform/iso-amyl alcohol (section 2.20) followed by ethanol precipitation (section 2.21), resuspended in 7-10 μl agarose gel loading buffer (diluted 3-fold in ddH_2O) and analysed by agarose gel electrophoresis (section 2.7). Gels contained 0.7% (w/v) agarose in TESS buffer and were prepared using the Bio-Rad Sub-Cell GT apparatus (tray size: 15 cm x 25 cm). Electrophoresis was conducted in TESS buffer at 1.67 V/cm for 36 hr, with buffer recirculation. Gels were dried and ^{32}P-labelled DNA visualised by autoradiography (section 2.10).

2.40 BRANCH MIGRATION ASSAYS

2.40.1 Branch Migration of α-Structures

Reaction mixtures (20 μl) containing 0.57 μM ^{32}P-labelled α-structures (recombination intermediates; section 2.31) in branch migration buffer A were preincubated for 5 min at 37°C. RuvB or RuvB^{D113E} were then added, at the concentrations indicated in the figures, and incubation was continued for 20 min. In RuvAB-mediated branch migration reactions, α-structures were preincubated with 15 nM RuvA for 5 min at 37°C prior to the addition of RuvB/RuvB^{D113E}, and reactions were allowed to proceed for 15 min. Reactions

were stopped and DNA products deproteinised by the addition of 1/4 vol branch migration stop buffer A (5x) followed by incubation for 10 min at 37°C. Samples were diluted with 1/9 vol agarose gel loading buffer and were analysed by electrophoresis through 1.2% agarose gels at 4.6 V/cm for 3.5 hr, with buffer recirculation (section 2.7). Ethidium bromide was included in the gel and electrophoresis buffer to stabilise the intermediates. ^{32}P-labelled DNA was detected by autoradiography (section 2.10) and quantified by PhosphorImager analysis (section 2.11).

2.40.2 Branch Migration of Synthetic X-Junctions

Reactions containing 1 nM ^{32}P-labelled X12 DNA (in terms of junctions; section 2.32) in branch migration buffer B were preincubated for 5 min at 37°C. RuvA (10 nM) was then added, followed by the addition of appropriate amounts of RuvB or RuvB^{D113E}. After 30 min incubation at 37°C, reactions were treated with 1/9 vol branch migration stop buffer B (10x) and incubated for a further 10 min. Samples were diluted with 1/3 vol neutral gel loading buffer and analysed by 8% neutral PAGE at 160 V for 2 hr (section 2.8). ^{32}P-labelled DNA was detected by autoradiography (section 2.10) and quantified by PhosphorImager analysis (section 2.11).

2.40.3 Branch Migration of Synthetic Y-Junctions

Reactions (5 μl) typically contained 4 nM ^{32}P-labelled Y-junction DNA (in terms of junctions; section 2.33) in branch migration buffer C. However, in some assays, the ATP (2 mM) in the buffer was either omitted or replaced with ATPγS (2 mM). After 5 min preincubation at 37°C, RuvA (0.1 μM) was added followed by the addition of RuvB/RuvB^{D113E} (0.2 or 1 μM), as indicated in the figures. Reactions were incubated for a further 15 min at 37°C, and then were put on ice

and treated with 1/9 vol branch migration stop buffer C (10x). Samples were diluted with 1/4 vol neutral gel loading buffer, centrifuged (14,000 rpm, 2 min, 4°C in an Eppendorf Model 5415 C benchtop centrifuge) and then immediately loaded onto 10% neutral polyacrylamide gels (section 2.8). ^{32}P-labelled DNA products were analysed by electrophoresis at 120 V for 5 hr at 4°C, and visualised by autoradiography (section 2.10).

In some branch migration assays, 3 μl samples were treated with stop buffer and analysed by neutral PAGE as described above, and the remaining 2 μl were subjected to denaturing PAGE. In the latter case, the samples were heated for 3 min at 95°C in formamide buffer and analysed by electrophoresis through 8% denaturing polyacrylamide gels (large, 38 x 50 cm) at 100W for 25 min (section 2.9).

CHAPTER THREE : RESULTS

EXPRESSION AND PURIFICATION OF RUVB^{D113E}

I. INTRODUCTION

Helicase motifs I and II are present in all known helicases and correspond to the A and B sites of the Walker nucleotide binding motif (Walker *et al.*, 1982). The crystal structures of a number of NTP-binding proteins have indicated that the Walker A motif forms a phosphate binding loop (P-loop) in which the highly conserved lysine residue interacts directly with the β and γ phosphates of the bound nucleotide (Fry *et al.*, 1986; Milburn *et al.*, 1990; Pai *et al.*, 1990; Saraste *et al.*, 1990; Story and Steitz, 1992). Mutagenesis studies of the RNA helicase eIF-4A have shown that replacement of the lysine residue in helicase motif I with asparagine abolishes ATP binding (Pause and Sonenberg, 1992; Rozen *et al.*, 1989). Motif II (the 'DEAD' box or DExx motif) has been implicated in NTP hydrolysis (Pause and Sonenberg, 1992) and it is thought that the N-proximal aspartate residue interacts, through a water molecule, with Mg^{2+} bound to NTP (Pai *et al.*, 1990; Story and Steitz, 1992). Substitution of glutamate for this amino acid in eIF-4A resulted in a helicase-defective protein capable of ATP hydrolysis, suggesting an additional role of the aspartate residue in the coupling of NTPase activity to RNA unwinding (Pause and Sonenberg, 1992).

RuvB possesses conserved helicase motifs (Figure 1.7) and has been shown to exhibit an *in vitro* DNA helicase activity in the presence of RuvA (Adams and West, 1995b; Tsaneva *et al.*, 1993; Tsaneva and West, 1994). However, the current model for the RuvAB branch migration complex bound to a Holliday junction (Figure 1.8B) suggests that strand exchange has already occurred before the DNA enters the RuvB rings, thereby questioning the need for DNA unwinding activity by RuvB *in vivo* (Hargreaves *et al.*, 1998; Hiom and West, 1995a; Parsons *et al.*, 1995a; Rafferty *et al.*, 1996).

To investigate the role of DNA helicase activity in RuvAB-mediated branch migration, the highly conserved aspartate residue in helicase motif II of RuvB (Asp113) was replaced with glutamate by site-directed mutagenesis. The *in vivo* characterisation, expression and purification of the resultant mutant protein, $RuvB^{D113E}$, are described in this chapter, and its biochemical characterisation is detailed in Chapters 4 and 5. In addition, the *in vivo* studies and attempted purification of a second site-directed mutant protein, $RuvB^{K68N}$, that contains a lysine to asparagine substitution in helicase motif I, are discussed.

II. SITE-DIRECTED MUTAGENESIS OF RUVB

Sequence alignments show that helicase motifs I and II are highly conserved in RuvB across a diverse range of bacterial species (Figure 3.1A). Positions of the amino acids mutated in *E. coli* RuvB, Lys68 and Asp113, and their proposed catalytic roles are indicated in Figures 3.1A and 3.1B. Site-directed mutations were introduced into the *ruvB* gene carried by plasmid pGTI19 (Sharples *et al.*, 1990) by Dr C. Mézard (Materials and Methods, section 2.5). The resultant plasmids, carrying the mutant alleles $ruvB^{K68N}$ and $ruvB^{D113E}$, were named pME4 and pME3, respectively.

III. *IN VIVO* STUDIES

PHENOTYPIC EFFECTS OF $RUVB^{D113E}$ EXPRESSION

Cells carrying *ruv* mutations are sensitive to DNA damaging agents, such as UV light, ionising irradiation and mitomycin C (Otsuji *et al.*, 1974; Sharples *et al.*, 1990). To determine whether $RuvB^{D113E}$ expression could complement the UV-sensitive phenotype of a *ruvB* mutant strain, plasmid pME3 was transformed

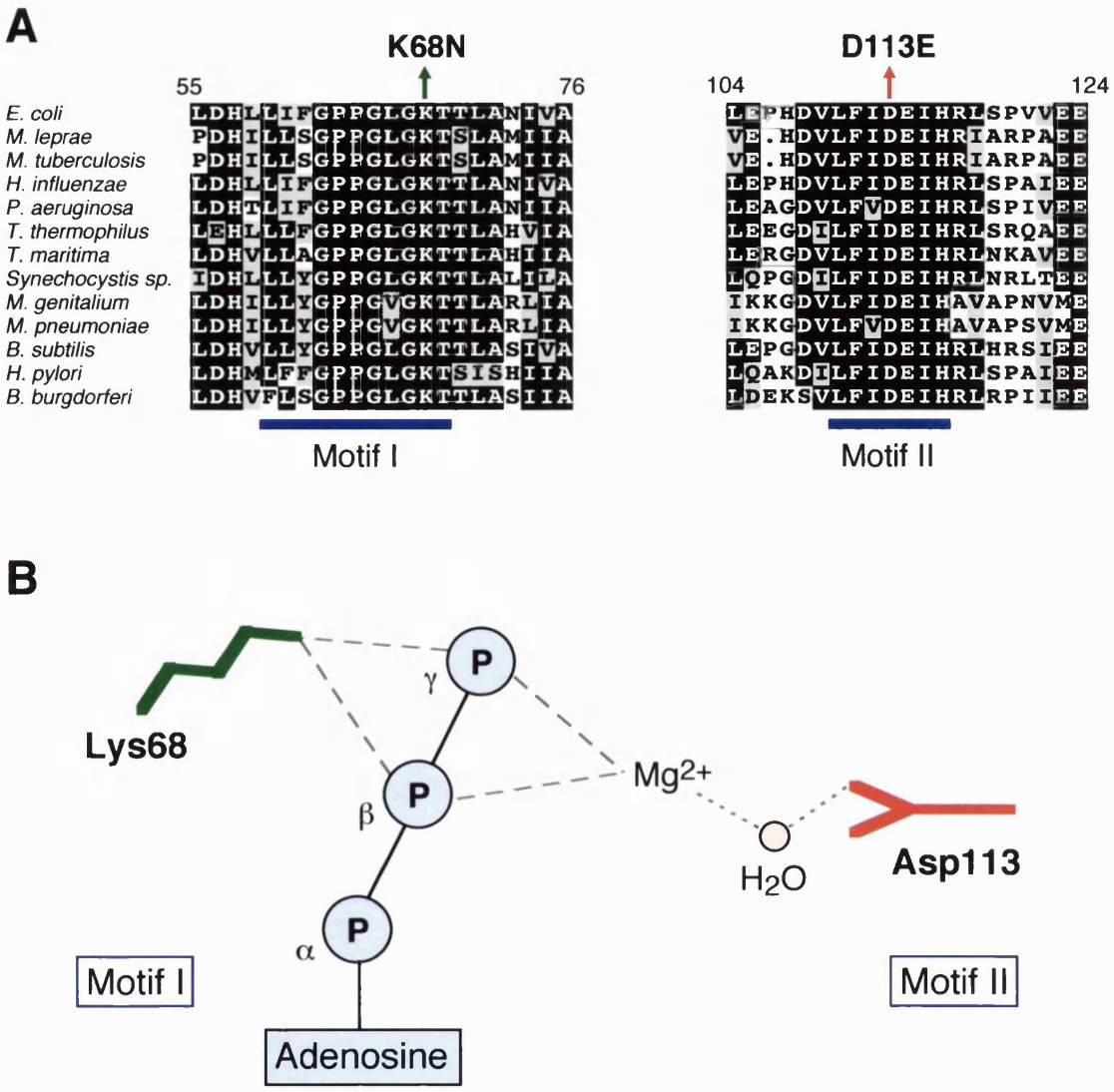

FIGURE 3.1. SITE-DIRECTED MUTAGENESIS OF *E. COLI* RUVB

A. Alignment of part of the *E. coli* RuvB sequence (residues 55-76 and 104-124) with the corresponding regions of 12 bacterial homologues. Protein sequences were aligned using PileUp (Wisconsin Package Version 10.0, Genetics Computer Group, Madison, Wisc.). Identical and similar amino acids are boxed in black and grey, respectively. The highly conserved helicase motifs I and II are indicated along with the positions of the K68N and D113E amino acid substitutions introduced into *E. coli* RuvB.

B. Schematic diagram indicating the proposed catalytic roles of Lys68 and Asp113 in *E. coli* RuvB. Helicase motif I forms a phosphate binding loop in which Lys68 is thought to interact with the β- and γ-phosphates of the bound ATP. Helicase motif II is thought to play a role in Mg^{2+}-coordinated ATP hydrolysis with Asp113 interacting with ATP-bound Mg^{2+} through a water molecule as indicated. The figure was adapted from Story and Steitz (1992).

into *E. coli* strain HI24 (*ruvB4*) (Otsuji *et al.*, 1974; Sharples *et al.*, 1990). Expression of the mutant protein resulted in partial complementation of the *ruvB4* mutation, as indicated by the partial restoration of UV resistance (Figure 3.2A, left panel). To examine the effect of $RuvB^{D113E}$ on the function of the wild-type protein, pME3 was also introduced into the ruv^+ strain AB1157. $RuvB^{D113E}$ expression resulted in a dominant negative phenotype, such that the ruv^+ cells carrying pME3 became UV sensitive (Figure 3.2A, right panel). In comparison, expression of wild-type RuvB (from pGTI19) fully complemented the UV-sensitive phenotype of HI24 and had no adverse effects on the ruv^+ strain AB1157 (Figure 3.2A, both panels).

Plasmids pGTI19 and pME3 are derived from the multicopy plasmid pUC19 (Yanisch-Perron *et al.*, 1985) and carry $ruvB/ruvB^{D113E}$ under the control of the vector *lac* promoter (Sharples *et al.*, 1990). However, although strains AB1157 and HI24 are $lacI^+$, the level of expression of the LacI repressor protein is insufficient to tightly regulate the promoter, resulting in constitutive over-expression of $RuvB/RuvB^{D113E}$ in these strains. The levels of plasmid-encoded RuvB and $RuvB^{D113E}$ were estimated by SDS-PAGE and Western blotting to be ~1,000-fold higher than that of chromosomally expressed RuvB (data not shown).

To study the effects of $RuvB^{D113E}$ at more physiological levels of expression, cells carrying pME3 were co-transformed with pREP4 (Qiagen), a low copy number plasmid which constitutively expresses the Lac repressor protein. In this background, $RuvB^{D113E}$ expression was estimated to be only 4- to 8-fold higher than chromosomal RuvB expression (data not shown). At these lower expression levels, no dominant negative effect was observed in AB1157 (Figure 3.2B, right panel) but $RuvB^{D113E}$ failed to complement the *ruvB4*

FIGURE 3.2. *IN VIVO* COMPLEMENTATION STUDIES

A. UV survival curves of *E. coli* strain HI24 (*ruvB4*) and its wild-type control AB1157 following transformation with plasmids pME3 (*ruvB*^{D113E}; ●), pGTI19 (*ruvB*$^{+}$; ■) or pUC19 (◆). Experiments were carried out as described in Materials and Methods.

B. UV survival curves were conducted as in A, except that HI24 and AB1157 were pre-transformed with pREP4 in order to control expression of RuvB/RuvB^{D113E} from the *lac* promoter.

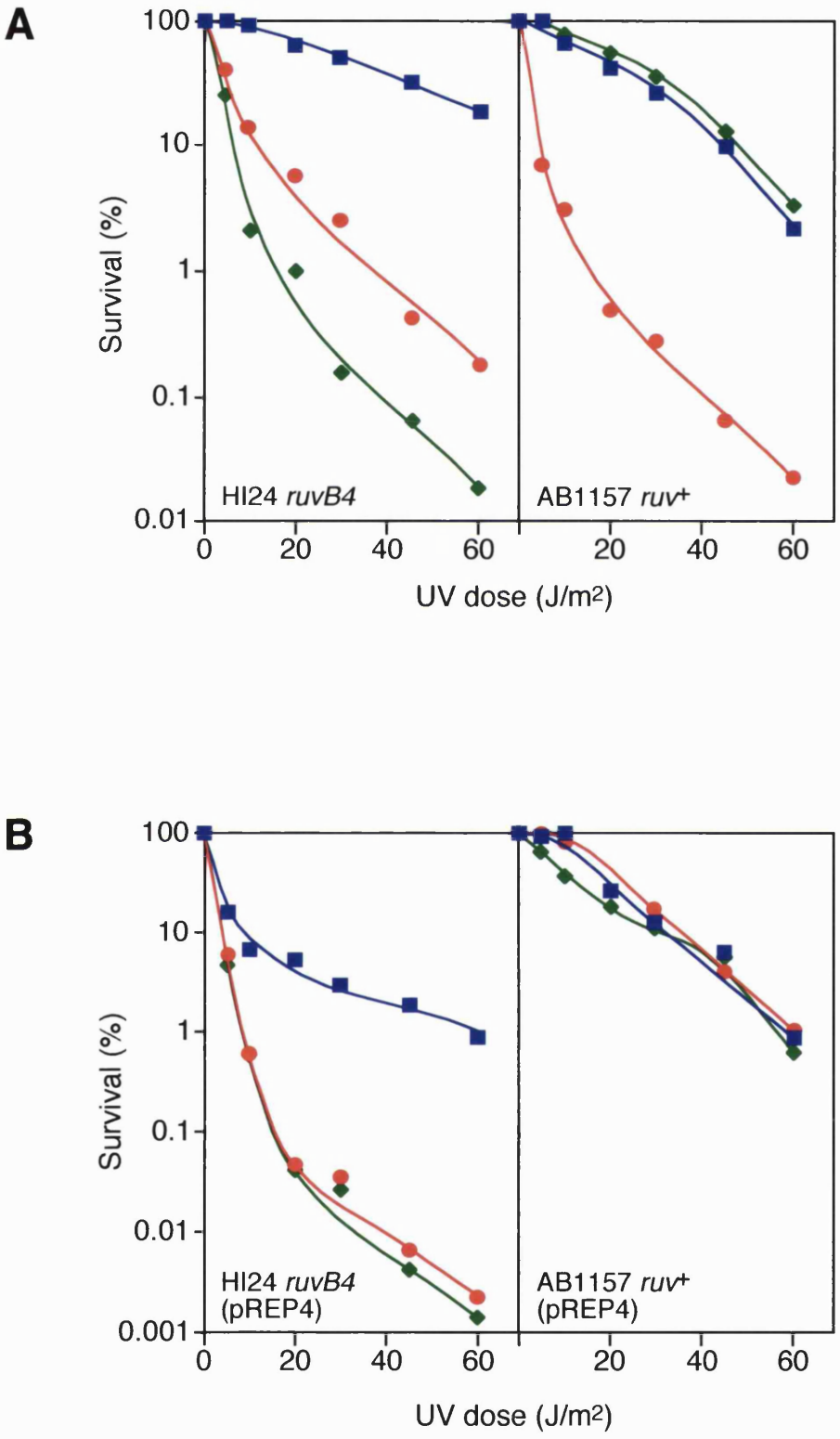
A
100
10
1
0.1
0.01
Survival (%)
HI24 ruvB4
AB1157 ruv+
0
20
40
60
20
40
60
UV dose (J/m2)
B
100
10
1
0.1
0.01
0.001
Survival (%)
HI24 ruvB4
(pREP4)
AB1157 ruv+
(pREP4)
0
20
40
60
20
40
60
UV dose (J/m2)

FIGURE 3.2

mutation in HI24 (left panel). Wild-type RuvB, expressed at the same level, restored UV resistance to H124 (Figure 3.2B, left panel).

PHENOTYPIC EFFECTS OF RUVB^{K68N} EXPRESSION

Complementation studies were conducted as described above except cells were transformed with pME4, a pUC19 derivative containing *ruvB*^{K68N} under control of the p*lac* promoter. In contrast with RuvB^{D113E}, the constitutive over-expression of RuvB^{K68N} failed to complement the UV-sensitive phenotype of strain HI24 *ruvB4* (Figure 3.3A, left panel). In fact, cells carrying pME4 showed an increased UV sensitivity compared to cells transformed with the pUC19 vector control. Over-expression of RuvB^{K68N} in the *ruv*$^{+}$ strain AB1157 resulted in a dominant negative effect, as observed for RuvB^{D113E} (Figure 3.3A, right panel). The UV sensitivities of strains AB1157 and HI24 transformed with both pME4 and pREP4 were comparable to the pUC19 controls, indicating that the low copy number expression of RuvB^{K68N} had no effect on cell survival following UV-irradiation in either the *ruvB4* or *ruv*$^{+}$ strain (Figure 3.3B, both panels).

IV. EXPRESSION OF RUVB^{D113E}

EXPRESSION IN *E. COLI* HRS1004

RuvB^{D113E} was initially over-expressed, from pME3, in *E. coli* strain HRS1004, a derivative of AB1157 containing a deletion of the *ruvAB* operon (Iwasaki *et al.*, 1989b). The *ruvB* deletion was essential to avoid contamination of the mutant protein with wild-type RuvB. Starter cultures of HRS1004 (pME3) were grown up overnight and used to inoculate medium for large-scale expression of RuvB^{D113E}. Although the *ruvB*^{D113E} gene in pME3 is under the control of the vector *lac* promoter, expression of the mutant protein was constitutive in the

FIGURE 3.3. *IN VIVO* COMPLEMENTATION STUDIES (RUVB^{K68N})

A. UV survival curves of *E. coli* strain HI24 (*ruvB4*) and its wild-type control AB1157 following transformation with plasmids pME4 (*ruvB*^{K68N}; ●), pGTI19 (*ruvB*; ■) or pUC19 (◆). Experiments were carried out as described in Materials and Methods.

B. UV survival curves were conducted as in A, except that HI24 and AB1157 were pre-transformed with pREP4 in order to control expression of RuvB/RuvB^{K68N} from the *lac* promoter.

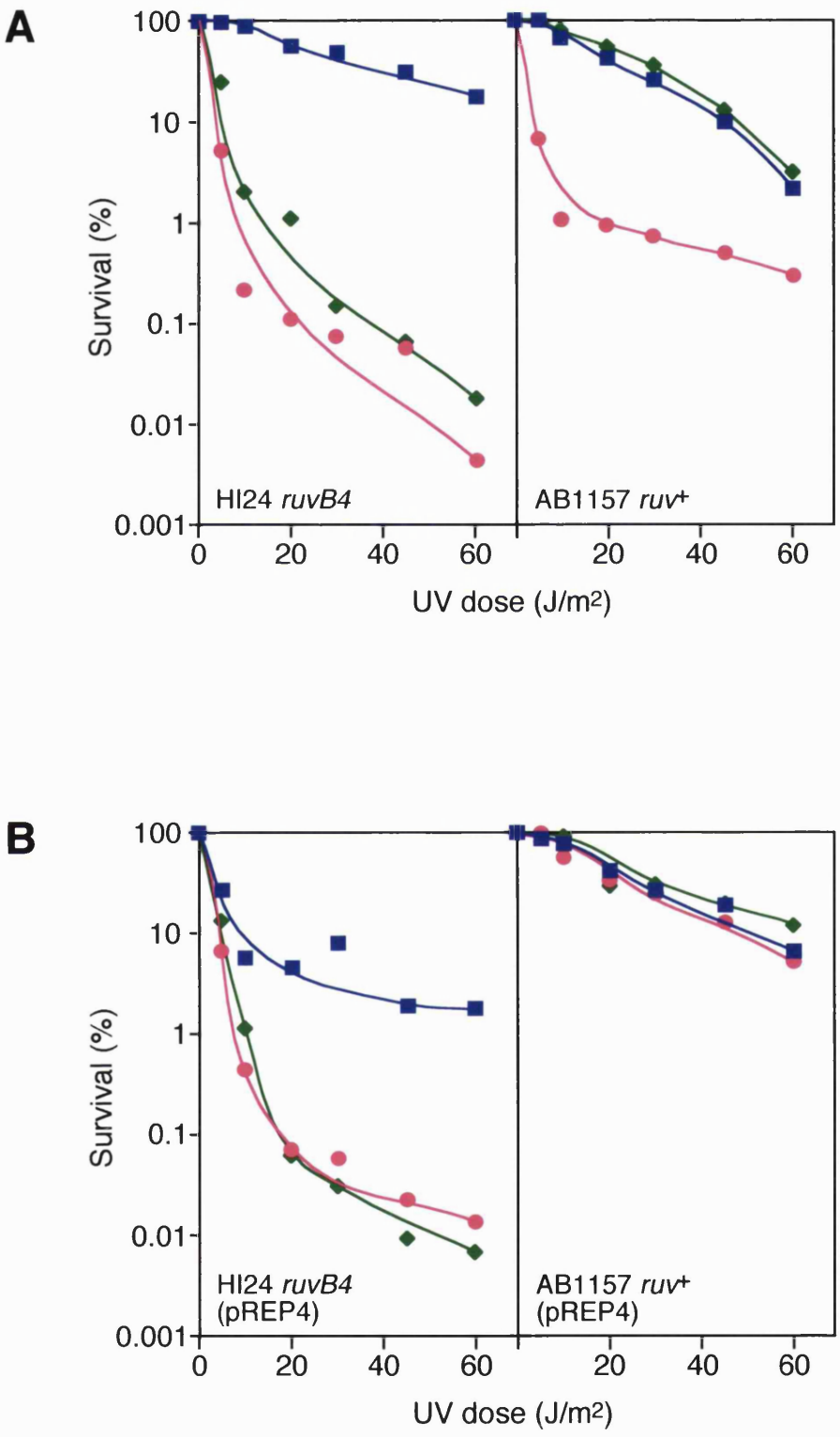
A
100
10
1
0.1
0.01
0.001
Survival (%)
HI24 ruvB4
AB1157 ruv+
0
20
40
60
20
40
60
UV dose (J/m2)
B
100
10
1
0.1
0.01
0.001
Survival (%)
HI24 ruvB4
(pREP4)
AB1157 ruv+
(pREP4)
0
20
40
60
20
40
60
UV dose (J/m2)

FIGURE 3.3

lacI^{+} host strain and therefore was not IPTG-inducible. Instead, cells carrying the multicopy plasmid were grown for 6-8 hr after which samples were analysed by SDS-PAGE.

In one expression study (Figure 3.4), moderate expression of RuvB^{D113E} was obtained in four out of six cultures (lanes e, f, i and j). However, several other attempts to over-express RuvB^{D113E} were unsuccessful. Similarly, wild-type RuvB expression in HRS1004 was inconsistent (data not shown). It is possible that high levels of RuvB or RuvB^{D113E} are deleterious for cell growth and that constitutive over-expression in the starter and expression cultures (Figure 3.4, lanes b-d) results in selection for 'non-expressing' cells.

EXPRESSION IN *E. COLI* FB820

To overcome the expression problems outlined above, a new expression strain (FB820) was constructed by Dr F. E. Benson. FB820 is a Δ*ruvAB* derivative of JM101 (Yanisch-Perron *et al.*, 1985) and contains the *lacI*^{q} gene on its F′ plasmid. This is a mutated version of the *lacI* gene that over-produces the Lac repressor protein. The entire *ruvAB* operon in JM101 was deleted, and replaced with the tetracycline resistance gene, by P1 transduction from HRS1004 (Iwasaki *et al.*, 1989b).

FB820 was used for all subsequent over-expression of wild-type and mutant RuvB proteins. The high levels of Lac repressor protein in this strain, expressed from the *lacI*^{q} gene, controls the p*lac* promoter of pME3 (or pGTI19) and allows IPTG-inducible expression of RuvB^{D113E}. Trial expression studies were conducted and showed that maximum over-expression was achieved by including glucose (0.2%, w/v) in the starter cultures to ensure tight control of the p*lac* promoter prior to induction (data not shown). Freshly-transformed FB820 (pME3) was grown in 11 litres of fermenter medium, as described in

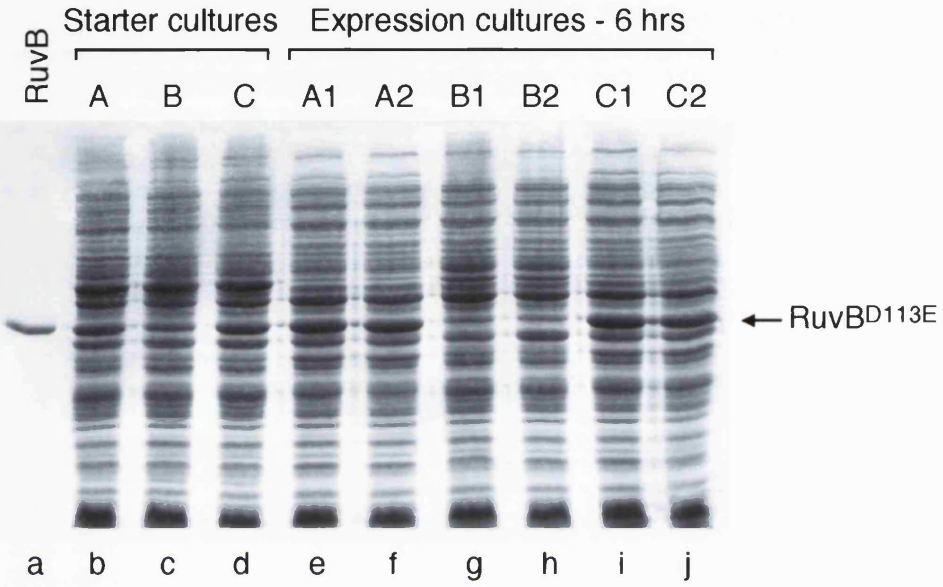

FIGURE 3.4. EXPRESSION OF RUVB^{D113E} IN *E. COLI* STRAIN HRS1004

Cells transformed with plasmid pME3 were grown up overnight (~12 hrs) at 30°C in Luria broth supplemented with 100 μg/ml carbenicillin. The starter cultures (A, B, C) were each used to inoculate 2 x 400 ml cultures as indicated. The cultures were grown with aeration for 6 hrs at 37°C, after which samples were analysed by 10% SDS-PAGE. Proteins were visualised by staining with Coomassie blue.

Materials and Methods (section 2.13), and induced by the addition of IPTG. After 6 hr induction, the amount of $RuvB^{D113E}$ in FB820 comprised approximately ~25% of total cell protein (Figure 3.5). Cells were harvested after 8 hr induction (Materials and Methods, section 2.13) and stored at -80°C.

V. PURIFICATION OF $RUVB^{D113E}$

POLYMIN P PRECIPITATION OF $RUVB^{D113E}$

Preliminary attempts to purify $RuvB^{D113E}$ followed a protocol developed for the wild-type protein (Tsaneva *et al.*, 1992a; Materials and Methods, section 2.13). Unfortunately, however, most of the mutant protein was found to bind irreversibly to the hydroxyapatite column used during this procedure (data not shown). Iwasaki *et al* (Iwasaki *et al.*, 1989a) have described an alternative scheme for the purification of RuvB which involves an initial Polymin P precipitation step. Small-scale trials were therefore conducted to see whether this would be a suitable purification step for $RuvB^{D113E}$.

The basic scheme for Polymin P precipitation is summarised in Figure 3.6A. Following cell lysis and high speed centrifugation, which were carried out as described for wild-type RuvB (Materials and Methods, section 2.13), 10% (v/v) Polymin P (pH 7.5) was added to the crude lysate to a final concentration of 0.5%. Subsequent buffer additions are based on the initial volume of lysate used. After stirring for 30 min on ice, the suspension was centrifuged at 10,000 rpm for 15 min at 4°C (Sorvall centrifuge, SS-34 or GSA rotor). The pellet was resuspended in 1/2 vol R-buffer containing 400 mM NaCl (Materials and Methods, section 2.3), stirred for 10 min (on ice) and centrifuged as before. This pellet was then resuspended in 1/5 vol R-buffer containing 1.1 M NaCl. Following centrifugation, this latter step was repeated to maximise protein

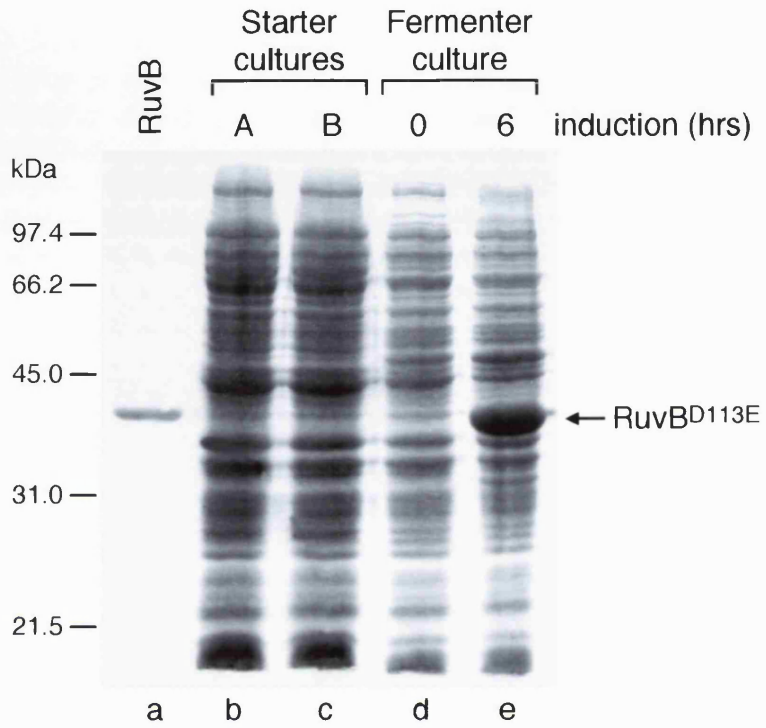

FIGURE 3.5. LARGE SCALE OVER-EXPRESSION OF RUVB^{D113E} IN *E. COLI* STRAIN FB820.

1 litre starter cultures of FB820 (pME3) (A, B) were grown up in Luria broth supplemented with 100 μg/ml carbenicillin and 0.2% glucose for ~9 hrs at 37°C. Fermenter medium (9 litres) was inoculated with the starter cultures (2 litres) and the cells grown under fermenter conditions as described in Materials and Methods. At an OD_{650} of 3.0, the cells were induced by the addition of 1 mM IPTG. Samples were taken 0 and 6 hrs after induction and analysed by 10% SDS-PAGE, along with starter culture samples. Proteins were visualised by Coomassie blue staining. The positions of the molecular weight markers are indicated.

FIGURE 3.6. POLYMIN P PURIFICATION OF RUVB^{D113E}

A. Trial scheme for purification of RuvB^{D113E} using Polymin P. Following cell lysis, proteins in the crude lysate were precipitated with Polymin P and then selectively eluted using increasing concentrations of NaCl. After each centrifugation step, a sample of the supernatant (SN) was kept for analysis.

B. 10% SDS-PAGE analysis of the SN samples obtained in a small-scale trial, showing the elution of RuvB^{D113E} at 1.1 M NaCl (lanes e and f). Proteins were visualised by Coomassie blue staining.

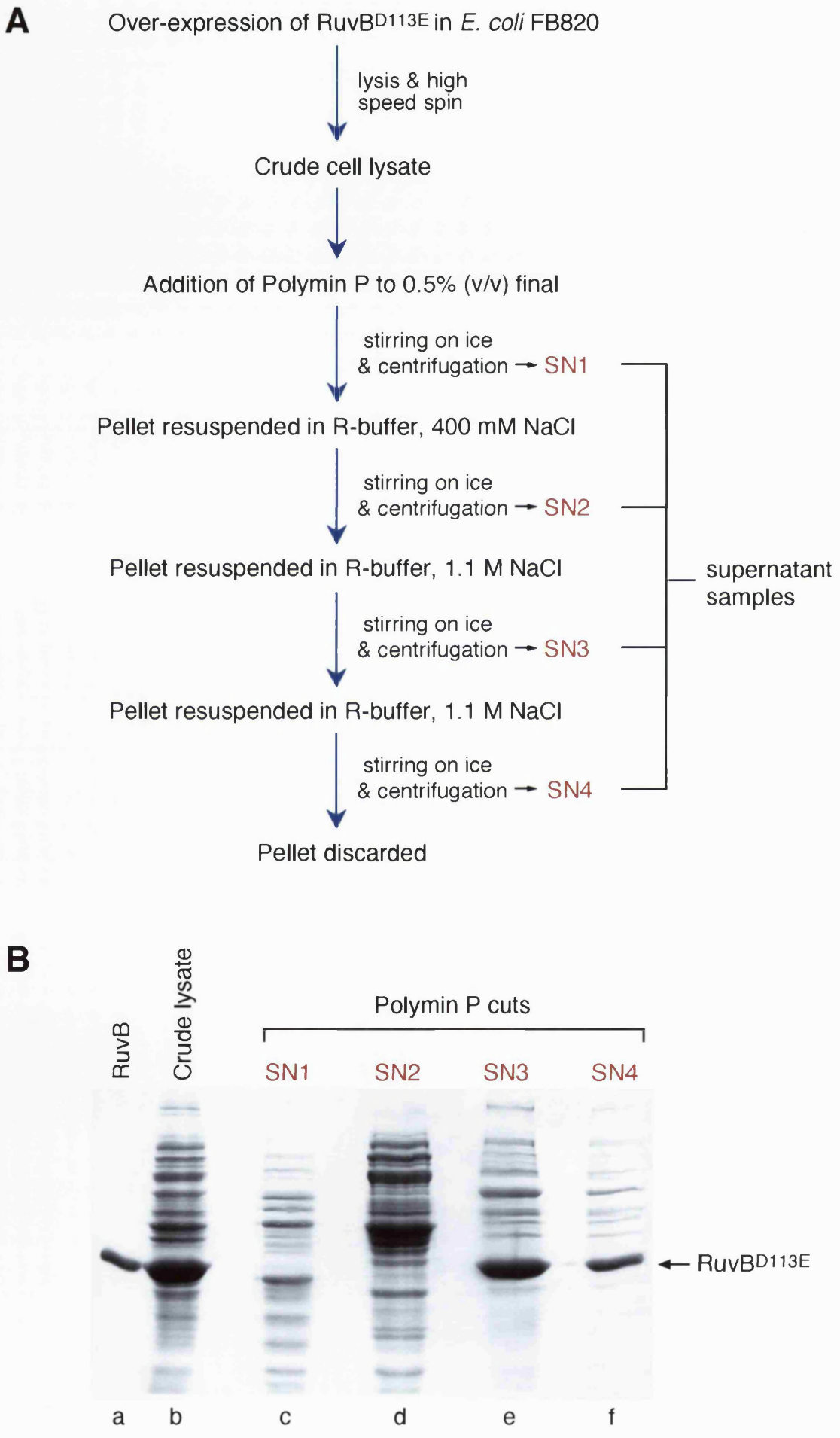
A
Over-expression of RuvB^{D113E} in *E. coli* FB820
lysis & high speed spin
Crude cell lysate
Addition of Polymin P to 0.5% (v/v) final
stirring on ice & centrifugation → SN1
Pellet resuspended in R-buffer, 400 mM NaCl
stirring on ice & centrifugation → SN2
Pellet resuspended in R-buffer, 1.1 M NaCl
stirring on ice & centrifugation → SN3
Pellet resuspended in R-buffer, 1.1 M NaCl
stirring on ice & centrifugation → SN4
Pellet discarded
supernatant samples
B
RuvB
Crude lysate
Polymin P cuts
SN1
SN2
SN3
SN4
RuvB^{D113E}
a
b
c
d
e
f

FIGURE 3.6

recovery. A Polymin P purification trial was conducted on 10 ml crude lysate. Samples of the supernatants obtained after each centrifugation step (SN1-4) were kept and analysed by SDS-PAGE (Figure 3.6B). Polymin P precipitation provided a powerful purification step for $RuvB^{D113E}$ since the majority of other proteins were removed from the pellet with 400 mM NaCl (lane d). In addition, some impurities were lost in the initial precipitation step (lane c). $RuvB^{D113E}$ eluted at 1.1 M NaCl and comprised ~50% of the total protein (lanes e and f), as compared to ~30% in the crude lysate.

Surprisingly, when the Polymin P-purified $RuvB^{D113E}$ was taken through the rest of purification scheme described by Tsaneva *et al* (Tsaneva *et al.*, 1992a), the elution problems originally experienced with the hydroxyapatite column were no longer encountered. This suggests that the binding to Polymin P affected the behaviour of $RuvB^{D113E}$, either directly or indirectly (e.g. by removing another factor present), aiding efficient elution from the hydroxyapatite column.

SCHEME FOR $RUVB^{D113E}$ PURIFICATION

Following the success of the Polymin P trials, a scheme was developed for the purification of $RuvB^{D113E}$ (Figure 3.7A). The scheme was based on the published protocol for wild-type RuvB (Tsaneva *et al.*, 1992a; section 2.13), but included an initial Polymin P precipitation step as well as a number of more subtle changes. 200 ml of frozen *E. coli* FB820 cells expressing $RuvB^{D113E}$ (equivalent to ~55 g wet cells) were thawed and lysed as described in Materials and Methods (section 2.13). Following high speed centrifugation, Polymin P purification of the crude lysate (fraction I; volume 230 ml) was conducted as described in the previous section, using a Waring blender (low speed, 2 x 30 sec) to resuspend each pellet in R-buffer. The supernatants obtained with the

FIGURE 3.7. PURIFICATION OF RUVB^{D113E}

A. Scheme for the purification of RuvB^{D113E}. Details of the purification are given in the text.

B. Samples at each stage in the purification scheme were analysed by 10% SDS-PAGE. Lane a, purified RuvB (2 μg); lane b, crude cell lysate; lane c, phosphocellulose column flow through after Polymin P precipitation; lanes d – f, fractions eluted from DEAE-Biogel, hydroxyapatite and Mono Q. Proteins were visualised by Coomassie blue staining. The positions of the molecular weight markers are indicated.

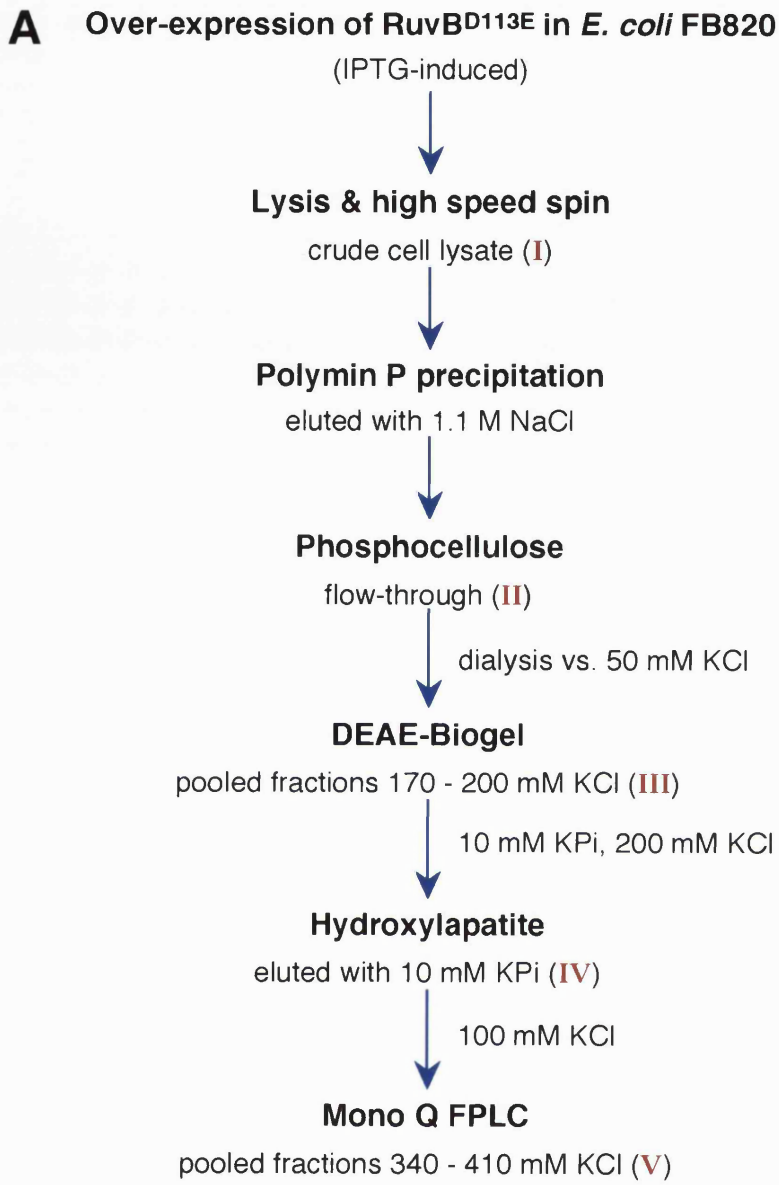
A
Over-expression of RuvB^{D113E} in *E. coli* FB820
(IPTG-induced)
Lysis & high speed spin
crude cell lysate (I)
Polymin P precipitation
eluted with 1.1 M NaCl
Phosphocellulose
flow-through (II)
dialysis vs. 50 mM KCl
DEAE-Biogel
pooled fractions 170 - 200 mM KCl (III)
10 mM KPi, 200 mM KCl
Hydroxylapatite
eluted with 10 mM KPi (IV)
100 mM KCl
Mono Q FPLC
pooled fractions 340 - 410 mM KCl (V)

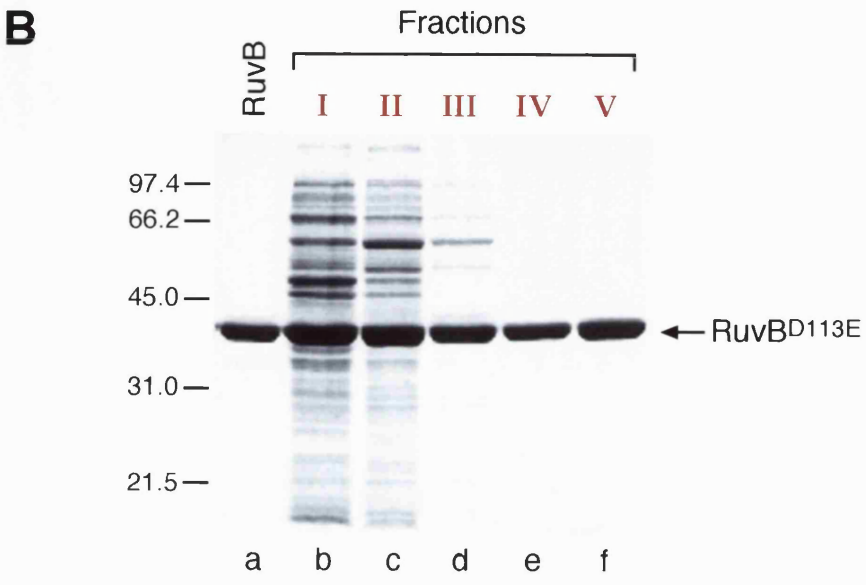
B
Fractions
RuvB
I
II
III
IV
V
97.4
66.2
45.0
31.0
21.5
RuvB^{D113E}
a
b
c
d
e
f

FIGURE 3.7

1.1 M NaCl cuts (SN3 and 4) were pooled and passed through a phosphocellulose column (50 ml) equilibrated with R-buffer containing 1.1 M NaCl. Phosphocellulose is a cation exchanger and was used to remove residual Polymin P present that might cause protein precipitation upon lowering the salt concentration for subsequent column chromatography.

The flow-through of the phosphocellulose column (fraction II) was dialysed against TEGD buffer containing 50 mM KCl (Materials and Methods, section 2.3) and loaded onto a DEAE Bio-Gel column (50 ml) equilibrated with the same buffer. The column was developed with a 50 – 300 mM KCl linear gradient in TEGD. Fractions containing $RuvB^{D113E}$, which eluted at 175 – 200 mM KCl, were pooled (fraction III), dialysed against P_2-buffer containing 200 mM KCl and applied to a hydroxyapatite column (40 ml) equilibrated with the same buffer. $RuvB^{D113E}$ (>95% purity) eluted as a sharp peak by washing with P_2-buffer (without KCl). The eluted $RuvB^{D113E}$ (fraction IV) was then dialysed against TEGD buffer containing 100 mM KCl and loaded onto a Mono Q FPLC column equilibrated in the same buffer. RuvB was eluted with a 100 – 600 mM KCl linear gradient. Peak fractions containing $RuvB^{D113E}$ (340 – 420 mM KCl) were pooled (fraction V) and dialysed against protein storage buffer B. Aliquots of the protein were fast-frozen in dry ice/ethanol and kept at -20°C (working stocks) or -80°C (for long term storage). The purification procedure yielded ~25 mg RuvB protein of >99% purity. A sample was taken at each step in the purification scheme and analysed by SDS-PAGE (Figure 3.7B).

VI. SUMMARY AND DISCUSSION

To determine whether the site-directed mutants $RuvB^{D113E}$ and $RuvB^{K68N}$ are functional *in vivo*, the proteins were expressed in both *ruvB* and *ruv*$^+$ strains and the resultant cells were assessed for their sensitivity to UV-irradiation. Over-

expression of RuvB^{D113E} was found to partially complement the UV-sensitive phenotype of the *ruvB* strain. It appears, therefore, that RuvB^{D113E} can promote limited cellular recovery following UV-induced DNA damage when present in abundance. This is in contrast with the site-directed mutant RuvB^{D113N} reported previously, which failed to complement the *ruvB* strain indicating that replacement of the aspartate residue in helicase motif II with asparagine abolished the repair activity of the protein *in vivo* (Mézard *et al.*, 1997). Over-expression of both RuvB^{D113E} and RuvB^{D113N} in the *ruv*$^{+}$ control strain, however, resulted in a dominant negative effect. These results suggest that high expression levels of the proteins interfere with the activity of wild-type RuvB in the cell. This is likely to be due to the formation of mixed hexamers, containing both wild-type and mutant RuvB, that are either unable to bind DNA or that form inactive RuvAB-junction complexes.

Over-expression of RuvB^{K68N} was unable to complement the UV-sensitive phenotype of the *ruvB* strain and resulted in a dominant negative effect in the *ruv*$^{+}$ strain, indicating that the mutant protein is defective in some biochemical activity necessary for cellular recovery following UV-irradiation. Similar results have been recently reported for two other RuvB Lys68 mutants, RuvB^{K68R} and RuvB^{K68A} (Hishida *et al.*, 1999). Biochemical characterisation of the purified proteins showed that they had a reduced ability to bind ATP and were defective in ATP hydrolysis and branch migration activity. Replacement of the lysine residue in helicase motif I of RNA helicase eIF-4A with asparagine (K82N) abolished ATP binding (Pause and Sonenberg, 1992; Rozen *et al.*, 1989). The positive charge of the lysine side-chain is thought to be required for interaction with the β- and γ-phosphates of ATP. The lysine to asparagine substitution in RuvB^{K68N} would remove the positive charge and so is likely to result in similar ATP binding defects as observed for eIF-4A^{K82N}.

It is interesting to note that, at a high level of expression, RuvB^{K68N} exhibited a relatively mild dominant negative effect, making the *ruv*$^{+}$ strain less UV sensitive than RuvB^{D113E}. Previous studies have shown that RuvB requires a nucleotide cofactor to bind DNA (Müller *et al.*, 1993b). Therefore, it is possible that the ability of RuvB^{K68N} protein to bind DNA is abolished or reduced, due to a defect in ATP binding, making it less competitive than the wild-type protein for junction binding.

RuvB^{D113E} was over-expressed in a Δ*ruvAB* derivative strain (FB820) containing the *lacI*^{q} gene. The presence of a *lac* repression system, as well as the addition of glucose to the starter cultures, was essential to ensure tight regulation of protein expression prior to induction. Leaky expression of the mutant protein, or indeed of wild-type RuvB, in the starter cultures resulted in poor and inconsistent protein expression. This suggests that high levels of wild-type or mutant RuvB may be detrimental to the cell, resulting in a selection for 'non-expressing' cells.

RuvB^{K68N} was also over-expressed in *E. coli* strain FB820. Unfortunately, however, attempts to purify this mutant protein using the scheme developed for RuvB^{D113E} were unsuccessful. RuvB^{K68N} was precipitated by Polymin P but did not elute from the pellet, even with 3 M NaCl (data not shown). Efforts to purify RuvB^{K68N} using the protocol described for wild-type RuvB also failed due to irreversible binding of the mutant protein to the hydroxyapatite column. Thus despite containing just single amino acid changes, RuvB^{D113E} and RuvB^{K68N} behaved differently to each other and to the wild-type protein during purification. This provided an early indication that the mutations may have induced conformational changes in RuvB. A modified purification scheme was designed for RuvB^{D113E} and the protein was purified to homogeneity. The next two chapters focus on the biochemical characterisation of this mutant protein.

CHAPTER FOUR : RESULTS

BIOCHEMICAL CHARACTERISATION OF RUVB^{D113E}

PART I

I. INTRODUCTION

The interaction of RuvB with dsDNA has been detected by band-shift assays (Müller *et al.*, 1993b) and visualised by electron microscopy (Stasiak *et al.*, 1994). RuvB-dsDNA complexes, formed in the presence of Mg^{2+} and ATPγS, were found to consist of double hexameric RuvB rings encircling the DNA (Stasiak *et al.*, 1994). RuvB protein also binds ATP and exhibits a weak ATPase activity (Iwasaki *et al.*, 1989a) that is stimulated by the presence of DNA and RuvA (Marrione and Cox, 1995; Marrione and Cox, 1996; Mitchell and West, 1994; Shiba *et al.*, 1991). Since DNA binding and ATP hydrolysis are required for RuvAB-catalysed helicase and branch migration reactions (Adams and West, 1995b; Mitchell and West, 1996; Tsaneva *et al.*, 1992b; Tsaneva *et al.*, 1993), the biochemical characterisation of RuvB^{D113E} initially focussed on these fundamental activities.

II. DNA BINDING BY RUVB^{D113E}

DNA BINDING BY RUVB^{D113E} IN ATPγS

DNA binding by RuvB has been studied using band-shift assays and is dependent on high concentrations of Mg^{2+} (>10 mM) and the presence of a nucleotide cofactor (Müller *et al.*, 1993b). RuvB-DNA complexes formed in the presence of ATPγS, a slowly hydrolysable ATP analogue, are more retarded than those formed in ATP (Müller *et al.*, 1993b). ATPγS is thought to stabilise the interaction between RuvB and DNA, allowing complexes to remain intact during gel electrophoresis.

To study the binding activity of RuvB^{D113E} relative to wild-type RuvB, both proteins were incubated with form I (supercoiled) dsDNA in the presence of 15 mM Mg^{2+} and ATPγS. The resulting protein-DNA complexes were fixed with glutaraldehyde and analysed by agarose gel electrophoresis. As shown in Figure 4.1A, wild-type RuvB formed defined protein-DNA complexes (lanes b-h). The degree of DNA retardation increased with the protein concentration (lanes b-d), until saturation was reached at a stoichiometry of one RuvB hexamer per ~26 bp (lane e). This is consistent with DNase I footprinting experiments (Hiom and West, 1995a) and electron microscopic studies (Stasiak *et al.*, 1994), which suggest that a single RuvB hexamer spans 24-27 bp and a double hexamer encompasses 49 bp. In contrast, only slight retardation of the DNA was observed with RuvB^{D113E} (at ≥7 μM) under the same reaction conditions (lanes i-o).

RuvB binds DNA poorly at Mg^{2+} concentrations of ≤10 mM. Under these conditions, RuvA is required to mediate the interaction of RuvB with DNA (Müller *et al.*, 1993b). To determine whether RuvA could facilitate the binding of RuvB^{D113E} to DNA, band-shift assays were conducted at 5 mM Mg^{2+} in the presence of RuvA (Figure 4.1B). Whilst highly-retarded RuvAB-DNA complexes were observed with wild-type RuvB (lanes c-h), only weak DNA binding by RuvAB^{D113E} was detected (lanes i-n).

DNA BINDING BY RUVB^{D113E} IN ATP/ATPγS

Observations made by electron microscopy (discussed in the next section) suggested that the poor DNA binding observed with RuvB^{D113E} was due to the presence of ATPγS. This was confirmed by band-shift reactions that were carried out using 0.5 mM ATP and varying concentrations of ATPγS (Figure 4.2A). Increasing the ATPγS concentration enhanced DNA-protein complex

FIGURE 4.1. DUPLEX DNA BINDING BY RUVB^{D113E} IN THE PRESENCE OF ATPγS

A. Band-shift assays were conducted for RuvB and RuvB^{D113E} in the presence of 1 mM ATPγS, as described in Materials and Methods. Protein-DNA complexes were fixed with glutaraldehyde and analysed by 0.8% agarose gel electrophoresis followed by ethidium bromide staining.

B. DNA binding by RuvB^{D113E} in the presence of RuvA. Reactions were carried out as described for A, except that the Mg^{2+} concentration was reduced to 5 mM and RuvB/RuvB^{D113E} were premixed with RuvA (4 μM) as indicated.

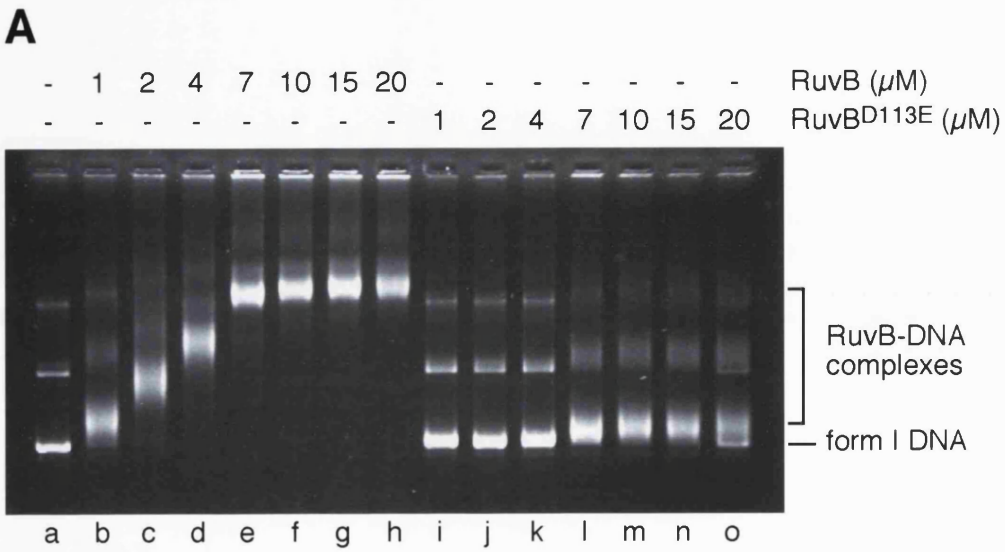
A
- 1 2 4 7 10 15 20 - - - - - - - RuvB (μM)
- - - - - - - - 1 2 4 7 10 15 20 RuvB^{D113E} (μM)
RuvB-DNA complexes
form I DNA
a b c d e f g h i j k l m n o

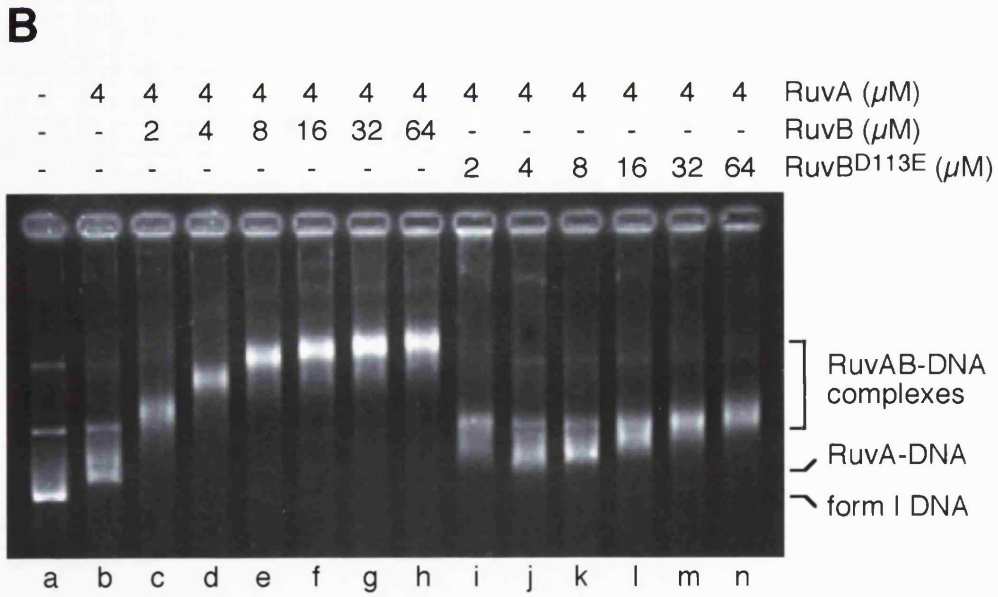
B
- 4 4 4 4 4 4 4 4 4 4 4 4 4 4 RuvA (μM)
- - 2 4 8 16 32 64 - - - - - - RuvB (μM)
- - - - - - - - 2 4 8 16 32 64 RuvB^{D113E} (μM)
RuvAB-DNA complexes
RuvA-DNA
form I DNA
a b c d e f g h i j k l m n

FIGURE 4.1

FIGURE 4.2. DUPLEX DNA BINDING BY RUVB^{D113E} IN THE PRESENCE OF ATP/ATPγS

A. Band-shift assays were conducted for RuvB and RuvB^{D113E} in the presence of 0.5 mM ATP and with the indicated concentrations of ATPγS, as described in Materials and Methods. Protein-DNA complexes were fixed with glutaraldehyde and analysed by 0.8% agarose gel electrophoresis followed by ethidium bromide staining.

B. DNA binding by RuvB^{D113E} in the presence of RuvA. Reactions were carried out as described for A, except that the Mg^{2+} concentration was reduced to 5 mM and RuvB or RuvB^{D113E} were premixed with RuvA (4 μM) as indicated.

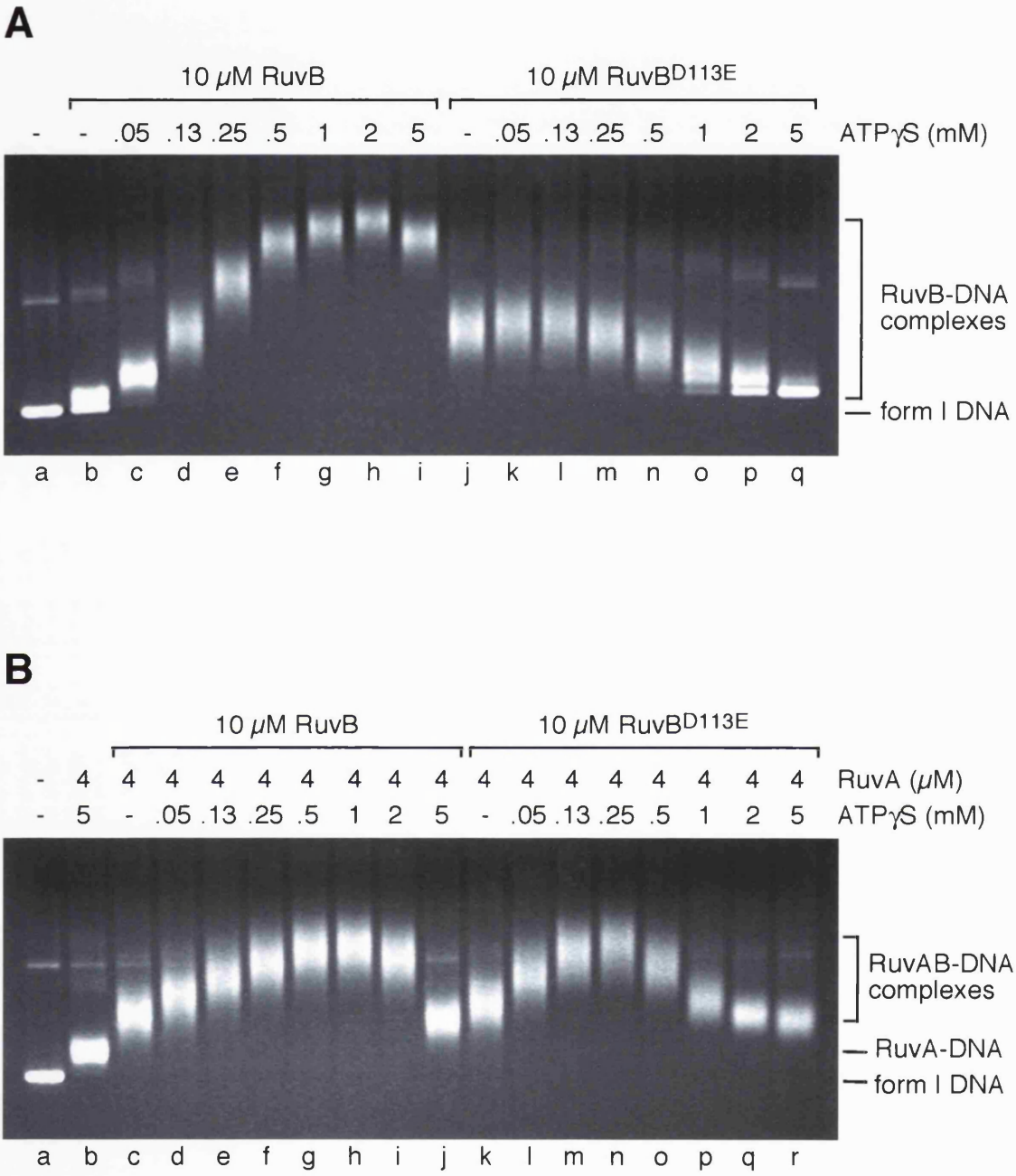
A
10 μM RuvB
10 μM RuvB^{D113E}
- - .05 .13 .25 .5 1 2 5 - .05 .13 .25 .5 1 2 5 ATPγS (mM)
RuvB-DNA complexes
form I DNA
a b c d e f g h i j k l m n o p q
B
10 μM RuvB
10 μM RuvB^{D113E}
- 4 4 4 4 4 4 4 4 4 4 4 4 4 4 4 4 4 RuvA (μM)
- 5 - .05 .13 .25 .5 1 2 5 - .05 .13 .25 .5 1 2 5 ATPγS (mM)
RuvAB-DNA complexes
RuvA-DNA
form I DNA
a b c d e f g h i j k l m n o p q r

FIGURE 4.2

formation by the wild-type protein (lanes c-i), whereas similar increases reduced the DNA binding by RuvB^{D113E} (lanes k-q). Interestingly, however, stable interaction between RuvB^{D113E} and dsDNA was detected in the presence of ATP alone (lane j), conditions in which only limited DNA binding by the wild-type protein is observed by band-shift assays (Müller *et al.*, 1993b; Figure 4.2A, lane b). Thus RuvB^{D113E} forms stable complexes with dsDNA in the presence of ATP but its DNA binding activity is inhibited by ATPγS. These results will be discussed further in later sections.

To test whether RuvA directs the loading of RuvB^{D113E} onto dsDNA, RuvAB-binding assays were conducted in the presence of 5 mM Mg^{2+} and varying ratios of ATP:ATPγS. Efficient DNA binding was observed for both RuvAB and RuvAB^{D113E}, although the degree of DNA retardation again varied depending on the cofactor conditions (Figure 4.2B). In the presence of RuvA, the binding of both proteins was stimulated by ATPγS, with maximum retardation observed at a ratio of 1:2 (RuvB) and 2:1 (RuvB^{D113E}) ATP:ATPγS, respectively (lanes h and n). Further increases in the concentration of ATPγS inhibited the binding of RuvB^{D113E} to DNA (lanes o - r), and at 5 mM ATPγS the interaction of the wild-type protein was also severely affected (lane j). In contrast with the previous experiment carried out in the absence of RuvA, stable protein-DNA complexes were detected in the presence of ATP alone with RuvB as well as RuvB^{D113E} (lanes c and k). It is possible that RuvA stabilises the binding of RuvB or reloads dissociated RuvB rings onto the DNA, thereby partially alleviating the need for ATPγS. In summary, these band-shift assays demonstrate that RuvB^{D113E} can form stable protein-DNA complexes, in the presence and absence of RuvA, and that the stability of this complex or the affinity of RuvB/RuvB^{D113E} for DNA can be modulated by variations in the ratio of ATP:ATPγS.

FORMATION OF HEXAMERIC RINGS BY RUVB^{D113E}

Previous studies have shown that, in the presence of Mg^{2+} and ATP or ATPγS, RuvB forms double hexameric rings that encircle the DNA (Stasiak *et al.*, 1994). To compare the low-resolution structures of wild-type RuvB and RuvB^{D113E}, the proteins were incubated with linear duplex DNA in the presence of 15 mM Mg^{2+} and 1 mM ATPγS. Protein-DNA complexes were fixed with glutaraldehyde, and visualised under an electron microscope by Dr A. Stasiak (University of Lausanne). RuvB^{D113E} formed doublet structures on the DNA (Figure 4.3B) that were indistinguishable from the double hexameric rings observed with wild-type RuvB (Stasiak *et al.*, 1994; Figure 4.3A). However, fewer RuvB^{D113E} rings were associated with the DNA compared with RuvB, which is consistent with the reduced DNA binding activity observed in the presence of ATPγS in earlier band-shift assays (Figures 4.1 and 4.2).

In addition to the DNA-bound double rings formed by RuvB^{D113E}, a large highly-structured aggregate of the mutant protein was observed that seemed to be free of DNA (Figure 4.3C). The aggregate appeared to be composed of interwound bundles of protein filament-like structures that each consisted of stacked RuvB^{D113E} rings. This self-association of RuvB^{D113E} may be responsible for the apparent reduced DNA binding activity of the protein in ATPγS. It should be noted that, apart from DNA binding and transient DNA unwinding (Chapter 5, section II), all other biochemical assays described are conducted in the presence of ATP alone, allowing direct comparisons to be made between RuvB and RuvB^{D113E}.

III. ATPASE ACTIVITY OF RUVB^{D113E}

To compare the DNA-dependent and DNA-independent ATPase activities of RuvB^{D113E} and RuvB, the proteins were incubated with ATP (spiked with [α-

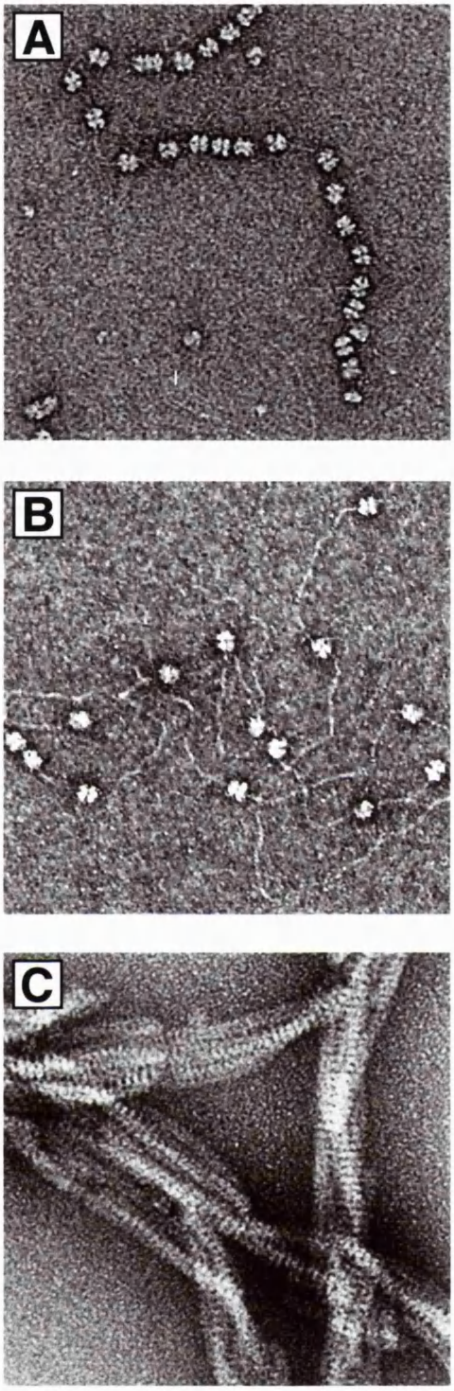

FIGURE 4.3. ELECTRON MICROSCOPIC VISUALISATION OF RUVB (A) AND RUVB^{D113E} (B, C) IN THE PRESENCE OF DUPLEX DNA.

Complexes formed in the presence of 15 mM Mg^{2+} and 1 mM ATPγS were prepared as described in Materials and Methods, and observed at a magnification of 70,000x.

^{32}P]ATP) in the presence or absence of form I DNA, under conditions (15 mM Mg^{2+}) that favour the association of RuvB with DNA (Müller *et al.*, 1993b). DNA-dependent reactions contained an excess of DNA compared to the amount of protein present. The products were analysed by thin-layer chromatography and the amount of [α-^{32}P]ADP present was quantified by PhosphorImager analysis (Figure 4.4A). In the absence of DNA, RuvB and RuvB^{D113E} exhibited low, but detectable, rates of ATP hydrolysis (0.79 and 0.30 mol ATP/min per mol protein, respectively). These weak intrinsic ATPase activities were stimulated 6- to 7-fold by the addition of form I DNA, resulting in rates of 5.7 and 1.8 mol ATP/min per mol protein for RuvB and RuvB^{D113E}, respectively. The results show that RuvB^{D113E} possesses DNA-dependent ATPase activity but with a k_{cat} value that is ~3-fold lower than that of the wild-type protein.

Previous studies have demonstrated that RuvA enhances the ATPase activity of RuvB by facilitating the loading of RuvB onto DNA (Marrione and Cox, 1996; Mitchell and West, 1996; Shiba *et al.*, 1991). To investigate the effect of RuvA on the DNA-dependent ATPase activity of RuvB^{D113E}, time course experiments were conducted in the presence and absence of RuvA (Figure 4.4B). In the absence of RuvA, RuvB and RuvB^{D113E} hydrolysed ATP at rates of 4.8 and 1.4 mol ATP/min per mol protein, respectively. Upon addition of RuvA, the rates of ATP hydrolysis by both proteins were stimulated ~4-fold. These results indicate that RuvA is able to interact with and load RuvB^{D113E} onto dsDNA and thereby enhance its ATPase activity.

FIGURE 4.4. ATPASE ACTIVITY OF RUVB^{D113E}.

A. Comparison of the ATPase activities of RuvB and RuvB^{D113E} in the presence and absence of duplex DNA. Large scale assays were performed as described in Materials and Methods. Reactions were initiated with the addition of 5 μM RuvB (■) or 5 μM RuvB^{D113E} (●). In control reactions, DNA was omitted (□ and ○). At the indicated times, samples were removed and subjected to thin-layer chromatography, and the percentage of ATP hydrolysed to ADP was determined by PhosphorImager analysis. Background levels of ADP (2% and 4%), observed in the absence of RuvB, have been subtracted.

B. Comparison of the DNA-dependent ATPase activities of RuvB and RuvB^{D113E} in the presence and absence of RuvA. Reactions were carried out as described for A, except that 4 μM RuvB (◆) or 4 μM RuvB^{D113E} (✦) were premixed with 1 μM RuvA. In control reactions, RuvA was omitted (◇ and ✧). Background levels of ADP (2.2% and 2.6%) have been subtracted.

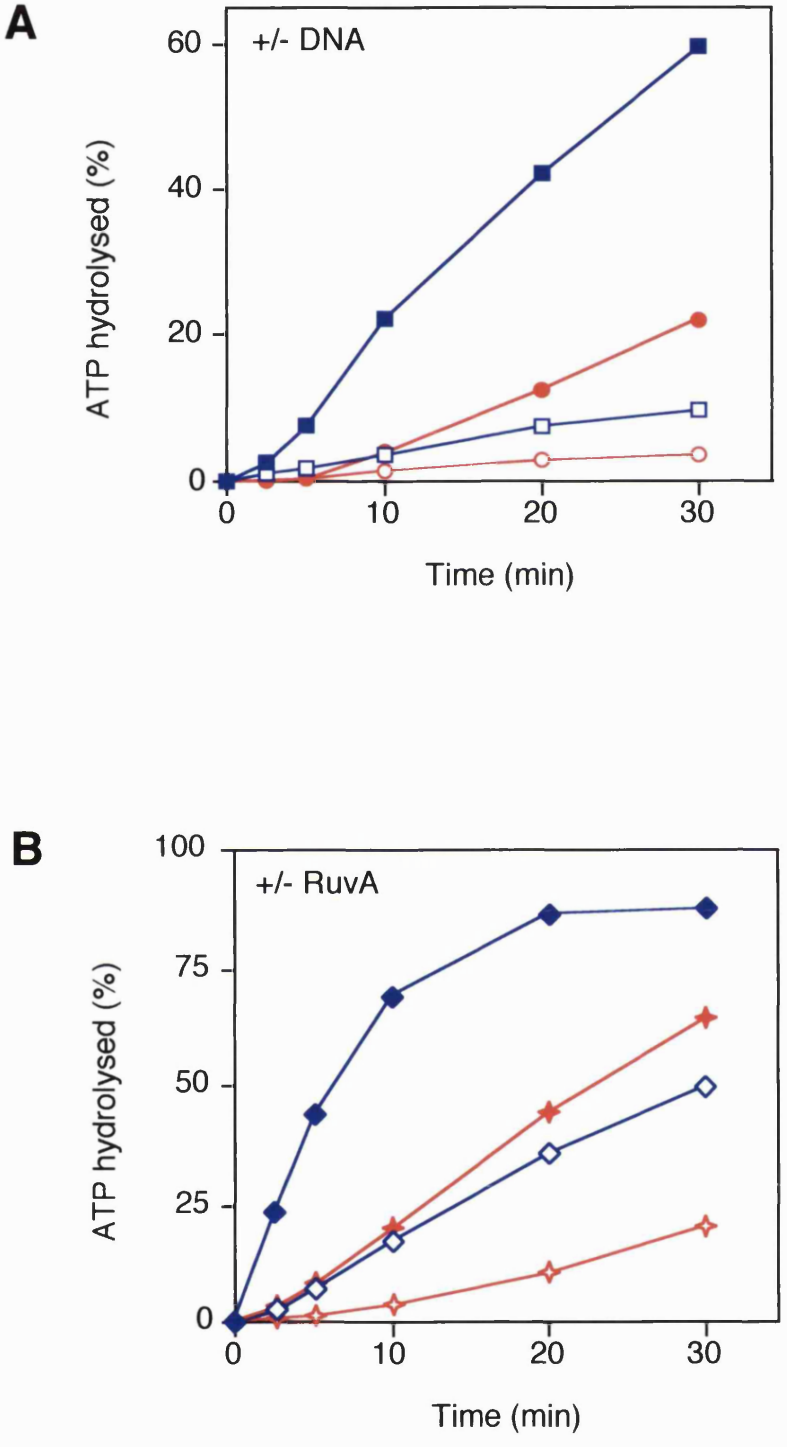
A
+/- DNA
ATP hydrolysed (%)
60
40
20
0
0
10
20
30
Time (min)
B
+/- RuvA
ATP hydrolysed (%)
100
75
50
25
0
0
10
20
30
Time (min)

FIGURE 4.4

IV. SUMMARY AND DISCUSSION

In this chapter, it has been shown that RuvB^{D113E} is capable of dsDNA binding, hexameric ring formation, interaction with RuvA and DNA-dependent ATPase activity. The interaction of the mutant protein with DNA was investigated using band-shift assays and found to exhibit different nucleotide cofactor preferences compared to wild-type RuvB. It was shown previously that ATPγS favours the stable association of RuvB with DNA and that only weak interactions are detected in the presence of ATP (Müller *et al.*, 1993b), observations that were confirmed in the present study. In contrast, however, DNA binding by RuvB^{D113E} occurred preferentially in the presence of ATP. It has been suggested that, whilst ATP binding is required for the formation of RuvB-DNA complexes, subsequent hydrolysis of ATP may result in the dissociation of RuvB from DNA (Müller *et al.*, 1993b). The stable interaction of RuvB^{D113E} with DNA in the presence of ATP may, therefore, be due to the reduced ATPase activity of the mutant protein. An alternative possibility that cannot be ruled out is that the Asp to Glu substitution causes a conformational change in the protein, such that hexameric rings assemble on the duplex DNA in a more locked configuration than the wild-type protein.

The band-shift studies showed that the binding of RuvB^{D113E} to DNA is inhibited by ATPγS. When protein-DNA complexes formed in the presence of ATPγS were visualised by electron microscopy, both double hexameric rings on the DNA and a large protein complex were observed for RuvB^{D113E}. The mutant protein therefore appears to have a tendency to aggregate in the presence of ATPγS, which would consequently prevent its interaction with DNA. Interestingly, the mutant protein RuvB^{D113N}, which contains an Asp113 to asparagine substitution, has also been shown to self-associate but to a lesser extent, forming short rod-like filaments (Mézard *et al.*, 1997).

X-ray crystallographic studies of NTP-hydrolysing proteins indicate that the highly conserved aspartate in the Walker B motif (corresponding to helicase motif II) interacts with Mg^{2+} through a water molecule (Pai *et al.*, 1990; Story and Steitz, 1992). The Mg^{2+} ion is, in turn, complexed to the terminal phosphates of the bound nucleotide (see Figure 3.1). Furthermore, the crystal structure of the DNA helicase PcrA, in a ternary complex with DNA and a non-hydrolysable analogue of ATP (adenylylimidodiphosphate, AMP-PNP), shows that the aspartate residue contacts a Mg^{2+} ion bound in the active site of the enzyme. Since coordination of a divalent ion is usually required for NTP hydrolysis (Schulz, 1992), mutations of this aspartate residue in helicase motif II are often associated with disrupted NTPase activity (Dombroski *et al.*, 1988; Gross and Shuman, 1995; Mézard *et al.*, 1997; Pause and Sonenberg, 1992; Soultanas *et al.*, 1999; Washington *et al.*, 1996). Replacement of Asp113 with glutamate in RuvB, however, only reduced its DNA-dependent ATPase activity by ~3-fold, whilst the equivalent mutation in RNA helicase eIF-4A had no effect on the ATPase activity of the protein (Pause and Sonenberg, 1992). Glutamate possess an identical side-chain to aspartate with the exception of an additional $-CH_2$ group. The ability of $RuvB^{D113E}$ to hydrolyse ATP could be due to the larger side-chain of the glutamate residue bypassing the water molecule and interacting directly with the ATP-bound Mg^{2+}, as proposed for eIF-4A (Pause and Sonenberg, 1992).

RuvA and RuvB interact in solution (Mitchell and West, 1994; Shiba *et al.*, 1993) and form a multi-subunit complex on Holliday junctions that promotes branch migration (Hiom and West, 1995a; Parsons *et al.*, 1995a; Parsons and West, 1993). Whilst the interaction between RuvA and $RuvB^{D113E}$ was not tested directly, RuvA facilitated binding of the mutant protein to DNA under conditions ($\leq$10 mM Mg^{2+}) in which RuvB is known to interact poorly with

DNA (Müller and West, 1993b). Furthermore, RuvA stimulated the DNA-dependent ATPase activity of $RuvB^{D113E}$ by the same factor as the wild-type protein. Taken together, these results indicate that RuvA interacts normally with $RuvB^{D113E}$ and loads it onto dsDNA.

CHAPTER FIVE : RESULTS

BIOCHEMICAL CHARACTERISATION OF RUVB^{D113E}

PART II

I. INTRODUCTION

RuvB possesses conserved helicase motifs (see Figure 1.7), shares structural similarities with other hexameric ring proteins and, under certain conditions, exhibits ATP-dependent helicase activity *in vitro* (Adams and West, 1995b; Egelman, 1996; Tsaneva *et al.*, 1993; Tsaneva and West, 1994; West, 1996). During branch migration, the two RuvB rings are assembled on the 'outgoing' (heteroduplex) arms of the RuvA-bound Holliday junction and are thought to drive the reaction by pumping duplex DNA through their central channels (Hiom *et al.*, 1996; Hiom and West, 1995a; Parsons *et al.*, 1995a). Thus the current model for RuvAB-mediated branch migration proposes that separation of the homoduplexes and strand exchange have occurred prior to reaching the RuvB rings, thereby questioning the role of RuvB-catalysed unwinding in this reaction.

The principle aim of introducing the Asp113 to glutamate substitution into RuvB was to dissociate the ATPase and helicase activities of the protein, thereby allowing the requirement for DNA unwinding in branch migration to be assessed specifically. Having established that RuvB^{D113E} binds DNA and hydrolyses ATP, prerequisites for the helicase and branch migration activities of RuvB (Adams and West, 1995b; Tsaneva *et al.*, 1992b; Tsaneva *et al.*, 1993), the mutant protein was further characterised *in vitro*.

II. DNA UNWINDING CATALYSED BY RUVB^{D113E}

DNA HELICASE ACTIVITY OF RUVAB^{D113E}

DNA helicase activity catalysed by RuvAB has been demonstrated *in vitro*, using standard substrates comprising a single-stranded circle with a short annealed fragment (Tsaneva *et al.*, 1993). To determine whether RuvAB^{D113E} possesses helicase activity, the release of a ^{32}P-labelled 66 nt oligonucleotide from circular ssDNA was measured (Figure 5.1). In the presence of RuvA, wild-type RuvB promoted efficient strand displacement (Figure 5.1A, lanes b-g) with ~80% product observed at 160 nM RuvB (Figure 5.1B). In contrast, RuvAB^{D113E} failed to displace the 66-mer fragment (lanes h - m), even at higher RuvB^{D113E} concentrations of up to 1.3 μM (data not shown). Similar results were obtained with a DNA helicase substrate carrying an annealed 40-mer oligonucleotide (data not shown).

To determine whether RuvB^{D113E} can release shorter fragments, helicase substrates with annealed 20 or 30 nt long oligonucleotides were prepared. Each substrate was used in reactions containing combinations of RuvA, RuvB and RuvB^{D113E} as shown in Figure 5.2. RuvA alone (lanes b and k), or RuvB/RuvB^{D113E} alone (lanes d, f, h, m, o and q) were unable to promote strand displacement. In the presence of RuvA, wild-type RuvB efficiently displaced the annealed oligonucleotides (lanes c and l). In contrast, RuvAB^{D113E} released only trace amounts of the 30 nt long fragment (lanes n and p), supporting the data presented in Figure 5.1 and indicating that the mutant protein is helicase-defective. Surprisingly, however, RuvAB^{D113E} were found to promote limited displacement of the 20-mer oligonucleotide (lanes e and g). To investigate this result further, a time course experiment was conducted and showed that the

FIGURE 5.1. HELICASE ACTIVITY OF RUVB^{D113E}: DISPLACEMENT OF A 66 NT FRAGMENT

A. Helicase substrate comprising a ^{32}P-labelled 66 nt oligonucleotide annealed to circular ssDNA was premixed with RuvA (30 nM) and incubated with the indicated amounts of RuvB or RuvB^{D113E}. Reactions were carried out as described in Materials and Methods. Products were deproteinised and analysed by 6% neutral PAGE followed by autoradiography. Lane n: heat-denatured control.

B. Quantification of the gel shown in A by PhosphorImager analysis. (■) RuvB, (●) RuvB^{D113E}. Displaced 66 nt fragments are expressed as a percentage of total ^{32}P-labelled DNA. In each case, a background amount of 66-mer observed in the absence of protein (lane a, 3.9%) has been subtracted.

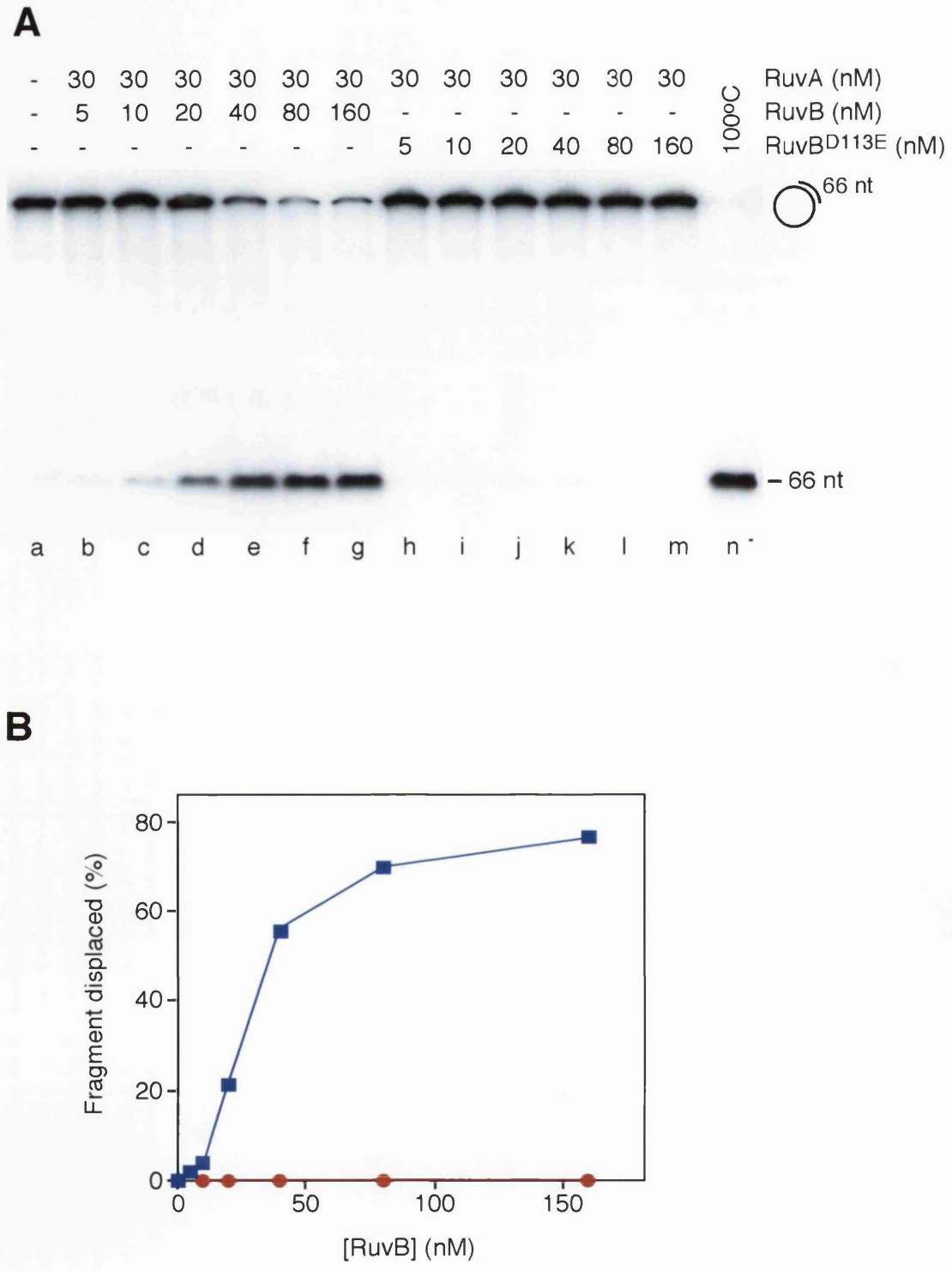
A
- 30 30 30 30 30 30 30 30 30 30 30 30
- 5 10 20 40 80 160 - - - - - -
- - - - - - - 5 10 20 40 80 160
100°C
RuvA (nM)
RuvB (nM)
RuvB^D113E (nM)
66 nt
– 66 nt
a b c d e f g h i j k l m n
B
Fragment displaced (%)
80
60
40
20
0
0
50
100
150
[RuvB] (nM)

FIGURE 5.1

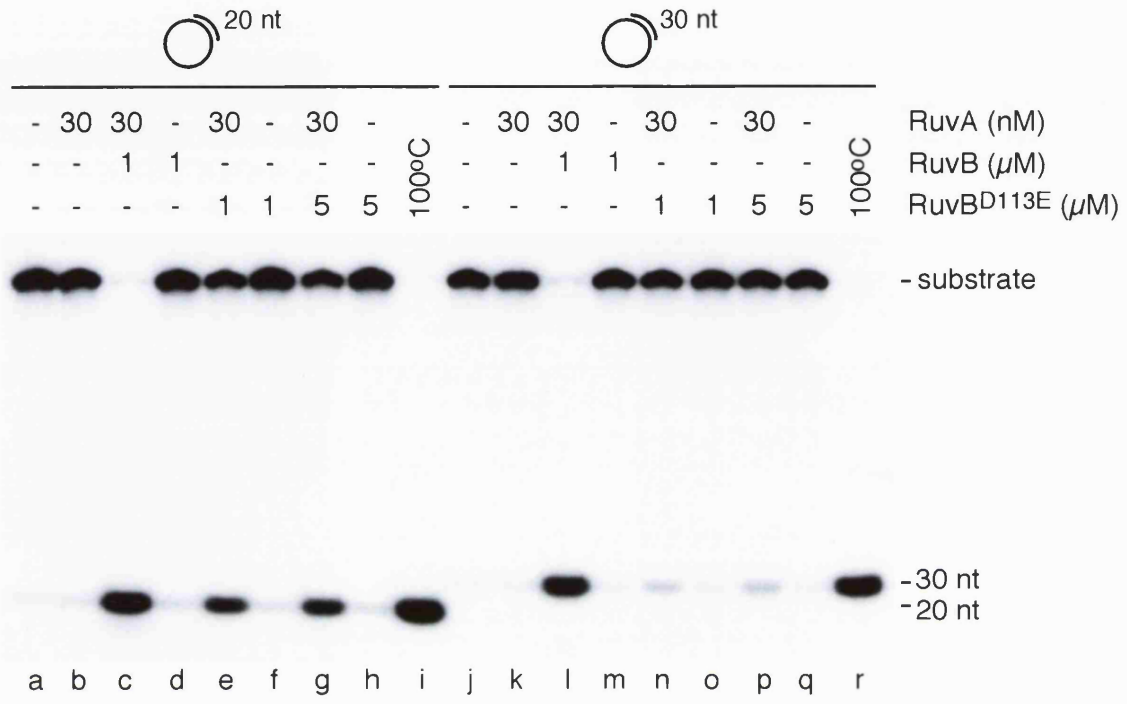

FIGURE 5.2. HELICASE ACTIVITY OF RUVB^{D113E}: DISPLACEMENT OF 20 NT AND 30 NT FRAGMENTS

Helicase substrates comprising a ^{32}P-end-labelled 20 nt or 30 nt oligonucleotide annealed to circular ssDNA were incubated with RuvB or RuvB^{D113E}, in the presence and absence of RuvA (30 nM) as indicated. Reactions were conducted as described in Materials and Methods. Products were deproteinised and analysed by 8% neutral PAGE followed by autoradiography. Lanes i and r: heat-denatured controls.

rate of displacement of the 20-mer fragment by RuvAB^{D113E} was ~30-fold lower than that observed with RuvAB (Figure 5.3).

TRANSIENT UNWINDING ACTIVITY OF RUVB^{D113E}

Using a sensitive topological assay, it has been shown that RuvAB, or RuvB alone, promote the transient unwinding of covalently closed duplex DNA (Adams and West, 1995b). This assay was carried out on RuvB^{D113E} to determine whether the mutant protein is able to transiently unwind dsDNA, despite being severely compromised in its strand displacement activity. A schematic diagram of the topological assay is shown in Figure 5.4A. The ATP-dependent unwinding of relaxed plasmid DNA, by RuvAB or RuvB, results in the introduction of compensating positive supercoils that are removed by eukaryotic (wheat germ) topoisomerase I. Upon deproteinisation, rewinding of the DNA in the regions opened by RuvAB results in a negatively supercoiled species that migrates faster on an agarose gel than the relaxed substrate. The unwinding reaction is thought to be transient, as its detection requires the presence of ATPγS in addition to ATP. The slowly hydrolysable analogue may stabilise the RuvAB complexes on the DNA, shortly after ATP-dependent unwinding has occurred.

At elevated concentrations of Mg^{2+} (12 to 30 mM), conditions that favour RuvB binding to DNA, wild-type RuvB can unwind DNA in the absence of RuvA (Adams and West, 1995b). To test whether RuvB^{D113E} alone is able to transiently unwind duplex DNA, ^{32}P-labelled relaxed plasmid DNA was incubated with wild-type and mutant RuvB in the presence of 30 mM Mg^{2+} and nucleotide cofactors. In light of the inhibitory effects of ATPγS on DNA binding by RuvB^{D113E}, assays were conducted in the presence of a constant amount of ATP and increasing amounts of ATPγS (Figure 5.4B). Fast migrating bands, the

FIGURE 5.3. COMPARISON OF THE RATE OF DISPLACEMENT OF A 20 NT FRAGMENT BY RUVB AND RUVB^{D113E}

A. Large scale reactions containing a 20 nt annealed substrate premixed with RuvA (30 nM) were initiated by the addition of RuvB (500 nM) or RuvB^{D113E} (500 nM). Helicase reactions were carried out as described in Materials and Methods. At the indicated times, samples were deproteinised and analysed by 8% neutral PAGE followed by autoradiography.

B. Quantification of the gel shown in A by PhosphorImager analysis. (■) RuvB, (●) RuvB^{D113E}. Displaced 20 nt fragments are expressed as a percentage of total ^{32}P-labelled DNA. An average background amount of 20-mer observed in the absence of protein (lanes a and b, 7.4%) has been subtracted.

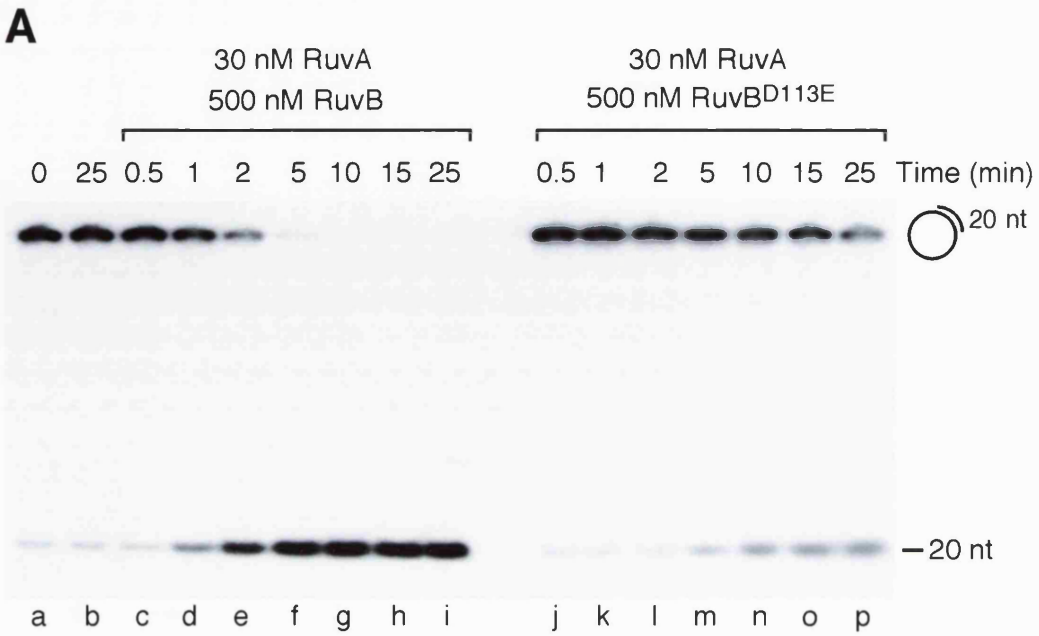
A
30 nM RuvA
500 nM RuvB
30 nM RuvA
500 nM RuvBD113E
0 25 0.5 1 2 5 10 15 25
0.5 1 2 5 10 15 25 Time (min)
20 nt
20 nt
a b c d e f g h i
j k l m n o p

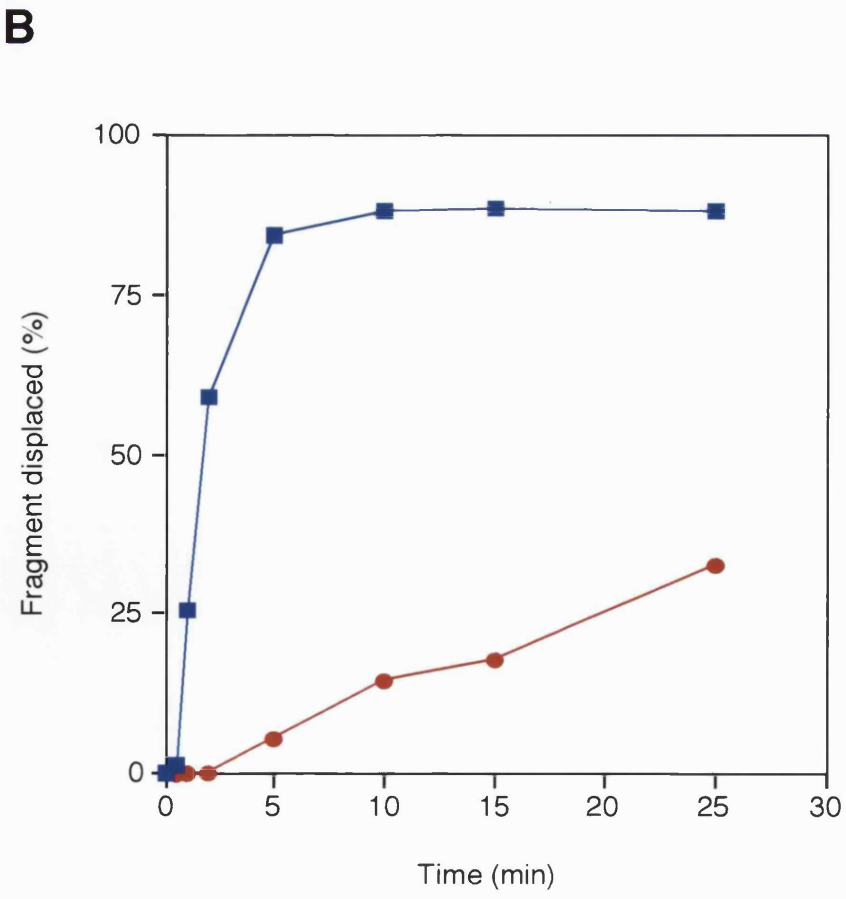
B
100
75
50
25
0
Fragment displaced (%)
0 5 10 15 20 25 30
Time (min)

FIGURE 5.3

FIGURE 5.4. TRANSIENT UNWINDING OF COVALENTLY CLOSED DNA

A. *In vitro* topological assay for detecting transient unwinding. The localised unwinding of relaxed covalently closed (cc) DNA (a) by RuvAB, or RuvB alone, results in the introduction of compensating positive supercoils (b) which are subsequently removed by eukaryotic topoisomerase I (euk Topo I) (c). Upon deproteinisation with SDS and proteinase K, rewinding of the DNA in the regions opened by RuvAB leads to negatively supercoiled products (d). Detection of unwinding products requires a mixture of ATP and ATPγS.

B. Transient unwinding activity of RuvB and $RuvB^{D113E}$ under different nucleotide conditions. Uniformly ^{32}P-labelled relaxed plasmid DNA was incubated with RuvB or $RuvB^{D113E}$ (4.8 μM) in reaction buffer containing 0.5 mM ATP and the indicated concentrations of ATPγS. Reactions were carried out as described in Materials and Methods. Wheat germ topoisomerase I was added where indicated, and the products were deproteinised and analysed by 0.7% agarose gel electrophoresis. Lane a: supercoiled DNA marker (M).

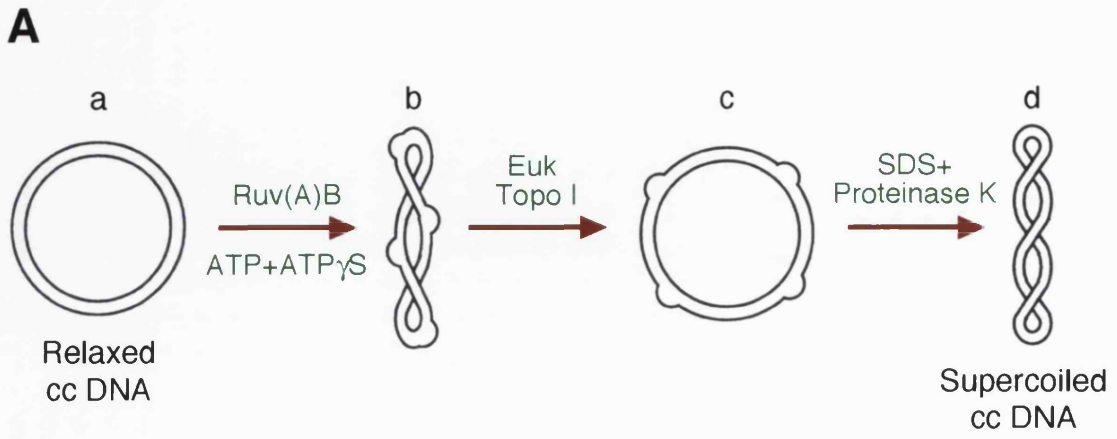
A
a
b
c
d
Ruv(A)B
ATP+ATPγS
Euk
Topo I
SDS+
Proteinase K
Relaxed
cc DNA
Supercoiled
cc DNA

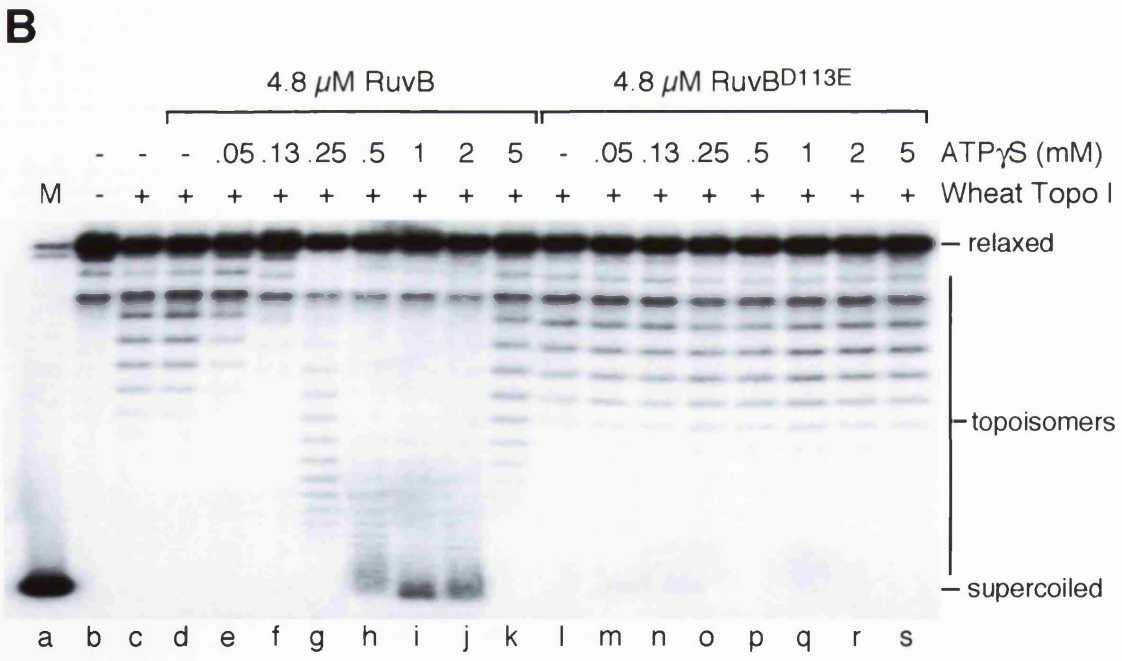
B
4.8 μM RuvB
4.8 μM RuvBD113E
- - - .05 .13 .25 .5 1 2 5 - .05 .13 .25 .5 1 2 5 ATPγS (mM)
M - + + + + + + + + + + + + + + + + Wheat Topo I
relaxed
topoisomers
supercoiled
a b c d e f g h i j k l m n o p q r s

FIGURE 5.4

products of DNA unwinding, were observed for wild-type RuvB (lanes g-k). Since the unwinding products (topoisomers) migrate at specific positions depending on the number of supercoils introduced, electrophoretic mobility represents a direct measure of the amount of unwinding. As observed previously (Adams and West, 1995b), maximum unwinding by RuvB occurred at an ATP:ATPγS ratio of ~1:2 (lane i). At this nucleotide ratio, the unwinding products migrated at the same position as native supercoiled DNA (compare lanes a and i). $RuvB^{D113E}$, however, failed to promote DNA unwinding under all nucleotide conditions tested (compare lanes l-s to control lane c), even when the protein concentration was increased by 10-fold (data not shown).

RuvA has been shown to stimulate RuvB-mediated DNA unwinding and is essential for activity at <15 mM Mg^{2+} (Adams and West, 1995b). When similar reactions to those described above were carried out in the presence of RuvA, DNA unwinding products were detected with $RuvB^{D113E}$ (Figure 5.5A, lanes m-p) as well as with the wild-type protein (lanes f-l). However, as expected from the earlier DNA binding studies, the proteins exhibited different nucleotide preferences. Whilst maximum DNA unwinding by RuvAB was observed at an ATP:ATPγS ratio of ~1:2 (lanes i-k), $RuvAB^{D113E}$-catalysed unwinding occurred in the absence (lane m) and at low concentrations (lanes n-p) of ATPγS with the optimum ATP:ATPγS ratio being 10:1 (lane n).

The abilities of RuvAB and $RuvAB^{D113E}$ to promote DNA unwinding, under optimal reaction conditions, are compared in Figure 5.5B. The degree of unwinding observed for wild-type and mutant RuvB was comparable and, in both cases, directly proportional to the protein concentration (compare lanes e-i and j-n). Taken together, the results of these experiments indicate that, under optimised nucleotide conditions, $RuvB^{D113E}$ can promote efficient transient unwinding of duplex DNA but only in the presence of RuvA.

FIGURE 5.5. TRANSIENT DNA UNWINDING ACTIVITY OF RUVB^{D113E} IN THE PRESENCE OF RUVA

A. Dependence of unwinding by RuvAB or RuvAB^{D113E} on the ATP:ATPγS ratio. Uniformly ^{32}P-labelled relaxed plasmid DNA was incubated with RuvA (2 μM) and RuvB or RuvB^{D113E} (2.4 μM) in reaction buffer containing 0.5 mM ATP and the indicated concentrations of ATPγS. Reactions were carried out as described in Materials and Methods. Wheat germ topoisomerase I was added where indicated, and the products were deproteinised and analysed by 0.7% agarose gel electrophoresis. Lane a: supercoiled DNA marker (M).

B. Comparison of the unwinding activities of RuvAB and RuvAB^{D113E}. Reactions were conducted as described for A, adding the indicated amounts of RuvB or RuvB^{D113E} and in the presence of optimum ATP/ATPγS conditions as determined in A. The RuvA control (lane d) contains 0.5 mM ATP and 0.05 mM ATPγS.

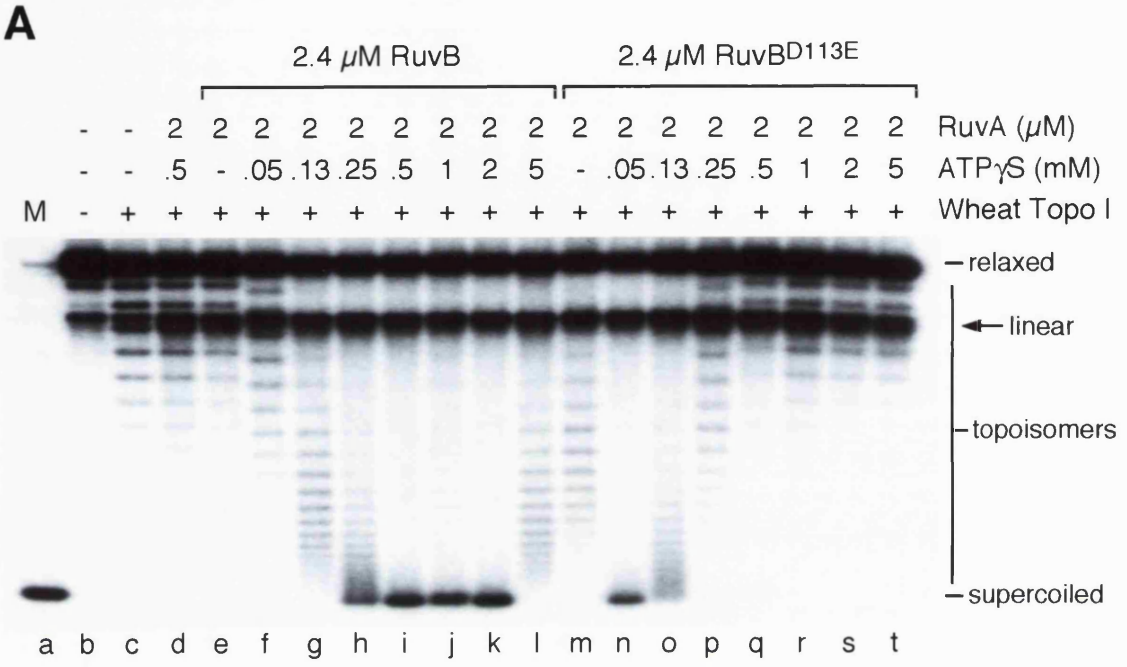
A
2.4 μM RuvB
2.4 μM RuvBD113E
RuvA (μM)
ATPγS (mM)
Wheat Topo I
M
relaxed
linear
topoisomers
supercoiled
a b c d e f g h i j k l m n o p q r s t

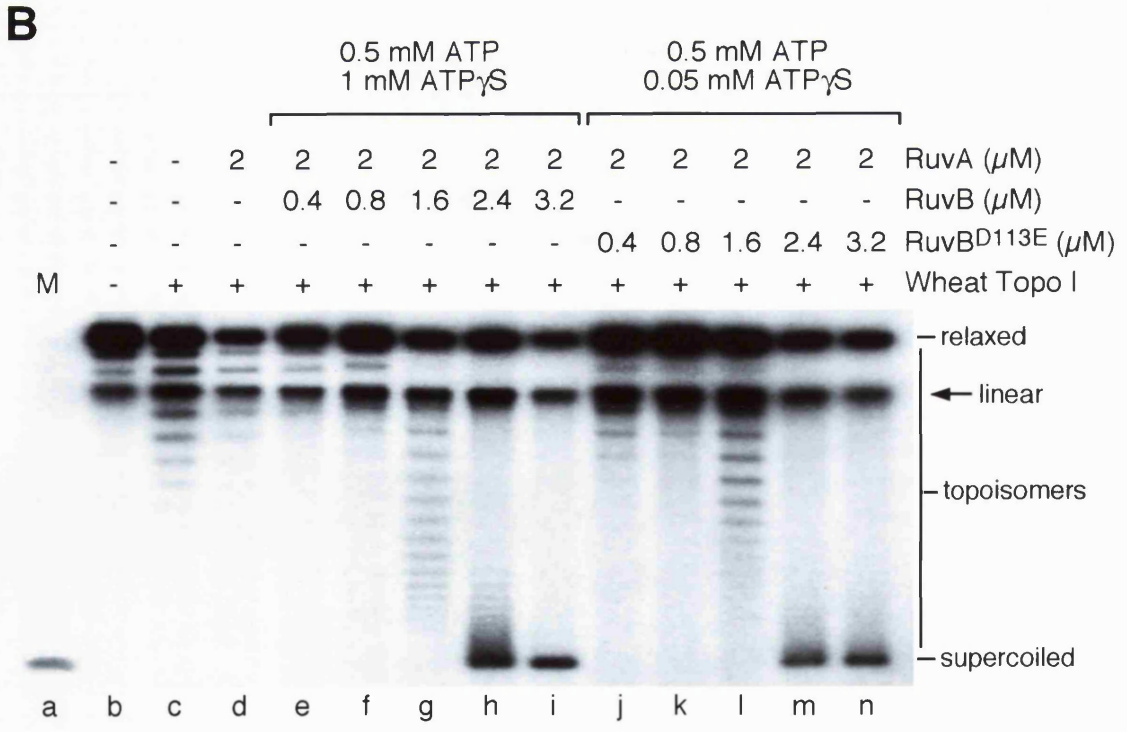
B
0.5 mM ATP
1 mM ATPγS
0.5 mM ATP
0.05 mM ATPγS
RuvA (μM)
RuvB (μM)
RuvBD113E (μM)
Wheat Topo I
M
relaxed
linear
topoisomers
supercoiled
a b c d e f g h i j k l m n

FIGURE 5.5

III. BRANCH MIGRATION ACTIVITY OF RUVB^{D113E}

IN VITRO ASSAY FOR BRANCH MIGRATION

Having established that RuvB^{D113E} is severely compromised in its strand displacement activity but partially or totally proficient in all other biochemical activities tested, I wanted to assess its ability to promote branch migration. The *in vitro* assay used to study RuvAB-mediated branch migration is outlined in Figure 5.6 and was conducted as described elsewhere (Eggleston *et al.*, 1997). Recombination intermediates (α-structures) were prepared by RecA-mediated strand exchange between gapped circular pDEA-7Z DNA (gDNA) and ^{32}P-labelled linear duplex pAKE-7Z DNA. With these substrates, strand exchange is driven through ~2.6 kbp of homology, up to a ~1.7 kbp region of heterologous sequences. Since RecA-mediated exchange is unable to bypass heterologies of ≥120 bp in size (Hahn *et al.*, 1988; Morel *et al.*, 1994), these sequences act as a block to the reaction.

In the presence of ATP, RuvAB act on deproteinised recombination intermediates and promote branch migration. Due to the heterologous block, branch migration is only permitted in the 'reverse' direction, leading to the dissociation of the α-structures and release of ^{32}P-labelled linear duplex DNA (Mitchell and West, 1996). The products can be separated by agarose gel electrophoresis and quantified by PhosphorImager analysis.

BRANCH MIGRATION OF RECOMBINATION INTERMEDIATES BY RUVB^{D113E}

RuvB alone promotes branch migration in the presence of stoichiometric amounts of protein and at elevated (≥15 mM) Mg^{2+} concentrations (Mitchell and West, 1996; Müller *et al.*, 1993a; Tsaneva *et al.*, 1992b; Figure 5.7A, lanes b-f). In

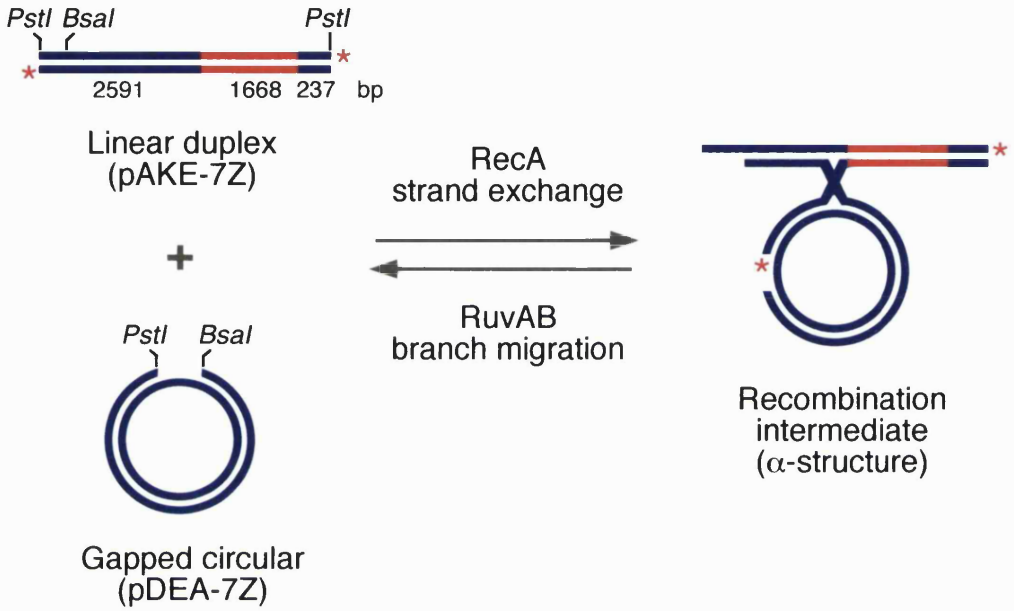

FIGURE 5.6. *IN VITRO* ASSAY FOR BRANCH MIGRATION

RecA protein promotes strand exchange between gapped circular duplex DNA (pDEA-7Z) and 3′ ^{32}P-end-labelled linear duplex DNA (pAKE-7Z), to form recombination intermediates (α-structures). The strand exchange reaction proceeds for ~2.6 kbp before being blocked by a ~1.7 kbp region of heterology in the linear duplex (red shading). The RuvAB proteins, or under certain conditions RuvB alone, promote branch migration away from the block (ie. reverse branch migration) leading to dissociation of the α-structures and giving rise to the two starting substrates, as shown. The red asterisk represents the position of the ^{32}P-end-label.

FIGURE 5.7. BRANCH MIGRATION ACTIVITY OF RUVB^{D113E} AND RUVAB^{D113E}

A. RuvB-mediated branch migration. Deproteinised ^{32}P-labelled recombination intermediates were incubated with the indicated concentrations of RuvB or RuvB^{D113E}, as described in Materials and Methods. Products were deproteinised and analysed by 1.2% agarose gel electrophoresis. Labelled DNA was visualised by autoradiography.

B. RuvAB-mediated branch migration. Reactions were carried out as described for A, except recombination intermediates were premixed with RuvA (15 nM) prior to the addition of RuvB or RuvB^{D113E}.

C. Quantification of the agarose gels shown in A and B by PhosphorImager analysis. (■) RuvB, (●) RuvB^{D113E}. Linear duplex products are expressed as a percentage of total ^{32}P-labelled DNA. Background values of linear duplex DNA observed in the absence of protein have been deducted.

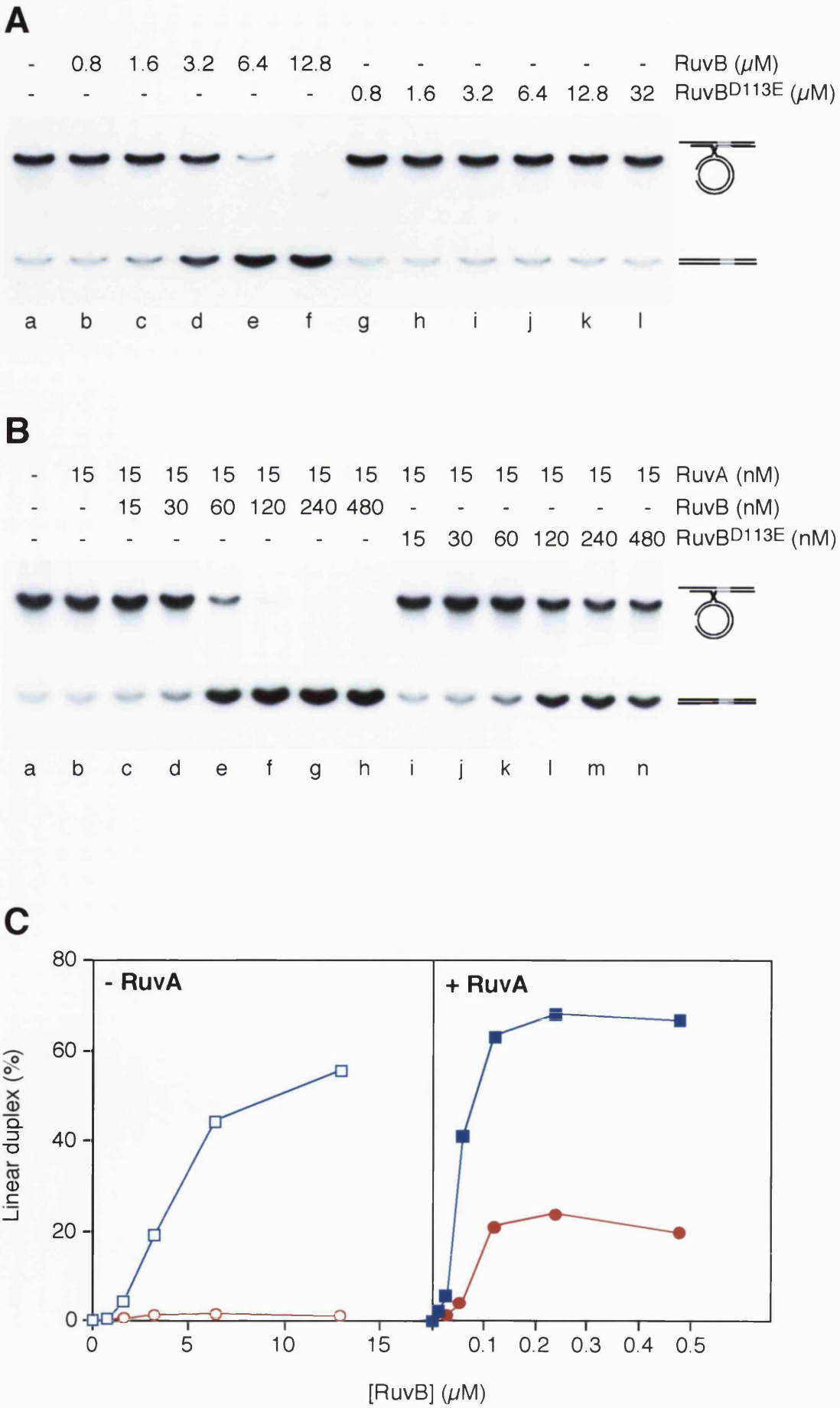
A
- 0.8 1.6 3.2 6.4 12.8 - - - - - - RuvB (μM)
- - - - - - 0.8 1.6 3.2 6.4 12.8 32 RuvB^{D113E} (μM)
a b c d e f g h i j k l
B
- 15 15 15 15 15 15 15 15 15 15 15 15 15 RuvA (nM)
- - 15 30 60 120 240 480 - - - - - - RuvB (nM)
- - - - - - - - 15 30 60 120 240 480 RuvB^{D113E} (nM)
a b c d e f g h i j k l m n
C
- RuvA
+ RuvA
Linear duplex (%)
80
60
40
20
0
0 5 10 15
0.1 0.2 0.3 0.4 0.5
[RuvB] (μM)

FIGURE 5.7

contrast, RuvB^{D113E} failed to promote branch migration in the absence of RuvA, even at high protein concentrations (Figure 5.7A, lanes g-l).

Although RuvB-mediated branch migration provides a useful *in vitro* assay, the RuvAB-dependent reaction is thought to be the most relevant mechanism *in vivo* since *ruvA* mutants exhibit a similar repair-defective phenotype to *ruvB* mutants (Lloyd *et al.*, 1984; Mandal *et al.*, 1993; Sharples *et al.*, 1990). Therefore, branch migration assays were conducted in the presence of RuvA (Figure 5.7B). These reactions were performed at low RuvB concentrations and at 10 mM Mg^{2+} (Mitchell and West, 1996). Significantly, RuvB^{D113E} catalysed branch migration in the presence of RuvA, albeit with reduced efficiency compared to the wild-type protein (compare lanes c-h and i–n). Compared to wild-type RuvB, ~3-fold more RuvB^{D113E} was required to obtain 20% linear duplex product (Figure 5.7C, right panel). The reduced efficiency of branch migration observed with RuvB^{D113E} is possibly due its reduced ATPase activity.

The heterologous block in the recombination intermediates is positioned ~2.6 kbp into the linear duplex (Figure 5.6). Therefore, assuming that the Holliday junction is driven to the block in all the substrate molecules, RuvAB-mediated branch migration has to occur over an appreciable distance for release of linear duplex product. Therefore, it should be noted that the activity observed for RuvAB^{D113E}, although reduced, is highly significant and clearly shows that the mutant protein is proficient in branch migration activity.

BRANCH MIGRATION OF SYNTHETIC JUNCTIONS

In addition to recombination intermediates made by RecA, the branch migration activity of RuvAB has also been demonstrated using small synthetic Holliday junctions (Iwasaki *et al.*, 1992; Parsons *et al.*, 1992; Parsons and West,

1993). To further study the branch migration activity of RuvB^{D113E}, assays were conducted using synthetic junctions. The junction used for these reactions, X12 (van Gool *et al.*, 1998), contained a 12 bp homologous core and was generated by annealing four 50-mer oligonucleotides. In the presence of RuvA, both RuvB and RuvB^{D113E} promoted branch migration to form duplex DNA products with splayed single-stranded arms (Figure 5.8A), although the activity of the mutant protein was significantly reduced compared to wild-type RuvB (Figure 5.8B). It should be noted, however, that the results of these experiments were variable and that, in some cases, the branch migration activity of RuvAB^{D113E} was more comparable to that of RuvAB. In agreement with previous findings (Parsons *et al.*, 1992; Parsons and West, 1993), branch migration by neither protein was observed in the absence of RuvA (Figure 5.8A, lanes h and n).

IV. INTERACTION OF RUVB^{D113E} WITH RUVC

FORMATION OF A COMPLEX BETWEEN RUVB^{D113E} AND RUVC

Genetic and biochemical studies indicate that RuvAB-mediated branch migration and RuvC-mediated resolution are coupled by the formation of a RuvABC-Holliday junction complex (Davies and West, 1998; Eggleston *et al.*, 1997; Lloyd *et al.*, 1984; Mahdi *et al.*, 1996; Mandal *et al.*, 1993; Sharples *et al.*, 1990; Sharples *et al.*, 1994a; van Gool *et al.*, 1998; Whitby *et al.*, 1996; Zerbib *et al.*, 1998). Direct interactions between RuvB and RuvC, in the absence of DNA, have been demonstrated by chemical cross-linking (Eggleston *et al.*, 1997). To determine whether RuvB^{D113E} is able to interact with RuvC, the proteins were mixed and complexes formed were covalently linked with glutaraldehyde. The cross-linked products were analysed by SDS-PAGE followed by Western blotting using anti-RuvB and anti-RuvC antibodies (Figure 5.9A).

FIGURE 5.8. BRANCH MIGRATION OF SYNTHETIC HOLLIDAY JUNCTIONS BY RUVB^{D113E}

A. ^{32}P-labelled synthetic Holliday junctions (X12) were incubated with RuvA (10 nM) and RuvB or RuvB^{D113E} as indicated (described in Materials and Methods). Labelled DNA products were deproteinised, analysed by 8% neutral PAGE and visualised by autoradiography.

B. Quantification of the gel shown in A by PhosphorImager analysis. (■) RuvB, (●) RuvB^{D113E}. Branch migration products (duplex DNA with splayed single-stranded arms) are expressed as a percentage of total ^{32}P-labelled DNA. A background level of product observed in the absence of protein (lane a, 0.8%) has been subtracted.

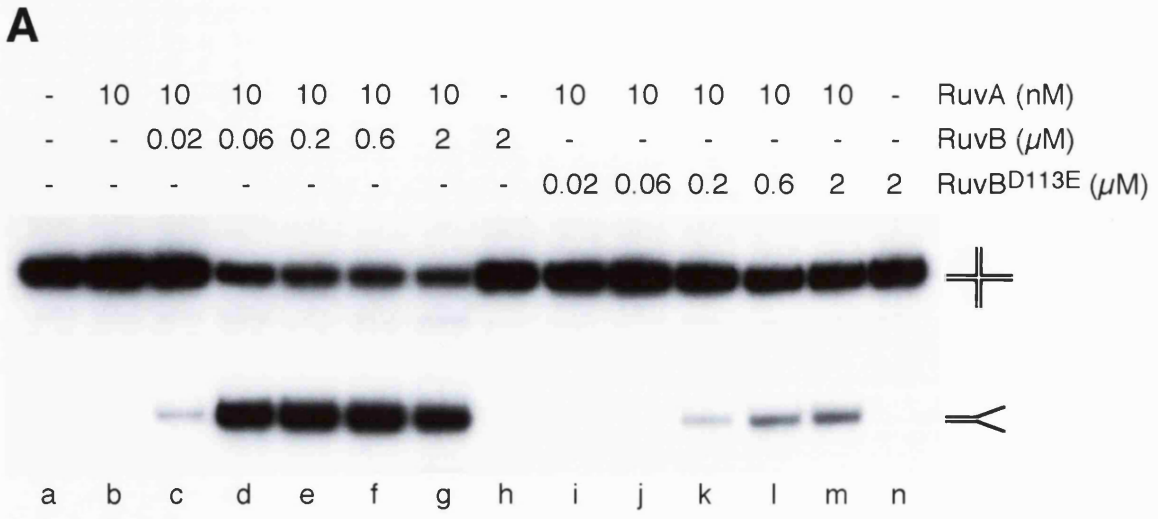
A
- 10 10 10 10 10 10 - 10 10 10 10 10 - RuvA (nM)
- - 0.02 0.06 0.2 0.6 2 2 - - - - - - RuvB (μM)
- - - - - - - - 0.02 0.06 0.2 0.6 2 2 RuvB^{D113E} (μM)
a b c d e f g h i j k l m n

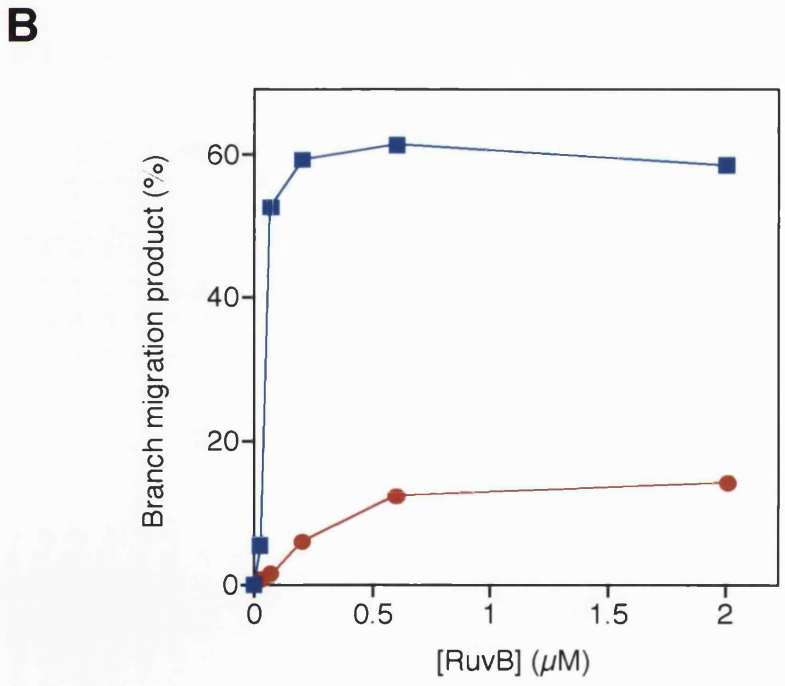
B
Branch migration product (%)
60
40
20
0
0 0.5 1 1.5 2
[RuvB] (μM)

FIGURE 5.8

FIGURE 5.9. INTERACTION OF RUVB^{D113E} WITH RUVC

A. Covalent cross-linking of RuvB^{D113E} and RuvC. RuvB or RuvB^{D113E} (1 μg) and RuvC (0.5 μg) were mixed in buffer as described in Materials and Methods. After 10 min incubation at 30°C, protein complexes were cross-linked by the addition of glutaraldehyde (GA), as indicated, and subjected to 10% SDS-PAGE (180 V; 75 min). Proteins were detected by Western blotting, as described in Materials and Methods, using rabbit polyclonal antibodies raised against RuvB (lanes a-f) or RuvC (g-l) followed by enhanced chemiluminescence (ECL) detection.

B. Stimulation of RuvC-junction binding by RuvB^{D113E}. ^{32}P-labelled synthetic junction (X12) was preincubated with the indicated amounts of RuvB or RuvB^{D113E} before adding RuvC (5 nM). Reactions were carried out as described in Materials and Methods. Protein-DNA complexes were analysed by 6% neutral PAGE followed by autoradiography. This band-shift experiment was conducted by Dr A. J. van Gool.

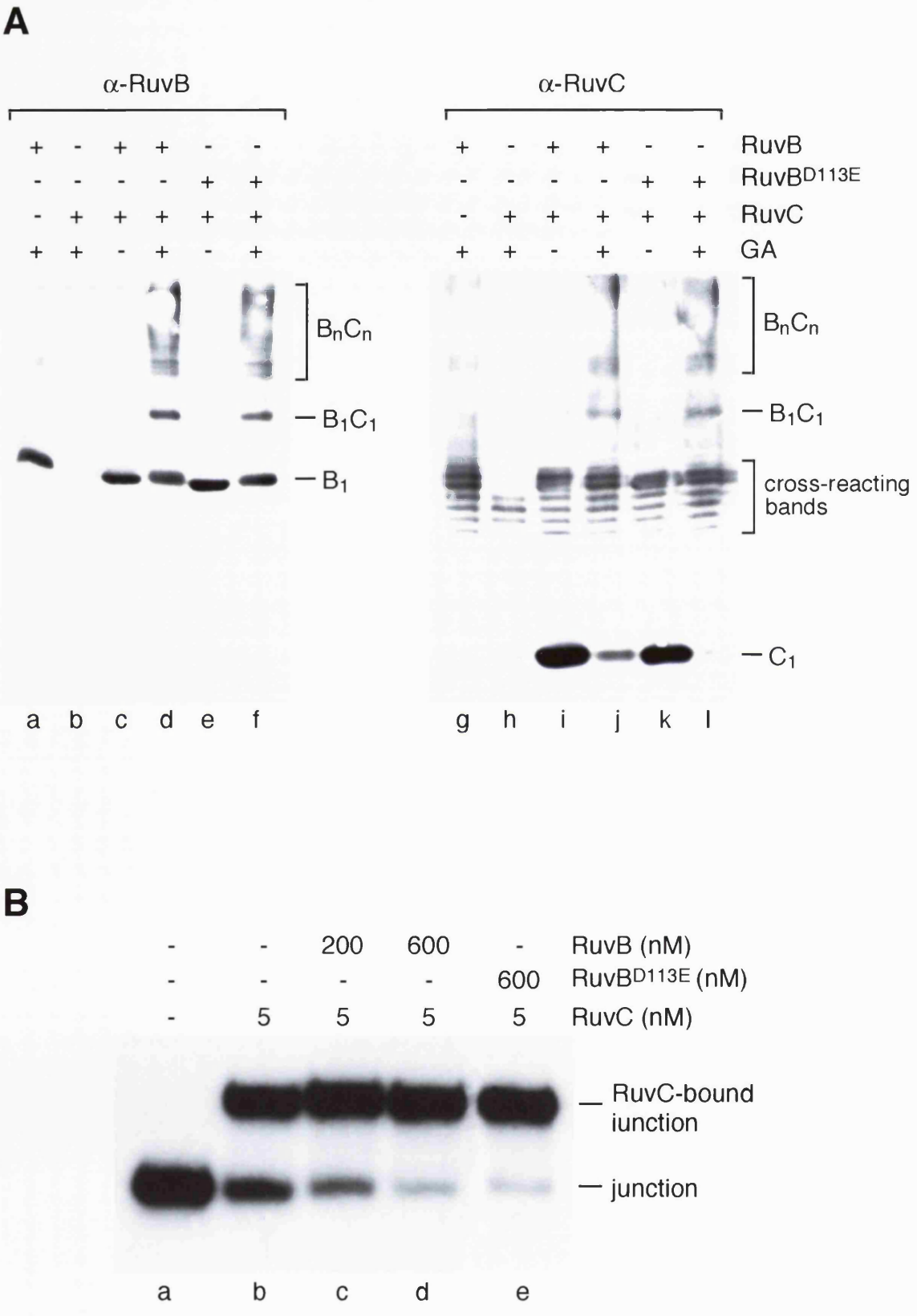
A
α-RuvB
α-RuvC
RuvB
RuvB^D113E
RuvC
GA
BnCn
B1C1
B1
cross-reacting bands
C1
a b c d e f g h i j k l
B
RuvB (nM)
RuvB^D113E (nM)
RuvC (nM)
RuvC-bound junction
junction
a b c d e

FIGURE 5.9

When mixtures of RuvC with either RuvB or $RuvB^{D113E}$ were treated with glutaraldehyde, novel cross-linked species were observed (Figure 5.9, lanes d, f, j and l). These complexes were not seen with either RuvB or RuvC alone (lanes a and h) or in the absence of cross-linking (lanes c, e, i and k). Furthermore, the complexes were detected with both anti-RuvB and anti-RuvC antibodies, indicating the presence of both proteins. One of the novel bands migrated between the 50 and 64 kDa markers, consistent with a complex comprising a monomer of RuvC (19 kDa) and a monomer of either RuvB or $RuvB^{D113E}$ (37 kDa) (designated B_1C_1). In addition, a number of higher molecular weight species of >98 kDa were also detected that presumably contain higher oligomeric forms of each protein (designated B_nC_n). The same cross-linked species were observed for both RuvB and $RuvB^{D113E}$ (compare lanes d and f, and lanes j and l), indicating that the mutant protein interacts with RuvC in the absence of DNA. The additional bands present in all lanes of the anti-RuvC Western blot (lanes g-l) are due to cross-reaction of the polyclonal antibody, possibly with a protein contaminant present in the gel loading buffer. These bands were not observed with an anti-RuvC monoclonal antibody (data not shown).

STIMULATION OF RUVC-HOLLIDAY JUNCTION BINDING BY $RUVB^{D113E}$

Previous band-shift studies have shown that RuvB stabilises the association of RuvC with synthetic Holliday junctions (van Gool *et al.*, 1998). To confirm the cross-linking results, reactions were kindly carried out by Dr A. J. van Gool to compare the stimulation of RuvC-junction binding by $RuvB^{D113E}$ with that of the wild-type protein (Figure 5.9B). Both proteins were found to stabilise the binding of RuvC to the X-junction to similar extents (compare lanes d and e).

Thus $RuvB^{D113E}$ appears to interact with RuvC both in solution and on Holliday junction DNA.

V. SUMMARY AND DISCUSSION

Helicase motif II (DExx) is highly conserved in RNA and DNA helicases (Gorbalenya and Koonin, 1993) and corresponds to the Walker B box of NTP-hydrolysing enzymes (Walker *et al.*, 1982). The aspartate residue plays a key role in catalysis, being implicated both in Mg^{2+}-coordinated NTP hydrolysis and in the harnessing of this chemical energy for helicase action (Pause and Sonenberg, 1992). The aspartate in helicase motif II of *E. coli* RuvB protein (Asp113) was replaced with glutamate by site-directed mutagenesis, and the over-expression, purification and characterisation of the resultant mutant protein, $RuvB^{D113E}$, have been described in Chapters 3 to 5.

The D113E mutation was introduced into RuvB with the aim of dissociating its ATPase and helicase activities, so that the role of DNA unwinding in branch migration could be assessed. As shown in the previous chapter, $RuvB^{D113E}$ is capable of ATP hydrolysis as well as being proficient in DNA binding, hexameric ring formation and in its interaction with RuvA. In this chapter, the helicase activity of the mutant protein was analysed using a strand displacement assay and was found to be severely compromised. In the presence of RuvA, $RuvB^{D113E}$ released a 20 nt long fragment from circular ssDNA with a 30-fold reduced rate compared to the wild-type protein and was unable to displace a fragment of >30 nt in length.

An uncoupling of ATPase and helicase activities was observed previously when the aspartate residue in helicase motif II of the RNA helicase eIF-4A was replaced with glutamate (Pause and Sonenberg, 1992). Helicases are thought to transduce the energy from NTP hydrolysis into an unwinding action

through protein conformational changes. In the crystal structures of helicases *E. coli* Rep (Korolev *et al.*, 1997), *B. stearothermophilus* PcrA (Subramanya *et al.*, 1996; Velankar *et al.*, 1999) and hepatitis C virus NS3 protein (Cho *et al.*, 1998; Kim *et al.*, 1998; Yao *et al.*, 1997), the nucleotide binding site was found to be located in a cleft between two 'RecA-like' subdomains (Story and Steitz, 1992; Story *et al.*, 1992). It is, therefore, ideally situated to mediate conformational changes between the domains as a result of NTP binding and hydrolysis. The helicase motifs are located around the NTP binding site and it has been proposed that contacts between conserved residues in these motifs, across the domain interface, are important for the coupling of ATP hydrolysis and DNA unwinding (Subramanya *et al.*, 1996). It is possible that replacing the highly conserved aspartate in helicase motif II of RuvB with glutamate may disrupt one of these contacts, thereby dissociating the ATPase and helicase activities. Mutations of other amino acid residues within the conserved motifs, resulting in a similar uncoupling effect, have been reported for T7 gp4 (Washington *et al.*, 1996), *E. coli* Rho (Pereira and Platt, 1995), mammalian eIF-4A (Pause and Sonenberg, 1992), *B. stearothermophilus* PcrA (Dillingham *et al.*, 1999; Soultanas *et al.*, 1999), and a number of viral helicases (Graves-Woodward *et al.*, 1997; Gross and Shuman, 1995; Jindal *et al.*, 1994).

The aim of this study was to investigate the role of DNA helicase activity in RuvAB-mediated branch migration. Being uncoupled in its ATPase and helicase activities, $RuvB^{D113E}$ provided the ideal tool to address this question. $RuvAB^{D113E}$ was shown to promote branch migration of both synthetic Holliday junctions and recombination intermediates made by RecA. In both cases, the activity was reduced compared to wild-type RuvB, probably due to its impaired ATPase activity. However, it should be noted that $RuvAB^{D113E}$ was capable of driving branch migration through a distance of ~2.6 kbp in the case

of the recombination intermediate substrates. This is a significant result given that the DNA helicase activity of RuvAB^{D113E} was severely compromised to the extent that it was unable to displace a fragment of >30 nt from ssDNA. Interestingly, the *E. coli* RecG protein, which also promotes branch migration *in vitro*, only exhibits a very weak DNA helicase activity (Whitby *et al.*, 1994).

In addition to the classical strand displacement assay, a specialised topological assay was employed to assess the DNA unwinding activity of RuvB^{D113E}. Using this assay, RuvAB^{D113E}, but not RuvB^{D113E} alone, were found to promote efficient transient unwinding of relaxed plasmid DNA. Interestingly, the branch migration activity of RuvB^{D113E} was also dependent on the presence of RuvA. Collectively, the results indicate that branch migration proceeds by a mechanism that does not require extensive helicase activity but that may involve limited transient separation of duplex DNA within the RuvB rings.

The ability of RuvAB^{D113E} to promote branch migration *in vitro* was reflected *in vivo*, by the partial complementation of a *ruvB* mutant strain by over-expression of RuvB^{D113E}. RuvB^{D113E} was, however, unable to complement the UV-sensitive phenotype of the strain at low expression levels. Furthermore, over-expression of the mutant protein in *ruv*$^{+}$ cells resulted in a dominant negative effect, indicating that RuvB^{D113E} is defective in some aspect of its repair activity. Recent biochemical studies have indicated that RuvAB-mediated branch migration and RuvC-mediated resolution are closely linked and that a complex of all three Ruv proteins is required for Holliday junction resolution *in vivo* (Davies and West, 1998; Eggleston *et al.*, 1997; van Gool *et al.*, 1998; Whitby *et al.*, 1996; Zerbib *et al.*, 1998). However, direct and functional interactions were detected between RuvB^{D113E} and RuvC *in vitro*. The UV-sensitive phenotype associated with RuvB^{D113E} may possibly be due to the need for extensive DNA unwinding for branch migration through heterologous DNA sequences (Adams

and West, 1996; Iype *et al.*, 1994; Parsons *et al.*, 1995b) and substrates containing DNA lesions (Tsaneva *et al.*, 1992b)

The purification and characterisation of $RuvB^{D113E}$ described in Chapters 3 to 5 have been published in: George, H., Mézard, C., Stasiak, A., and West, S. C. (1999). Helicase-defective $RuvB^{D113E}$ promotes RuvAB-mediated branch migration *in vitro*. *J. Mol. Biol.* **293**, 505-519.

CHAPTER SIX : RESULTS

DNA OPENING WITHIN THE RUVB RING: A REQUIREMENT FOR BRANCH MIGRATION?

I. INTRODUCTION

The work conducted with the mutant protein $RuvB^{D113E}$ indicates that extensive helicase activity is not required for RuvAB-mediated branch migration. It is possible, however, that the duplex DNA is transiently opened within each RuvB hexameric ring. This would provide a single strand allowing RuvB to pump the DNA through its central cavity with a defined polarity.

To further investigate the mechanism of action of the RuvB motor protein, an interstrand cross-link was introduced into a branch migration substrate in order to prevent strand separation. The cross-link was positioned such that it would be encountered by RuvB during branch migration. If DNA opening within the RuvB ring is absolutely required for branch migration to occur, then the presence of the cross-link would be expected to block the reaction. These studies were conducted using the wild-type RuvB protein.

II. PREPARATION OF THE CROSS-LINKED JUNCTION

To provide the simplest model system, a synthetic 3-armed (Y) junction was used for these studies as opposed to a classical 4-armed Holliday junction. RuvAB has been shown to promote efficient branch migration of Y-junctions *in vitro* (Hiom *et al.*, 1996; Lloyd and Sharples, 1993b; Tsaneva and West, 1994). To introduce a site-directed interstrand cross-link into the junction, this work made use of a chemically synthesised monoadduct between a psoralen derivative and thymidine, called a *cis*-syn 2-carbomethoxypsoralen furan-side thymidine monoadduct. This was kindly synthesised by Dr W. R. Kobertz (MIT) (Kobertz and Essigmann, 1996), and was incorporated into a 26 nt long oligonucleotide

(oligo 1) by Dr D. A. Nauman as described (Kobertz and Essigmann, 1997). The psoralen-containing oligo 1 (denoted oligo 1^{ps}) was 5' ^{32}P-end-labelled and annealed with the other oligonucleotides to form a 3-armed junction (Figure 6.1A). Upon exposure to long-wave UV light (320-410 nm), the psoralen monoadduct reacts with an adjacent thymidine on the complementary strand to form an interstrand cross-link, or diadduct.

With X-junctions, RuvB can assemble on either pair of arms and will therefore promote branch migration in both directions. However, previous studies have shown that by using asymmetric Holliday junctions, containing two long and two short arms, RuvB binding can be biased to one pair of arms, i.e. to the long arms (Hiom and West, 1995a; van Gool *et al.*, 1999). In the current study, it was important to ensure that the RuvB ring was targeted to the arm containing the cross-link. Therefore, an asymmetric Y-structure was used with two short (12 bp) arms, and one long (44 bp) arm containing the cross-link 3-4 bp from the junction point (Figure 6.1A). The RuvB hexamer has been shown to span ~25 bp (Hiom and West, 1995a), and as a consequence will only assemble on the long arm containing the diadduct. The asymmetric assembly of RuvAB on the Y substrate results in unidirectional branch migration, as shown in Figure 6.1B. For the end products of the reaction (i.e. duplex DNA with splayed single-stranded arms and a displaced single strand) to be observed, however, RuvB must pump the cross-linked duplex through its central cavity.

An additional factor was also taken into account when designing the substrate. In previous studies which used Y-structures with equal length arms, branch migration also occurred with a unique polarity (Hiom *et al.*, 1996; Lloyd and Sharples, 1993b; Tsaneva and West, 1994). In these cases, the assembly of RuvB was not biased by different arm lengths. Instead, the observations are thought to relate to the asymmetric structure that 3-armed junctions have been

FIGURE 6.1. CROSS-LINKED Y-JUNCTION SUBSTRATE

A. The synthetic three-armed junction Y-2 used in this study is composed of oligos 1-4 and was prepared as described in Materials and Methods. The junction comprises one long (44 bp) arm and two short (12 bp) arms. Oligo 1 contains a psoralen monoadduct which, upon long-wave UV-irradiation, forms an interstrand cross-link in the long arm at the position shown. In addition, two control Y-junction substrates were prepared, one containing a psoralen monoadduct (Y-1) and the other without psoralen modification (Y). All three Y-junction substrates were 5′ ^{32}P-end-labelled in oligo 1 and contain a 4 bp homologous core (indicated in bold-type).

B. Theoretical branch migration of Y-2 by RuvAB. Due to the asymmetry of the Y-junction, the RuvAB complex assembles with the RuvB ring bound to the long arm containing the psoralen cross-link. To promote branch migration, the RuvB ring pumps duplex DNA through its central cavity in the direction indicated and will therefore need to traverse the interstrand cross-link to release branch migration products (splayed duplex and oligo 4).

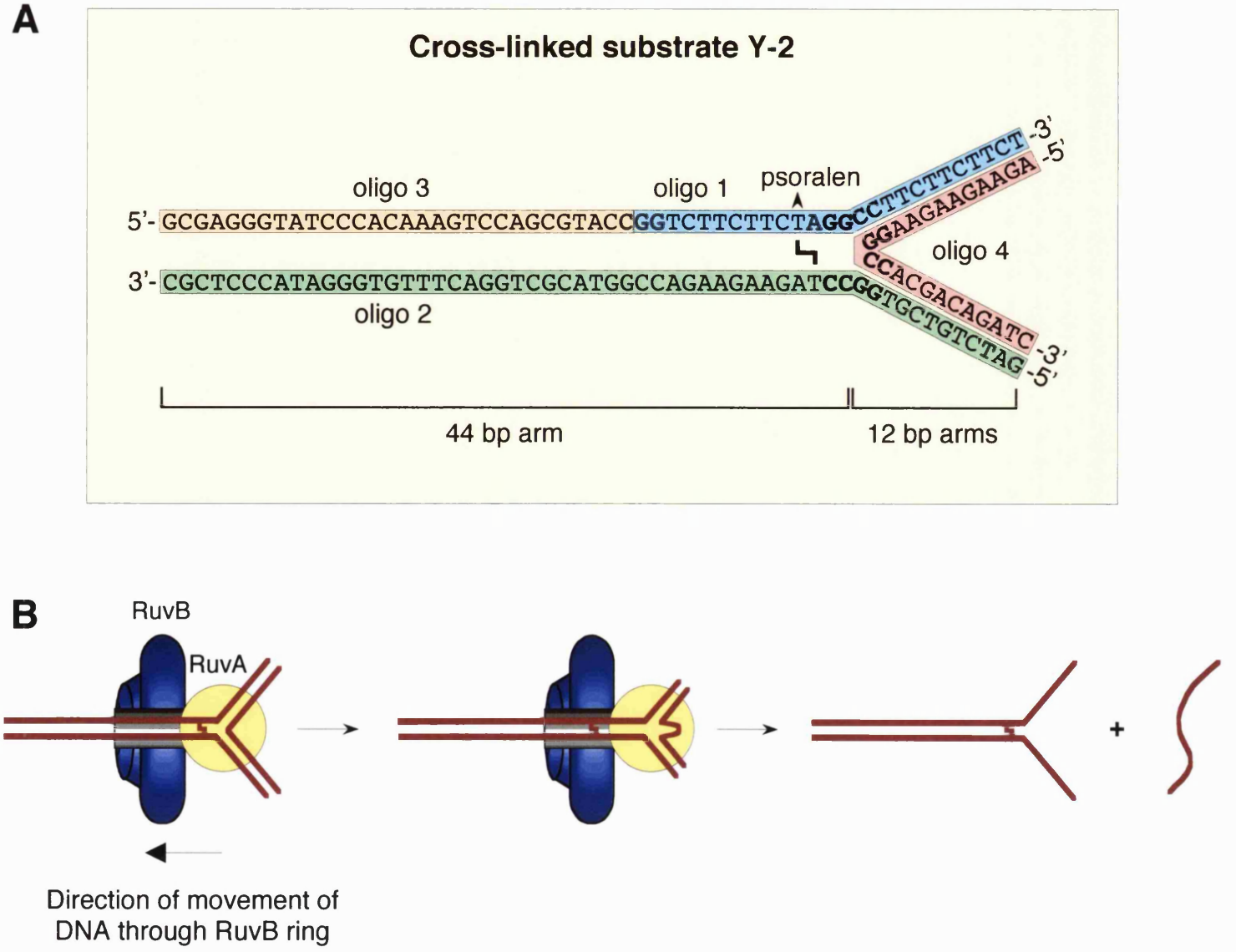
A
Cross-linked substrate Y-2
oligo 3
oligo 1
psoralen
5'- GCGAGGGTATCCCACAAAGTCCAGCGTACCGGTCTTCTTCTAGGCCTTCTTCTTCT -3'
GGAAGAAGAAGA -5'
oligo 4
3'- CGCTCCCATAGGGTGTTTCAGGTCGCATGGCCAGAAGAAGATCCGGTGCTGTCTAG -5'
CCACGACAGATC -3'
oligo 2
44 bp arm
12 bp arms
B
RuvB
RuvA
+
Direction of movement of
DNA through RuvB ring

FIGURE 6.1

shown to adopt in the presence of Mg^{2+} (Guo *et al.*, 1990; Lu *et al.*, 1991a), resulting in the asymmetric assembly of the RuvAB complex (Hiom *et al.*, 1996). It has been shown that the geometry of a 3-armed junction is dependent on the sequence of the flanking and penultimate bases at the junction point, and that junctions containing identical sequences at these positions in all three arms (i.e. a 4 bp homologous core) are symmetric (Lu *et al.*, 1991a). Therefore, to avoid any intrinsic asymmetry of the cross-linked Y-structure that might affect the efficiency by which RuvB binds and drives branch migration on the long arm, a 4 bp homologous core was included at the junction point (Figure 6.1A).

In addition to the Y-junction containing the psoralen cross-link (referred to as Y-2), two control Y-junctions were prepared: (i) Y-1, which contained the monoadduct but was not cross-linked, and (ii) Y, a similar substrate without psoralen modification. Each junction was 5' ^{32}P-end-labelled on oligo 1.

It should be noted that the Y substrates used in this study contain a single strand nick in the long arm, between oligos 1 and 3. Several attempts were made to ligate the nick using T4 DNA ligase. In these trials, oligo 3 was 5' ^{32}P-end-labelled and oligo 1 was phosphorylated using cold ATP. Although efficient ligation was achieved with the control Y junction (i.e. without psoralen modification), it proved to be extremely difficult to ligate the Y-2 substrate (data not shown). Psoralen cross-links induce local distortions in the DNA and it is possible that the cross-link in Y-2, which is near to the nicked region, inhibits the ligation reaction. Attempts were made to ligate the Y-junction first, prior to UV-induced cross-linking. Unfortunately, however, the efficiency of cross-linking was reduced significantly by the preceding ligation reaction. Since the preparation of Y-2 already involved several steps that incurred significant yield losses, it was not possible to introduce a ligation step that would reduce the

yields further, especially considering the limited amount of oligo 1^{ps} available for this work.

III. BINDING OF THE CROSS-LINKED Y-2 JUNCTION BY RUVA

Psoralen cross-links are known to distort the local DNA structure (Hwang *et al.*, 1996; Spielmann *et al.*, 1995). Therefore, since the cross-link in Y-2 is located close to the junction point where RuvA binds, band-shift assays were carried out to confirm that the modified junction could be bound by RuvA. As shown in Figure 6.2, RuvA bound Y-2 and the control junctions, Y (unmodified) and Y-1 (containing a psoralen monoadduct), with comparable efficiency. As observed previously with 4-armed (X) junctions (Parsons *et al.*, 1992; Whitby *et al.*, 1996), two defined protein-DNA complexes were detected with each Y-junction (lanes c, f and i). These complexes are thought to result from the binding of either one or two tetramers of RuvA. Some dissociation of RuvA-DNA complexes occurred upon electrophoresis but no differences were observed between Y-2 and the control substrates Y and Y-1, showing that the instability of RuvA binding is not a result of the interstrand cross-link.

IV. RUVAB-MEDIATED BRANCH MIGRATION OF Y-2

To determine whether the interstrand cross-link blocks RuvAB-mediated branch migration, the Y-junctions were incubated with RuvA, RuvB or RuvAB (Figure 6.3A). Significantly, RuvAB promoted efficient branch migration with all three substrates (lanes c, d, j, k, o and p), giving rise to the expected ^{32}P-labelled splayed arm product which migrated at the same position as a marker composed of oligos 1, 2 and 3 (M1; lane f). An additional marker, consisting of oligos 1, 2 and 4 (M2; lane g), was also included to confirm that the faster migrating product was not simply due to the dissociation of oligo 3. Branch

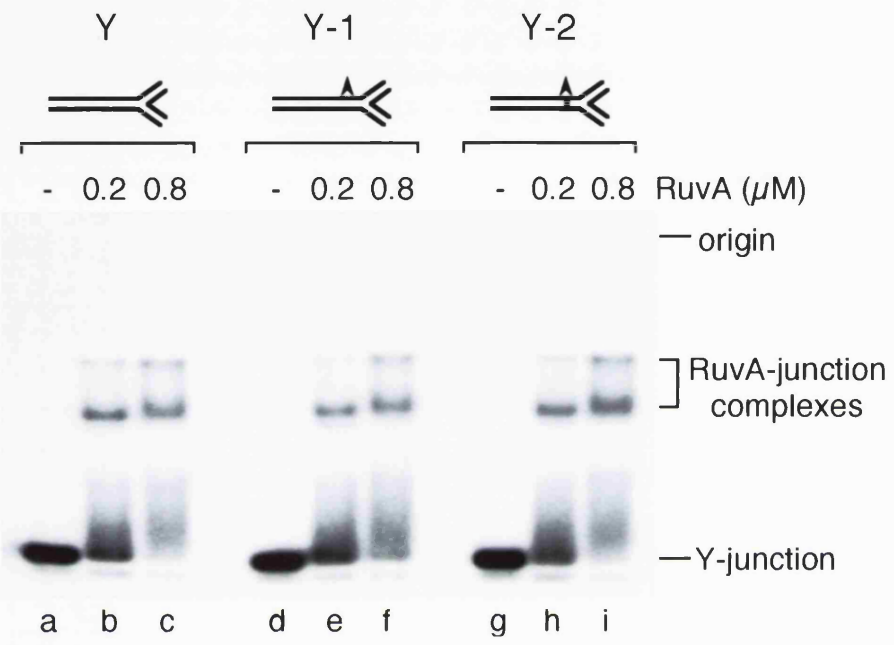

FIGURE 6.2. BINDING OF JUNCTION Y-2 BY RUVA

Band-shift assays were conducted for Y-2 and control junctions Y and Y-1, as described in Materials and Methods, and with the indicated amounts of RuvA. RuvA-junction complexes were separated on a low ionic strength 4% polyacrylamide gel and detected by autoradiography.

FIGURE 6.3. BRANCH MIGRATION OF JUNCTION Y-2 BY RUVAB

A. Y-junction substrates (5′ ^{32}P-end-labelled in oligo 1) were incubated with RuvA (0.1 μM) and RuvB as indicated. Reactions were conducted as described in Materials and Methods. DNA products were deproteinised, analysed by 10% neutral PAGE and visualised by autoradiography. Markers M1 (lane f) and M2 (lane g) contain ^{32}P-labelled oligo 1 annealed with oligos 2 and 3, or with oligos 2 and 4, respectively.

B. Analysis of the branch migration products by denaturing PAGE. 2 μl samples from the branch migration reactions in A were denatured by heating for 3 min at 95°C in the presence of formamide and analysed by 8% denaturing PAGE. ^{32}P-labelled DNA was detected by autoradiography. Markers M3 (lane f) and M4 (lane g) contain ^{32}P-labelled oligo 1 cross-linked to oligo 2, or oligo 1 alone, respectively.

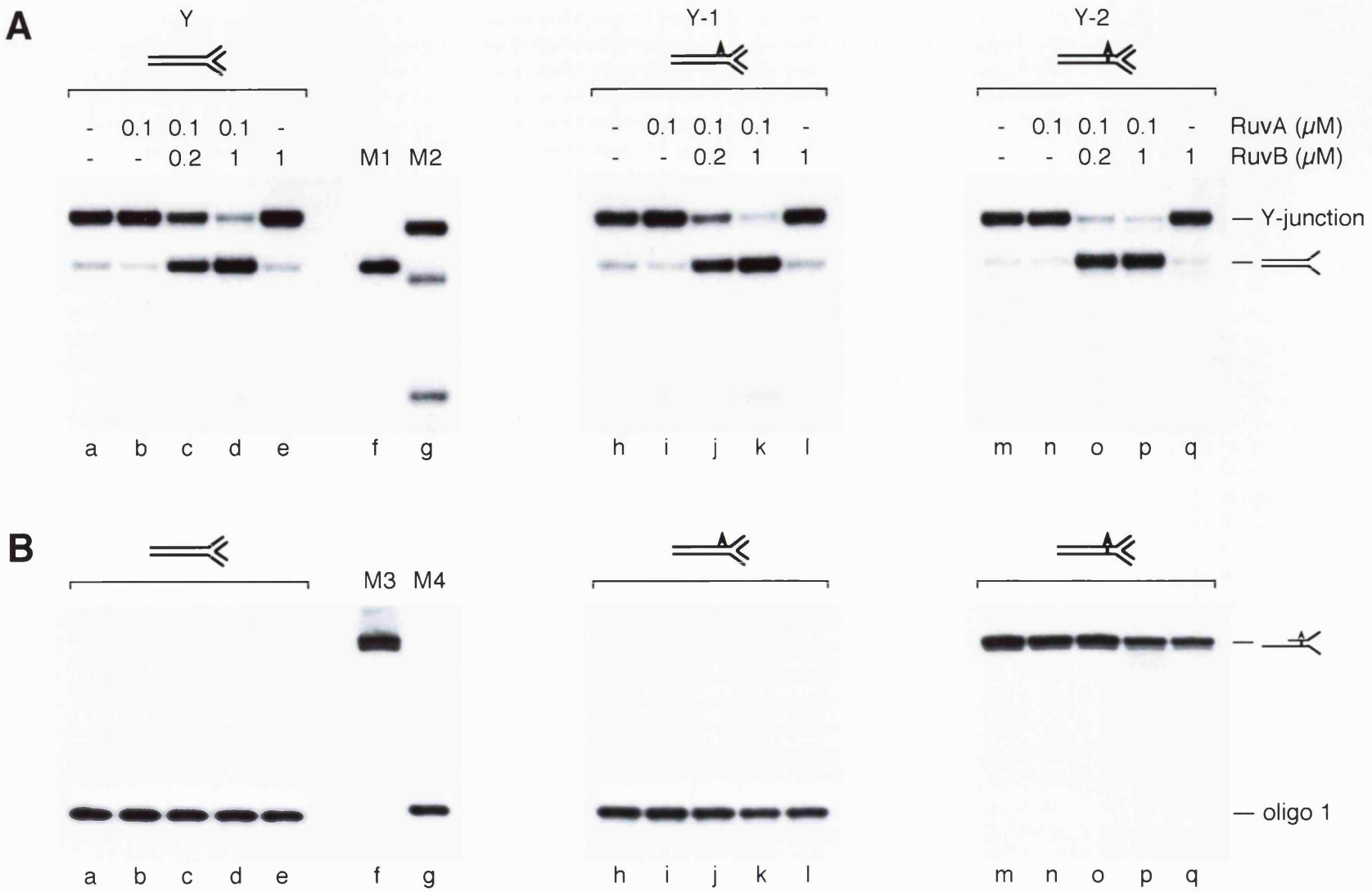
A
Y
Y-1
Y-2
- 0.1 0.1 0.1 -
- - 0.2 1 1
M1 M2
RuvA (μM)
RuvB (μM)
— Y-junction
a b c d e f g
h i j k l
m n o p q
B
M3 M4
— oligo 1

FIGURE 6.3

migration products were not detected in the presence of RuvA alone (lanes b, i and n) or RuvB alone (lanes e, l and q).

CONFIRMATION OF CROSS-LINKING IN Y-2

It is remarkable that the presence of the interstrand cross-link had no adverse effect on the branch migration reaction. It was therefore essential to confirm the presence of the cross-link in Y-2. To do this, the products of branch migration (as shown in Figure 6.3A) were analysed by denaturing polyacrylamide gel electrophoresis (Figure 6.3B). With junction Y-2, a slow migrating band was observed which corresponded to ^{32}P-labelled oligo 1^{ps} cross-linked to oligo 2 (compare lanes m-q with marker M3 in lane f). In contrast, denaturation of the unmodified junction (Y), or the junction containing the psoralen monoadduct (Y-1), resulted in a band that migrated at the same position as the ^{32}P-labelled oligo 1 marker (compare lanes a-e and h-l with marker M4 in lane g). Even upon longer exposure, no faster migrating band was detected for Y-2, indicating that all of the substrate molecules were cross-linked.

ATP-DEPENDENCE OF BRANCH MIGRATION

RuvAB-mediated branch migration is an ATP-dependent process (Tsaneva *et al.*, 1992b). To test the requirement of ATP hydrolysis and hence confirm the involvement of branch migration in the release of oligo 4 from Y-2, reactions were conducted in the presence of ATP, ATPγS, or in the absence of a nucleotide cofactor (Figure 6.4). Products were only observed in the presence of ATP (lane d), confirming that the release of oligo 4 is a result of active branch migration by RuvAB, and that junction binding alone (in the presence of ATPγS) is not sufficient to observe the faster migrating product (lane f).

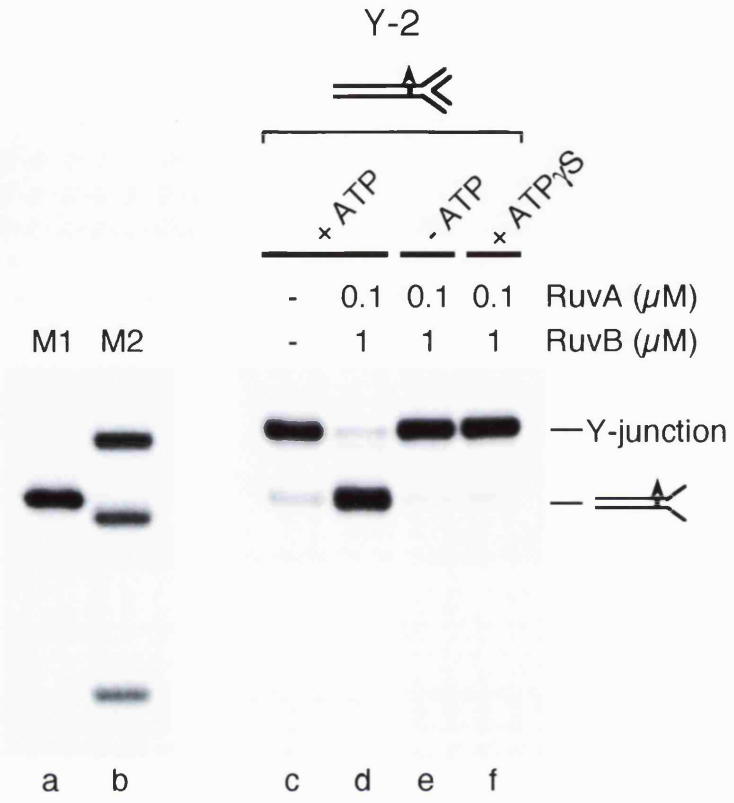

FIGURE 6.4. ATP-DEPENDENCE OF RUVAB-MEDIATED BRANCH MIGRATION OF JUNCTION Y-2

Branch migration reactions containing ^{32}P-labelled junction Y-2 were conducted as described in Materials and Methods, in the presence of ATP (2 mM), ATPγS (2 mM), or in the absence of a nucleotide cofactor. RuvA (0.1 μM) and RuvB (1 μM) were added as indicated. ^{32}P-labelled DNA products were deproteinised, analysed by 10% PAGE and visualised by autoradiography. Markers M1 (lane a) and M2 (lane b) correspond to ^{32}P-end-labelled oligo 1 annealed with oligos 2 and 3, or with oligos 2 and 4, respectively.

V. SUMMARY AND DISCUSSION

The aim of this study was to investigate whether transient opening of dsDNA occurs within the RuvB ring during RuvAB-mediated branch migration. To address this question, branch migration assays were conducted using an asymmetric three-armed junction, Y-2, containing a psoralen interstrand cross-link. The cross-link prevents strand separation and was positioned in the long arm of the junction, near to the crossover. By using an asymmetric junction, with one long arm and two short arms, the assembly of the RuvB ring was restricted to the long arm containing the cross-link. The design of the junction Y-2 therefore ensured that the interstrand cross-link would be encountered by RuvB during branch migration. RuvAB were found to promote ATP-dependent branch migration of Y-2, indicating that the RuvB ring was able to translocate along cross-linked duplex DNA.

The data presented in this chapter show that complete duplex opening within the RuvB ring is not required for branch migration and rule out a single strand base-by-base tracking mechanism for DNA translocation. It is possible, however, that ssDNA translocation occurs by a mechanism that does not involve the separation of every base pair within the RuvB ring. Indeed, the psoralen diadduct could be bypassed provided RuvB possesses a large step size. However, although transient DNA opening by RuvB has been demonstrated under certain reaction conditions (Adams and West, 1995b), chemical probing of an active RuvAB-Holliday junction complex failed to detect duplex opening within the RuvB rings (C.A. Parsons and S.C.W., unpublished data).

The results of this study may instead provide the first support for an alternative model in which duplex DNA is pumped through the RuvB ring without strand separation. If this is the case, however, what factors determine

directionality? In ssDNA translocation models, directionality is imposed by the phosphodiester backbone of the bound single strand. Duplex DNA, however, is composed of two antiparallel strands and so does not possess such polarity. Electron microscopic studies have shown that the RuvB hexamer possesses a large and small tier and that in the RuvAB-Holliday junction complex the two RuvB rings are oppositely oriented (Yu *et al.*, 1997). This bipolar arrangement results in the DNA being pumped out through the small end of each RuvB ring during branch migration. Thus the polarity of the rings relative to the junction, as directed by RuvA during complex assembly, could impose the directionality of translocation.

With the data presented in this chapter, it is not possible to distinguish between a translocation mechanism whereby the duplex DNA is partially opened within the RuvB ring, and one in which the DNA remains fully base-paired. However, the latter is a tempting possibility, especially considering that DNA is most stable in its double-stranded form.

The work described in this chapter will be published in: George, H., Kuraoka, I., Nauman, D. A., Kobertz, W. R., Wood, R. D., and West, S. C. (2000). RuvAB-mediated branch migration does not involve extensive DNA opening within the RuvB hexamer. *Curr. Biol., in press.*

CHAPTER SEVEN : GENERAL DISCUSSION

The principal aim of this work was to investigate the mechanism by which the *E. coli* RuvA and RuvB proteins promote branch migration during homologous recombination and recombinational repair; in particular to understand how the RuvB branch migration motor promotes the passage of DNA through its central cavity.

I. RUVB – A HELICASE OR MOLECULAR PUMP?

RuvB possesses conserved helicase motifs, exhibits an *in vitro* DNA helicase activity with RuvA, and shares structural similarities with the emerging family of hexameric helicases (Adams and West, 1995b; Egelman, 1996; Tsaneva *et al.*, 1993; Tsaneva and West, 1994; West, 1996). These observations suggested that RuvB-catalysed DNA unwinding may be central to the mechanism of branch migration. However, recent data on the mechanism of RuvAB-mediated branch migration indicate otherwise. The two RuvB rings have been shown to encircle the 'outgoing' heteroduplex arms of the RuvA-bound junction, and four negatively-charged pins near the centre of the RuvA tetramer are thought to facilitate separation of the strands as they pass from one helical axis to the other (Hargreaves *et al.*, 1998; Hiom *et al.*, 1996; Hiom and West, 1995a; Parsons *et al.*, 1995a; Rafferty *et al.*, 1996). Therefore, separation of the homoduplexes and strand exchange have already occurred prior to reaching the RuvB rings. Thus, to drive the process of branch migration, RuvB does not necessarily have to unwind the DNA but instead needs to pump duplex DNA through its central cavity. This poses the question of whether RuvB is a helicase *per se* or a highly-specialised molecular pump.

Site-directed mutagenesis of RuvB has been used to investigate the role of DNA helicase activity in branch migration. The aspartate residue in helicase

motif II, a highly conserved residue in all helicases that is thought play a key role in the coupling of ATPase and helicase activity, was replaced with glutamate. The resulting mutant protein, $RuvB^{D113E}$, was able to promote RuvAB-mediated branch migration despite being severely compromised in its DNA helicase activity (as measured by the strand displacement assay). Thus the results indicated that extensive helicase activity is not required for RuvAB-mediated branch migration. However, it is possible that transient unwinding of duplex DNA may occur within the RuvB rings to provide a single strand for translocation. To test this hypothesis, an interstrand cross-link was introduced into a three-armed junction such that it would be encountered by RuvB during branch migration. The cross-link, which prevents DNA strand separation, did not inhibit RuvAB-mediated branch migration. The results thus indicated that complete opening of the duplex as it passes through the RuvB ring is not necessary for branch migration. At present, however, it is not known whether limited opening of the dsDNA occurs within the ring or whether the DNA remains fully base-paired during translocation.

Taken together, the results of this work provide strong evidence to suggest that RuvB does not behave as a true helicase in branch migration but rather acts as a molecular pump.

II. MECHANISM OF DNA TRANSLOCATION BY RUVB

At present, the precise mechanism by which the RuvB rings promote the passage of DNA through their central channels during branch migration is poorly understood. As well as catalysing strand separation, many helicases use the energy derived from NTP hydrolysis to fuel their translocation along DNA. RuvB contains a number of conserved helicase motifs and, whilst our data

suggest that it does not behave like a classical helicase, RuvB may employ a 'helicase-like' mechanism of translocation for driving branch migration.

RuvB shares striking structural similarities with other hexameric ring helicases, despite there being limited sequence homology between the proteins. Various studies have suggested that the replicative hexameric helicases T7 gp4 and T4 gp41 encircle and translocate along one DNA strand of a replication fork, excluding the other from the centre of the ring (Hacker and Johnson, 1997; Raney *et al.*, 1996; Yong and Romano, 1996; Yu *et al.*, 1996b). Given the structural conservation, it is possible that the same motor that pumps ssDNA through the central cavity of these hexameric helicases, resulting in helicase function, could pump dsDNA through the central cavity of RuvB, resulting in branch migration (Egelman, 1998).

Based on our knowledge of RuvB, and on observations made with other hexameric helicases, I propose three models for DNA translocation by RuvB (Figure 7.1). All of these models invoke a 'bind-release' mechanism in which successive rounds of DNA binding and release are coupled to cycles of ATP binding and hydrolysis, respectively. Indeed band-shift studies have shown that ATP binding is required for the formation of stable RuvB-DNA complexes, and that subsequent hydrolysis to ADP might destabilise this interaction leading to dissociation of RuvB from DNA (Müller *et al.*, 1993b). The state of the bound nucleotide has been shown to modulate interactions of T7 gp4 and DnaB with DNA in a similar fashion (Hingorani and Patel, 1993; Jezewska and Bujalowski, 1996).

FIGURE 7.1. MODELS FOR DNA TRANSLOCATION BY RUVB

A. 'Cycling model', in which the DNA (indicated in cross-section by a yellow star) is passed sequentially around the hexamer, from the catalytic subunit (indicated in red) of one dimer to the next. DNA binding and release are thought to be coupled to ATP binding and hydrolysis, respectively. The predicted state of the bound nucleotide at each catalytic subunit during translocation is indicated.

B. 'Shuttling model', a similar mechanism to A but involving the flipping of the DNA between two adjacent catalytic subunits.

C. 'Inchworm model', whereby a single catalytic subunit contains two non-identical DNA binding sites, a leading site (L) and a tail site (T). Conformational changes of the two DNA binding sites, in response to ATP binding and hydrolysis, result in translocation of the DNA (indicated in side view by a yellow bar).

In each model, the arrows indicate the direction of movement of the DNA.

A. 'Cycling model'

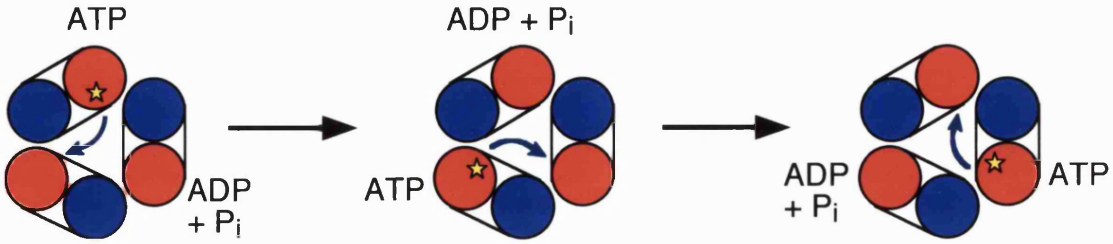

B. 'Shuttling model'

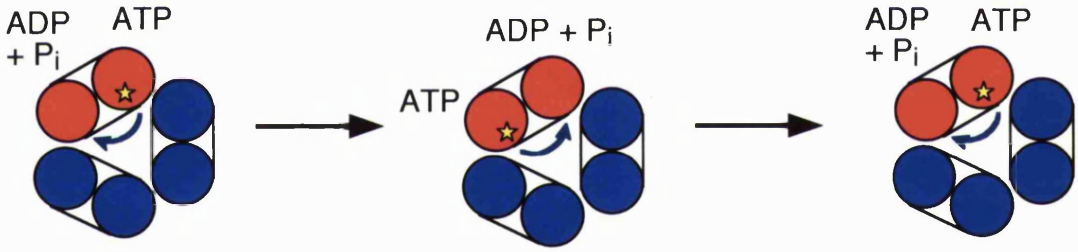

C. 'Inchworm model'

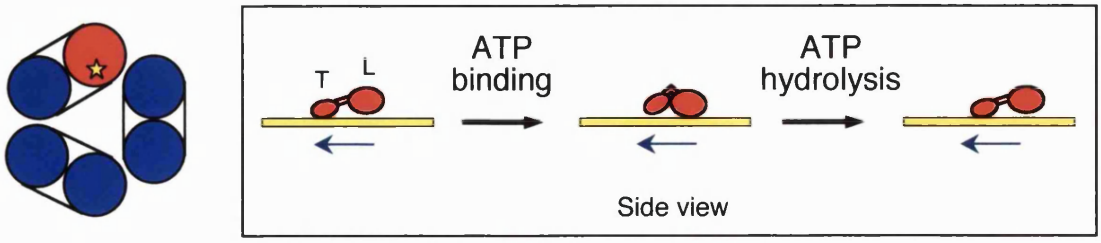

FIGURE 7.1

CYCLING MODEL

In the 'cycling model' (Figure 7.1A), translocation is coupled to a rotational movement of the DNA within the RuvB hexamer. Since RuvB is dimeric in solution (Tsaneva *et al.*, 1992a), it is possible that the hexamer comprises a trimer of dimers and that translocation occurs as DNA is passed sequentially from dimer to dimer around the ring, as shown in Figure 7.1A. In such a model, each dimer is presumed to be asymmetric with one catalytic and one non-catalytic subunit. Indeed, DnaB (Bujalowski and Klonowska, 1993), Rho (Geiselmann and von Hippel, 1992; Stitt, 1988) and T7 gp4 (Hingorani and Patel, 1996; Hingorani *et al.*, 1997) have been shown to contain three high affinity and three low affinity ATP-binding sites, indicating the presence of three asymmetric dimers.

A model where the ssDNA is rotated between three catalytic subunits, each at different stages of catalysis depending on the state of the bound nucleotide, has been proposed for T7 gp4 and shows remarkable similarity to the cyclical binding change mechanism of F_1-ATPase (Abrahams *et al.*, 1994; Boyer, 1993; Hingorani *et al.*, 1997). This is particularly interesting since F_1-ATPase, a component of the ATP synthase, possesses a 'RecA-like' nucleotide binding core that is also common to a number of helicases, including Rho, T7 gp4 and *B. stearothermophilus* PcrA (Abrahams *et al.*, 1994; Miwa *et al.*, 1995; Opperman and Richardson, 1994; Sawaya *et al.*, 1999; Story and Steitz, 1992; Subramanya *et al.*, 1996; Washington *et al.*, 1996). Furthermore, F_1-ATPase is a ring-shaped heterohexamer ($\alpha_3\beta_3$) with the γ subunit of the ATPase situated within the central cavity of the ring, analogous to the way in which the hexameric helicases bind DNA (Abrahams *et al.*, 1994).

SHUTTLING MODEL

The 'shuttling model' (Figure 7.1B) is a variation of the first model, except in this case the DNA is flipped between two adjacent subunits upon cycles of ATP binding and hydrolysis. The model is supported by the finding that RuvAB-mediated branch migration occurs with comparable efficiency in reactions containing either ATP or a 1:2 ratio of ATP/ATPγS (Mitchell and West, 1996). Furthermore, kinetic studies show that under single turnover conditions each RuvB hexamer hydrolyses only two molecules of ATP, suggesting that only two subunits may be involved in each translocation cycle (Marrione and Cox, 1995). Assuming RuvB is a trimer of dimers, these two catalytic subunits may reside in the same dimer, as shown in Figure 7.1B, or in adjacent dimers.

INCHWORM MODEL

The third model (Figure 7.1C) requires two non-identical binding sites in a single catalytic subunit - a leading site and a tail site (Lohman, 1993; Yarranton and Gefter, 1979). Wigley and colleagues have proposed an 'inchworm' model for the monomeric helicase PcrA (Velankar *et al.*, 1999). The leading site (in domain 2A) and tail site (in domain 1A) of PcrA are located either side of a cleft which contains the nucleotide binding site (Subramanya *et al.*, 1996; Velankar *et al.*, 1999). Upon ATP binding, the cleft closes altering the conformation of the protein. As a result, the leading site binds the duplex region adjacent to the fork, and the tail site slides along the ssDNA towards it. At the same time, several base pairs of the duplex DNA are destabilised at the junction. Upon ATP hydrolysis, the cleft re-opens causing the tail site to grab the ssDNA and the leading site to slide along the DNA to the next unwound base pair, ready

for another cycle of duplex opening and translocation (Velankar *et al.*, 1999). As a result, the protein moves along the DNA in an inchworm fashion, unwinding the duplex as it goes.

RuvB could adopt a similar mechanism of DNA translocation to PcrA, the main difference being that both DNA binding sites would be present in a single catalytic subunit of the hexamer (Figure 7.1C). RuvB (Stasiak *et al.*, 1994), DnaB (San Martin *et al.*, 1995) and T7 gp4 (Egelman *et al.*, 1995) have all been shown to possess bilobed subunits, resulting in hexameric rings with a large and small tier. Interestingly, a recent study shows that the DNA binding site of DnaB contains two subsites with different affinities for ssDNA (Jezewska *et al.*, 1998b). The strong ssDNA binding site is in the vicinity of the small domain of the protein, and the weak binding subsite is located in the large domain. The strong binding site is proposed to bind the 5′ ssDNA tail whereas the incoming duplex is thought to be accommodated within the weak site. These results are consistent with the structural polarity of RuvB and T7 gp4, both of which are known to pump DNA out through the small end of the hexameric ring (Egelman *et al.*, 1995; Yu *et al.*, 1997). RuvB and T7 gp4 could also contain two non-identical DNA binding sites, one in each lobe. If so, it is tempting to speculate that the nucleotide binding site is located in the 'hinge' region between these two lobes, making it ideally situated to effect conformational changes between the two lobes in response to the binding and hydrolysis of NTP. It should be noted that an inchworm mechanism for RuvB would leave the other five subunits in the hexamer redundant in terms of catalysis. They would presumably play a critical structural role, however, allowing RuvB to encircle the DNA and therefore ensure a high processivity.

It is not known, at present, whether RuvB translocates along fully base-paired dsDNA or if transient DNA opening occurs with the hexameric ring. However, an inchworm mechanism could be envisaged in both cases. In the model proposed for PcrA, a wave of base flipping between adjacent pockets along the ssDNA binding site is thought to result in ssDNA translocation by one base at a time. However, considering that RuvB was found to efficiently bypass an interstrand cross-link, if RuvB translocates along ssDNA then it would have to exhibit a larger step size. Alternatively, the dsDNA may remain base-paired during translocation by RuvB. Velankar *et al* (1999) suggested that a PcrA-type translocation mechanism may operate in proteins that are translocators with conserved motifs rather than true helicases, such as type I restriction endonucleases (Gorbalenya and Koonin, 1991), and this may also be extended to specialised motor proteins such as RuvB.

III. CONCLUDING REMARKS

Since their discovery, the *E. coli* RuvA and RuvB proteins have been the subject of a number of biochemical and structural studies. As a result, our understanding of these proteins and their actions has progressed rapidly in recent years. However, a number of important questions remain to be answered before the mechanism of RuvAB-mediated branch migration is fully understood.

This work has investigated the mechanism by which the RuvB branch migration motor drives branch migration. The results have supported the hypothesis that RuvB does not function as a classical helicase *in vivo* but instead uses the energy of ATP hydrolysis to pump DNA through its central channel. However, further studies are needed to be able to determine which, if indeed

any, of the three DNA translocation models proposed above is relevant to RuvB. In particular, a long-awaited crystal structure of RuvB is likely to prove invaluable for our understanding, as has been the case for PcrA.

An important question that needs to be addressed is whether any transient opening of dsDNA occurs within the RuvB motor during branch migration. Considering that strand exchange, from homoduplex to heteroduplex DNA, is thought to have occurred prior to reaching RuvB, it is tempting to speculate that the duplexes remain fully base-paired as they pass through the rings. Certainly DNA is most stable in its double-stranded form and there is no apparent biological need for strand separation within the RuvB ring. In this work, RuvB was shown to efficiently bypass a single interstrand cross-link in duplex DNA. However, to prove that no strand separation occurs within the RuvB ring, a series of interstrand cross-links would have to be introduced into the substrate.

The field of helicases is an exciting and expanding area of work. The recent emergence of crystal structures has suggested that helicases possess a RecA-like nucleotide binding core, which may indicate a common mechanism of action. However, it should be noted that helicases have very diverse functions and thus may have developed specialised mechanisms to carry out their specific roles in the cell. An extreme example is the δ′ subunit of the clamp loader, which has a conserved RecA-like core but whose sequence has diverged to the extent that the protein no longer binds nucleotides (Egelman, 1998; Guenther *et al.*, 1997). RuvB possesses conserved helicase motifs and shares striking structural similarities with other hexameric helicases. However, RuvB also appears to be specialised, in this case as an ATP-dependent molecular pump. Insight into the mechanism by which RuvB harnesses the energy from

ATP hydrolysis for DNA translocation may provide important information on the mechanism of action of other hexameric helicases.

BIBLIOGRAPHY

Abdel-Monem, M., Durwald, H. and Hoffman-Berling, H. (1976) Enzymic unwinding of DNA. II. Chain separation by an ATP-dependent DNA unwinding enzyme. *Eur. J. Biochem.*, **65**, 441-449.

Aboussekhra, A., Chanet, R., Adjiri, A. and Fabre, F. (1992) Semidominant suppressors of *srs2* helicase mutations of *Saccharomyces cerevisiae* map in the *RAD51* gene, whose sequence predicts a protein with similarities to prokaryotic RecA proteins. *Mol. Cell. Biol.*, **12**, 3224-3234.

Abrahams, J.P., Leslie, A.G.W., Lutter, R. and Walker, J.E. (1994) Structure at 2.8Å resolution of F_1-ATPase from bovine heart mitochondria. *Nature*, **370**, 621-628.

Adams, D.E., Tsaneva, I.R. and West, S.C. (1994) Dissociation of RecA filaments from duplex DNA by the RuvA and RuvB DNA repair proteins. *Proc. Natl. Acad. Sci. U.S.A.*, **91**, 9901-9905.

Adams, D.E. and West, S.C. (1995a) Relaxing and unwinding on Holliday: DNA helicase-mediated branch migration. *Mutat. Res.*, **337**, 149-159.

Adams, D.E. and West, S.C. (1995b) Unwinding of closed circular DNA by the *Escherichia coli* RuvA and RuvB recombination/repair proteins. *J. Mol. Biol.*, **247**, 404-417.

Adams, D.E. and West, S.C. (1996) Bypass of DNA heterologies during RuvAB-mediated three- and four-strand branch migration. *J. Mol. Biol.*, **263**, 582-596.

Al-Deib, A.A., Mahdi, A.A. and Lloyd, R.G. (1996) Modulation of recombination and DNA repair by the RecG and PriA helicases of *Escherichia coli* K-12. *J. Bacteriol.*, **178**, 6782-6789.

Albala, J.S., Thelan, M.P., Prange, C., Fan, W., Christensen, M., Thompson, L.H. and Lennon, G.G. (1997) Identification of a novel human *RAD51* homolog, *RAD51B*. *Genomics*, **46**, 476-479.

Ariyoshi, M., Vassylyev, D.G., Iwasaki, H., Fujishima, A., Shinagawa, H. and Morikawa, K. (1994a) Preliminary crystallographic study of *Esherichia coli* RuvC protein. *J. Mol. Biol.*, **241**, 281-282.

Ariyoshi, M., Vassylyev, D.G., Iwasaki, H., Nakamura, H., Shinagawa, H. and Morikawa, K. (1994b) Atomic structure of the RuvC resolvase: A Holliday junction-specific endonuclease from *E. coli*. *Cell*, **78**, 1063-1072.

Asai, T. and Kogoma, T. (1994) D-loops and R-loops: Alternative mechanisms for the initiation of chromosome replication in *Escherichia coli*. *J. Bacteriol.*, **176**, 1807-1812.

Bachmann, B.J. (1972) Pedigrees of some mutant strains of *Escherichia coli* K-12. *Bacteriol. Rev.*, **36**, 525-557.

Basile, G., Aker, M. and Mortimer, R.K. (1992) Nucleotide-sequence and transcriptional regulation of the yeast recombinational repair gene *RAD51*. *Mol. Cell. Biol.*, **12**, 3235-3246.

Bauer, A., Huber, O. and Kemler, R. (1998) Pontin52, an interaction partner of beta-catenin, binds to the TATA box binding protein. *Proc. Natl. Acad. Sci. U.S.A.*, **95**, 14787-14792.

Baumann, P., Benson, F.E. and West, S.C. (1996) Human Rad51 protein promotes ATP-dependent homologous pairing and strand transfer reactions *in vitro*. *Cell*, **87**, 757-766.

Bedale, W.A. and Cox, M.M. (1996) Evidence for the coupling of ATP hydrolysis to the final (extension) phase of RecA protein-mediated DNA strand exchange. *J. Biol. Chem.*, **271**, 5725-5732.

Bell, L. and Byers, B. (1979) Occurrence of crossed strand-exchange forms in yeast during meiosis. *Proc. Natl. Acad. Sci. U.S.A.*, **76**, 3445-3449.

Benbow, R.M., Zuccarelli, A.J. and Sinsheimer, R.L. (1975) Recombinant DNA molecules of ϕX174. *Proc. Natl. Acad. Sci. U.S.A.*, **72**, 235-239.

Bennett, R.J., Dunderdale, H.J. and West, S.C. (1993) Resolution of Holliday junctions by RuvC resolvase: Cleavage specificity and DNA distortion. *Cell*, **74**, 1021-1031.

Bennett, R.J. and West, S.C. (1995) Structural analysis of the RuvC-Holliday junction complex reveals an unfolded junction. *J. Mol. Biol.*, **252**, 213-226.

Bennett, R.J. and West, S.C. (1996) Resolution of Holliday junctions in genetic recombination: RuvC protein nicks DNA at the point of strand exchange. *Proc. Natl. Acad. Sci. U.S.A.*, **93**, 12217-12222.

Benson, F.E., Collier, S. and Lloyd, R.G. (1991) Evidence of abortive recombination in *ruv* mutants of *Escherichia coli* K-12. *Mol. Gen. Genet.*, **225**, 266-272.

Benson, F.E., Illing, G.T., Sharples, G.J. and Lloyd, R.G. (1988) Nucleotide sequencing of the *ruv* region of *E. coli* K-12 reveals a LexA regulated operon encoding two genes. *Nucleic Acids Res.*, **16**, 1541-1550.

Benson, F.E. and West, S.C. (1994) Substrate specificity of the *Escherichia coli* RuvC protein: Resolution of 3- and 4-stranded recombination intermediates. *J. Biol. Chem.*, **269**, 5195-5201.

Benz, J., Trachsel, H. and Baumann, U. (1999) Crystal structure of the ATPase domain of translation initiation factor 4A from *Saccharomyces cerevisiae* - the prototype of the DEAD box protein family. *Structure Fold. Des.*, **7**, 671-679.

Bernstein, J.A. and Richardson, C.C. (1988a) A 7-kDa region of the bacteriophage T7 gene 4 protein is required for primase but not for helicase activity. *Proc. Natl. Acad. Sci. U.S.A.*, **85**, 396-400.

Bernstein, J.A. and Richardson, C.C. (1988b) Purification of the 56-kDa component of the bacteriophage T7 primase/helicase and characterization of its nucleoside 5'- triphosphatase activity. *J. Biol. Chem.*, **263**, 14891-14899.

Bernstein, J.A. and Richardson, C.C. (1989) Characterization of the helicase and primase activities of the 63-kDa component of the bacteriophage T7 gene 4 protein. *J. Biol. Chem.*, **264**, 13066-13073.

Bertrand-Burggraf, E., Kemper, B. and Fuchs, R.P.P. (1994) Endonuclease VII of phage T4 nicks n-2-acetylaminofluorene-induced DNA structures *in vitro*. *Mutat. Res.*, **314**, 287-295.

Bianco, P.R., Tracy, R.B. and Kowalczykowski, S.C. (1998) DNA strand exchange proteins: a biochemical and physical comparison. *Front. Biosci.*, **17**, 570-603.

Bird, L.E., Subramanya, H.S. and Wigley, D.B. (1998) Helicases: a unifying structural theme? *Curr. Opin. Struct. Biol.*, **8**, 14-18.

Bishop, D.K., Park, D., Xu, L.Z. and Kleckner, N. (1992) *DMC1*: A meiosis-specific yeast homolog of *E. coli recA* required for recombination, synaptonemal complex formation, and cell cycle progression. *Cell*, **69**, 439-456.

Boyer, P.D. (1993) The binding change mechanism for ATP synthase - some probabilities and possibilities. *Biochem. Biophys. Acta*, **1140**, 215-250.

Bradford, M.M. (1976) A rapid and sensitive method for the quantitation of microgram quantities of protein utilizing the principle of protein-dye binding. *Anal. Biochem.*, **72**, 248-254.

Bujalowski, W. and Jezewska, M.J. (1995) Interactions of *Escherichia coli* primary replicative helicase DnaB protein with single-stranded DNA: The nucleic acid does not wrap around the protein hexamer. *Biochemistry*, **34**, 8513-8519.

Bujalowski, W. and Klonowska, M.M. (1993) Negative cooperativity in the binding of nucleotides to *Escherichia coli* replicative helicase DnaB protein. Interactions with fluorescent nucleotide analogs. *Biochemistry*, **32**, 5888-5900.

Bujalowski, W., Klonowska, M.M. and Jewewska, M.S. (1994) Oligomeric structure of *Escherichia coli* primary helicase DnaB protein. *J. Biol. Chem.*, **269**, 31350-31358.

Bult, C.J., White, O., Olsen, G.J., Zhou, L., Fleischmann, R.D., Sutton, G.G., Blake, J.A., Fitzgerald, L.M., Clayton, R.A. and Gocayne, J.D. (1996) Complete genomic sequence of the methanogenic archaeon, *Methanococcus jannaschii*. *Science*, **273**, 1058-1073.

Byers, B. and Hollingsworth, N.M. (1994) Meiosis: DNA branching during meiotic recombination. *Curr. Biol.*, **4**, 448-451.

Camerini-Otero, R.D. and Hsieh, P. (1995) Homologous recombination proteins in prokaryotes and eukaryotes. *Annu. Rev. Genet.*, **29**, 509-552.

Cartwright, R., Dunn, A.M., Simpson, P.J., Tambini, C.E. and Thacker, J. (1998a) Isolation of novel human and mouse genes of the *recA/RAD51* recombination/repair gene family. *Nucleic Acids Res.*, **26**, 1653-1659.

Cartwright, R., Tambini, C.E., Simpson, P.J. and Thacker, J. (1998b) The *XRCC2* DNA repair gene from human and mouse encodes a novel member of the *recA/RAD51* family. *Nucleic Acids Res.*, **26**, 3084-3089.

Cassuto, E. and Howard-Flanders, P. (1986) The binding of RecA protein to duplex DNA molecules is directional and is promoted by a single stranded region. *Nucleic Acids Res.*, **14**, 1149-1158.

Cassuto, E., West, S.C. and Howard-Flanders, P. (1982) Can RecA protein promote homologous pairing between duplex regions of DNA. *EMBO J.*, **1**, 821-825.

Chamberlain, D., Keeley, A., Aslam, M., Arenaslicea, J., Brown, T., Tsaneva, I.R. and Perkins, S.J. (1998) A synthetic Holliday junction is sandwiched between two tetrameric *Mycobacterium leprae* RuvA structures in solution: new insights from neutron-scattering, contrast variation and modelling. *J. Mol. Biol.*, **284**, 385-400.

Chiu, S.K., Wong, B.C. and Chow, S.A. (1990) Homologous pairing in duplex DNA regions and the formation of four stranded paranemic joints promoted by RecA protein. Effect of gap length. *J. Biol. Chem.*, **265**, 21262-21268.

Cho, H.S., Ha, N.C., Kang, L.W., Chung, K.M., Back, S.H., Jang, S.K. and Oh, B.H. (1998) Crystal structure of RNA helicase from genotype 1b hepatitis C virus. A feasible mechanism of unwinding duplex RNA. *J. Biol. Chem.*, **273**, 15045-15052.

Churchill, M.E.A., Tullius, T.D., Kallenbach, N.R. and Seeman, N.C. (1988) A Holliday recombination intermediate is two-fold symmetric. *Proc. Natl. Acad. Sci. U.S.A.*, **85**, 4653-4656.

Clark, A.J. and Margulies, A.D. (1965) Isolation and characterization of recombination deficient mutants of *Escherichia coli* K12. *Proc. Natl. Acad. Sci. U.S.A.*, **53**, 451-459.

Clark, A.J. and Sandler, S.J. (1994) Homologous genetic recombination: the pieces begin to fall into place. *Crit. Rev. Microbiol.*, **20**, 125-142.

Clegg, R.M., Murchie, A.I.H. and Lilley, D.M.J. (1994) The solution structure of the four-way DNA junction at low salt conditions: A fluorescence resonance energy transfer analysis. *Biophys. J.*, **66**, 99-109.

Cole, S.T., Brosch, R., Parkhill, J., Garnier, T., Churcher, C., Harris, D., Gordon, S.V., Eiglmeier, K., Gas, S., Barry, C.E. *et al.* (1998) Deciphering the biology of *Mycobacterium tuberculosis* from the complete genome sequence. *Nature*, **393**, 537-544.

Conley, E.C. and West, S.C. (1989) Homologous pairing and the formation of nascent synaptic intermediates between regions of duplex DNA by RecA protein. *Cell*, **56**, 987-995.

Conley, E.C. and West, S.C. (1990) Underwinding of DNA associated with duplex-duplex pairing by RecA protein. *J. Biol. Chem.*, **265**, 10156-10163.

Connolly, B., Parsons, C.A., Benson, F.E., Dunderdale, H.J., Sharples, G.J., Lloyd, R.G. and West, S.C. (1991) Resolution of Holliday junctions *in vitro* requires the *Escherichia coli ruvC* gene product. *Proc. Natl. Acad. Sci. U.S.A.*, **88**, 6063-6067.

Connolly, B. and West, S.C. (1990) Genetic recombination in *Escherichia coli*: Holliday junctions made by RecA protein are resolved by fractionated cell-free extracts. *Proc. Natl. Acad. Sci. U.S.A.*, **87**, 8476-8480.

Cooper, J.P. and Hagerman, P.J. (1987) Gel electrophoretic analysis of the geometry of a DNA four-way junction. *J. Mol. Biol.*, **198**, 711-719.

Cordeiro-Stone, M., Zaritskaya, L.S., Price, L.K. and Kaufmann, W.K. (1997) Replication fork bypass of a pyrimidine dimer blocking leading strand DNA synthesis. *J. Biol. Chem.*, **272**, 13945-13954.

Cox, M.M. (1994) Why does RecA protein hydrolyse ATP? *Trends Biochem. Sci.*, **19**, 217-222.

Cox, M.M. and Lehman, I.R. (1981a) Directionality and polarity in RecA protein-promoted branch migration. *Proc. Natl. Acad. Sci. U.S.A.*, **78**, 6018-6022.

Cox, M.M. and Lehman, I.R. (1981b) RecA protein of *E. coli* promotes branch migration, a kinetically distinct phase of DNA strand exchange. *Proc. Natl. Acad. Sci. U.S.A.*, **78**, 3433-3437.

Cox, M.M., McEntee, K. and Lehman, I.R. (1981) A simple and rapid procedure for the large scale purification of the RecA protein of *Escherichia coli*. *J. Biol. Chem.*, **256**, 4676-4678.

Cox, M.M., Soltis, D.A., Livneh, Z. and Lehman, I.R. (1983) On the role of single-stranded DNA binding protein in RecA protein-promoted DNA strand exchange. *J. Biol. Chem.*, **258**, 2577-2585.

DasGupta, C., Wu, A.M., Kahn, R., Cunningham, R.P. and Radding, C.M. (1981) Concerted strand exchange and formation of Holliday structures by *E. coli* RecA protein. *Cell*, **25**, 507-516.

Davies, A.A. and West, S.C. (1998) Formation of RuvABC-Holliday junction complexes *in vitro*. *Curr. Biol.*, **8**, 725-727.

de Massy, B., Studier, F.W., Dorgai, L., Appelbaum, E. and Weisberg, R.A. (1984) Enzymes and sites of genetic recombination: Studies with gene 3 endonuclease of phage T7 and with site affinity mutants of phage lambda. *Cold Spring Harb. Symp. Quant. Biol.*, **49**, 715-726.

de Massy, B., Weisberg, R.A. and Studier, F.W. (1987) Gene 3 endonuclease of bacteriophage T7 resolves conformationally branched structures in double-stranded DNA [published erratum appears in J. Mol. Biol. 1987 Aug 5;196(3):following 742]. *J. Mol. Biol.*, **193**, 359-376.

Dean, F.B., Borowiec, J.A., Eki, T. and Hurwitz, J. (1992) The simian virus-40 T-antigen double hexamer assembles around the DNA at the replication origin. *J. Biol. Chem.*, **267**, 14129-14137.

deLaat, W.L., Jaspers, N.G.J. and Hoeijmakers, J.H.J. (1999) Molecular mechanism of nucleotide excision repair. *Genes Dev.*, **13**, 768-785.

DiCapua, E., Schnarr, M., Ruigrok, R.W.H., Lindner, P. and Timmins, P.A. (1990) Complexes of RecA protein in solution. A study by small angle neutron scattering. *J. Mol. Biol.*, **214**, 557-570.

Dickie, P., McFadden, G. and Morgan, A.R. (1987) The site-specific cleavage of synthetic Holliday junction analogs and related branched DNA structures by bacteriophage T7 endonuclease I. *J. Biol. Chem.*, **262**, 14826-14836.

Dillingham, M.S., Soultanas, P. and Wigley, D.B. (1999) Site-directed mutagenesis of motif III in PcrA helicase reveals a role in coupling ATP hydrolysis to strand separation. *Nucl. Acids Res.*, **27**, 3310-3317.

Dombroski, A.J., Brennan, C.A., Spear, P. and Platt, T. (1988) Site-directed alterations in the ATP-binding domain of Rho protein affect its activities as a termination factor. *J. Biol. Chem.*, **263**, 18802-18809.

Dong, F., Gogol, E.P. and von Hippel, P.H. (1995) The phage T4-coded DNA replication helicase (gp41) forms a hexamer upon activation by nucleoside triphosphate. *J. Biol. Chem.*, **270**, 7462-7473.

Doniger, J., Warnwe, R.C. and Tessman, I. (1973) Role of circular dimer DNA in the primary recombination mechanism of bacteriophage S13. *Nature New Biol.*, **242**, 9-12.

Dosanjh, M.K., Collins, D.W., Fan, W.F., Lennon, G.G., Albala, J.S., Shen, Z.Y. and Schild, D. (1998) Isolation and characterization of *RAD51C*, a new human member of the *RAD51* family of related genes. *Nucleic Acids Res.*, **26**, 1179-1184.

Doutriaux, M.P., Couteau, F., Bergounioux, C. and White, C. (1998) Isolation and characterization of the *RAD51* and *DMC1* homologs from *Arabidopsis thaliana*. *Mol. Gen. Genet.*, **257**, 283-291.

Duckett, D.R., Giraud-Panis, M.J.E. and Lilley, D.M.J. (1995) Binding of the junction-resolving enzyme T7 endonuclease I to DNA; Separation of binding and catalysis by mutation. *J. Mol. Biol.*, **246**, 95-107.

Duckett, D.R., Murchie, A.I.H., Diekmann, S., Von Kitzing, E., Kemper, B. and Lilley, D.M.J. (1988) The structure of the Holliday junction and its resolution. *Cell*, **55**, 79-89.

Duckett, D.R., Murchie, A.I.H. and Lilley, D.M.J. (1990) The role of metal ions in the conformation of the four-way junction. *EMBO J.*, **9**, 583-590.

Dunderdale, H.J., Benson, F.E., Parsons, C.A., Sharples, G.J., Lloyd, R.G. and West, S.C. (1991) Formation and resolution of recombination intermediates by *E. coli* RecA and RuvC proteins. *Nature*, **354**, 506-510.

Dunderdale, H.J., Sharples, G.J., Lloyd, R.G. and West, S.C. (1994) Cloning, over-expression, purification and characterization of the *Escherichia coli* RuvC Holliday junction resolvase. *J. Biol. Chem.*, **269**, 5187-5194.

Dunn, J.J. and Studier, F.W. (1983) Complete nucleotide sequence of bacteriophage T7 DNA and the locations of T7 genetic elements. *J. Mol. Biol.*, **166**, 477-535.

Dyda, F., Hickman, A.B., Jenkins, T.M., Engelman, A., Craigie, R. and Davies, D.R. (1994) Crystal structure of the catalytic domain of HIV-1 integrase: similarity to other polynucleotidyl transferases. *Science*, **266**, 1981-1986.

Dynan, W.S., Jendrisak, J.J. and Hager, D.A. (1981) Purification and characterization of wheat germ DNA topoisomerase I (nicking-closing enzyme). *J. Biol. Chem.*, **256**, 5860-5865.

Echols, H. and Goodman, M.F. (1991) Fidelity mechanisms in DNA replication. *Ann. Rev. Biochem.*, **60**, 477-511.

Edelhoch, H. (1967) Spectroscopic determination of tryptophan and tyrosine in proteins. *Biochemistry*, **6**, 1948-1954.

Egelman, E.H. (1996) Homomorphous hexameric helicases: tales from the ring cycle. *Structure*, **4**, 759-762.

Egelman, E.H. (1998) Bacterial helicases. *J. Struct. Biol.*, **124**, 123-128.

Egelman, E.H. and Stasiak, A. (1986) Structure of helical RecA-DNA complexes. Complexes formed in the presence of ATP-γ-S or ATP. *J. Mol. Biol.*, **191**, 677-698.

Egelman, E.H., Yu, X., Wild, R., Hingorani, M.M. and Patel, S.S. (1995) Bacteriophage T7 helicase-primase proteins form rings around single-stranded DNA that suggest a general structure for hexameric helicases. *Proc. Natl. Acad. Sci. U.S.A.*, **92**, 3869-3873.

Eggleston, A.K., Mitchell, A.H. and West, S.C. (1997) *In vitro* reconstitution of the late steps of genetic recombination in *E. coli*. *Cell*, **89**, 607-617.

Eggleston, A.K. and West, S.C. (1997) Recombination initiation: Easy as A, B, C, D....χ? *Curr. Biol.*, **7**, 745-749.

Elborough, K.M. and West, S.C. (1990) Resolution of synthetic Holliday junctions in DNA by an endonuclease activity from calf thymus. *EMBO J.*, **9**, 2931-2936.

Ellis, N.A., Groden, J., Ye, T.Z., Straughen, J., Lennon, D.J., Ciocci, S., Proytcheva, M. and German, J. (1995) The Bloom's syndrome gene product is homologous to RecQ helicases. *Cell*, **83**, 655-666.

Evans, D.H. and Kolodner, R. (1987) Construction of a synthetic Holliday junction analog and characterization of its interaction with a *Saccharomyces cerevisiae* endonuclease that cleaves Holliday junctions. *J. Biol. Chem.*, **262**, 9160-9165.

Farabaugh, P.J. (1978) Sequence of the *lacI* gene. *Nature*, **274**, 765-769.

Ferguson, D.O. and Holloman, W.K. (1996) Recombinational repair of gaps in DNA is asymmetric in *Ustilago maydis* and can be explained by a migrating D-loop model. *Proc. Natl. Acad. Sci. U.S.A.*, **93**, 5419-5424.

Finger, L.R. and Richardson, J.P. (1982) Stabilization of the hexameric form of *Escherichia coli* protein Rho under ATP hydrolysis conditions. *J. Mol. Biol.*, **156**, 203-219.

Fleischmann, R.D., Adams, M.D., White, O., Clayton, R.A., Kirkness, E.F., Kerlavage, A.R., Bult, C.J., Tomb, J.F., Dougherty, B.A. and Merrick, J.M. (1995) Whole genome random sequencing and assembly of *Haemophilus influenzae* Rd. *Science*, **269**, 496-512.

Fouts, E.T., Yu, X., Egelman, E.H. and Botchan, M.R. (1999) Biochemical and electron microscopic image analysis of the hexameric E1 helicase. *J. Biol. Chem.*, **274**, 4447-4458.

Fraser, C.M., Gocayne, J.D., White, O., Adams, M.D., Clayton, R.A., Fleischmann, R.D., Bult, C.J., Kerlavage, A.R., Sutton, G. and Kelley, J.M. (1995) The minimal gene complement of *Mycoplasma genitalium*. *Science*, **270**, 397-403.

Friedberg, E.C., Walker, G.C. and Siede, W. (1995) *DNA Repair and Mutagenesis.* American Society for Microbiology, Washington.

Fry, D.C., Kuby, S.A. and Mildvan, A.S. (1986) ATP-binding site of adenylate kinase: Mechanistic implications of its homology with *ras*-encoded p21, F1-ATPase, and other nucleotide-binding proteins. *Proc. Natl. Acad. Sci. U.S.A.*, **83**, 907-911.

Fu, T.J., Tse-Dinh, Y.C. and Seeman, N.C. (1994) Holliday junction crossover topology. *J. Mol. Biol.*, **236**, 91-105.

Fukuoh, A., Iwasaki, H., Ishioka, K. and Shinagawa, H. (1997) ATP-dependent resolution of R-loops at the ColE1 replication origin by *Escherichia coli* RecG protein, a Holliday junction-specific helicase. *EMBO J.*, **16**, 203-209.

Game, J.C. (1993) DNA double-strand breaks and the *RAD50-RAD57* genes in *Saccharomyces*. *Semin. Cancer Biol.*, **4**, 73-83.

Geiselmann, J., Seifreid, S.E., Yager, T.D., Liang, C. and von Hippel, P.H. (1992a) Physical properties of the *Escherichia coli* transcription termination factor Rho. 2. Quaternary structure of the Rho hexamer. *Biochemistry*, **31**, 121-132.

Geiselmann, J. and von Hippel, P.H. (1992) Functional interactions of ligand cofactors with *Escherichia coli* transcription termination factor Rho. I. Binding of ATP. *Prot. Sci.*, **1**, 850-860.

Geiselmann, J., Wang, Y., Seifried, S.E. and Von Hippel, P.H. (1993) A physical model for the translocation and helicase activities of *Escherichia coli* transcription termination protein Rho. *Proc. Natl. Acad. Sci. U.S.A.*, **90**, 7754-7758.

Geiselmann, J., Yager, T.D., Gill, S.C., Calmettes, P. and von Hippel, P.H. (1992b) Physical properties of the *Escherichia coli* transcription termination factor Rho. 1. Association states and geometry of the Rho hexamer. *Biochemistry*, **31**, 111-121.

George, H., Mézard, C., Stasiak, A. and West, S.C. (1999) Helicase-defective $RuvB^{D113E}$ promotes RuvAB-mediated branch migration *in vitro*. *J. Mol. Biol.*, **293**, 505-519.

Gogol, E.P., Seifried, S.E. and von Hippel, P.H. (1991) Structure and assembly of the *Escherichia coli* transcription termination factor Rho and its interaction with RNA. I. Cryoelectron microscopic studies. *J. Mol. Biol.*, **221**, 1127-1138.

Gorbalenya, A.E. and Koonin, E.V. (1991) Endonuclease (R) subunits of type-I and type-III restriction-modification enzymes contain a helicase-like domain. *FEBS Lett.*, **291**, 277-281.

Gorbalenya, A.E. and Koonin, E.V. (1993) Helicases: amino acid sequence comparisons and structure-function relationships. *Curr. Opin. Struct. Biol.*, **3**, 419-429.

Gorbalenya, A.E., Koonin, E.V., Donchenko, A.P. and Blinov, V.M. (1989) Two related superfamilies of putative helicases involved in replication, recombination, repair and expression of DNA and RNA genomes. *Nucl. Acid Res.*, **17**, 4713-4730.

Grant, S.G., Jessee, J., Bloom, F.R. and Hanahan, D. (1990) Differential plasmid rescue from transgenic mouse DNAs into *Escherichia coli* methylation-restriction mutants. *Proc. Natl. Acad. Sci. U.S.A.*, **87**, 4645-4649.

Graves-Woodward, K.L., Gottlieb, J., Challberg, M.D. and Weller, S.K. (1997) Biochemical analyses of mutations in the HSV-1 helicase-primase that alter ATP hydrolysis, DNA unwinding, and coupling between hydrolysis and unwinding. *J. Biol. Chem.*, **272**, 4623-4630.

Griffith, J. and Shores, C.G. (1985) RecA protein rapidly crystallizes in the presence of spermidine: a valuable step in its purification and physical characterization. *Biochemistry*, **24**, 158-162.

Gross, C.H. and Shuman, S. (1995) Mutational analysis of vaccinia virus nucleoside triphosphate phosphohydrolase II, a DExH box RNA helicase. *J. Virol.*, **69**, 4727-4736.

Guenther, B., Onrust, R., Sali, A., O'Donnell, M. and Kuriyan, J. (1997) Crystal structure of the δ' subunit of the clamp-loader complex of *E. coli* DNA polymerase III. *Cell*, **91**, 335-345.

Guo, Q., Lu, M., Churchill, M.E.A., Tullius, T.D. and Kallenbach, N.R. (1990) Asymmetric structure of a three-arm DNA junction. *Biochemistry*, **29**, 10927-10933.

Haber, J.E. (1999) DNA recombination: the replication connection. *Trends Biochem. Sci.*, **24**, 271-275.

Habu, T., Taki, T., West, A., Nishimune, Y. and Morita, T. (1996) The mouse and human homologs of *DMC1*, the yeast meiosis-specific homologous recombination gene, have a common unique form of exon skipped transcript in meiosis. *Nucleic Acids Res.*, **24**, 470-477.

Hacker, K.J. and Johnson, K.A. (1997) A hexameric helicase encircles one DNA strand and excludes the other during DNA unwinding. *Biochemistry*, **36**, 14080-14087.

Hahn, T.R., West, S.C. and Howard-Flanders, P. (1988) RecA-mediated strand exchange reactions between duplex DNA molecules containing damaged bases, deletions and insertions. *J. Biol. Chem.*, **263**, 7431-7436.

Hanawalt, P.C., Cooper, P.K., Ganesan, A.K. and Smith, C.A. (1979) DNA repair in bacteria and mammalian cells. *Annu. Rev. Biochem.*, **48**, 783-836.

Hargreaves, D., Rice, D.W., Sedelnikova, S.E., Artymiuk, P.J., Lloyd, R.G. and Rafferty, J.B. (1998) Crystal structure of *E. coli* RuvA with bound DNA Holliday junction at 6Å resolution. *Nature Struct. Biol.*, **5**, 441-446.

Heuser, J. and Griffith, J. (1989) Visualization of RecA protein and its complexes with DNA by quick-freeze/deep etch electron microscopy. *J. Mol. Biol.*, **210**, 473-484.

Higgins, N.P., Kato, K. and Strauss, B. (1976) A model for replication repair in mammalian cells. *J. Mol. Biol.*, **101**, 417-425.

Himmelreich, R., Hilbert, H., Plagens, H., Pirkl, E., Li, B.C. and Herrmann, R. (1996) Complete sequence analysis of the genome of the bacterium *Mycoplasma pneumoniae*. *Nucleic Acids Res.*, **24**, 4420-4449.

Hingorani, M.M. and Patel, S.S. (1993) Interactions of bacteriophage T7 DNA primase helicase protein with single-stranded and double-stranded DNAs. *Biochemistry*, **32**, 12478-12487.

Hingorani, M.M. and Patel, S.S. (1996) Cooperative interactions of nucleotide ligands are linked to oligomerization and DNA binding in bacteriophage T7 gene 4 helicase. *Biochemistry*, **35**, 2218-2228.

Hingorani, M.M., Washington, M.T., Moore, K.C. and Patel, S.S. (1997) The dTTPase mechanism of T7 DNA helicase resembles the binding change mechanism of the F_1-ATPase. *Proc. Natl. Acad. Sci. U.S.A.*, **94**, 5012-5017.

Hiom, K., Tsaneva, I.R. and West, S.C. (1996) The directionality of RuvAB-mediated branch migration: *in vitro* studies with three-armed junctions. *Genes to Cells*, **1**, 443-451.

Hiom, K. and West, S.C. (1995a) Branch migration during homologous recombination: assembly of a RuvAB-Holliday junction complex *in vitro*. *Cell*, **80**, 787-793.

Hiom, K. and West, S.C. (1995b) Characterisation of RuvAB-Holliday junction complexes by glycerol gradient centrifugation. *Nucleic Acids Res.*, **23**, 3621-3626.

Hishida, T., Iwasaki, H., Ishioka, K. and Shinagawa, H. (1996) Molecular analysis of the *Pseudomonas aeruginosa* genes, *ruvA*, *ruvB* and *ruvC*, involved in processing of homologous recombination intermediates. *Gene*, **182**, 63-70.

Hishida, T., Iwasaki, H., Yagi, T. and Shinagawa, H. (1999) Role of Walker motif A of RuvB protein in promoting branch migration of Holliday junctions. Walker motif A mutations affect ATP binding, ATP hydrolyzing, and DNA binding activities of RuvB. *J. Biol. Chem.*, **274**, 25335-25342.

Holliday, R. (1964) A mechanism for gene conversion in fungi. *Genet. Res. Camb.*, **5**, 282-304.

Holzmann, K., Gerner, C., Korosec, T., Poltl, A., Grimm, R. and Sauermann, G. (1998) Identification and characterization of the ubiquitously occurring nuclear matrix protein NMP 238. *Biochem. Biophys. Res. Commun.*, **252**, 39-45.

Hong, X.K., Cadwell, G.W. and Kogoma, T. (1995) *Escherichia coli* RecG and RecA proteins in R-loop formation. *EMBO J.*, **14**, 2385-2392.

Horiguchi, T., Miwa, Y. and Shigesada, K. (1997) The quaternary geometry of transcription termination factor Rho: assignment by chemical cross-linking. *J. Mol. Biol.*, **269**, 514-528.

Howard-Flanders, P., Rupp, W.D., Wilkins, B.M. and Cole, R.S. (1968) DNA replication and recombination after UV irradiation. *Cold Spring Harb. Symp. Quant. Biol.*, **33**, 195-207.

Howard-Flanders, P. and Theriot, L. (1966) Mutants of *Escherichia coli* K-12 defective in DNA repair and genetic recombination. *Genetics*, **53**, 1137-1150.

Howard-Flanders, P., West, S.C. and Stasiak, A.J. (1984) Role of RecA spiral filaments in genetic recombination. *Nature*, **309**, 215-220.

Hwang, G.S., Kim, J.K. and Choi, B.S. (1996) The solution structure of a psoralen cross-linked DNA duplex by NMR and relaxation matrix refinement. *Biochem. Biophys. Res. Comm.*, **219**, 191-197.

Hyde, H., Davies, A.A., Benson, F.E. and West, S.C. (1994) Resolution of recombination intermediates by a mammalian endonuclease activity functionally analogous to *Escherichia coli* RuvC resolvase. *J. Biol. Chem.*, **269**, 5202-5209.

Iwasaki, H., Shiba, T., Makino, K., Nakata, A. and Shinagawa, H. (1989a) Overproduction, purification, and ATPase activity of the *Escherichia coli* RuvB protein involved in DNA repair. *J. Bacteriol.*, **171**, 5276-5280.

Iwasaki, H., Shiba, T., Nakata, A. and Shinagawa, H. (1989b) Involvement in DNA repair of the *ruvA* gene of *Escherichia coli*. *Molec. Gen. Genet.*, **219**, 328-331.

Iwasaki, H., Takahagi, M., Nakata, A. and Shinagawa, H. (1992) *Escherichia coli* RuvA and RuvB proteins specifically interact with Holliday junctions and promote branch migration. *Genes Dev.*, **6**, 2214-2220.

Iwasaki, H., Takahagi, M., Shiba, T., Nakata, A. and Shinagawa, H. (1991) *Escherichia coli* RuvC protein is an endonuclease that resolves the Holliday structure. *EMBO J.*, **10**, 4381-4389.

Iype, L.E., Wood, E.A., Inman, R.B. and Cox, M.M. (1994) RuvA and RuvB proteins facilitate the bypass of heterologous DNA insertions during RecA protein-mediated DNA strand exchange. *J. Biol. Chem.*, **269**, 24967-24978.

Jaspers, N.G.J. and Hoeijmakers, J.H.J. (1995) DNA repair: nucleotide excision repair in the test-tube. *Curr. Biol.*, **5**, 700-702.

Jeanmougin, F., Thompson, J.D., Gouy, M., Higgins, D.G. and Gibson, T.J. (1998) Multiple sequence alignment with Clustal X. *Trends Biochem. Sci.*, **23**, 403-405.

Jensch, F. and Kemper, B. (1986) Endonuclease VII resolves Y-junctions in branched DNA *in vitro*. *EMBO J.*, **5**, 181-189.

Jezewska, M.J. and Bujalowski, W. (1996) Global conformational transitions in *Escherichia coli* primary replicative helicase DnaB protein induced by ATP, ADP, and single-stranded DNA binding: multiple conformational states of the helicase hexamer. *J. Biol. Chem.*, **271**, 4261-4265.

Jezewska, M.J., Rajendran, S., Bujalowska, D. and Bujalowski, W. (1998a) Does single-stranded DNA pass through the inner channel of the protein hexamer in the complex with the *Escherichia coli* DnaB helicase: fluorescence energy transfer studies. *J. Biol. Chem.*, **273**, 10515-10529.

Jezewska, M.J., Rajendran, S. and Bujalowski, W. (1997) Strand specificity in the interactions of *Escherichia coli* primary replicative helicase DnaB protein with a replication fork. *Biochemistry*, **36**, 10320-10326.

Jezewska, M.J., Rajendran, S. and Bujalowski, W. (1998b) Functional and structural heterogeneity of the DNA binding site of the *Escherichia coli* primary replicative helicase DnaB protein. *J. Biol. Chem.*, **273**, 9058-9069.

Jindal, H.K., Yong, C.B., Wilson, G.M., Tam, P. and Astell, C.R. (1994) Mutations in the NTP-binding motif of minute virus of mice (MVM) NS-1 protein uncouple ATPase and DNA helicase functions. *J. Biol. Chem.*, **269**, 3283-3289.

Johnson, R.T. and Squires, S. (1992) The XP-D complementation group - insights into xeroderma-pigmentosum, cockaynes-syndrome and trichothiodystrophy. *Mutat. Res.*, **273**, 97-118.

Jwang, B.R. and Radding, C.M. (1992) Torsional stress generated by RecA protein during DNA strand exchange separates strands of a heterologous insert. *Proc. Natl. Acad. Sci. U.S.A.*, **89**, 7596-7600.

Kahn, R., Cunningham, R.P., DasGupta, C. and Radding, C.M. (1981) Polarity of heteroduplex formation promoted by *Escherichia coli* RecA protein. *Proc. Natl. Acad. Sci. U.S.A.*, **78**, 4786-4790.

Kallenbach, N.R., Ma, R.I. and Seeman, N.C. (1983) An immobile nucleic acid junction constructed from oligonucleotides. *Nature*, **305**, 829-831.

Kaneko, T., Tanaka, A., Sato, S., Kotani, H., Sazuka, T., Miyajima, N., Sugiura, M. and Tabata, S. (1995) Sequence analysis of the genome of the unicellular Cyanobacterium *Synechocystis* sp. strain PCC6803. I. Sequence features in the 1 Mb region from map positions 64% to 92% of the genome. *DNA Res.*, **2**, 153-166.

Kanemaki, M., Kurokawa, Y., Matsuura, T., Makino, Y., Masani, A., Okazaki, K., Morishita, T. and Tamura, T. (1999) TIP49b, a new RuvB-like DNA helicase, is included in a complex together with another RuvB-like DNA helicase, TIP49a. *J. Biol. Chem.*, **274**, 22437-22444.

Kanemaki, M., Makino, Y., Yoshida, T., Kishimoto, T., Koga, A., Yamamoto, K., Yamamoto, M., Moncollin, V., Egly, J.M., Muramatsu, M. *et al.* (1997) Molecular cloning of a rat 49-kDa TBP-interacting protein (TIP49) that is highly homologous to the bacterial RuvB. *Biochem. Biophys. Res. Commun.*, **235**, 64-68.

Kanne, D., Straub, K., Hearst, J.E. and Rapoport, H. (1982) Isolation and characterization of pyrimidine-psoralen-pyrimidine photodiadducts from DNA. *J. Amer. Chem. Soc.*, **104**, 6754-6764.

Kans, J.A. and Mortimer, R.K. (1991) Nucleotide sequence of the *RAD57* gene of *Saccharomyces cerevisiae*. *Gene*, **105**, 139-140.

Karlin, S. and Brocchieri, L. (1996) Evolutionary conservation of *recA* genes in relation to protein structure and function. *J. Bacteriol.*, **178**, 1881-1894.

Karlin, S., Weinstock, G.M. and Brendel, V. (1995) Bacterial classifications derived from RecA protein sequence comparisons. *J. Bacteriol.*, **177**, 6881-6893.

Keeney, S., Giroux, C.N. and Kleckner, N. (1997) Meiosis-specific DNA double-strand breaks are catalyzed by Spo11, a member of a widely conserved protein family. *Cell*, **88**, 375-384.

Kemper, B. and Garabett, M. (1981) Studies in T4-head maturation. 1. Purification and characterization of gene 49 controlled endonuclease. *Eur. J. Biochem.*, **115**, 123-132.

Kemper, B., Jensch, F., Depka-Prondzynski, M., Fritz, H.J., Borgmeyer, U. and Mizuuchi, K. (1984) Resolution of Holliday structures by endonuclease VII as observed in interactions with cruciform DNA. *Cold Spring Harb. Symp. Quant. Biol.*, **49**, 815-825.

Kikuchi, N., Gohshi, T., Kawahire, S., Tachibana, T., Yoneda, Y., Isobe, T., Lim, C.R., Kohno, K., Ichimura, T., Omata, S. *et al.* (1999) Molecular shape and ATP binding activity of rat p50, a putative mammalian homologue of RuvB DNA helicase. *J. Biochem. (Tokyo)*, **125**, 487-494.

Kim, J.I., Cox, M.M. and Inman, R.B. (1992a) On the role of ATP hydrolysis in RecA protein-mediated DNA strand exchange. 1. Bypassing a short heterologous insert in one DNA substrate. *J. Biol. Chem.*, **267**, 16438-16443.

Kim, J.I., Cox, M.M. and Inman, R.B. (1992b) On the role of ATP hydrolysis in RecA protein-mediated DNA strand exchange. 2. 4-strand exchanges. *J. Biol. Chem.*, **267**, 16444-16449.

Kim, J.L., Morgenstern, K.A., Griffith, J.P., Dwyer, M.D., Thomson, J.A., Murcko, M.A., Lin, C. and Caron, P.R. (1998) Hepatitis C virus NS3 RNA helicase domain with a bound oligonucleotide: the crystal structure provides insights into the mode of unwinding. *Structure*, **6**, 89-100.

Kleff, S. and Kemper, B. (1988) Initiation of heteroduplex loop repair by T4-encoded endonuclease VII *in vitro*. *EMBO J.*, **7**, 1527-1535.

Kleff, S., Kemper, B. and Sternglanz, R. (1992) Identification and characterization of yeast mutants and the gene for a cruciform cutting endonuclease. *EMBO J.*, **11**, 699-704.

Kobertz, W.R. and Essigmann, J.M. (1996) Total synthesis of a *cis*-syn 2-carbomethoxypsoralen furan-side thymidine monoadduct. *J. Amer. Chem. Soc.*, **118**, 7101-7107.

Kobertz, W.R. and Essigmann, J.M. (1997) Solid-phase synthesis of oligonucleotides containing a site-specific psoralen derivative. *J. Amer. Chem. Soc.*, **119**, 5960-5961.

Koffel-Schwartz, N., Coin, F., Veaute, X. and Fuchs, R.P.P. (1996) Cellular strategies for accommodating replication-hindering adducts in DNA: Control by the SOS response in *Escherichia coli*. *Proc. Natl. Acad. Sci. U.S.A.*, **93**, 7805-7810.

Komori, K., Sakae, S., Shinagawa, H., Morikawa, K. and Ishino, Y. (1999) A Holliday junction resolvase from *Pyrococcus furiosus*: Functional similarity to *Escherichia coli* RuvC provides evidence for conserved mechanism of homologous recombination in Bacteria, Eukarya, and Archaea. *Proc. Natl. Acad. Sci. U.S.A.*, **96**, 8873-8878.

Konforti, B.B. and Davis, R.W. (1992) ATP hydrolysis and the displaced strand are two factors that determine the polarity of RecA-promoted DNA strand exchange. *J. Mol. Biol.*, **227**, 38-53.

Korolev, S., Hsieh, J., Gauss, G.H., Lohman, T.M. and Waksman, G. (1997) Major domain swiveling revealed by the crystal structures of complexes of *Escherichia coli* Rep helicase bound to single-stranded DNA and ADP. *Cell*, **90**, 635-647.

Korolev, S., Yao, N., Lohman, T.M., Weber, P.C. and Waksman, G. (1998) Comparisons between the structures of HCV and Rep helicases reveal structural similarities between SF1 and SF2 super-families of helicases. *Protein Sci.*, **7**, 605-610.

Kowalczykowski, S.C., Dixon, D.A., Eggleston, A.K., Lauder, S.D. and Rehrauer, W.M. (1994) Biochemistry of homologous recombination in *Escherichia coli*. *Microbiol. Revs*, **58**, 401-465.

Kowalczykowski, S.C. and Krupp, R.A. (1987) Effects of *E. coli* SSB protein on the single stranded DNA dependent ATPase activity of *E. coli* RecA protein: Evidence that SSB facilitates the binding of RecA protein to regions of secondary structure within single-stranded DNA. *J. Mol. Biol.*, **193**, 97-113.

Kowalczykowski, S.C. and Krupp, R.A. (1995) DNA strand exchange promoted by RecA protein in the absence of ATP: implications for the mechanism of energy transduction in protein-promoted nucleic acid transactions. *Proc. Natl. Acad. Sci. U.S.A.*, **92**, 3478-3482.

Kuzminov, A. (1995) Collapse and repair of replication forks in *Escherichia coli*. *Mol. Microbiol.*, **16**, 373-384.

Laemmli, U.K. (1970) Cleavage of structural proteins during the assembly of the head of bacteriophage T4. *Nature*, **227**, 680-685.

Li, Z.F., Golub, E.I., Gupta, R. and Radding, C.M. (1997) Recombination activities of *Hs*Dmc1 protein, the meiotic human homolog of RecA protein. *Proc. Natl. Acad. Sci. U.S.A.*, **94**, 11221-11226.

Little, J.W. (1984) Autodigestion of LexA and phage lambda repressors. *Proc. Natl. Acad. Sci. U.S.A.*, **81**, 1375-1379.

Little, J.W., Edmiston, S.H., Pacelli, L.Z. and Mount, D.W. (1980) Cleavage of the *Escherichia coli* LexA protein by the RecA protease. *Proc. Nat. Acad. Sci. U.S.A.*, **77**, 3225-3229.

Little, J.W. and Mount, D.W. (1982) The SOS regulatory system of *E. coli*. *Cell*, **29**, 11-22.

Liu, N., Lamerdin, J.E., Tebbs, R.S., Schild, D., Tucker, J.D., Shen, M.R., Brookman, K.W., Siciliano, M.J., Walter, C.A., Fan, W.F. *et al.* (1998) Xrcc2 and Xrcc3, new human Rad51-family members, promote chromosome stability and protect against DNA cross-links and other damages. *Mol. Cell.*, **1**, 783-793.

Lloyd, R.G. (1991) Conjugal recombination in resolvase-deficient *ruvC* mutants of *Escherichia coli* K12 depends on *recG*. *J. Bacteriol.*, **173**, 5414-5418.

Lloyd, R.G., Benson, F.E. and Shurvinton, C.E. (1984) Effect of *ruv* mutations on recombination and DNA repair in *Escherichia coli* K12. *Mol. Gen. Genet.*, **194**, 303-309.

Lloyd, R.G. and Buckman, C. (1991) Genetic analysis of the *recG* locus of *Escherichia coli* K-12 and of its role in recombination and DNA repair. *J. Bacteriol.*, **173**, 1004-1011.

Lloyd, R.G. and Low, K.B. (1996) Homologous recombination. In Neidhardt, F.C. (ed.) *Escherichia coli and Salmonella: Cellular and Molecular Biology*. ASM Press, pp. 2236-2255.

Lloyd, R.G. and Sharples, G.J. (1993a) Dissociation of synthetic Holliday junctions by *E. coli* RecG protein. *EMBO J.*, **12**, 17-22.

Lloyd, R.G. and Sharples, G.J. (1993b) Processing of recombination intermediates by the RecG and RuvAB proteins of *Escherichia coli*. *Nucleic Acids Res.*, **21**, 1719-1725.

Lohman, T.M. (1993) Helicase-catalyzed DNA unwinding. *J. Biol. Chem.*, **268**, 2269-2272.

Lohman, T.M. and Bjornson, K.P. (1996) Mechanisms of helicase-catalyzed DNA unwinding. *Ann. Rev. Biochem.*, **65**, 169-214.

Lovett, S.T. (1994) Sequence of the *RAD55* gene of *Saccharomyces cerevisiae*: Similarity of Rad55 to prokaryotic RecA and other RecA-like proteins. *Gene*, **142**, 103-106.

Lu, M., Guo, Q. and Kallenbach, N.R. (1991a) Effect of DNA sequence on the structure of three-arm DNA junctions. *Biochemistry*, **30**, 5815-5820.

Lu, M., Guo, Q., Studier, F.W. and Kallenbach, N.R. (1991b) Resolution of branched DNA substrates by T7 endonuclease I and its inhibition. *J. Biol. Chem.*, **266**, 2531-2536.

Lynn, R.M. and Wang, J.C. (1989) Peptide sequencing and site-directed mutagenesis identify tyrosine-319 as the active site tyrosine of *Escherichia coli* DNA topoisomerase I. *Proteins*, **6**, 231-239.

MacFarland, K.J., Shan, Q., Inman, R.B. and Cox, M.M. (1997) RecA as a motor protein: testing models for the role of ATP hydrolysis in DNA strand exchange. *J. Biol. Chem.*, **272**, 17675-17685.

Maeshima, K., Morimatsu, K. and Horii, T. (1996) Purification and characterization of *X*Rad51.1 protein, *Xenopus RAD51* homologue: recombinant *X*Rad51.1 promotes strand exchange reaction. *Genes to Cells*, **1**, 1057-1068.

Maeshima, K., Morimatsu, K., Shinohara, A. and Horii, T. (1995) *RAD51* homologs in *Xenopus laevis*: Two distinct genes are highly expressed in ovary and testis. *Gene*, **160**, 195-200.

Mahdi, A.A., Sharples, G.J., Mandal, T.N. and Lloyd, R.G. (1996) Holliday junction resolvases encoded by homologous *rusA* genes in *Escherichia coli* K-12 and phage-82. *J. Mol. Biol.*, **257**, 561-573.

Mandal, T.N., Mahdi, A.A., Sharples, G.J. and Lloyd, R.G. (1993) Resolution of Holliday intermediates in recombination and DNA repair: indirect suppression of *ruvA*, *ruvB*, and *ruvC* mutations. *J. Bacteriol.*, **175**, 4325-4334.

Marrione, P.E. and Cox, M.M. (1995) RuvB protein-mediated ATP hydrolysis: functional asymmetry in the RuvB hexamer. *Biochemistry*, **34**, 9809-9818.

Marrione, P.E. and Cox, M.M. (1996) Allosteric effects of RuvA protein, ATP, and DNA on RuvB protein-mediated ATP hydrolysis. *Biochemistry*, **35**, 11228-11238.

Masai, H., Asai, T., Kubota, Y., Arai, K. and Kogoma, T. (1994) *Escherichia coli* PriA protein is essential for inducible and constitutive stable DNA replication. *EMBO J.*, **13**, 5338-5345.

Masson, J.-Y., Davies, A.A., Hajibagheri, N., Van Dyck, E., Benson, F.E., Stasiak, A.Z., Stasiak, A. and West, S.C. (1999) The meiosis-specific recombinase Dmc1 forms ring structures and interacts with hRad51. *EMBO J.*, **18**, 6552-6560.

Mastrangelo, I.A., Bezanilla, M., Hansma, P.K., Hough, P.V. and Hansma, H.G. (1994) Structures of large T antigen at the origin of SV40 DNA replication by atomic force microscopy. *Biophys. J.*, **66**, 293-298.

Mastrangelo, I.A., Hough, P.V.C., Wall, J.S., Dobson, M., Dean, F.B. and Hurwitz, J. (1989) ATP-dependent assembly of double hexamers of SV40 T antigen at the viral origin of DNA replication. *Nature*, **338**, 658-662.

Matson, S.W., Bean, D.W. and George, J.W. (1994) DNA helicases: Enzymes with essential roles in all aspects of DNA metabolism. *BioEssays*, **16**, 13-22.

McSwiggen, J.A., Bear, D.G. and von Hippel, P.H. (1988) Interactions of *Escherichia coli* transcription termination factor Rho with RNA. I. Binding stoichiometries and free energies. *J. Mol. Biol.*, **199**, 609-622.

Menetski, J.P., Bear, D.G. and Kowalczykowski, S.C. (1990) Stable DNA heteroduplex formation catalyzed by the *Escherichia coli* RecA protein in the absence of ATP hydrolysis. *Proc. Natl. Acad. Sci. U.S.A.*, **87**, 21-25.

Mézard, C., Davies, A.A., Stasiak, A. and West, S.C. (1997) Biochemical properties of $RuvB^{D113N}$: a mutation in helicase motif II of the RuvB hexamer affects DNA binding and ATPase activities. *J. Mol. Biol.*, **271**, 704-717.

Milburn, M.V., Tong, L., deVos, A.M., Brunger, A., Yamaizumi, Z., Nishimura, S. and Kim, S.H. (1990) Molecular switch for signal transduction: structural differences between active and inactive forms of protooncogenic ras proteins. *Science*, **247**, 939-945.

Mitchell, A.H. and West, S.C. (1994) Hexameric rings of *Escherichia coli* RuvB protein: Cooperative assembly, processivity, and ATPase activity. *J. Mol. Biol.*, **243**, 208-215.

Mitchell, A.H. and West, S.C. (1996) Role of RuvA in branch migration reactions catalyzed by the RuvA and RuvB proteins of *Escherichia coli*. *J. Biol. Chem.*, **271**, 19497-19502.

Miwa, Y., Horiguchi, T. and Shigesada, K. (1995) Structural and functional dissections of transcription termination factor Rho by random mutagenesis. *J. Mol. Biol.*, **254**, 815-837.

Mizuuchi, K., Kemper, B., Hays, J. and Weisberg, R.A. (1982) T4 endonuclease VII cleaves Holliday structures. *Cell*, **29**, 357-365.

Møllegaard, N.E., Murchie, A.I.H., Lilley, D.M.J. and Nielsen, P.E. (1994) Uranyl photoprobing of a four-way DNA junction: evidence for specific metal ion binding. *EMBO J.*, **13**, 1508-1513.

Morel, P., Stasiak, A., Ehrlich, S.D. and Cassuto, E. (1994) Effect of length and location of heterologous sequences on RecA-mediated strand exchange. *J. Biol. Chem.*, **269**, 19830-19835.

Mueller, J.E., Newton, C.J., Jensch, F., Kemper, B., Cunningham, R.P., Kallenbach, N.R. and Seeman, N.C. (1990) Resolution of Holliday junction analogs by T4 endonuclease VII can be directed by substrate structure. *J. Biol. Chem.*, **265**, 13918-13924.

Müller, B., Burdett, I. and West, S.C. (1992) Unusual stability of recombination intermediates made by *Escherichia coli* RecA protein. *EMBO J.*, **11**, 2685-2693.

Müller, B., Jones, C. and West, S.C. (1990) T7 endonuclease I resolves Holliday junctions formed *in vitro* by RecA protein. *Nucleic Acids Res.*, **18**, 5633-5636.

Müller, B., Tsaneva, I.R. and West, S.C. (1993a) Branch migration of Holliday junctions promoted by the *Escherichia coli* RuvA and RuvB proteins: I. Comparison of the RuvAB- and RuvB-mediated reactions. *J. Biol. Chem.*, **268**, 17179-17184.

Müller, B., Tsaneva, I.R. and West, S.C. (1993b) Branch migration of Holliday junctions promoted by the *Escherichia coli* RuvA and RuvB proteins: II. Interaction of RuvB with DNA. *J. Biol. Chem.*, **268**, 17185-17189.

Muniyappa, K., Shaner, S.L., Tsang, S.S. and Radding, C.M. (1984) Mechanism of the concerted action of RecA protein and helix-destabilizing proteins in homologous recombination. *Proc. Natl. Acad. Sci. U.S.A.*, **81**, 2757-2761.

Murchie, A.I.H., Clegg, R.M., von Kitzing, E., Duckett, D.R., Diekmann, S. and Lilley, D.M.J. (1989) Fluorescence energy transfer shows that the four-way DNA junction is a right-handed cross of antiparallel molecules. *Nature*, **341**, 763-766.

Murchie, A.I.H. and Lilley, D.M.J. (1993) T4 endonuclease VII cleaves DNA containing a cisplatin adduct. *J. Mol. Biol.*, **233**, 77-85.

Nassif, N., Penney, J., Pal, S., Engels, W.R. and Gloor, G.B. (1994) Efficient copying of nonhomologous sequences from ectopic sites via P-element-induced gap repair. *Mol. Cell. Biol.*, **14**, 1613-1625.

Nayak, S. and Bryant, F.R. (1999) Differential rates of NTP hydrolysis by the mutant [S69G]RecA protein: Evidence for a coupling of NTP turnover to DNA strand exchange. *J. Biol. Chem.*, **274**, 25979-25982.

Nishimoto, H., Takayama, M. and Minagawa, T. (1979) Purification and some properties of deoxyribonuclease whose synthesis is controlled by gene 49 of bacteriophage T4. *Eur. J. Biochem.*, **100**, 433-440.

Ogawa, T., Wabico, H., Tsurimoto, T., Horii, T., Masukata, H. and Ogawa, H. (1979) Characteristics of purified RecA protein and the regulation of its synthesis *in vitro*. *Cold Spring Harb. Symp. Quant. Biol.*, **43**, 909-915.

Ogawa, T., Yu, X., Shinohara, A. and Egelman, E.H. (1993) Similarity of the yeast Rad51 filament to the bacterial RecA filament. *Science*, **259**, 1896-1899.

Opperman, T. and Richardson, J.P. (1994) Phylogenetic analysis of sequences from diverse bacteria with homology to the *Escherichia coli rho* gene. *J. Bacteriol.*, **176**, 5033-5043.

Oram, M., Keeley, A. and Tsaneva, I. (1998) Holliday junction resolvase in *Schizosaccharomyces pombe* has identical endonuclease activity to the Cce1 homolog Ydc2. *Nucleic Acids Res.*, **26**, 594-601.

Orr-Weaver, T., Szostak, J.W. and Rothstein, R.J. (1981) Yeast transformation: a model system for the study of recombination. *Proc. Natl. Acad. Sci. U.S.A.*, **78**, 6354-6358.

Ortiz-Lombardía, M., González, A., Eritja, R., Aymamí, J., Azorín, F. and Coll, M. (1999) Crystal structure of a DNA Holliday junction [In Process Citation]. *Nat. Struct. Biol.*, **6**, 913-917.

Otsuji, N., Iyehara, H. and Hideshima, Y. (1974) Isolation and characterization of an *Escherichia coli ruv* mutant which forms nonseptate filaments after low doses of ultraviolet light irradiation. *J. Bacteriol.*, **117**, 337-344.

Pai, E.F., Krengel, U., Petsko, G.A., Goody, R.S., Kabsch, W. and Wittinghofer, A. (1990) Refined crystal structure of the triphosphate conformation of H-*ras* p21 at 1.35Å resolution: implications for the mechanism of GTP hydrolysis. *EMBO J.*, **9**, 2351-2359.

Panyutin, I.G., Biswas, I. and Hsieh, P. (1995) A pivotal role for the structure of the Holliday junction in DNA branch migration. *EMBO J.*, **14**, 1819-1826.

Panyutin, I.G. and Hsieh, P. (1993) Formation of a single base mismatch impedes spontaneous DNA branch migration. *J. Mol. Biol.*, **230**, 413-424.

Panyutin, I.G. and Hsieh, P. (1994) The kinetics of spontaneous DNA branch migration. *Proc. Natl. Acad. Sci. U.S.A.*, **91**, 2021-2025.

Paques, F., Leung, W.Y. and Haber, J.E. (1998) Expansions and contractions in a tandem repeat induced by double-strand break repair. *Mol. Cell. Biol.*, **18**, 2045-2054.

Parsons, C.A., Kemper, B. and West, S.C. (1990) Interaction of a four-way junction in DNA with T4 endonuclease VII. *J. Biol. Chem.*, **265**, 9285-9289.

Parsons, C.A., Murchie, A.I.H., Lilley, D.M.J. and West, S.C. (1989) Resolution of model Holliday junctions by yeast endonuclease: Effect of DNA structure and sequence. *EMBO J.*, **8**, 239-246.

Parsons, C.A., Stasiak, A., Bennett, R.J. and West, S.C. (1995a) Structure of a multisubunit complex that promotes DNA branch migration. *Nature*, **374**, 375-378.

Parsons, C.A., Stasiak, A. and West, S.C. (1995b) The *E. coli* RuvAB proteins branch migrate Holliday junctions through heterologous DNA sequences in a reaction facilitated by SSB. *EMBO J.*, **14**, 5736-5744.

Parsons, C.A., Tsaneva, I., Lloyd, R.G. and West, S.C. (1992) Interaction of *Escherichia coli* RuvA and RuvB proteins with synthetic Holliday junctions. *Proc. Natl. Acad. Sci. U.S.A.*, **89**, 5452-5456.

Parsons, C.A. and West, S.C. (1988) Resolution of model Holliday junctions by yeast endonuclease is dependent upon homologous DNA sequences. *Cell*, **52**, 621-629.

Parsons, C.A. and West, S.C. (1993) Formation of a RuvAB-Holliday junction complex *in vitro*. *J. Mol. Biol.*, **232**, 397-405.

Passy, S.I., Yu, X., Li, Z., Radding, C.M., Masson, J.-Y., West, S.C. and Egelman, E.H. (1999) Human Dmc1 protein binds DNA as an octameric ring. *Proc. Natl. Acad. Sci. U.S.A.*, **96**, 10684-10688.

Patel, S.S. and Hingorani, M.M. (1993) Oligomeric structure of bacteriophage T7 DNA primase/helicase proteins. *J. Biol. Chem.*, **268**, 10668-10675.

Pause, A. and Sonenberg, N. (1992) Mutational analysis of a DEAD box RNA helicase: the mammalian translation initiation factor eIF-4A. *EMBO J.*, **11**, 2643-2654.

Pereira, S. and Platt, T. (1995) A mutation in the ATP binding domain of Rho alters its RNA binding properties and uncouples ATP hydrolysis from helicase activity. *J. Biol. Chem.*, **270**, 30401-30407.

Petes, T.D., Malone, R.E. and Symington, L.S. (1991) Recombination in yeast. *The molecular and cellular biology of the yeast Saccharomyces: Genome dynamics, protein synthesis and energetics*. Cold Spring Harbor Laboratory Press, New York, Vol. 1, pp. 407-521.

Picksley, S.M., Parsons, C.A., Kemper, B. and West, S.C. (1990) Cleavage specificity of bacteriophage T4 endonuclease VII and bacteriophage T7 endonuclease I on synthetic branch migratable Holliday junctions. *J. Mol. Biol.*, **212**, 723-735.

Pittman, D.L., Weinberg, L.R. and Schimenti, J.C. (1998) Identification, characterization, and genetic mapping of *RAD51D*, a new mouse and human *RAD51/recA*-related gene. *Genomics*, **49**, 103-111.

Potter, H. and Dressler, D. (1976) On the mechanism of genetic recombination: Electron microscopic observation of recombination intermediates. *Proc. Natl. Acad. Sci. U.S.A.*, **73**, 3000-3004.

Pugh, B.F. and Cox, M.M. (1987a) RecA protein binding to the heteroduplex product of DNA strand exchange. *J. Biol. Chem.*, **262**, 1337-1343.

Pugh, B.F. and Cox, M.M. (1987b) Stable binding of RecA protein to duplex DNA. *J. Biol. Chem.*, **262**, 1326-1336.

Qiu, X.B., Lin, Y.L., Thome, K.C., Pian, P., Schlegel, B.P., Weremowicz, S., Parvin, J.D. and Dutta, A. (1998) An eukaryotic RuvB-like protein (RuvBL1) essential for growth. *J. Biol. Chem.*, **273**, 27786-27793.

Rafferty, J.B., Sedelnikova, S.E., Hargreaves, D., Artymiuk, P.J., Baker, P.J., Sharples, G.J., Mahdi, A.A., Lloyd, R.G. and Rice, D.W. (1996) Crystal structure of DNA recombination protein RuvA and a model for its binding to the Holliday junction. *Science*, **274**, 415-421.

Raney, K.D., Carver, T.E. and Benkovic, S.J. (1996) Stoichiometry and DNA unwinding by the bacteriophage T4 41:59 helicase. *J. Biol. Chem.*, **271**, 14074-14081.

Register, J.C. and Griffith, J. (1985) The direction of the RecA protein assembly onto single strand DNA is the same as the direction of strand assimilation during exchange. *J. Biol. Chem.*, **260**, 12308-12312.

Reha-Kranz, L.J. and Hurwitz, J. (1978) The *dnaB* gene product of *Escherichia coli*: Purification, homogeneity and physical properties. *J. Biol. Chem.*, **253**, 4043-4050.

Rehrauer, W.M. and Kowalczykowski, S.C. (1993) Alteration of the nucleoside triphosphate (NTP) catalytic domain within *Escherichia coli* RecA protein attenuates NTP hydrolysis but not joint molecule formation. *J. Biol. Chem.*, **268**, 1292-1297.

Resnick, M.A. (1976) The repair of double-strand breaks in DNA: a model including recombination. *J. Theoret. Biol.*, **59**, 97-106.

Rice, M.C., Smith, S.T., Bullrich, F., Havre, P. and Kmiec, E.B. (1997) Isolation of human and mouse genes based on homology to *REC2*, a recombinational repair gene from the fungus *Ustilago maydis*. *Proc. Natl. Acad. Sci. U.S.A.*, **94**, 7417-7422.

Rice, P. and Mizuuchi, K. (1995) Structure of the bacteriophage Mu transposase core: a common structural motif for DNA transposition and retroviral integration. *Cell*, **82**, 209-220.

Roberts, J.W., Roberts, C.W., Craig, N.L. and Phizicky, E.M. (1979) Activity of the *E. coli recA* gene product. *Cold Spring Harb. Symp. Quant. Biol.*, **43**, 917-920.

Rockmill, B., Sym, M., Scherthan, H. and Roeder, G.S. (1995) Roles for two RecA homologs in promoting meiotic chromosome synapsis. *Genes Dev.*, **9**, 2684-2695.

Roe, S.M., Barlow, T., Brown, T., Oram, M., Keeley, A., Tsaneva, I.R. and Pearl, L.H. (1998) Crystal structure of an octameric RuvA-Holliday junction complex. *Molec. Cell*, **2**, 361-372.

Roman, L.J. and Kowalczykowski, S.C. (1989) Characterization of the helicase activity of the *Escherichia coli* RecBCD enzyme using a novel helicase assay. *Biochemistry*, **28**, 2863-2872.

Rosselli, W. and Stasiak, A. (1990) Energetics of RecA-mediated recombination reactions. Without ATP hydrolysis RecA can mediate polar strand exchange but is unable to recycle. *J. Mol. Biol.*, **216**, 335-352.

Rosselli, W. and Stasiak, A. (1991) The ATPase activity of RecA is needed to push the DNA strand exchange through heterologous regions. *EMBO J.*, **10**, 4391-4396.

Rozen, F., Pelletier, J., Trachsel, H. and Sonenberg, N. (1989) A lysine substitution in the ATP-binding site of eucaryotic initiation factor 4A abrogates nucleotide-binding activity. *Mol. Cell. Biol.*, **9**, 4061-4063.

Rupp, W.D. and Howard-Flanders, P. (1968) Discontinuities in the DNA synthesized in an excision-defective strain of *Escherichia coli* following ultraviolet irradiation. *J. Mol. Biol.*, **31**, 291-304.

Rupp, W.D., Wilde, C.E., Reno, D.L. and Howard-Flanders, P. (1971) Exchanges between DNA strands in ultraviolet-irradiated *Escherichia coli*. *J. Mol. Biol.*, **61**, 25-44.

Saito, A., Iwasaki, H., Ariyoshi, M., Morikawa, K. and Shinagawa, H. (1995) Identification of four acidic amino acids that constitute the catalytic center of the RuvC Holliday junction resolvase. *Proc. Natl. Acad. Sci. U.S.A.*, **92**, 7470-7474.

Sambrook, E.F., Fritsch, E.F. and Maniatis, T. (1989) *Molecular Cloning: A Laboratory Manual*. Cold Spring Harbor Laboratory Press, Cold Spring Harbor, New York.

San Martin, M.C., Gruss, C. and Carazo, J.M. (1997) Six molecules of SV40 large T antigen assemble in a propeller-shaped particle around a channel. *J. Mol. Biol.*, **268**, 15-20.

San Martin, M.C., Stamford, N.P.J., Dammerova, N., Dixon, N.E. and Carazo, J.M. (1995) A structural model for the *Escherichia coli* DnaB helicase based on electron microscopy data. *J. Struct. Biol.*, **114**, 167-176.

Sandler, S.J., Satin, L.H., Samra, H.S. and Clark, A.J. (1996) *recA*-like genes from three archaean species with putative protein products similar to Rad51 and Dmc1 proteins of the yeast *Saccharomyces cerevisiae*. *Nucleic Acids Res.*, **24**, 2125-2132.

Saraste, M., Sibbald, P.R. and Wittinghofer, A. (1990) The P-loop - a common motif in ATP- and GTP-binding proteins. *TIBS*, **15**, 430-434.

Sawaya, M.R., Guo, S., Tabor, S., Richardson, C.C. and Ellenberger, T. (1999) Crystal structure of the helicase domain from the replicative helicase-primase of bacteriophage T7 [In Process Citation]. *Cell*, **99**, 167-177.

Scherzinger, E., Ziegelin, G., Bárcena, M., Carazo, J.M., Lurz, R. and Lanka, E. (1997) The RepA protein of plasmid RSF1010 is a replicative DNA helicase. *J. Biol. Chem.*, **272**, 30228-30236.

Schulz, G.E. (1992) Binding of nucleotides by proteins. *Curr. Opin. Struct. Biol.*, **2**, 61-67.

Schutte, B.C. and Cox, M.M. (1987) Homology-dependent changes in adenosine 5'-triphosphate hydrolysis during RecA protein promoted DNA strand exchange: evidence for long paranemic complexes. *Biochemistry*, **26**, 5616-5625.

Schwacha, A. and Kleckner, N. (1995) Identification of double Holliday junctions as intermediates in meiotic recombination. *Cell*, **83**, 783-791.

Scott, J.F., Eisenberg, S., Bertsch, L.L. and Kornberg, A. (1977) A mechanism of duplex DNA replication revealed by enzymatic studies of phage øX174: Catalytic strand separation in advance of replication. *Proc. Natl. Acad. Sci. U.S.A.*, **74**, 193-197.

Seif, R. (1982) New properties of simian virus 40 large T antigen. *Mol. Cell Biol.*, **2**, 1463-1471.

Seigneur, M., Bidnenko, V., Ehrlich, S.D. and Michel, B. (1998) RuvAB acts at arrested replication forks. *Cell*, **95**, 419-430.

Seitz, E.M., Brockman, J.P., Sandler, S.J., Clark, A.J. and Kowalczykowski, S.C. (1998) RadA protein is an archaeal RecA protein homolog that catalyzes DNA strand exchange. *Genes Dev.*, **12**, 1248-1253.

Shah, R., Bennett, R.J. and West, S.C. (1994a) Activation of RuvC Holliday junction resolvase *in vitro*. *Nucleic Acids Res.*, **22**, 2490-2497.

Shah, R., Bennett, R.J. and West, S.C. (1994b) Genetic recombination in *E. coli*: RuvC protein cleaves Holliday junctions at resolution hotspots *in vitro*. *Cell*, **79**, 853-864.

Shah, R., Cosstick, R. and West, S.C. (1997) The RuvC dimer resolves Holliday junctions by a dual incision mechanism that involves base-specific contacts. *EMBO J.*, **16**, 1464-1472.

Shan, Q. and Cox, M.M. (1996) RecA protein dynamics in the interior of RecA nucleoprotein filaments. *J. Mol. Biol.*, **257**, 756-774.

Shan, Q. and Cox, M.M. (1997) RecA filament dynamics during DNA strand exchange reactions. *J. Biol. Chem.*, **272**, 11063-11073.

Shan, Q., Cox, M.M. and Inman, R.B. (1996) DNA strand exchange promoted by $RecA^{K72R}$: Two reaction phases with different Mg^{2+} requirements. *J. Biol. Chem.*, **271**, 5712-5724.

Shaner, S.L. and Radding, C.M. (1987) Translocation of *Escherichia coli* RecA protein from a single-stranded tail to contiguous duplex DNA. *J. Biol. Chem.*, **262**, 9211-9219.

Sharp, P.A., Sugden, B. and Sambrook, J. (1973) Detection of two restriction endonuclease activities in *Haemophilus parainfluenzae* using analytical agarose-ethidium bromide electrophoresis. *Biochemistry*, **12**, 3055-3063.

Sharples, G.J., Benson, F.E., Illing, G.T. and Lloyd, R.G. (1990) Molecular and functional analysis of the *ruv* region of *Escherichia coli* K-12 reveals three genes involved in DNA repair and recombination. *Mol. Gen. Genet.*, **221**, 219-226.

Sharples, G.J., Chan, S.N., Mahdi, A.A., Whitby, M.C. and Lloyd, R.G. (1994a) Processing of intermediates in recombination and DNA repair: Identification of a new endonuclease that specifically cleaves Holliday junctions. *EMBO J.*, **13**, 6133-6142.

Sharples, G.J. and Lloyd, R.G. (1991) Resolution of Holliday junctions in *E. coli*: Identification of the *ruvC* gene product as a 19 kDa protein. *J. Bacteriol.*, **173**, 7711-7715.

Sharples, G.J., Whitby, M.C., Ryder, L. and Lloyd, R.G. (1994b) A mutation in helicase motif-III of *Escherichia coli* RecG protein abolishes branch migration of Holliday junctions. *Nucleic Acids Res.*, **22**, 308-313.

Shiba, T., Iwasaki, H., Nakata, A. and Shinagawa, H. (1991) SOS-inducible DNA repair proteins, RuvA and RuvB, of *Escherichia coli*: Functional interactions between RuvA and RuvB for ATP hydrolysis and renaturation of the cruciform structure in supercoiled DNA. *Proc. Natl. Acad. Sci. U.S.A.*, **88**, 8445-8449.

Shiba, T., Iwasaki, H., Nakata, A. and Shinagawa, H. (1993) *Escherichia coli* RuvA and RuvB proteins involved in recombination repair: physical properties and interactions with DNA. *Mol. Gen. Genet.*, **237**, 395-399.

Shida, T., Iwasaki, H., Saito, A., Kyogoku, Y. and Shinagawa, H. (1996) Analysis of substrate specificity of the RuvC Holliday junction resolvase with synthetic Holliday junctions. *J. Biol. Chem.*, **271**, 26105-26109.

Shim, S.C. and Kim, Y.Z. (1983) Photoreaction of 8-methoxypsoralen with thymidine. *Photochem. Photobiol.*, **38**, 265-271.

Shinagawa, H., Makino, K., Amemura, M., Kimura, S., Iwasaki, H. and Nakata, A. (1988) Structure and regulation of the *Escherichia coli ruv* operon involved in DNA repair and recombination. *J. Bacteriol.*, **170**, 4322-4329.

Shinagawa, H., Shiba, T., Iwasaki, H., Makino, K., Takahagi, T. and Nakata, A. (1991) Properties of the *Escherichia coli* RuvA and RuvB proteins involved in DNA repair, recombination and mutagenesis. *Biochimie*, **73**, 505-508.

Shinohara, A., Ogawa, H., Matsuda, Y., Ushio, N., Ikeo, K. and Ogawa, T. (1993) Cloning of human, mouse and fission yeast recombination genes homologous to *RAD51* and *recA*. *Nature Genet.*, **4**, 239-243.

Shinohara, A., Ogawa, H. and Ogawa, T. (1992) Rad51 protein involved in repair and recombination in *Saccharomyces cerevisiae* is a RecA-like protein. *Cell*, **69**, 457-470.

Shurvinton, C.E. and Lloyd, R.G. (1982) Damage to DNA induces expression of the *ruv* gene of *Escherichia coli*. *Mol. Gen. Genet.*, **185**, 352-355.

Smith, D.R., Richterich, P., Rubenfield, M., Rice, P.W., Butler, C., Lee, H.M., Kirst, S., Gundersen, K., Abendschan, K., Xu, Q. *et al.* (1997) Multiplex sequencing of 1.5 Mb of the *Mycobacterium leprae* genome. *Genome Res.*, **7**, 802-819.

Smith, K.C. and Meun, D.H. (1970) Repair of radiation-induced damage in *Escherichia coli*. I. Effect of *rec* mutations on post-replication repair of damage due to ultraviolet radiation. *J. Mol. Biol.*, **51**, 459-472.

Soultanas, P., Dillingham, M.S., Velankar, S.S. and Wigley, D.B. (1999) DNA binding mediates conformational changes and metal ion coordination in the active site of PcrA helicase. *J. Mol. Biol.*, **290**, 137-148.

Spielmann, H.P., Dwyer, T.J., Sastry, S.S., Hearst, J.E. and Wemmer, D.E. (1995) DNA structural reorganization upon conversion of a psoralen furan-side monoadduct to an interstrand cross-link: implications for DNA repair. *Proc. Natl. Acad. Sci. U.S.A.*, **92**, 2345-2349.

Spiess, E., Zimmerman, H. and Lunsdorf, H. (1987) Negative staining of proteins and filaments. In Sommerville, J. and Scheer, U. (eds.), *Electron Microscopy in Molecular Biology*. IRL Press, Oxford, pp. 147-166.

Stasiak, A. and DiCapua, E. (1982) The helicity of DNA in complexes with RecA protein. *Nature*, **299**, 185-186.

Stasiak, A., DiCapua, E. and Koller, T. (1981) Elongation of duplex DNA by RecA protein. *J. Mol. Biol.*, **151**, 557-564.

Stasiak, A., Tsaneva, I.R., West, S.C., Benson, C.J.B., Yu, X. and Egelman, E.H. (1994) The *Escherichia coli* RuvB branch migration protein forms double hexameric rings around DNA. *Proc. Natl. Acad. Sci. U.S.A.*, **91**, 7618-7622.

Stitt, B.L. (1988) *Escherichia coli* transcription termination protein Rho has three hydrolytic sites for ATP. *J. Biol. Chem.*, **263**, 11130-11137.

Story, R.M. and Steitz, T.A. (1992) Structure of the RecA protein-ADP complex. *Nature*, **355**, 374-376.

Story, R.M., Weber, I.T. and Steitz, T.A. (1992) The structure of the *Escherichia coli* RecA protein monomer and polymer. *Nature*, **355**, 318-325.

Subramanya, H.S., Bird, L.E., Brannigan, J.A. and Wigley, D.B. (1996) Crystal structure of a DExx box DNA helicase. *Nature*, **384**, 379-383.

Sung, P. (1994) Catalysis of ATP-dependent homologous DNA pairing and strand exchange by yeast Rad51 protein. *Science*, **265**, 1241-1243.

Sung, P. and Robberson, D.L. (1995) DNA strand exchange mediated by a Rad51-ssDNA nucleoprotein filament with polarity opposite to that of RecA. *Cell*, **82**, 453-461.

Symington, L.S. and Kolodner, R. (1985) Partial purification of an enzyme from *Saccharomyces cerevisiae* that cleaves Holliday junctions. *Proc. Natl. Acad. Sci. U.S.A.*, **82**, 7247-7251.

Szostak, J.W., Orr-Weaver, T.L., Rothstein, R.J. and Stahl, F.W. (1983) The double-strand break repair model for recombination. *Cell*, **33**, 25-35.

Takahagi, M., Iwasaki, H., Nakata, A. and Shinagawa, H. (1991) Molecular analysis of the *Escherichia coli ruvC* gene, which encodes a Holliday junction specific endonuclease. *J. Bacteriol.*, **173**, 5747-5753.

Takahagi, M., Iwasaki, H. and Shinagawa, H. (1994) Structural requirements of substrate DNA for binding to and cleavage by RuvC, a Holliday junction resolvase. *J. Biol. Chem.*, **269**, 15132-15139.

Tambini, C.E., George, A.M., Rommens, J.M., Tsui, L.-C., Scherer, S.W. and Thacker, J. (1997) The *XRCC2* DNA repair gene: Identification of a positional candidate. *Genomics*, **41**, 84-92.

Taylor, A.F. and Smith, G.R. (1980) Unwinding and rewinding of DNA by the RecBC enzyme. *Cell*, **22**, 447-457.

Terasawa, M., Shinohara, A., Hotta, Y., Ogawa, H. and Ogawa, T. (1995) Localization of RecA-like recombination proteins on chromosomes of the lily at various meiotic stages. *Genes Dev.*, **9**, 925-934.

Thacker, J. (1999) A surfeit of *RAD51*-like genes? *Trends Genet.*, **15**, 166-168.

Thompson, B.J., Camien, M.N. and Warner, R.C. (1976) Kinetics of branch migration in double-stranded DNA. *Proc. Natl. Acad. Sci. U.S.A.*, **73**, 2299-2303.

Thompson, B.J., Escarmis, C., Parker, B., Slater, W.C., Doniger, J., Tessman, I. and Warner, R.C. (1975) Figure-8 configuration of dimers of S13 and ϕX174 replicative form DNA. *J. Mol. Biol.*, **91**, 409-419.

Tomb, J.F., White, O., Kerlavage, A.R., Clayton, R.A., Sutton, G.G., Fleischmann, R.D., Ketchum, K.A., Klenk, H.P., Gill, S., Dougherty, B.A. *et al.* (1997) The complete genome sequence of the gastric pathogen *Helicobacter pylori*. *Nature*, **388**, 539-547.

Tong, J. and Wetmur, J.G. (1996) Cloning, sequencing, and expression of *ruvB* and characterization of RuvB proteins from two distantly related thermophilic eubacteria. *J. Bacteriol.*, **178**, 2695-2700.

Torres-Ramos, C.A., Prakash, S. and Prakash, L. (1997) Requirement of yeast DNA polymerase delta in post-replicational repair of UV-damaged DNA. *J. Biol. Chem.*, **272**, 25445-25448.

Tsaneva, I.R., Illing, G.T., Lloyd, R.G. and West, S.C. (1992a) Purification and properties of the RuvA and RuvB proteins of *Escherichia coli*. *Mol. Gen. Genet.*, **235**, 1-10.

Tsaneva, I.R., Müller, B. and West, S.C. (1992b) ATP-dependent branch migration of Holliday junctions promoted by the RuvA and RuvB proteins of *E. coli*. *Cell*, **69**, 1171-1180.

Tsaneva, I.R., Müller, B. and West, S.C. (1993) RuvA and RuvB proteins of *Escherichia coli* exhibit DNA helicase activity *in vitro*. *Proc. Natl. Acad. Sci. U.S.A.*, **90**, 1315-1319.

Tsaneva, I.R. and West, S.C. (1994) Targeted versus non-targeted DNA helicase activity of the RuvA and RuvB proteins of *Escherichia coli*. *J. Biol. Chem.*, **269**, 26552-26558.

Uhlin, B.E. and Clark, A.J. (1981) Overproduction of the *E. coli* RecA protein without stimulation of its proteolytic activity. *J. Bacteriol.*, **148**, 386-390.

Umezu, K., Chi, N.W. and Kolodner, R.D. (1993) Biochemical interaction of the *Escherichia coli* RecF, RecO, and RecR proteins with RecA protein and single-stranded-DNA binding-protein. *Proc. Natl. Acad. Sci. U. S. A.*, **90**, 3875-3879.

Umezu, K. and Kolodner, R.D. (1994) Protein interactions in genetic recombination in *Escherichia coli*: interactions involving RecO and RecR overcome the inhibition of RecA by single-stranded DNA binding protein. *J. Biol. Chem.*, **269**, 30005-30013.

Valenzuela, M.S. and Inman, R.B. (1975) Visualization of a novel junction in bacteriophage lambda DNA. *Proc. Natl. Acad. Sci. U.S.A.*, **72**, 3024-3028.

Van Dyck, E., Hajibagheri, N.M.A., Stasiak, A. and West, S.C. (1998) Visualisation of human Rad52 protein and its complexes with hRad51 and DNA. *J. Mol. Biol.*, **284**, 1027-1038.

van Gool, A.J., Hajibagheri, N.M.A., Stasiak, A. and West, S.C. (1999) Assembly of the Escherichia coli RuvABC resolvasome directs the orientation of Holliday junction resolution. *Genes & Dev.*, **13**, 1861-1870.

van Gool, A.J., Shah, R., Mézard, C. and West, S.C. (1998) Functional interactions between the Holliday junction resolvase and the branch migration motor of *Escherichia coli*. *EMBO J.*, **17**, 1838-1845.

Velankar, S.S., Soultanas, P., Dillingham, M.S., Subramanya, H.S. and Wigley, D.B. (1999) Crystal structures of complexes of PcrA DNA helicase with a DNA substrate indicate an inchworm mechanism. *Cell*, **97**, 75-84.

Vincent, S.D., Mahdi, A.A. and Lloyd, R.G. (1996) The RecG branch migration protein of *Escherichia coli* dissociates R-loops. *J. Mol. Biol.*, **264**, 713-721.

Walker, J.E., Saraste, M., Runswick, M.J. and Gay, N.J. (1982) Distantly related sequences in the α- and β-subunits of ATP synthase, myosin, kinases and other ATP-requiring enzymes and a common nucleotide binding fold. *EMBO J.*, **1**, 945-951.

Washington, M.T., Rosenberg, A.H., Griffin, K., Studier, F.W. and Patel, S.S. (1996) Biochemical analysis of mutant T7 primase/helicase proteins defective in DNA binding, nucleotide hydrolysis, and the coupling of hydrolysis with DNA unwinding. *J. Biol. Chem.*, **271**, 26825-26834.

Wessel, R., Schweizer, J. and Stahl, H. (1992a) Simian virus 40 T-antigen DNA helicase is a hexamer which forms a binary complex during bidirectional unwinding from the viral origin of DNA replication. *J. Virol.*, **66**, 804-815.

Wessel, R., Schwizer, J. and Stahl, H. (1992b) Simian virus 40 T-antigen DNA helicase is a hexamer which forms a binary complex during bidirectional unwinding from the viral origin of DNA replication. *J. Virol.*, **66**, 804-815.

West, S.C. (1992) Enzymes and molecular mechanisms of homologous recombination. *Ann. Rev. Biochem.*, **61**, 603-640.

West, S.C. (1996) DNA helicases: New breeds of translocating motors and molecular pumps. *Cell*, **86**, 177-180.

West, S.C. (1997) Processing of recombination intermediates by the RuvABC proteins. *Ann. Rev. Genet.*, **31**, 213-244.

West, S.C. (1998) RuvA gets X-rayed on Holliday. *Cell*, **94**, 699-701.

West, S.C., Cassuto, E. and Howard-Flanders, P. (1981a) Heteroduplex formation by RecA protein: Polarity of strand exchanges. *Proc. Natl. Acad. Sci. U.S.A.*, **78**, 6149-6153.

West, S.C., Cassuto, E. and Howard-Flanders, P. (1981b) Mechanism of *E. coli* RecA protein-directed strand exchanges in postreplication repair of DNA. *Nature*, **294**, 659-662.

West, S.C., Cassuto, E. and Howard-Flanders, P. (1982) Postreplication repair in *E. coli*: Strand exchange reactions of gapped DNA by RecA protein. *Mol. Gen. Genet.*, **187**, 209-217.

West, S.C., Cassuto, E., Mursalim, J. and Howard-Flanders, P. (1980) Recognition of duplex DNA containing single-stranded regions by RecA protein. *Proc. Natl. Acad. Sci. U.S.A.*, **77**, 2569-2573.

West, S.C., Countryman, J.K. and Howard-Flanders, P. (1983) Enzymatic formation of biparental figure-8 molecules from plasmid DNA and their resolution in *Escherichia coli*. *Cell*, **32**, 817-829.

West, S.C. and Howard-Flanders, P. (1984) Duplex-duplex interactions catalyzed by RecA protein allow strand exchanges to pass double strand breaks in DNA. *Cell*, **37**, 683-691.

Whitby, M.C., Bolt, E.L., Chan, S.N. and Lloyd, R.G. (1996) Interactions between RuvA and RuvC at Holliday junctions: inhibition of junction cleavage and formation of a RuvA-RuvC-DNA complex. *J. Mol. Biol.*, **264**, 878-890.

Whitby, M.C. and Dixon, J. (1997) A new Holliday junction resolving enzyme from *Schizosaccharomyces pombe* that is homologous to Ccel from *Saccharomyces cerevisiae*. *J. Mol. Biol.*, **272**, 509-522.

Whitby, M.C., Ryder, L. and Lloyd, R.G. (1993) Reverse branch migration of Holliday junctions by RecG protein: A new mechanism for resolution of intermediates in recombination and DNA repair. *Cell*, **75**, 341-350.

Whitby, M.C., Vincent, S.D. and Lloyd, R.G. (1994) Branch migration of Holliday junctions: identification of RecG protein as a junction specific DNA helicase. *EMBO J.*, **13**, 5220-5228.

White, M.F. and Lilley, D.M.J. (1996) The structure-selectivity and sequence-preference of the junction-resolving enzyme CCE1 of *Saccharomyces cerevisiae*. *J. Mol. Biol.*, **257**, 330-341.

White, M.F. and Lilley, D.M.J. (1997) Characterization of a Holliday junction-resolving enzyme from *Schizosaccharomyces pombe*. *Mol. Cell. Biol.*, **17**, 6465-6471.

Wong, I. and Lohman, T.M. (1992) Allosteric effects of nucleotide cofactors on *Escherichia coli* Rep helicase DNA binding. *Science*, **256**, 350-355.

Yamada, K., Fukuoh, A., Iwasaki, H. and Shinagawa, H. (1999) Novel properties of the *Thermus thermophilus* RuvB protein, which promotes branch migration of Holliday junctions. *Mol. Gen. Genet.*, **261**, 1001-1011.

Yanisch-Perron, C., Vieira, J. and Messing, J. (1985) Improved M13 phage cloning vectors and host strains: nucleotide sequences of the M13mp18 and pUC19 vectors. *Gene*, **33**, 103-119.

Yao, N., Hesson, T., Cable, M., Hong, Z., Kwong, A.D., Le, H.V. and Weber, P.C. (1997) Structure of the hepatitis C virus RNA helicase domain. *Nat. Struct. Biol.*, **4**, 463-467.

Yarranton, G.T. and Gefter, M.L. (1979) Enzyme-catalyzed DNA unwinding: Studies on *Escherichia coli* Rep protein. *Proc. Natl. Acad. Sci. U.S.A.*, **76**, 1658-1662.

Yeung, A.T., Jones, B.K. and Chu, C.T. (1988) Photoreactivities and thermal properties of psoralen cross-links. *Biochemistry*, **27**, 3204-3210.

Yonesaki, T. and Minagawa, T. (1985) T4 phage gene *uvsX* product catalyzes homologous DNA pairing. *EMBO J.*, **4**, 3321-3327.

Yong, Y. and Romano, L.J. (1996) Benzo[α]pyrene-DNA adducts inhibit the DNA helicase activity of the bacteriophage T7 gene 4 protein. *Chem. Res. Toxicol.*, **9**, 179-187.

Yoshida, K., Kondoh, G., Matsuda, Y., Habu, T., Nishimune, Y. and Morita, T. (1998) The mouse *recA*-like gene *DMC1* is required for homologous chromosome synapsis during meiosis. *Mol. Cell.*, **1**, 707-718.

Yoshimura, Y., Morita, T., Yamamoto, A. and Matsushiro, A. (1993) Cloning and sequence of the human *recA*-like gene cDNA. *Nucleic Acids Res.*, **21**, 1665.

Yu, C.E., Oshima, J., Fu, Y.H., Wijsman, E.M., Hisama, F., Alisch, R., Matthews, S., Nakura, J., Miki, T., Ouais, S. *et al.* (1996a) Positional cloning of the Werner's syndrome gene. *Science*, **272**, 258-262.

Yu, X. and Egelman, E.H. (1992) Structural data suggest that the active and inactive forms of the RecA filament are not simply interconvertible. *J. Mol. Biol.*, **227**, 334-346.

Yu, X. and Egelman, E.H. (1993) DNA conformation induced by the bacteriophage-T4 UvsX protein appears identical to the conformation induced by the *Escherichia coli* RecA protein. *J. Mol. Biol.*, **232**, 1-4.

Yu, X. and Egelman, E.H. (1997) The RecA hexamer is a structural homologue of ring helicases. *Nature Struct. Biol.*, **4**, 101-104.

Yu, X., Hingorani, M.M., Patel, S.S. and Egelman, E.H. (1996b) DNA is bound within the central hole to one or two of the six subunits of the T7 DNA helicase. *Nature Struct. Biol.*, **3**, 740-743.

Yu, X., Jezewska, M.J., Bujalowski, W. and Egelman, E.H. (1996c) The hexameric *Escherichia coli* DnaB helicase can exist in different quaternary states. *J. Mol. Biol.*, **259**, 7-14.

Yu, X., West, S.C. and Egelman, E.H. (1997) Structure and subunit composition of the RuvAB-Holliday junction complex. *J. Mol. Biol.*, **266**, 217-222.

Zerbib, D., Mézard, C., George, H. and West, S.C. (1998) Coordinated actions of RuvABC in Holliday junction processing. *J. Mol. Biol.*, **281**, 621-630.